# POLIURETANOZKO ITSASGARRIEN SINTESIA LIGNINAN OINARRITUTAKO BIOPOLIOLAK ERABILIZ

## POLYURETHANE ADHESIVE SYNTHESIS USING LINGIN-BASED BIO-POLYOLS


eman ta zabal zazu

Universidad del País Vasco

Euskal Herriko Unibertsitatea

**Fabio Hernández Ramos**


**2023ko urtarrila**

*“Hello there”*

*Obi-Wan Kenobi*

# Poliuretanozko-itsasgarrien sintesia ligninan oinarritutako biopoliolak erabiliz

## Polyurethane adhesive synthesis using lignin-based bio-polyols

**Fabio Hernández Ramos**-ek aurkeztutako disertazioa

Euskal Herriko Unibertsitateak

Material Berriztagarrien Ingeniaritzako programan

Doktore Titulua lortzeko baldintzak betez

*Jalel Labidi eta Xabier Erdocia doktoreen zuzendaritzapean*

Ingeniaritza Kimikoa eta Ingurumenaren Ingeniearitza Saila

DONOSTIA – SAN SEBASTIÁN

2023

Dokumentu hau euskaraz eta ingelesez idatzita dago. Euskaraz dauden atalak hauek dira:

I. ATALA osoa

II. ATALA osoa

III. ATALEKO I. eta II. Argitalpenak

IV. ATALEKO Ondorioak eta Etorkizuneko Lanak, eta I., II., eta III. eranskinak

*“No, try not. Do or do not. There is no try”*

*Master Yoda*

# Esker onak

Onartu beharra daukat hau ez zela nire etorkizuneko asmoen artean sartzen, baina hara non 41 urterekin nire bokazioa aurkitu dudan. Ez gustatzen ez zitzaidalako, baizik eta neure buruarekiko segurtasun faltagatik ez nuelako uste horretarako gai nintzenik. Baina, egin dut, gozatu eta sufritu dut, gorrotatu eta maitatu egin dut eta, batez ere, egunez egun landu dut, orduak sartuz, peiperrak irakurriz, mantala zikinduz, beira eta ekipamenduren bat edo beste apurtuz, eta harraskan hamaika ordu pasatuz. Hala ere, Frodo Bolsonek izan zuen bezala, abentura honetan jende zoragarria izan da niri laguntzen, dena ondo atera zedin. Horregatik, eskerrik beroenak eman nahi dizkizuet.

Hasteko, eskerrak eman nahi dizkiot nire zuzendari izan den Jalel Labidi doktoreari tesi hau egiteko aukera emateagatik, non lignina eta poliuretanoei buruz ikasteaz gain, neure burua pixka bat gehiago ezagutzeko aukera izan dut. Xabier Erdocia doktoreari, bost urte hauetan emandako laguntzagatik eta azkenean dena ondo ateratzen dela ikasi dugulako. Horrregatik, nire eskerrik beroenak eskaintzen dizkizut. María González Alriols doktoreari, nire ikasle garaitik gaur egunera arte beti irribarre eta hitz atseginez lagundu didana. Bruno Miguel Morais doktoreari ere eskerrak eman nahiko nizkioke Viseuko Instituto Politeknikoko egonaldian emandako laguntzagatik.

Nire koadrilari, bereziki, Imanol, Mikel, Luis eta Iñigo Calvo doktoreari, hay da, “Brothers of Metal” taldeari, Txiki tabernan musika ona entzuten emandako gau guztiengatik.

Osasun Sport Clinik klinikako Aintzaneri, errehabilitazio eta entrenamendu goizak atseginagoak egiteagatik, merezi duzulako onena opa dizut. Sergio eta Luciari, ez etsitzeagatik. Egunen batean zuen aholku guztiak jarraitzeko gai izango naiz.

BioRP taldeko kide guztiei, berriak zein zaharrak, bost urte hauetan zehar eman didazuen laguntzagatik. Baina, batez ere, abentura luze hau nirekin estu-estu partekatu duzuenoi, dagoeneko ez zarete lankideak bakarrik, lagun handiak bihurtu zaretelako, aholku eta laguntza bila, edo eta mojito, festa edo tontakeriak behar ditudanean jo dezakedana. Mila esker Rut, Leyre (nire kongresu-emaztea), Izaskun eta Patricia Doktoreei eta, jakina, baita Faridari ere. Eta ez, ez naiz zutaz ahazten, Amaia Morales Doktorea, nahiz eta hasiera batean zu ere ez zinen nire gustukoa izan, gaur egun, zalantzarik gabe, nire pertsona faboritoenetako batean bihurtu zara.

Eskerrik asko Julen Vadillori zure aholku eta laguntzagatik. Izaskun, Tamara, Joseba, Iratxe, Mireia eta Nereari zuen denbora eta laguntzagatik. Eta nola ez, Loliri, inoiz aurkitzen ez dudan arren, beti hor egoten baita behar denerako.

Mila esker, baita ere, nire guraso eta anai-arrebei, nire etaparik ilunetan ere izan duten pazientziagatik. Familia politikoari ere eskerrak eman nahiko nizkioke familian hartu nautelako.

Azkenik, Cris, nire (AMORE)ri. Txikitan ezagutu genuen elkar, auzoan jolasten, eta bizitzak gure bideak aldi batez banandu zituen, biok gehien behar genuenean berriro elkartzeko. Elkarrekin bide bat egitea erabaki dugu, garrantzitsuena, bizitzarena, eta ziur nago elkarrekin agertzen diren eragozpen guztiei aurre egingo dizkiegula, azken hilabete zoro hauetan bezala.

Eta noski, eskerrik asko Lukari, nire eguzkia eta izarrak izateagatik.

## Nomenclature

| | |
|---|---|
| Acid number | $A_n$ |
| Activation Energy | $E_a$ |
| (3-aminopropyl)trimethoxysilane | APTMS |
| Attenuated Total Reflection-Fourier Transformed Infrared | ATR-FTIR |
| Automated bonding evaluation system | ABES |
| Average molecular weight | $M_W$ |
| Bio-polyols formulated with CG for elastic PUs from Eucalyptus globulus | $EOPE_{CG}$ |
| Bio-polyols formulated with CG for elastic PUs from Pinus radiata | $POPE_{CG}$ |
| Bio-polyols formulated with CG for rigid PUs from Eucalyptus globulus | $EOPR_{CG}$ |
| Bio-polyols formulated with CG for rigid PUs from Pinus radiata | $POPR_{CG}$ |
| Black Liquor | BL |
| Box-Benkhen Design | BBD |
| Carbon | C |
| Crude Glycerol | CG |
| Derivative Thermogravimetric | DTG |
| Dimethyl Carbonate | DMC |
| Equivalent Weight | EW |
| Eucalyptus globulus organosolv black liquor | EOBL |
| Eucalyptus globulus organosolv lignin | EOL |
| Eucalyptus globulus organosolv lignin after ultrasound treatment | EOUL |
| Eucalyptus globulus organosolv Polyol for Elastic PU | EOPE |
| Eucalyptus globulus organosolv Polyol for Rigid PU | EOPR |
| Eucalyptus globulus organosolv Polyol for Elastic PU | EOPE |
| Eucalyptus globulus organosolv Polyol for Rigid PU | EOPR |
| Eucalyptus Organosolv Polyol | EOP |
| Fatty Acids Methyl Esters | FAMEs |

| | |
|---|---|
| Free Fatty Acids | FFA |
| Functionality | *f* |
| Gas chromatography-Mass spectrometry | CG-MS |
| Gel Permeation Cromatography | GPC |
| Hexamethylenediamine | HDMA |
| Hard Segment | HS |
| Hard Segment weight fraction | $HS_W$ |
| Hydroxyl number | $I_{OH}$ |
| Isocyanate group | NCO |
| Ixocyanate to OH ratio | NCO:OH |
| Kissingr-Akahira-Sunose | KAS |
| Lignin-based polyurethane adhesive | LPA |
| Lignin-based NIPU adhesive | LNA |
| LNA with the silane coupling agent | CLNA |
| Maximum mass fraction of the rigid segment mixed in the soft segment | $W_H$ |
| 4,4'-Methylene diphenyl diisocyanate | MDI |
| Non-isocyanate polyurethane | NIPU |
| Number Average Molecular Weight | $M_n$ |
| Ozawa-Flyn-Wall | OFW |
| Pine organosolv Polyol | POP |
| Pinus radiata organosolv black liquor | POBL |
| Pinus radiata organosolv lignin | POL |
| Pinus radiata organosolv Polyol for Elastic PU | POPE |
| Pinus radiata organosolv Polyol for Rigid PU | POPR |
| Pinus radiata organosolv lignin after ultrasound treatment | POUL |
| Polydispersity Index | PDI |
| Polyethylene Glycol | PEG |
| Polyethylene glycol/Glycerol weight ratio | PEG/Gly |

| | |
|---|---|
| Polyurethane | PU |
| Preexponential factor | A |
| Response Surface Methodology | RSM |
| Soft Segment | SS |
| Soft segment weight fraction | $SS_W$ |
| Theoretical Hard Segment | $HS_t$ |
| Thermogravimetric Analysis | TGA |
| Weight fraction of H-bonded urethane groups | $X_{HB}$ |
| Weight fraction of the mixed phase | $MP_W$ |

# Table of Contents

**Lignin-based non isocyanate polyurethane adhesives. Synthesis and determination of adhesion properties and thermal degradation kinetic**

# *1. ATALA*

## SARRERA

*“You can’t stop change any more than*

*you can stop the suns from setting”*

*Shmi Skywaker*

## 1.1. Behin batean

Eguzki Sistema, Esne Bideko Orion Besoan kokatua, duela 4.570 miloi urte inguru sortu zen, ziur asko izar kumulu batean, izarretako gas eta hautsez eratutako hodei bat eguzki-nebulosa bat sortzeko kolapsatu zenean[1]. Grabitatearen ondorioz, nebulosaren erdigunean gero eta material gehiago pilatzen joan zen, presio hidrogeno atomoak helioan fusionatzeko gai izan zen arte, Eguzki izeneko izar bat sortuz. Eguzkiaren sorreraren ondoren, gainerako materiala, lehenik, planeta gaseosoak (Jupiter, Saturno, Urano eta Neptuno), gero planeta harritsuak (Merkurio, Venus, Lurra eta Marte) eta planeta nanoak (Pluton, Zeres, Haumea, Makemake, Eris, Sedna eta Phattie) osatzeko bildu zen. Azkenik, nebulosa desagertu zenean, Eguzki Sistema Eguzkiak, planetek eta haien ilargiek, planeta nanoez eta hondakinek osatzen zuten. Azken hauek, batez ere asteroide gerrikoan, Kuiper gerrikoan eta Oorten hodeian aurki daitezke. Sortu zenetik, Eguzki Sistemak 27 orbita inguru osatu ditu zentro galaktikoaren inguruan [2], non Lurra planeta antzua izatetik bizitzaz betetako planeta izatera igaro den.

Lehen bizi-formak, bakterioak, ziurrenik itsaspeko ingurune hidrotermaletan agertu ziren duela 3.770 miloi urte baino gehiago [3]. Beranduago, prokarioto izeneko zelula mota berri bat agertu zen, Lurreko bizitzaren gertaera garrantzitsu bat sortuz oxigenoa sortzeko ahalmena zuten prokarioto fototrofoen eboluzioarekin, bereziki Zianobakterioak, horietatik abiatuta kloroplastoek eboluzionatu egin baitzuten, beste organismo batzuen eboluziorako bidea erraztuz, algak eta landareak kasu [4,5]. Zianobakterioei esker, oxigeno atmosferikoaren mailak gora egin zuen duela 2450-2220 miloi urte, eta horrek Oxidazio Gertakari Handia izeneko iraungipen-gertaera eragin zuen [6].

Oxigenoaren presentziak Lurreko bizitzaren eboluzioaren prozesu garrantzitsuenetako bat ekarri zuen, zelula eukariotoen eboluzioa hain

zuzen ere [7]. Zelula mota hauek, bakteriokin eta archaeekin alderatuta, zelula konplexuagoak dira, mintz plasmatiko baten barruan ondo banatutako nukleo bat eta organulu desberdinak dituztenak. Honen ondorioz, zelula eukariotoek sistema berri eta konplexuagoen sorrera ekarri zuten, animalien, landareen, onddoen eta protisten erreinuen eboluzioa ahalbidetuz [8].

Landareek duela 500 miloi urte inguru lurzorua kolonizatzen hasi ziren, algak, lehorreko lehen landareen arbasoak, itsas kostaldeetako ingurune lehorretara egokitu behar izan zirenean, lurra konkistatu zuen egokitze-prozesu bati hasiera emanez. Hala ere, lehorreko lehen landareen agerpena ez zen gertatu 50 miloi urte geroago arte. Ordobizikoaren amaieran [9].

Lehen lehorreko landare horiek, lehorreko baldintza berrietara egokitzeko, eboluzio-erronka desberdinei egin behar izan zieten aurre. Besteak beste, UV-Ben esposizioari eta lehen urak ematen zuen euskarri estrukturalaren ezari egokitu behar izan ziren. Era berean, estrategia berriak ere garatu behar izan zituzten, hala nola lehortzea saihesteko mekanismoak eta belarjaleak eta patogenoak bezalako beste espezie batzuen aurkako babes-neurriak [10]. Lurreko landare berri hauen garapenerako egokitzapen guztiak ezinbestekoak izan ziren arren, metabolismo fenilpropanoide delakoaren bilakaera, zalantzarik gabe, garrantzitsuenetarikoa izan zen. Izan ere, horri esker, landareak UV-B kaltegarrietatik (280-320 nm) babesteko gai ziren fenilpropanoide unitateak metatzeko gai izan ziren [11]. Hala ere, trakeofitak agertu arte, 10 miloi urte geroago, landareek ez zuten fenilpropanoide unitate horiek zelula-horman ezartzeko ahalmena garatu lignina molekula metatzeko. Lignina molekularen agerpenak landareei tente hazteko errefortzu-estrukturala eman zien, zelulosak eskaintzen duen trakzioarekiko erresistentzia osatuz [12], eta hauen sistema baskularraren garapena ahalbidetu zuen [11]. Azkenik, egokitzapen horiek guztiek gaur egun lurreko landare baskular guztiek dituzten ezaugarri bereizgarriak sortu

zituzten, hala nola xilema, kutikula, estomak, aire interzelularreko espazioa, floema, endodermisa eta lurreko ekosisteman bizirauteko eta kolonizatzeko beharrezkoa den belaunaldien txandakatzea [13].

Bestalde, arestian aipatu bezala, zelula eukariotoek ezin konta ahala animalia-espezietan eboluzionatu ziren, horien artean Homo Sapiens-a. Homo Sapiens-ek bere ingurunea arrazionalki ezagutu eta uler dezake, eta konplexutasun handiko eragiketa kontzeptual eta sinbolikoak egiteko gai da, hala nola hizkuntza, arrazoiketa abstraktua eta introspekzio- eta espekulazio-gaitasuna. Beraz, gizakia animalien eboluzioaren gailurtzat har daiteke gaur egun arte. Hala ere, adimen handi hori aho biko arma bihur liteke, gizakia bere desagertzera eraman dezakeena.

## 1.2. Gizateria eta klima-aldaketa

Lehen aipatu bezala, gizateriaren eboluzioa animalien eboluzioaren gailurtzat har daiteke. Hala ere, gizakiak eta bere ingurunea moldatzeko duen gaitasunak ingurumenean aldaketa larriak eragin ditu. Aldaketa horiek animalia- eta landare-espezie asko desagertzea eragin du, eta, gainera, giza espeziearen beraren biziraupena izugarri zailduko luketen klima-aldaketak eragin ditzakete. Gizateriak duela milaka urtetik bere ingurunea eraldatzeko gaitasuna izan duen arren, aldaketa horiek ez zuten kliman eraginik izan XVIII. Mendearen amaierara arte. Gertaera hori gizateriaren asmakizunik handienetako batekin bat etorri zen, lurrun-makina, espeziearen etorkizuna betiko aldatuko zuena [14]. James Wattek 1784an garatua, asmakizun honek gizateria inoiz ikusitako garapen teknologikora katapultatu zuen, Lehen Iraultza Industriala (*First Industrial Revolution* FIR) deiturikoan, eskuzko ekoizpenaren metodoa mekaniko izatera aldatu zuena, produktibitatearen hobekuntza ekarriz [15]. Tamalez, erregai gisa ikatza erabiltzen zuen gailu berri horrek $CO_2$-ren emisio antropogenikoak, eta NOx eta SOX bezalako beste gas batzuen emisioak azkar handitzea eragin zuen. Ikatza FIRen

energia ekoizteko lehengai nagusia izan zen bezala, petrolioa izan zen Bigarren Industria Iraultzaren (*Second Industrial Revolution* SIR) garapena bultzatu zuena, garraiorako eta energia ekoizteko erregai gisa ez ezik, oinarrizko produktu askoren lehengai gisa ere erabili baitzen. Hain da garrantzitsua petrolioa gure gizartean, ezen XX. mendea petrolioaren mendea baita, non 2009an munduko 20 enpresa handienetatik 7 petrolio-enpresak ziren [16]. Baina, gizarteak erregai fosilekiko (ikatza, petrolioa, gasa eta abar) duen gehiegizko mendekotasuna eragin zuzena izan du ingurumenan. Horrela, berotegi-efektuko gasen kontzentrazioak gora egin dute azken 200 urteetan, emisio antropogenikoen hazkundearen ondorioz [17]. I.1. Irudiak azken 10000 urteetako $CO_2$ kontzentrazioaren bilakaera erakusten du. Ikus daitekeenez, XIX. mendearen erdialdera arte $CO_2$ atmosferikoaren kontzentrazioa konstante mantendu zen, eta mendeak aurrera egin ahala handitzen hasi zen. $CO_2$ isurien hazkundea XX. mendearen bigarren erdialdean areagotu ziren, hazkunde demografikoaren ondorioz energia-beharra eta ondasunen kontsumoa areagotu egin baitzen [18].

Hala ere, erregai fosilekiko mendekotasuna murrizteko diseinatutako politikak dauden arren, ezarritako helburuak betetzetik oso urrun daude. Izan ere, 2021ean, munduko energia primarioaren eskaria % 5,8 handitu zen, eta petrolioaren munduko ekoizpena eguneko 1,4 miloi upeletan handitu zen [21]. Gainera, Europar Batasunak (EB) gas naturala energia garbitzat hartzeko hartutako erabaki eztabaidagarriak [22] arriskuan jar lezake 2050erako Ebren zero isurketen helburua.

Bestalde, kutsadura atmosferikoaz gain, petrolioa ondasunak ekoizteko lehengai gisa erabiltzeak bestelako ingurumen-hondamendiak sortzen ditu. Besteak beste, petroliotik eratorritako material plastikoen erabilerak eragindako kutsadura da aipagarrienetako bat.

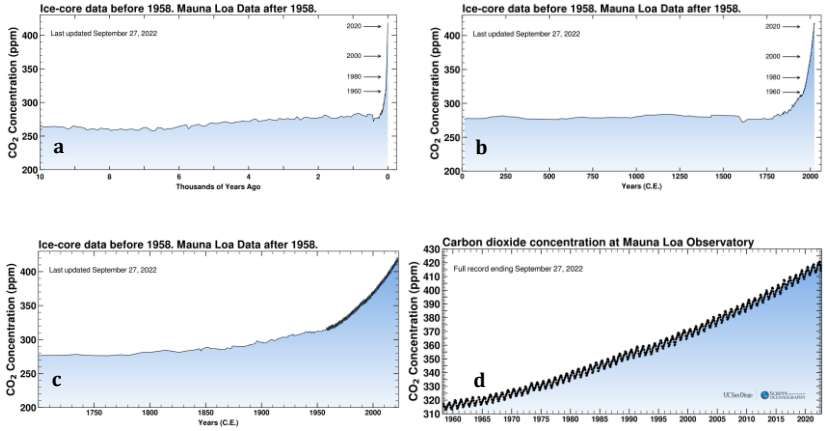


I.1. Irudia. a [19]-tik moldatua, b eta c [17]-tik moldatua, d Kaliforniako Unibertsitateko Scripps Institution of Oceanography, San Diego erakundearen kortesia da [20]

Lehen plastiko sintetikoa, zeluloidea, John Wesley Hyatt-ek garatu zuen 1869an. Material hau billar-bolak egiteko erabiltzen zen marfila ordezkatzeko helburu noblearekin garatu zen, horrela elefanteak iraungipen seguru batetik salbatzeko [23]. Harrezkeroztik, plastiko sintetikoak eguneroko bizitzaren parte izatera eta giza jardueraren garapenean funtsezko elementu izatera pasa dira [24]. Izan ere, plastiko berriaren munduko ekoizpenak etengabe gora egun du urtez urte, 1950ean 1,5 Mt ekoiztetik 2020an 364 Mt ekoiztera pasatuz (I.2. Irudia) [25]. Tamalez, hondakin plastikoen zati txiki bat baino ez da biltzen, eta horrek esan nahi du kontsumo osteko hondakin plastiko asko kontrolik gabe ingurumenera botatzen direla. Izan ere, EBn, bildutako plastiko kopurua 2006an 23.79 Mt izatetik 2020an 29,5 Mt izatera igo den arren, ez da nahikoa urtero ingurumenean eragiten diren kalte larriak arintzeko. Dena den, aldi horretan plastikoen isurketa zabortegietan % 46.6an murriztu dela, eta birziklapenaren eta balorizazio energetikoaren erabilera, berriz, % 117,7 eta % 77,1ean, hurrenez hurren, hazi direla ikus daiteke I.3. Irudian.

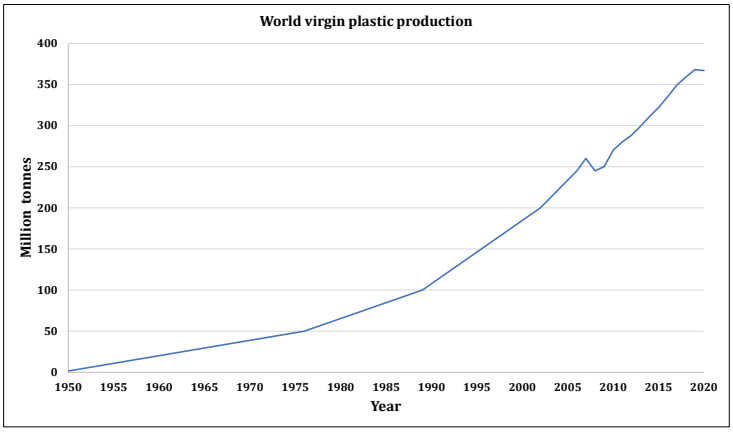


I.2. Irudia. Plastiko berrien munduko ekoizpena. Termoplastikoak, poliuretanoak, termoegonkorrak, elastomeroak, itsasgarria, estaldurak eta zigilatzaileak eta PP-zuntzak barne. Ez ditu kontsideratzen PET, PA eta Polyacryl-zuntzk [25]-etik lortutako datuak

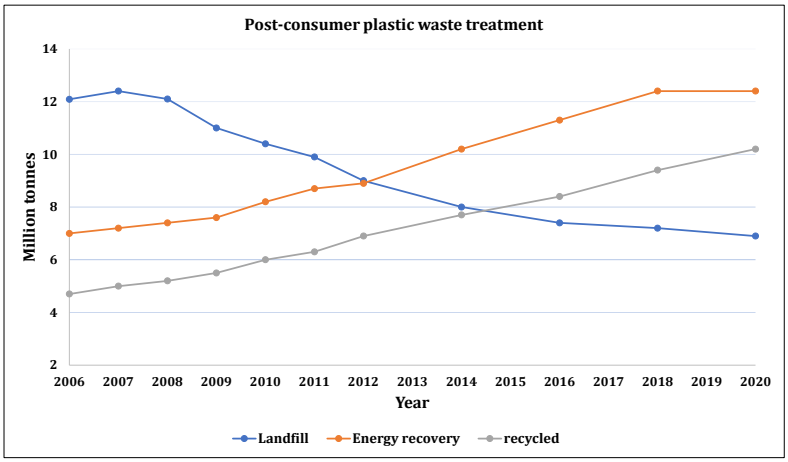


I.3. Irudia. Kontsumo osteko hondakin plastikoen tratamendua EU27+3an. [26]-tik egokitua

## 1.3. Poliuretanoak

Material plastikoek osatzen duten familia handiaren artean, PUak garrantzi handikoak dira industriarentzat, polimero moldakorrenak baitira beren propietate mekanikoengatik eta eskaintzen duten aplikazio sorta handiari

esker, besteak beste, PUen artean, termoplastikoak, aparrak, elastomeroak, itsasgarriak, estaldurak eta zigilatzaileak aurki daitezke [27–29].

Otto Bayer doktoreak 1937an lehen PUa sintetizatu zuenetik, PUren munduko ekoizpena 20 miloi tonaraino hazi da [30] 69200 miloi dolar garbiko merkatu-balioa lortuz 2019an, eta urteko %5,0-5,6 inguruan haztea espera dena 2025era arte [31].

PUak isozianatoen, kate-hedagailuen eta talde hidroxiloak dituzten molekulen (poliesterreko edo polieterreko poliolak, batez ere) arteko poliadizio-erreakzio baten bidez osatutako konposatuak dira. Hidroxilo talde baten eta isozianato talde baten arteko adizio-erreakzioak uretano talde bat sortzen du I.4. Irudian azaltzen den bezala. Beraz, poliolen, kate-hedatzaileen eta diisozianato-molekulen arteko kondentsazio-erreakzioaren bidez, PUak sorrarazten dituen lotura uretano errepikakor bat sortzen da [32]. Erreakzioan beste konposatu batzuk ere erabil daitezke, hala nola katalizatzaileak, baita beste gehigarri batzuk ere, emultsionatzaileak, egonkortzaileak, pigmentuak, kargak eta plastifikatzaileak besteak beste.

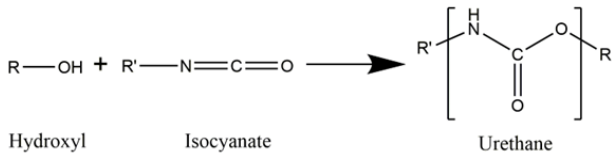


I.4. Irudia. Uretano taldeak sortzeko hidroxilo eta isozianato taldeen arteko adizio-erreakzioa

Poliola, isozianatoa eta kate-hedagailua lotura kobalenteen bidez lotzen dira, polimeroaren funtsezko egitura osatzen duen eta lotura uretanoen unitate errepikakorrak dituen kate nagusi bat osatzeko [33] (I.5. Irudia).

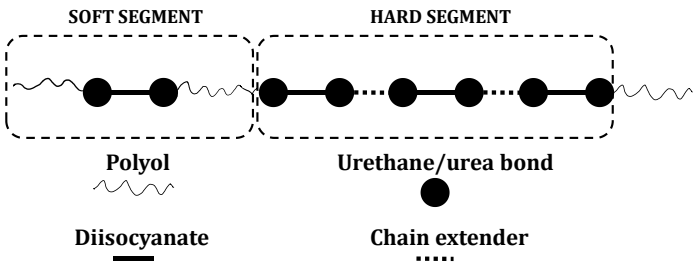


I.5. Irudia. PUaren egitura primarioa

Poliolak PUren segmentu malgua (*Soft Segment* SS) izeneko egitura osatzen duen bitartean, isozianatoak eta kate-hedagailuak segmentu zurruna (*Hard Segment* HS) osatzen dute (I.6. Irudia). SS eta HSren arteko bateraezintasun termodinamikoa dela eta, fase-bereizketa bat sortzen da PUaren egituran, bloke biguna (*Soft Block* SB) eta bloke zurruna (*Hard Block* HB) deritzon mikrodomeinuak sortuz [34]. Lehenengoak malgutasuna ematen dio estrukturari, eta bigarrenak, berriz, zurruntasuna [35].

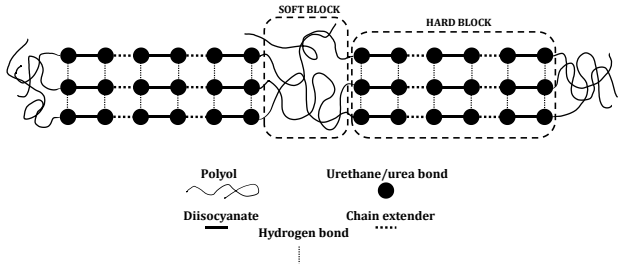


I.6. Irudia. HS eta SS osatutako PUen egitura sekundarioa

Poliola, isozianatoa eta kate-hedagailua nola elkartzen diren, erabilitako sintesi-metodoaren arabera kontrola daiteke. Poliuretanoak, nagusiki, "one-shot" metodoa eta bi etapako edo prepolimeroaren metodoa deituriko bi prozesuen bidez sintetizatzen dira [36].

- "One-shot" metodoa

  Metodo honen bidez osagai guztiak aldi berean nahasten dira. Horrela, isozianatoa aske da sistemako edozein osagaiarekin

erreakzionatzeko zorizko luzerako HBak eratuz, eta, beraz, oso tamaina aldakorreko domeinuak lortuz [37]. I.7. Irudian metodo honen bidez sintetizatutako PU baten egitura molekularraren eskema irudikatzen da.

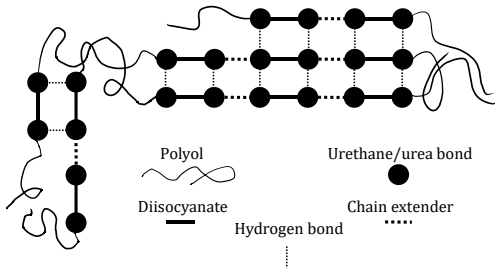


I.7. Irudia. "One-shot" metodoaren bidez sintetizatutako PU baten egitura molekularraren eskema

❖ Prepolimeroaren metodoa

Prepolimeroaren metodoa, funtsean, bi etapako metodo bat da. Lehen urratsean, isozianato taldeak poliolarekin guztiz edo partzialki erreakzionatzen du, kateen muturretan NCO kontzentrazio txikia duen prepolimero bat sortzeko. Bigarren etapan, prepolimeroa kate-hedagailu batekin erreakzionarazten da, kateetako NCO terminal taldeek erreakzionatu ahal izan dezaten. Horrela, tamaina txikiko eta uniformeagoak diren HS blokeak sortzen dira "one-shot" metodoarekin eratzen direnekin alderatuta, eta horrek propietate mekanikoak hobetzen ditu [37]. Oro har, bi etapako metodo honen bidez sortzen diren HSak bi isozianato-unitate eta kate-hedagailu unitate batez osatuta daude. Prepolimeroaren metodoaren bidez sintetizatutako PU baten egitura molekularra I.8. Irudian agertzen den eskeman irudikatzen da.

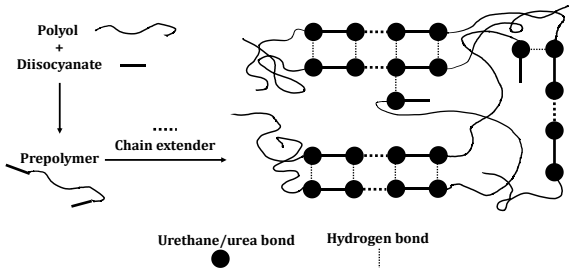


I.8. Prepolimeroaren metodoaren bidez sintetizatutako PU baten egitura molekularraren eskema

### 1.3.1. Poliolak

Lehen esan bezala, PUen industria garrantzi handikoa da gaur egun. Horregatik, poliolak PUen funtsezko osagaietako bat direla kontuan hartuta, haien merkatua ere oso garrantzitsua da. Izan ere, 2019an polioleen industriek 26200 miloi dolar inguru sortu zituen, eta 2024 urterako 34400 milioira arte haztea espero da [39]. Poliolak, petrolioaren deribatuak izan ohi diren eta gutxienez bi talde hidroxilo edo amina dituzten substantzia kimiko bezala definitzen diren konposatuak dira [40].

Poliolak pisu molekularraren arabera bi kategoria nagusietan sailka daitezke: pisu molekular baxuko edo poliol monomerikoak eta pisu molekular handiko edo poliol polimerikoak (oligopoliol). Poliol monomerikoak kate-hedagailu gisa erabili daitezke diol bat denean, edo agente saregile gisa bi hidroxilo talde baino gehiago dituenean (trioleak, tetraolak, etab. ) [41].

Poliol polimerikoak berriz, 10000 g/mol arteko pisu molekularra duten polimeroak izan ohi dira, gehienez 8 hidroxilo talde dituztenak [42] eta bi kategoria nagusitan azpisailka daitezke, polieter eta poliester polioletan, alegia. Azken aplikazioaren arabera, hobe da poliol polieter edo poliester bat. Adibidez, lehenengoek kate-malgutasun handiagoa eta sakabanagarritasun

hobea eskaintzen dute ingurune urtarretan, baina erresistentzia txikiagoa dute argiaren eta zahartzearen aurrean, poliesterrezko poliolekin alderatuz gero.

### 1.3.2. Isozianatoak

Isozianatoak oro har amina primario baten fosgenazio erreakzioaren bidez sortzen dira, I.1. Ekuazioan adierazten den bezala.

$$R - NH_2 + COCl_2 \rightarrow R - NCO + 2HCl \qquad \text{I.1. Ekuazioa}$$

Isozianatoak aromatiko eta alifatiko gisa sailka daitezke beren egituraren arabera; horien artean, aromatikoak dira PUak ekoizteko gehien erabiltzen direnak, erreaktibioagoak eta arrisku gutxiagokoak baitira [36]. Hauen artean, Tolueno diisozianatoa (TDI) eta 4,4'-Difenilmetano diisozianatoa (MDI) dira erabilienak; hara ere, biak kantzerigeno, mutageniko eta reprotoxiko gisa sailkatua daude PUko industriak langileen osasunerako osa arriskutsuak izanik [43]. Diisozianato aromatikoetan oinarritutako PUek portaera termiko eta mekaniko ona dute; baina, oxidazio baxua edo ultramoreen aurrean egonkortasuna ona izateko, diisozianato alifatikoak erabiltzea komenigarria da [36].

### 1.3.3. Poliuretano motak

PUek hainbat modutara sailka daitezkeen produktu-aukera zabala eskaintzen dute. Karak (2017)-ek [36] eta Akindoyo et al., (2016)-ek [33] dioten bezala, sailkapen hori, I.1. Taulan ikus daitekeen bezala, egitura, portaera termiko, jatorria eta aplikazioa kontutan hartuta egin daiteke.

I.1. Taula. PU mota nagusiak irizpide desberdinen arabera

| *PU classification* | | | |
|---|---|---|---|
| Structure | Origin | Thermal behaviour | Product application |
| Linear | Synthetic | Thermoplastic | Foams<br>Fibres |
| Branch-chained<br>Crosslinked | Bio-sourced | Thermosetting | CASE (coatings, adhesives, sealants and elastomers)<br>Smart materials (ionomers) |

### 1.3.3.1. Poliuretano-itsasgarriak

Itsasgarri bat, bi gainazaletan aplikatzen denean, biak lotura itsaskor iraunkor baten biez lotzeko gai den material bat da [44]. Hezurrak, larruak, arrainak, esnea eta landareak bezalako produktu naturaletatik eratorritako itsasgarriak milaka urteetan zehar erabili dira. Hala ere, itsasgarri sintetikoak ez ziren industrialki erabiltzen hasi 40ko hamarkadaren erdialdera arte, eta geroztik haien erabilera izugarri handitu da. Hain da aplikagarria hainbat industria-eremutan, zaila baita itsasgarririk ez duen produktu bat aurkitzea [45].

Industrian eskuragarri dauden itsasgarrien artean, hala nola epoxiak, akrilikoak, poliamidak, silikonak, polisulfuroak, urea, melamina eta fenol-formaldehidoak [46], PU itsasgarriak dira moldakorrenak eta errendimendu handienekoak zizailuarekiko eta trakzioarekiko erresistentzia handia dutelako. Izan ere, gainazalak hezetzeko, hainbat substratutan hidrogeno-zubiak eratzeko eta hidrogeno atomo aktibo edo talde funtzionalak dituzten substratuekin lotura kobalenteak eratzeko gaitasuna dute [36,47]. Bestalde, PU itsasgarriek ingurumen-arazo eta osasun-arazo gutxiago eragiten dituzte itsasgarri arruntekin alderatuta, urea, melamina eta fenol-formaldehidoa

kasu, PU itsasgarriek ez baitute konposatu organiko lurrunkorrak igortzen PUaren bizitza erabilgarrian zehar [48]. Hori gutxi el balitz, erresistentzia handiagoa izateaz eta konposatu organiko lurrunkorrik ez isurtzeaz gain, PU itsasgarriek prentsaketa-denbora laburragoak behar izaten dituzte, malguak izaten dira eta hainbat substratu itsasteko gai dira, hala nola, egurra, metala, beira, plastikoa, kautxua, zeramika eta ehun-zuntza [49]. Hala ere, kontuan izan behar da PUen propietateak sintesian erabiltzen diren isozianatoaren eta poliolaren izaeraren araberakoak direla. PU itsasgarriak osagai bateko sistemetan edo bi osagaiko sistemetan sailka daitezke, formulazioan dauden faseen arabera eta oso erabiliak dira zuraren ingeniaritzako produktuetan duten propietateak direla eta.

### 1.3.4. Poliuretanoen sintesirako alternatiba ekologikoagoak

Esan bezala, PUak ekoizteko beharrezkoak diren produktu kimikoak industria petrokimikotik lortzen ohi dira. Beraz, PUaren industriak ingurumenean duen eragina konpondu beharreko arazoa da, gero eta murriztaileagoak diren araudiak bete nahi badute. Erronka horri aurre egiteko, PUaren industriak bi jarduera-bide har ditzake. Lehenengoa ingurumenerako oso kaltegarria den isozianatoa erabiltzear uztea da, isozianatorik gabeko poliuretanoak (*non isocyanate polyurethane* NIPU) sintetizatuz.

NIPUak sintetizatzeko lau modu diferente daude I.9. Irudian agertzen den bezala. Horien artean, ingurumenaren ikuspegitik, karbonato ziklikoen eta poliaminen arteko poliadizio-erreakzioa egokiena da. Hala ere, polikondentsazio erreakzioetan dimetil karbonatoa (DMC) erabiltzea ere estrategia ona izan daiteke, DMCa glizeroletik lor daitekeelako fosgenaziorik behar ez duten hainbat prozesuren bidez, eta, gainera ingurumenarentzat berdea kontsideratzen den agente karboximetilante ez-ziklikotzat hartzen da [50]. Izan ere, Enichem CO. (Italia), 1970ean, metanolaren karbonilazio

oxidatibotik abiatuta eta katalizatzaile metaliko bat erabiliz DMC-a sintetizatu zuenetik, hau, besteak beste, estaduren, itsasgarrien eta aerosolen formulazioetarako oso erabilia den disolbatzaile bihurtu da [51].

Jarraitu daitekeen bigarren estrategia petroliotik eratorritako poliolak, isozianatoak eta kate-hedagailuen ordez jatorri biologikoko beste batzuk erabiltzean datza. Izan ere, azken hamarkadetan konposatu hauek biomasatik lortzeko aukera aztertzen ari da, landare-olioak [52], gantz-azidoak [53,54], gantz-azidoen ester metilikoa (*fatty acid* methyl esther FAME) [55,56], glizerol gordina [57] eta biomasa lignozelulosikotik eratorritako konposatuak [58] gehien aztertutako lehengaiak izanik.

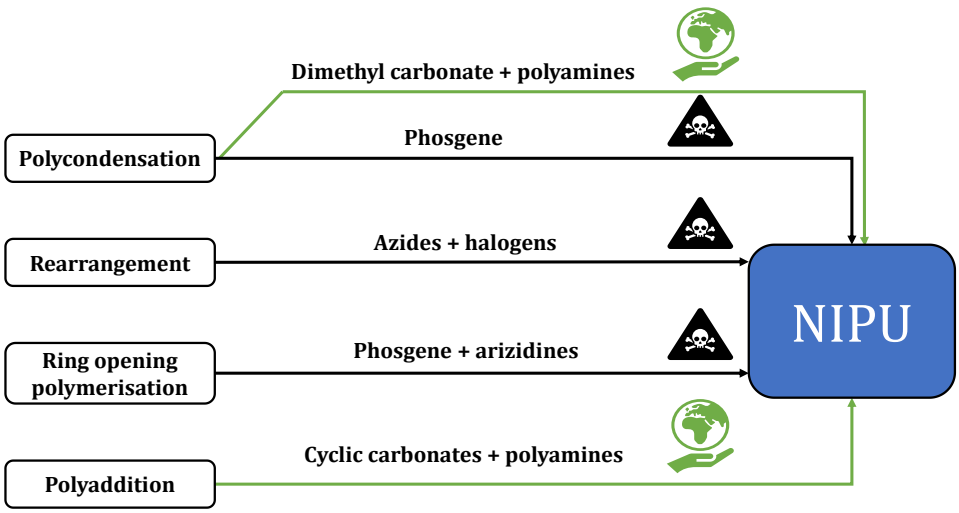


I.9. Irudia. NIPUak sintetizatzeko prozesu ezberdinak

## 1.4. Etorkizun berdeagoaren aldeko biofindegiak

EBa asmo handiko prozesu batean murgilduta dago etorkizun jasangarriago bat eraikitzeko, hainbat estrategia garatuz, hala nola Europako Itun Berdea, EBn berotegi-efektuko gasen emisioak (*greenhouse gas emissions* GHG) % 55a murriztu nahi dituena 2030erako , eta zero isuri garbira 2050erako, Ekonomia Zirkularreko Ekintza Plana, Biodibertsitate Estrategia eta

"baserritik mahaira" estrategia. EBk proposatzen duen etorkizun honetan, biofindegiek zeregin garrantzitsua dute ezarritako helburuak betezen laguntzeko.

### 1.4.1. Biofindegiak eta biomasa

#### 1.4.1.1. Biofindegia

Biofindegiaren kontzeptua petrolioaren ohiko finketaren kontzeptuaren antzekoa da, baina petrolio gordina lehengai gisa erabili beharrean, hainbat biomasa mota erabiltzen dira, likido, solido edo gas moduan. Beraz, biofindegia ekonomiaren, ingurumenaren eta gizartearen aldetik onuragarriak diren eta biomasa merkaturatu daitezkeen bioproduktu bihurtzeko erabiltzen diren prozesuen multzo gisa definitu daiteke. Bioproduktu horien artean elikagaien eta pentsuen koprodukzioa, produktu kimikoen, materialen eta bionergiaren ekoizpena daude, besteak beste [59]. Biofindegiak sailkatzeko era desberdinak daude, hala nola integrazio-maila, eraldaketa prozesuaren eta erabilitako biomasaren arabera sailka daitzeke [60–62] I.10. Irudian erakusten den bezela.

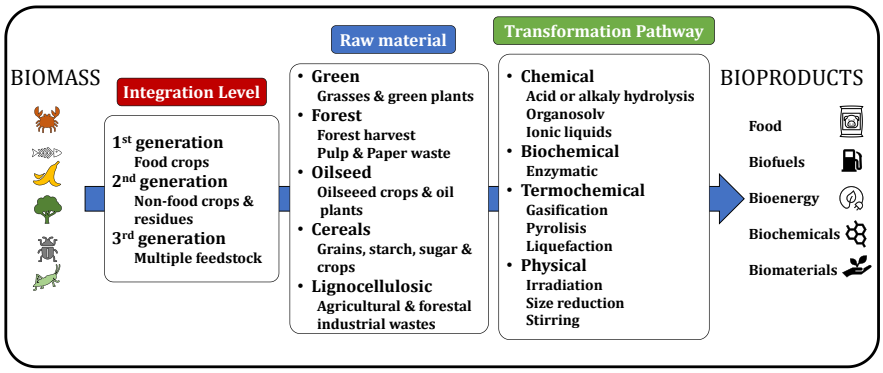


I.10. Irudia. Biofindegi baten sailkapen-diagrama

Lehen eta bigarren belaunaldiko biofindegiek lehengai mota bakarra erabiltzen dute prozesuan. Hala ere, lehen belaunaldiko biofindegiak azukre

edo olio ugariko lehengaiak soilik bioerregaiak ekoizteko erabiltzen dituzten bitartean, bigarren belaunaldikoek iturri desberdinetako lehengaiak erabil ditzakete produktu ugari ekoizteko. Gainera, nabarmendu behar da lehen belaunaldiko biofindegiek elikagai-laboreak erabili ohi dituztela elikagai horien prezioak handituz; bigarren belaunaldikoek, berriz, arazo hori saihesten dute, ez baitute elikagai-laborerik erabiltzen. Azkenik, hirugarren belaunaldiko biofindegiak teknologikoki aurreratuagoak dira eta ia edozein hondakin organiko erabil dezakete hainbat teknologia erabiliz produktu-sorta handi bat lortzeko.

#### 1.4.1.2. Biomasa

Biomasaren hainbat definizio daude, eta horietatik, agian, honako hau da onartuena: “Biomasa materia organikotik eta biologikoki sortzen diren produktu energetiko berriztagarrien eta lehengaien multzoa da”. Aipatzekoa da definizio horrek kanpoan uzten dituela biologikoki sortutako konposatu batzuk, hala nola ikatza, petrolioa edo gasa. Beraz, hondakin-produktuen eta nekazaritzako, akuikulturako, basogintzako eta horiekin lotutako industrietako hondakinen frakzio biodegradagarri guztiak, bai eta industria- eta udal-hondakinen frakzio biodegradagarriak ere, biomasatzat hartzen dira, biomasa lignozelulosikoa barne. Ondorioz, biomasa bioerregaiak, materialak eta erantsi handiko produktu kimikoak ekoizteko ahalmen handia duen baliabide berriztagarri ugarienetako bat da.

## 1.5. Biomasa lignozelulosikoa

Biomasa lignozelulosikoa baliabide berriztagarri nagusietako bat da; izan ere, lehengai ugaria, merkea eta ingurumena errespetatzen duena baita; gainera, oso produktu interesgarriak ekoizteko potentzial handiko baliabidea da, hala nola bioerregaiak, konposatu kimikoak eta materialak [63,64].

Biomasa lignozelulosikoa, batez ere zelulosaz, hemizelulosaz eta ligninaz osatutako material konposatu natural konplexu bat bezala definitu daiteke, landare zelula-hormen barruan sare konplexu gisa banatzen direnak (I.11. Irudia) [66].

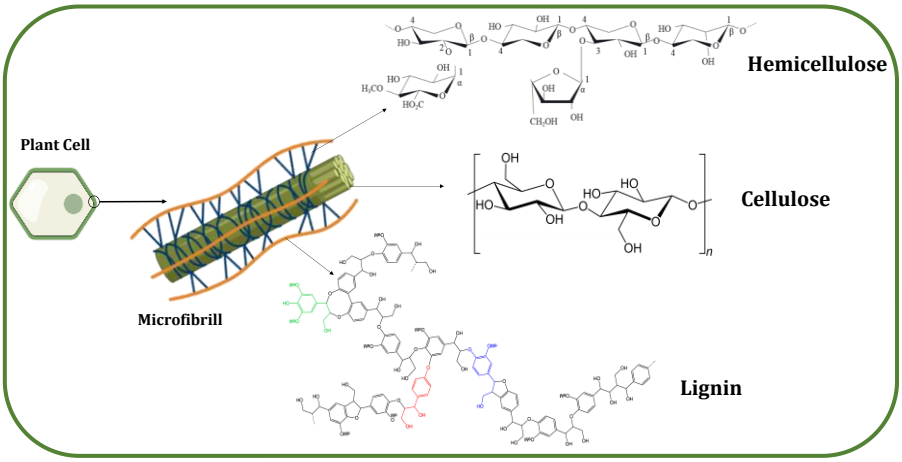


I.11. Landare-horma zelularraren egiturazko osagaien irudikapena

Hiru osagai hauen konposizioa nabarmen alda daiteke lehengaiaren eta ingurumen-faktoreen arabera [67], baita egiturazkoak ez diren beste konposatuenak ere [68] (proteina, pektinak, estraktu eta errautsak) I.2. Taulan adierazten den bezala.

I.2. Taula. Biomasa lignozelulosiko mota ezberdinen konposizio kimikoa ([67]-tik egokitua)

| Lehengaia | Zelulosa (%) | Hemizelulosa (%) | Lignina (%) |
|---|---|---|---|
| Zur gogorra | 45-55 | 24-40 | 18-25 |
| Zur biguna | 45-50 | 25-35 | 25-35 |
| Belarra | 25-40 | 25-50 | 10-30 |

### 1.5.1. Zelulosa

Zelulosa Lurreko biopolimero berriztagarri ugariena da, eta biomasa lignozelulosikoaren osagai nagusia da honen guztizko pisuaren %30-50a inguru hartzen baitu [69].

Zelulosa, zelula-horman, honela paketatzen da: oinarrizko unitatea, β-D-glukopiranosa, elkarren artean katigatuta agertzen da β-1-4 lotura glikosikikoen bitartez zuntz izeneko egitura linealak osatuz [70]. Zuntzak elkarrekin lotzen dira β-D-glukopiranosa unitateko hidroxilo-taldeen artean zortzen diren hidrogeno-zubien bidez, eremu kristalinoetan eta amorfoetan antolatzen diren makrofibrak sortuz [71]. Azkenik, makrofibrak egiturazko beste osagai batzuekin paketatzen dira horma zelularra sortzeko.

Zelulosa, hainbat aplikaziotan erabiltzeko material bikaina bihurtzen duten zenbait propietate desiragarriak ditu, besteak beste, hidrofilia, kiralitate, biodegradagarritasuna eta beste talde funtzionalekin loturak eratzeko erraztasuna. Propietate hauei esker, zelulosa hidrogelen aerogelen, filmen eta mintzen sintesian erabiltzen da, besteak beste [72].

### 1.5.2. Hemizelulosa

Hemizelulosak, landareen zelula paretetan aurkitzen den eta hainbat egitura-unitateez (xiloglukanoz, xilanoz, mananoz, glukomananoz eta β-(1,3 eta 1,4)-glukanoz) osatuta egon daitezkeen polisakarido amorfo adarkatu gisa defini daitezkeen konposatuak dira [73]. Hemizelulosak biomasa lignozelulosikoaren guztizko pisuaren %20-35 dira [74], eta zelulosa- eta lignina-frakzioen arteko aglutinatzaile gisa jarduten dute, biomasaren matrizeari zurruntasuna gehituz [75]. Zelula-paretaren egiturazko beste osagaien aplikagarritasunarekin alderatura, hemizelulosek erabilera mugatuagoa dute; hala ere, elikagaien industriarako (oligosakaridoak) eta

kimika-industriarako (azido organikoak) balio erantsi handiko produktuak ekoizteko ahalmen handia erakutsi dute.

### 1.5.3. Lignina

Lignina, zelulosaren ondoren, lurreko bigarren biopolimero ugariena da, gainera jatorri berriztagarriko biopolimero fenolikorik ugariena [76]. Biomasa lignozelulosiko pisuaren %15tik %40ra arte osa dezake, eta zelulosa eta hemizelulosak mikrobioen degradaziotik babesten ditu eta landareen zelula-hormei erresistentzia eta hidrofobotasuna ematen die [77]. Tamalez, ligninaren jatorrizko egitura ez da guztiz ezaguna, ezin baita hau aldatu gabe isolatu [78]. Izan ere, lignina isolatzeko metodo desberdin asko daude, bakoitzak bere ezaugarri eta berezitasunekin, lignina mota diferenteak ematen dituztenak.

Mundu mailan lignina ekoizle nagusia pasta eta paperaren industria da, ekoiztutako lignina guztiaren %97ko produkzioarekin, hoietatik %88a lignosulfonatoak eta %9 lignina kraft izanik [79]. Bi lignina mota hauek %1,5 eta %5 arteko sufre-pisua dute, eta balio erantsi txikiko aplikazioetarako erabiltzen dira, adibidez beroa eta elektrizitatea sortzeko [80]. Hala ere, badira sufrea erabiltzen ez duten beste prozesu batzuk, prozesu alkalinoak, organosolv prozesuak, lurrun-leherketa, hidrolisi azido diluitua edo berriago diren beste prozesu batzuk non likido ionikoak edo disolbatzaile eutektiko sakonak erabiltzen diren deslignifikazio prozesua egiteko esate baterako [81–86]. Metodo horien bidez lortutako ligninek lignosulfonatoak edo Kraft lignina baino purutasun eta propietate egokiagoak dituzte balio erantsi handiko aplikazioetan balorizatu ahal izateko.

Deslignifikazio-metodoaren eta erabilitako lehengaiaren arabera lignina mota desberdinak egon arren, lignina, fenilpropanozko hiru unitate diferenteen polimerizazioaz (alkohol p-kumarilikoa, alkohol koniferilikoa

eta alkohol sinapilikoa) eratutako hiru dimentsioko egitura irregular retikulatua duen polimeroa dela ondo onartua dago (I.12. Irudia).

Alkohol aromatiko horietatik abiatuta, p-hidroxi fenil (H), guaiazilo (G) eta siringilo (S) izeneko unitate polimeriko fenolikoak sintetizatzen dira (I.13. Irudia) [88,89]. Fenil-unitate hauek proportzio desberdinean agertzen dira landare-espeziearen arabera. Horrela, koniferoetatik eratorritako ligninek alkohol koniferilikoa du gehienbat, %90-95% inguruan, hostozabaletatik eratorritako ligninak, berriz, %25-50 alkohol koniferilikoz eta %50-75 alkohol sinapilikoz daude osatuta; eta gramineo jatorria duten ligninak hiru alkohol monomerikoez osatuta daude [90,91].

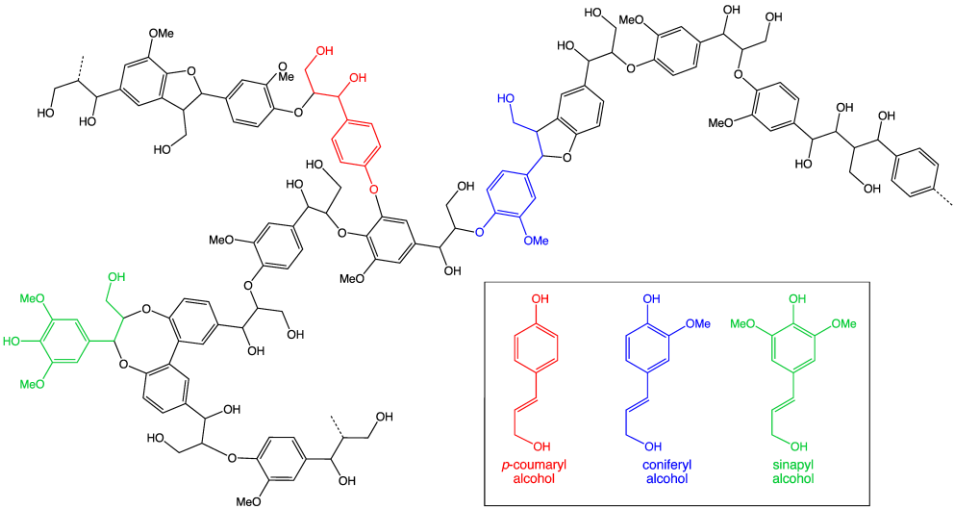


I.12. Lignina molekularen eta sintetizatzeko beharrezkoak diren alkohol aromatikoen egitura ([87]-tik egokitua)

H, G eta S unitate fenolikoak elkarren artean lotuta daude lehengaiaren arabera aldakor diren lotura eterren bidez, β-O-4, α-O-4 eta 4-O-5, eta karbono-karbono, 5-5, β-5, β-1 eta β-β, loturen bidez [92]. Hala eta guztiz ere, lotura ohikoena β-O-4 lotura da, %43tik %65era alda daitekeena [93].

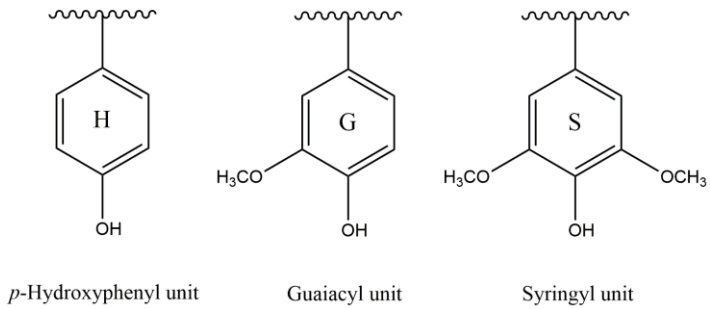


I.13. Irudia. Lignina-unitate fenolikoak

Ligninak, molekularen erreaktibotasunean eragiten duten eta erabilitako lehengaiaren eta erauzketa-metodoaren arabera proportzio aldakorra duten talde funtzional desberdinak ditu, hauen artean, hidroxilo fenolikoak eta alifatikoak, karbonilo, metoxi eta karboxilo taldeak. I.3. Taulan, lignina molekularen talde funtzional nagusien ehunekoa agertzen da.

I.3. Taula. Ligninaren talde funtzional desberdinen ehunekoa (% wt.) [95]

| Talde funtzionalak | Ehunekoa (%wt.) |
|---|---|
| Metoxi | 8,7-19,3 |
| Hidroxilo fenolikoa | 2,2-4,5 |
| Hidroxilo alifatikoa | 3,1-10,1 |
| Karboxilo | 2,9-7,1 |
| Karbonilo | 2,1-4,5 |

Lignina molekularen egitura kimikoari eta duen funtzionalitate handiari esker, lignina oso konposatu interesgarria da bio oinarritutako material berriak garatzeko, hala nola, karbono-zuntzak, mintzak, hidrogelak, poliolak, eta hainbat erregai eta produktu kimiko ezberdinak [96]. Gainera, lehen esan bezala, duen talde hidroxilo fenoliko eta alifatiko kontzentrazio handiari esker, lignina oso lehengai interesgarri bihurtu da poliuretanoak sintetizatzeko [29]. Hala ere, egituraren konplexutasuna, errepikagarritasun ezak, eta beharrezkoa den garapen teknologikorik ezak, ligninaren aplikazio teknikoa zailtzen dute [80].

## 1.6. Ligninan oinarritutako poliuretanoak

Biomasa lignozelulosikoa lehengai oso interesgarria da PUak sintetizatzeko beharrezkoak diren eta petroliotik eratorritako osagaiak erabat edo partzialki ordezkatzeko [49]. Biomasa lignozelulosikoa osatzen duten osagai guztien artean, lignina da, bere izaera fenolikoagatik eta duen funtzionaltasun altuagatik, PU industriarako aukera interesgarriena. Izan ere, hainbat estrategia erabil daitezke PUak sintetizatzeko lignina erabiliz. Adibidez, modifikaziorik gabe karga gisa erabil daiteke PUak formulatzeko [97], PUen aitzindari izan daitezkeen ligninan oinarritutako isozianatoak [98], karbonato ziklikoak [99] edo poliaminak [100] sintetizatzeko ere erabil daiteke lignina modifikatuz, edo NIPUak [101] edo poliolak [39] sintetizatzeko ere. Horietatik, agian, poliolen eta NIPUen sintesia dira lignina PU industrian erabiltzeko estrategiarik esperantzagarrienak.

### 1.6.1. Ligninan oinarritutako poliolak

Lignina molekularen ezaugarri paregabeek industriarako baliagarriak diren jatorri biologikoko poliolak sintetizatzeko baliabide aparta bihurtzen dute [39]. Zoritxarrez, ezaugarri berezi horiek berak dira lignina molekularen erreaktibotasun baxuaren erantzuleak [102]. Ezbehar hori gainditzeko, hainbat estrategia garatu dira, betiere molekularen erreaktibotasuna areagotzeko helburuarekin. Prozesu hauek hiru familia handitan sailka daitezke: ligninaren despolimerizazioa, ligninaren aldakuntza gune kimiko aktibo berriak sortuz eta hidroxilo taldeen funtzionalizazioa [103]. Hiru estrategia horietan bildutako teknika guztien artean, biopolioleen sintesia, lignina alkohol polihidrikoekin likidotuz, izan da interes gehien piztu duenetako bat [103,104].

#### 1.6.1.1. Likidotze prozesua

Likidotzea bihurketa termokimikoko teknologia bat da, zeinean biomasa fase likido baten aurrean eta beroa aplikatuz, 200 eta 400 °C bitarteko tenperaturetan, zati molekular txikietara degradatzen den [73]. Likidotze erreakzioa egiteko erabiltzen den disolbatzailearen arabera prozesua bi multzo nagusitan sailka daiteke: likidotze prozesu hidrotermikoa (*hydrothermal liquefaction* HTL) eta likidotze prozesu solbotermikoa (*solvothermal liquefaction* STL) [105]. Lehenengoan disolbatzaile nagusia ura da; STL prozesuan, berriz, disolbatzaile ez-urtsu desberdinak erabil daitezke, hala nola fenola, tetralin γ-balerolactona edo PEG edo glizerola bezalako alkohol polihidrikoak [106,107]. Azken prozesu hori, alkohol polihidrikoen bidezko likidotzea, PUak ekoizteko ligninan oinarritutako poliolak sintetizatzeko prozesurik erabiliena da. Normalean, lignina likidotzeko erreakzioetan erabiltzen diren disolbatzaile erabilienak PEG, glizerola edo 1,4-butanodiola dira. Erreakzioa burutzeko katalizatzaile azidoak zein basikoak erabil daitezke [104,107]; hala ere, katalizadore azidoak erabiltzen diren prozesuetan basikoak erabiltzen diren prozesuetan baino tenperatura baxuagoak behar direnez gehien erabiltzen diren katalizadoreak azidoak dira, non azido sulfurikoa katalizatzaile erabiliena den [108]. Ligninaren likidotze-erreakzioetan, solido/likido erlazioak, erabilitako disolbatzaile mota, katalizatzailearen kontzentrazioak eta erabilitako baldintzek (tenperatura eta denbora) eragin handia dute sintetizatutako poliolaren azken propietateetan, hidroxilo eta azido kopuruan adibidez [109].

STL prozesuaren bidez lignina likidotzeko erreakzioa erreaktore atmosferikoak erabiliz egin ohi da, tenperatura altuak (240 °C) eta erreakzio-denbora luzeak (3 h) erabiliz [110]. Hala ere, erreakzio-baldintza horiek berberek erreakzioaren errendimendua gutxitzea eragin dezakete[111]. Horregatik, mikrouhin bidezko irradiazio-teknologia alternatiba gisa proposatu da [112], beroketa prozesua azkarragoa eta homogeneoagoa

delako, eta erreakzio-denbora minutu batzuetara murrizten delako [104,108,113,114].

### 1.6.1.2. Glizerol gordina likidotze-prozesuetan

Lehen aipatu den bezala, ligninaren likidotze-prozesuan erabiltzen den glizerola jatorri petrokimikokoa izan ohi da; hala ere, badago aukera jasangarriago bat: biodieselaren industriatik datorrena, glizerol gordina. Izan ere, 2009 eta 2019 artean, Europako biodieselaren ekoizpena 21000 miloi tonatan handitu da (I.14. Irudia) glizerol mota honen gainprodukzioa sorraraziz, hamar tona biodiesel bakoitzeko tona bat glizerol gordin sortzen baita azpiproduktu gisa. Behin purifikatua, glizerol gordina hainbat industria desberdinetan erabil daiteke, elikagai, farmazia eta kosmetika industrietan besteak beste [115].

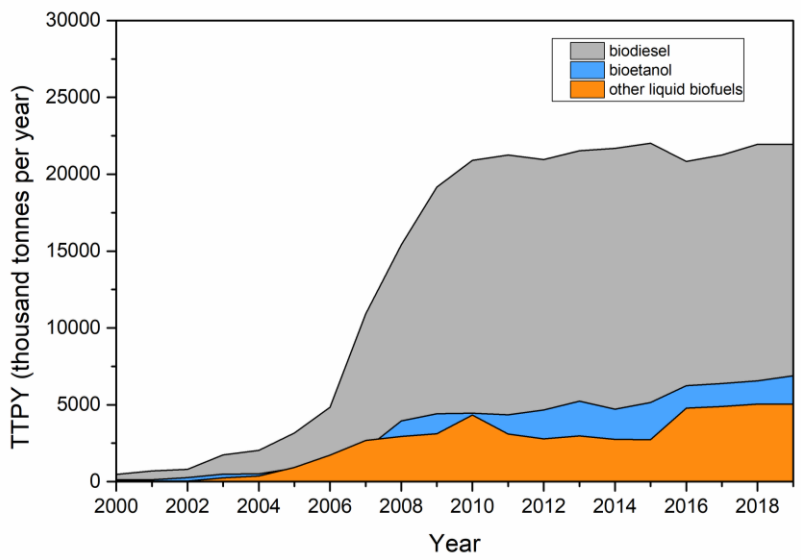


I.14. Irudia. Bioerregai likidoak ekoizteko gaitasuna Europan 2000 eta 2109 artean. Datuak [116]-tik lortuak

Glizerol gordinaren gainprodukzioaren ondorioz, fintzea ez da ekonomikoki errentagarria. Honezkero, industrialki onesteko erabilera bat bilatzea

ezinbestekoa da. Aplikazio posible bat ligninan oinarritutako likidotze bidezko poliolen ekoizpenean disolbatzaile gisa erabiltzea izango litzateke [104,118–121].

### 1.6.2. Lignina oinarritutako isozianato gabeko poliuretanoak

Lignina eta honen deribatu batzuk aintzindari bezala eta poliadizio-erreakzioa erabiliz hainbat termoplastiko eta termoegonkor diren NIPUak sintetizatzeko erabili dira, eta hauen artean gehien ikertu direnak termoegonkorrak dira. Modu honetan Sternberg eta Pilla (2020)-k [122] isozianato gabeko eta oinarri biologiko, forma-memoria eta propietate termiko eta mekaniko onak zituen apar bat sintetizatu zuten ligninaz formulatutako karbonato zikliko bat diamina batekin erreakzionaraziz.

Beste lan batean, soda ligninatik eratorritako karbonato zikliko bat erabili zen erretxina termoegonkor bat prestatzeko poli(etilenglikol)bis karbonato ziklikoa eta diamina batekin erreakzionatuz [123]. Arto-buruaren hidrolisi entzimatikotik eratorritako lignina beste ikerketa batean erabili zen propietate mekaniko eta termiko bikainak, birprozegarritasun eta birziklagarritasun handia, forma-memoria eta autokurazio-propietateak eta hainbat aplikaziotan erabil zitekeen konposatu termoplastiko bat ekoizteko [124]. Lignosulfonatoak NIPUak sintetizatzeko ere erabil daitezke, nahiz eta aplikazio-eremua ezberdina izan daitek lignina kraften eta lignina organosolven aplikazio-eremuei. Lignosulfonatoen propietate bereziengatik gertatzen da hori [125]. Bestalde, azido ferulikoa, siringaresinola eta kreosola bezalako ligninaren deribatu batzuk ere erabil daitezke NIPUak sintetizatzeko. Menard et al., (2017) [126] gai izan ziren hainbat NIPU sintetizatzeko azido ferulikoa karbonato ziklikoen aitzindari gisa erabiliz, eta horiek hainbat aminarekin erreakzionatuz material termoplastiko eta termoegonkor diferenteak sortu zituzten. Modu berean, beste ikerketa batean, baina karbonato ziklikoen aintzindari gisa siringaresinol eta amina

ezberdinak erabiliz, konposatu termoplastiko eta termoegonkorrak sintetizatu ziren [127]. Beste lan batean, kreosolean oinarritutako bis(karbonato zikliko) bat erabili zen amorfo edukiera handiko NIPUak sintetizatzeko [128].

## 1.7. Ligninan oinarritutako Poliuretanozko itsasgarriak

Lignina PU itsasgarri batean poliol gisa txertatzeak polimeroaren azken eduki aromatikoa hobetzen du, eta trantsizio-tenperatura eta itsasgarriaren egonkortasun termikoa handitzen ditu; izan ere, lignina egonkor mantentzen da tenperatura altuetan eta termoegonkor gisa jokatzen du [129]. Gainera, lignina segmentu bigun bezala erabiltzen den arren, normalean sare formatzaile bezala jarduten du, eta bere egitura aromatikoak segmentu zurrun bezala jokatzen du itsasgarrien erresistentzia mekanikoa hobetuz [49]. Hala ere, ligninaren egitura aromatikoa dela eta, PUaren HSaren eta SSaren arteko faseen bereizketa handitzen du, eta horrek PU itsasgarrien propietate mekanikoak okerrera egin ditzake [130]. Beraz, beharrezkoa da isozianatoaren eta ligninaren arteko proportzio egokia aurkitzea, faseak behar bezala bereizteko.

Azpimarratzekoa da PUen itsasgarriak sintetizatzeko erabiltzen den lignina eraldatu eta eraldatu gabe erabil daitekeela. Lehenengo kasua lignina PUzko itsasgarrien formulazioan txertatzeko soluziorik errazena da. Alabaina, kasu gehienetan, lignina tetrahidrofurano (THF) bezalako disolbatzaile organiko batekin disolbatu behar da [131]. Gainera, ligninak polimeroari eman diezaiokeen gehiegizko zurruntasuna dela eta, askotan eraldatu gabeko lignina PEG, errizino olioa eta glizerola bezalako beste poliol batzuekin erabiltzen da [97]. Bigarren metodoan, lignina eraldatu egiten da bere erreaktibotasuna eta gainerako osagaietan duen sakabanaketa hobetzeko. Esate baterako, Chen et al., (2020) [132] lignina molekularen erreaktibotasuna handitu zuten metoxi taldeak desmetilazio-prozesu baten

bidez erreaktibioagoak diren hidroxilo fenolikoetan bihurtuz. Bigarren metodo honetan ere beste poliol batzuk erabiltzen dira ligninaren txertaketaren ondoriozko hauskortasuna murrizteko eta PU itsasgarrien harikortasuna handitzeko [133].

Azkenik, ligninak PUzko itsasgarrien formulazioetan duen eraginari dagokionez, propietate termikoen [134,135] zein mekanikoen [136] hobekuntza handia nabarmendu behar da. Gainera PUzko itsasgarrietan lignina gehituz, hainbat substraturekiko atxikipen-maila handia lortzen da, PU itsasgarriena baino handiago ere izan daitekeena [137]. Lignina eraldatuta edo eraldatu gabe erabiltzen den alde batera utzita, PUzko itsasgarriak, oro har, toxiko diren MDI eta TDI bezalako diisozianatoak erabiliz sintetizatzen dira [130].

Ingurumena gehiago errespetatzen duen eta hain toxikoa ez den alternatiba bat NIPU itsasgarriak sintetizatzean datza. Gainera, bere merkatu-nitxo potentzialetako bat egurrezko panelen industria da, non itsasgarririk erabiliena formaldehidoan oinarritutakoa den. Formaldehidoan oinarritutako itsasgarri mota hauek konposatu organiko hegazkorrak (*volatile organic compounds* VOC) izurtzen ditu manipulazio, fabrikazio eta erabileran prozesuetan [138]. Lehen aipatu den bezala, DMC disolbatzailea NIPUak eta beste material batzuk sintetizatzeko oso aproposa den konposatua da. Disolbatzaile hau gai da NIPUak sortzeko hexametilendiaminarekin (HDMA) polikondentsazio-erreakzioen bidez erreakzionarazi egiten denean. Erreakzio mota honen bidezko NIPUen sintesia oso ondo bereizitako bi urratsetan datza [139]. Lehenengo urratsean, DMCa erabiliz lignina karbonatazio-erreakzio baten bidez funtzionalizatzen da, bertan bigarren urratsean erreakzionatzen duen bitarteko bat sortzen da. Bitarteko hau, HDMA bezalako diamina batekin erreakzionarazten denean uretano lotura sortu ditzake [140].

Azken urteotan, hainbat azterlan burutu dira bio-oinarritutako NIPUak formulatzeko polikondentsazio-erreakzioen bidez. Azterlan horietan, DMC eta HDMA disolbatzaileak biomasa lignozelulosikotik eratorritako glukosarekin [50,141], humina ez-furanikoekin [142], taninoekin [141,143] eta ligninarekin [140,144] erreakzionarazi egiten dira polikondentsazio erreakzioak erabiliz hainbat NIPU material ekoizteko. Arias et al., (2022) [139] autoreek egindako azterlanaren arabera, laborategi eskalan eta bizi-zikloaren analisiaren metodologia (*life cycle analysis* LCA) ingurumen-inpaktua ebaluatzeko erraminta gisa erabilita, lignina organosolv, DMC eta HDMAren arteko polikondentsazio-erreakzioaren bidez sintetizatutako NIPU itsasgarri bat itsasgarri sintetikoen alternatiba bideragarria zela frogatu zen.

## 1.8. Tesiaren helburuak

Tesi honen helburu nagusia zuraren industrian erabil zitezkeen isozianatorekin eta isozianatorik gabeko poliuretano-itsasgarriak sintetizatzea izan zen. Horretarako bi egur mota desberdinetako ligninak erabili ziren: *Eucalyptus globulus* eta *Pinus radiata* hain zuzen ere. Lignina hauek erabiliz eta alkohol polihidrikoak disolbatzaile gisa erabiliz, biopoliolak sintetizatu ziren mikrohuin bidezko likidotze prozesu baten bidez. Hasteko, mikrouhin teknologia bidezko likidotze erreakzioa optimizatu behar izan zen poliuretanoak sintetizatzeko beharrezko propietateak zituzten biopoliolak lortzeko. Horretarako, Box Behnken diseinu esperimental bat erabili zen erantzun-gainazalaren metodologia (RSM) erabiliz. Erreakzioa optimizatu eta gero, lortutako biopoliolak poliuretano-itsasgarriak sintetizatzeko erabili ziren bi metodo desberdinen bidez. Lehenengo metodoa poliadizio-erreakzio bat izan zen, diisozianato komertzial bat erabiliz; bigarrenean, berriz, isozianatorik gabeko poliuretanoak sintetizatu ziren polikondentsazio-erreakzioen bidez, DMC eta

HDMA erabiliz. I.15. Irudian tesi honetan jarraitutako prozedura esperimentalaren azalpen eskematiko bat aurkezten da, jarraian laburbiltzen dena.

**I. Argitalpena**: Lanaren zati honetan, bi lehengaiak, *Eucalyptus globulus* eta *Pinus ratiata* zurak, deslignifikatu egin ziren tesiaren beste ataletan erabiliko ziren lignina laginak lortzeko. Bestalde, lignina prezipitatzean geratzen den hondakin likidoa erabiliz, biopoliol desberdinak lortu ziren likido-likido erauzketa prozesu baten bidez.

**II. Argitalpena**: Bigarren zati honetan, biopoliolak sintetizatzeko erreakzio-baldintza optimizatu ziren gradu teknikoko disolbatzaileak erabiliz (PEG-400 eta Glizerola). Erreakzio baldintzak optimizatzeko Box Behnken diseinu esperimental bat burutu zen RSM metodologia erabiliz.

**III. Argitalpena**: Aurretik optimizatutako erreakzio-baldintzak erabiliz, eta gradu teknikoko glizerolaren ordez sukaldeko olio erabilitik lortutako glizerol gordin ez-puru bat erabiliz, biopoliolak sintetizatu ziren.

**IV. Argitalpena**: II. Argitalpenean optimizatutako errakzio-baldintzetaz baliatuz, errakzioaren eskalatze bat egin zen gradu teknikoko disolbatzaileak zein glizerol gordin ez-purua erabiliz. Lortutako biopoliolak eta MDI diisozianato komertziala erabiliz, poliuretanozko itsasgarriak sintetizatu ziren.

**V. Argitalpena**: Lanaren azken zati honetan, IV. argitalpenean egindako eskalatze prozesuan lortutako biopoliolak isozianatorik gabeko poliuretanoak sintetizatzeko erabili ziren, polikondentsazio-erreakzio baten bidez, DMC eta HDMA erabiliz.

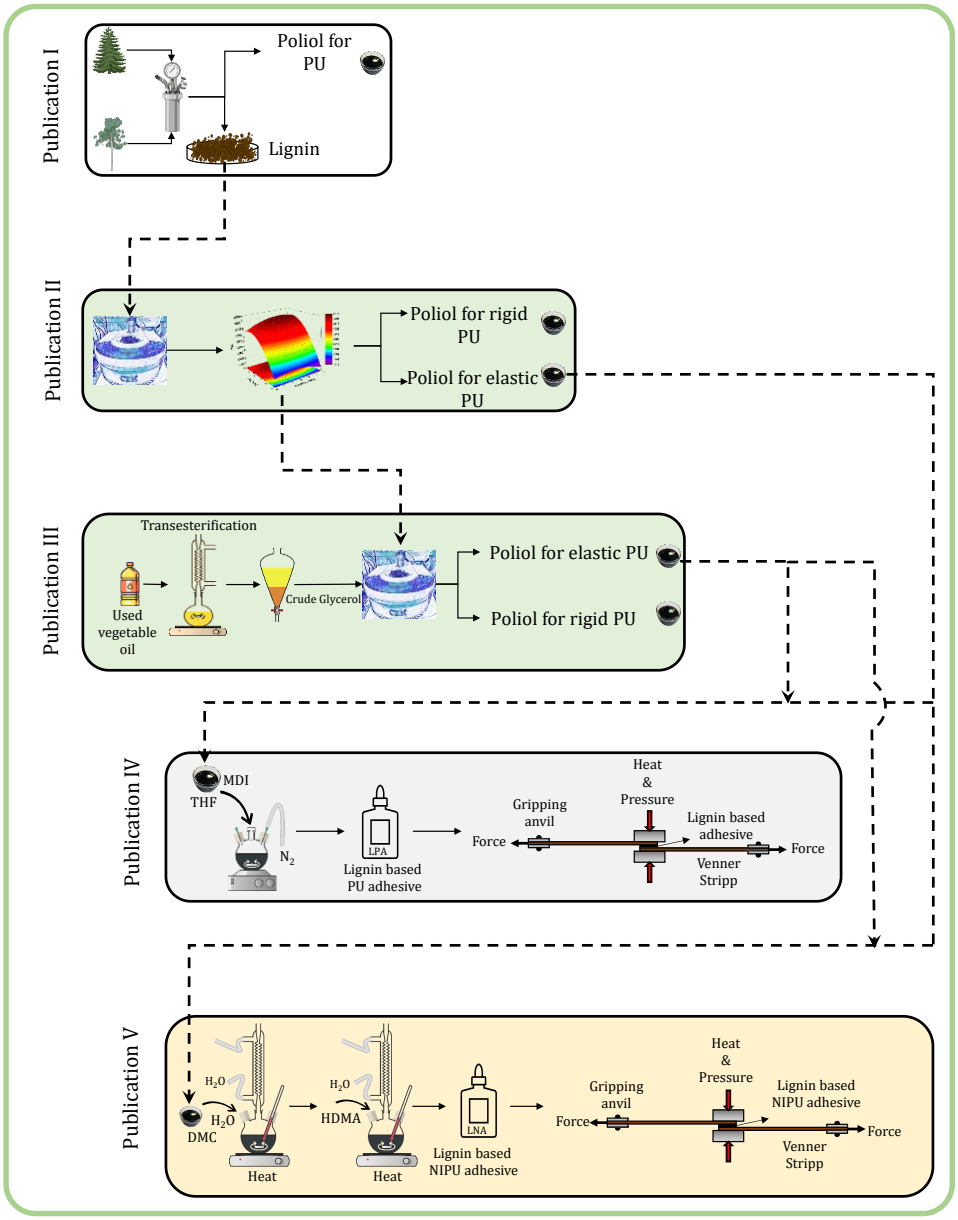


I.14. Irudia. Prozedura esperimentalaren azalpen eskematikoa

## 1.9. Erreferentziak

[1] A. Bonanno, H. Schlattl, L. Paternò, Astron. Astrophys. 390(3) (2002) 1115–8. 10.1051/0004-6361:20020749.

[2] S.F. Portegies Zwart, Astrophys. J. 696(1 PART 2) (2009) 2007–10. 10.1088/0004-637X/696/1/L13.

[3] M.S. Dodd, D. Papineau, T. Grenne, J.F. Slack, M. Rittner, F. Pirajno, J. O'Neil, C.T.S. Little, Nature 543(7643) (2017) 60–4. 10.1038/nature21377.

[4] B.E. Schirrmeister, A. Antonelli, H.C. Bagheri, BMC Evol. Biol. 11(1) (2011). 10.1186/1471-2148-11-45.

[5] B.E. Schirrmeister, M. Gugger, P.C.J. Donoghue, Palaeontology 58(5) (2015) 769–85. 10.1111/pala.12178.

[6] P. Sánchez-Baracaldo, T. Cardona, New Phytol. 225(4) (2020) 1440–6. 10.1111/nph.16249.

[7] E.U. Hammarlund, E. Flashman, S. Mohlin, F. Licausi, Science (80-. ). 370(6515) (2020). 10.1126/science.aba3512.

[8] P.A. Cohen, R.B. Kodner, Trends Ecol. Evol. 37(3) (2022) 246–56. 10.1016/j.tree.2021.11.005.

[9] J.K. Weng, C. Chapple, New Phytol. 187(2) (2010) 273–85. 10.1111/j.1469-8137.2010.03327.x.

[10] J.A. RAVEN, Bot. J. Linn. Soc. 88(1–2) (1984) 105–26. 10.1111/j.1095-8339.1984.tb01566.x.

[11] B. Lowry, D. Lee, C. Hébant, Taxon 29(2–3) (1980) 183–97.

10.2307/1220280.

[12] R.M. Bateman, P.R. Crane, W.A. Dimichele, P.R. Kenrick, N.P. Rowe, T. Speck, W.E. Stein, Annu. Rev. Ecol. Evol. Syst. 29 (1998) 263–92. 10.1146/annurev.ecolsys.29.1.263.

[13] A.R. Barceló, L.V.G. Ros, A.E. Carrasco, Trends Plant Sci. 12(11) (2007) 486–91. 10.1016/j.tplants.2007.09.002.

[14] P.J. Crutzen, Nature 415(January) (2002) 2002.

[15] Y. Chen, Engineering 3(5) (2017) 588–95. 10.1016/J.ENG.2017.04.009.

[16] L. Coleman, Energy Policy 40(1) (2012) 318–24. 10.1016/j.enpol.2011.10.012.

[17] C. MacFarling Meure, D. Etheridge, C. Trudinger, P. Steele, R. Langenfelds, T. Van Ommen, A. Smith, J. Elkins, Geophys. Res. Lett. 33(14) (2006) 2000–3. 10.1029/2006GL026152.

[18] R.B. Domínguez-Espíndola, D.M. Arias, C. Rodríguez-González, P.J. Sebastian, Appl. Therm. Eng. 216(June) (2022). 10.1016/j.applthermaleng.2022.119009.

[19] D. Lüthi, M. Le Floch, B. Bereiter, T. Blunier, J.M. Barnola, U. Siegenthaler, D. Raynaud, J. Jouzel, H. Fischer, K. Kawamura, T.F. Stocker, Nature 453(7193) (2008) 379–82. 10.1038/nature06949.

[20] Permissions and data sources | The Keeling Curve. Available at: https://keelingcurve.ucsd.edu/permissions-and-data-sources/. Accessed January 1, 2023.

[21] BP, [Online] London BP Stat. Rev. World Energy. (2022) 1–60.

[22] E. Parlamient, Taxonomy: MEPs do not object to inclusion of gas and nuclear activities | News | European Parliament. Available at: https://www.europarl.europa.eu/news/en/press-room/20220701IPR34365/taxonomy-meps-do-not-object-to-inclusion-of-gas-and-nuclear-activities. Accessed September 29, 2022.

[23] C.J. Rhodes, Sci. Prog. 102(3) (2019) 218–48. 10.1177/0036850419867204.

[24] R. Geyer, J.R. Jambeck, K.L. Law, Sci. Adv. 3(7) (2017) 25–9. 10.1126/sciadv.1700782.

[25] Plasticseurope, Plastics Europe. Available at: https://plasticseurope.org/resources/market-data/page/2/. Accessed October 1, 2022.

[26] Plastics Europe, Plast. - Facts 2021 (2021) 34.

[27] V.K. Ponnusamy, D.D. Nguyen, J. Dharmaraja, S. Shobana, J.R. Banu, R.G. Saratale, S.W. Chang, G. Kumar, Bioresour. Technol. (2019). 10.1016/j.biortech.2018.09.070.

[28] J.E.Q. Quinsaat, E. Feghali, D.J. Van De Pas, R. Vendamme, K.M. Torr, ACS Appl. Polym. Mater. (2021). 10.1021/acsapm.1c01081.

[29] H. Haridevan, D.A.C. Evans, A.J. Ragauskas, D.J. Martin, P.K. Annamalai, Green Chem. (2021). 10.1039/d1gc02744a.

[30] J. Peyrton, L. Avérous, Mater. Sci. Eng. R Reports (2021). 10.1016/j.mser.2021.100608.

[31] F.M. de Souza, P.K. Kahol, R.K. Gupta, Advances in Science, Technology

and Innovation, 2021, p. .

[32] N. Mahmood, Z. Yuan, J. Schmidt, C. Xu, Renew. Sustain. Energy Rev. (2016) 317–29. 10.1016/j.rser.2016.01.037.

[33] J.O. Akindoyo, M.D.H. Beg, S. Ghazali, M.R. Islam, N. Jeyaratnam, A.R. Yuvaraj, RSC Adv. (2016). 10.1039/c6ra14525f.

[34] M. Izadi, H. Mardani, H. Roghani-Mamaqani, M. Salami-Kalajahi, K. Khezri, ChemistrySelect 6(11) (2021) 2692–9. 10.1002/slct.202004307.

[35] S. Arévalo-Alquichire, M. Morales-Gonzalez, K. Navas-Gómez, L.E. Diaz, J.A. Gómez-Tejedor, M.A. Serrano, M.F. Valero, Polymers (Basel). 12(3) (2020). 10.3390/polym12030666.

[36] N. Karak, Biobased Smart Polyurethane Nanocomposites: From Synthesis to Applications, Royal Society of Chemistry, 2017, pp. 1–40.

[37] X. Sang, R. Wang, X. Chen, L. Zhang, M. An, Y. Shen, Adv. Mater. Res. 284–286 (2011) 1746–9. 10.4028/www.scientific.net/AMR.284-286.1746.

[38] C.S. Wong, K.H. Badri, Mater. Sci. Appl. 03(02) (2012) 78–86. 10.4236/msa.2012.32012.

[39] J. Perez-arce, A. Centeno-pedrazo, J. Labidi, J.R. Ochoa-gomez, E.J. Garcia-suarez, Polymers (Basel). 13(4) (2021) 1–12. 10.3390/polym13040651.

[40] P. Parcheta, J. Datta, Crit. Rev. Environ. Sci. Technol. 47(20) (2017) 1986–2016. 10.1080/10643389.2017.1400861.

[41] Y.Y. Li, X. Luo, S. Hu, Bio-based Polyols and Polyurethanes, 2015, pp.

1–79.

[42] M. Ionescu, [Set Polyols for Polyurethanes, Volume 1+2], 2019, pp. 27–46.

[43] P. Stachak, I. Łukaszewska, E. Hebda, K. Pielichowski, Materials (Basel). 14(13) (2021). 10.3390/ma14133497.

[44] S. Ebnesajjad, Handbook of Adhesives and Surface Preparation: Technology, Applications and Manufacturing, Elsevier Inc., 2010, pp. 3–13.

[45] L.F.M. da Silva, A. Öchsner, R.D. Adams, Handb. Adhes. Technol. Second Ed. 1–2 (2018) 1–1805. 10.1007/978-3-319-55411-2.

[46] B. Burchardt, Advances in polyurethane structural adhesives, Woodhead Publishing Limited, 2010.

[47] K.C. Frisch, Adhesion Science and Engineering, Elsevier B.V., 2002, pp. 759–812.

[48] R. V. Gadhave, P.A. Mahanwar, P.T. Gadekar, Open J. Polym. Chem. 07(04) (2017) 57–75. 10.4236/ojpchem.2017.74005.

[49] M. Alinejad, C. Henry, S. Nikafshar, A. Gondaliya, S. Bagheri, N. Chen, S.K. Singh, D.B. Hodge, M. Nejad, Polymers (Basel). 11(7) (2019). 10.3390/polym11071202.

[50] X. Xi, A. Pizzi, L. Delmotte, Polymers (Basel). 10(4) (2018) 1–21. 10.3390/polym10040402.

[51] R. Khiari, M.C. Brochier-Salon, M.F. Mhenni, E. Mauret, M.N. Belgacem, ChemSusChem 9(16) (2016) 2143–8. 10.1002/cssc.201600430.

[52] A. Fridrihsone, F. Romagnoli, V. Kirsanovs, U. Cabulis, J. Clean. Prod. 266 (2020) 121403. 10.1016/j.jclepro.2020.121403.

[53] P.M. Paraskar, R.D. Kulkarni, J. Polym. Environ. 29(1) (2020) 54–70. 10.1007/s10924-020-01849-x.

[54] X. Junming, J. Jianchun, L. Jing, J. Appl. Polym. Sci. 126(4) (2012) 1377–84. 10.1002/app.36740.

[55] S. Mohd Norhisham, T.I. Tuan Noor Maznee, H. Nurul Ain, P.P. Kosheela Devi, A. Srihanum, M.N. Norhayati, S.K. Yeong, A.H. Hazimah, C.M. Schiffman, A. Sendijarevic, V. Sendijarevic, I. Sendijarevic, Int. J. Adhes. Adhes. 73(October 2016) (2017) 38–44. 10.1016/j.ijadhadh.2016.10.012.

[56] T.N.M. Tuan Ismail, N.A. Ibrahim, M.A. Mohd Noor, S.S. Hoong, K.D. Poo Palam, S.K. Yeong, Z. Idris, C.M. Schiffman, I. Sendijarevic, E. Abd Malek, N. Zainuddin, V. Sendijarevic, JAOCS, J. Am. Oil Chem. Soc. 95(4) (2018) 509–23. 10.1002/aocs.12044.

[57] S. Cui, Z. Liu, Y. Li, Ind. Crops Prod. 108(July) (2017) 798–805. 10.1016/j.indcrop.2017.07.043.

[58] Y.Y. Li, X. Luo, S. Hu, Bio-based Polyols and Polyurethanes, 2015, pp. 1–79.

[59] B. Annevelink, L.G. Chavez, R. Van Ree, I.V. Gursel, Global biorefinery status report 2022, IEA Bioenergy, 2022.

[60] BioPlat, Suschem, I. y C. Ministerio de Economia, Minist. Econ. Ind. Y Compet. (2017) 1–92.

[61] E. de Jong, G. Jungmeier, Biorefinery Concepts in Comparison to

Petrochemical Refineries, Elsevier B.V., 2015.

[62] Y. Liu, Y. Lyu, J. Tian, J. Zhao, N. Ye, Y. Zhang, L. Chen, Renew. Sustain. Energy Rev. 139(January) (2021) 110716. 10.1016/j.rser.2021.110716.

[63] M. Zhou, O.A. Fakayode, A.E. Ahmed Yagoub, Q. Ji, C. Zhou, Renew. Sustain. Energy Rev. 156(December 2021) (2022) 111986. 10.1016/j.rser.2021.111986.

[64] H. Kawaguchi, K. Takada, T. Elkasaby, R. Pangestu, M. Toyoshima, P. Kahar, C. Ogino, T. Kaneko, A. Kondo, Bioresour. Technol. (2022). 10.1016/j.biortech.2021.126165.

[65] A. Saravanan, P. Senthil Kumar, S. Jeevanantham, S. Karishma, D.-V.N. Vo, Bioresour. Technol. (2022). 10.1016/j.biortech.2021.126203.

[66] P. Khemthong, C. Yimsukanan, T. Narkkun, A. Srifa, T. Witoon, S. Pongchaiphol, S. Kiatphuengporn, K. Faungnawakij, Biomass and Bioenergy (2021). 10.1016/j.biombioe.2021.106033.

[67] S. Malherbe, T.E. Cloete, Rev. Environ. Sci. Biotechnol. 1(2) (2002) 105–14. 10.1023/A:1020858910646.

[68] L. Sillero, R. Prado, M.A. Andrés, J. Labidi, Ind. Crops Prod. 137(May) (2019) 276–84. 10.1016/j.indcrop.2019.05.033.

[69] H.H. Cheng, L.M. Whang, Bioresour. Technol. (2022). 10.1016/j.biortech.2021.126097.

[70] A. Dadwal, S. Sharma, T. Satyanarayana, Int. J. Biol. Macromol. (2021). 10.1016/j.ijbiomac.2021.08.024.

[71] L. Bai, A. Ding, G. Li, H. Liang, Chemosphere 308(P3) (2022) 136426.

10.1016/j.chemosphere.2022.136426.

[72] S. Sugiarto, R.R. Pong, Y.C. Tan, Y. Leow, T. Sathasivam, Q. Zhu, X.J. Loh, D. Kai, Mater. Today Chem. 26 (2022) 101022. 10.1016/j.mtchem.2022.101022.

[73] J.Y. Kim, H.W. Lee, S.M. Lee, J. Jae, Y.K. Park, Bioresour. Technol. (2019). 10.1016/j.biortech.2019.01.055.

[74] S. Kassaye, K.K. Pant, S. Jain, Fuel Process. Technol. (2016). 10.1016/j.fuproc.2015.12.032.

[75] D. Kumari, R. Singh, Renew. Sustain. Energy Rev. (2018). 10.1016/j.rser.2018.03.111.

[76] J. Deng, S.F. Sun, E.Q. Zhu, J. Yang, H.Y. Yang, D.W. Wang, M.G. Ma, Z.J. Shi, Ind. Crops Prod. (2021). 10.1016/j.indcrop.2021.113412.

[77] C.G. Yoo, X. Meng, Y. Pu, A.J. Ragauskas, Bioresour. Technol. (2020). 10.1016/j.biortech.2020.122784.

[78] S. Gillet, M. Aguedo, L. Petitjean, A.R.C. Morais, A.M. Da Costa Lopes, R.M. Łukasik, P.T. Anastas, Green Chem. (2017). 10.1039/c7gc01479a.

[79] D.S. Bajwa, G. Pourhashem, A.H. Ullah, S.G. Bajwa, Ind. Crops Prod. 139(February) (2019) 111526. 10.1016/j.indcrop.2019.111526.

[80] P. Jędrzejczak, M.N. Collins, T. Jesionowski, Ł. Klapiszewski, Int. J. Biol. Macromol. (2021). 10.1016/j.ijbiomac.2021.07.125.

[81] A.W. Bhutto, K. Qureshi, K. Harijan, R. Abro, T. Abbas, A.A. Bazmi, S. Karim, G. Yu, Energy (2017). 10.1016/j.energy.2017.01.005.

[82] D. Sidiras, D. Politi, G. Giakoumakis, I. Salapa, Bioresour. Technol.

(2022). 10.1016/j.biortech.2021.126158.

[83] Y. Yu, J. Wu, X. Ren, A. Lau, H. Rezaei, M. Takada, X. Bi, S. Sokhansanj, Renew. Sustain. Energy Rev. (2022). 10.1016/j.rser.2021.111871.

[84] P. Das, R.B. Stoffel, M.C. Area, A.J. Ragauskas, Biomass and Bioenergy 120(November 2018) (2019) 350–8. 10.1016/j.biombioe.2018.11.029.

[85] Z. Usmani, M. Sharma, P. Gupta, Y. Karpichev, N. Gathergood, R. Bhat, V.K. Gupta, Bioresour. Technol. (2020). 10.1016/j.biortech.2020.123003.

[86] Z. Chen, A. Ragauskas, C. Wan, Ind. Crops Prod. (2020). 10.1016/j.indcrop.2020.112241.

[87] W. Graham Forsythe, M.D. Garrett, C. Hardacre, M. Nieuwenhuyzen, G.N. Sheldrake, Green Chem. 15(11) (2013) 3031–8. 10.1039/c3gc41110a.

[88] L. Zhang, T.U. Rao, J. Wang, D. Ren, S. Sirisommboonchai, C. Choi, H. Machida, Z. Huo, K. Norinaga, Fuel Process. Technol. (2022). 10.1016/j.fuproc.2021.107097.

[89] D. Kai, M.J. Tan, P.L. Chee, Y.K. Chua, Y.L. Yap, X.J. Loh, Green Chem. (2016). 10.1039/c5gc02616d.

[90] D. Huang, R. Li, P. Xu, T. Li, R. Deng, S. Chen, Q. Zhang, Chem. Eng. J. (2020). 10.1016/j.cej.2020.126237.

[91] C. Chio, M. Sain, W. Qin, Renew. Sustain. Energy Rev. 107(March) (2019) 232–49. 10.1016/j.rser.2019.03.008.

[92] E. Leng, Y. Guo, J. Chen, S. Liu, J. E, Y. Xue, Fuel (2022).

10.1016/j.fuel.2021.122102.

[93] X. Wu, N. Luo, S. Xie, H. Zhang, Q. Zhang, F. Wang, Y. Wang, Chem. Soc. Rev. (2020). 10.1039/d0cs00314j.

[94] X. Meng, C. Crestini, H. Ben, N. Hao, Y. Pu, A.J. Ragauskas, D.S. Argyropoulos, Nat. Protoc. 14(9) (2019) 2627–47. 10.1038/s41596-019-0191-1.

[95] W. Gao, P. Fatehi, Can. J. Chem. Eng. (2019). 10.1002/cjce.23620.

[96] Y. Meng, J. Lu, Y. Cheng, Q. Li, H. Wang, Int. J. Biol. Macromol. (2019). 10.1016/j.ijbiomac.2019.05.198.

[97] S. Magina, N. Gama, L. Carvalho, A. Barros-Timmons, D.V. Evtuguin, Materials (Basel). 14(22) (2021) 1–18. 10.3390/ma14227072.

[98] T.A.P. Hai, M. Tessman, N. Neelakantan, A.A. Samoylov, Y. Ito, B.S. Rajput, N. Pourahmady, M.D. Burkart, Biomacromolecules 22(5) (2021) 1770–94. 10.1021/acs.biomac.0c01610.

[99] M.A.C. Mhd. Haniffa, K. Munawar, Y.C. Ching, H.A. Illias, C.H. Chuah, Chem. - An Asian J. 16(11) (2021) 1281–97. 10.1002/asia.202100226.

[100] M. Ghasemlou, F. Daver, E.P. Ivanova, B. Adhikari, Eur. Polym. J. 118(May) (2019) 668–84. 10.1016/j.eurpolymj.2019.06.032.

[101] J. Sternberg, O. Sequerth, S. Pilla, Prog. Polym. Sci. (2021). 10.1016/j.progpolymsci.2020.101344.

[102] B.M. Upton, A.M. Kasko, Chem. Rev. 116(4) (2016) 2275–306. 10.1021/acs.chemrev.5b00345.

[103] S. Laurichesse, L. Avérous, Prog. Polym. Sci. 39(7) (2014) 1266–90.

10.1016/j.progpolymsci.2013.11.004.

[104] K. Gosz, P. Kosmela, A. Hejna, G. Gajowiec, Ł. Piszczyk, Wood Sci. Technol. 52(3) (2018) 599–617. 10.1007/s00226-018-0991-4.

[105] J. Zhang, N. Hori, A. Takemura, J. Clean. Prod. 277 (2020) 124015. 10.1016/j.jclepro.2020.124015.

[106] M.R. Haverly, T.C. Schulz, L.E. Whitmer, A.J. Friend, J.M. Funkhouser, R.G. Smith, M.K. Young, R.C. Brown, Fuel (2018). 10.1016/j.fuel.2017.09.072.

[107] M. Vale, M.M. Mateus, R. Galhano dos Santos, C. Nieto de Castro, A. de Schrijver, J.C. Bordado, A.C. Marques, J. Clean. Prod. 212 (2019) 1036–43. 10.1016/j.jclepro.2018.12.088.

[108] S.H.F. da Silva, I. Egüés, J. Labidi, Ind. Crops Prod. 137(March) (2019) 687–93. 10.1016/j.indcrop.2019.05.075.

[109] E. barbary M. Hassan, N. Shukry, Ind. Crops Prod. 27(1) (2008) 33–8. 10.1016/j.indcrop.2007.07.004.

[110] S. Hu, Y. Li, Ind. Crops Prod. 57 (2014) 188–94. 10.1016/j.indcrop.2014.03.032.

[111] S. Hu, X. Luo, Y. Li, ChemSusChem 7(1) (2014) 66–72. 10.1002/cssc.201300760.

[112] U.A. Amran, S. Zakaria, C.H. Chia, Z. Fang, M.Z. Masli, Energy and Fuels (2017). 10.1021/acs.energyfuels.7b02098.

[113] B.L. Xue, J.L. Wen, R.C. Sun, Materials (Basel). 8(2) (2015) 586–99. 10.3390/ma8020586.

[114] S.H.F. da Silva, P.S.B. dos Santos, D. Thomas da Silva, R. Briones, D.A. Gatto, J. Labidi, J. Wood Chem. Technol. 37(5) (2017) 343–58. 10.1080/02773813.2017.1303513.

[115] J.C. Thompson, B.B. He, Appl. Eng. Agric. 22(2) (2006) 261–5. 10.13031/2013.20272.

[116] Eurostat, Statistics | Eurostat. Available at: https://ec.europa.eu/eurostat/databrowser/view/NRG_INF_LBPC__custom_1487898/default/table. Accessed May 10, 2022.

[117] L.R. Kumar, R. Kaur, R.D. Tyagi, P. Drogui, Bioresour. Technol. 323(December 2020) (2021) 124565. 10.1016/j.biortech.2020.124565.

[118] L.C. Muller, S. Marx, H.C.M. Vosloo, J. Renew. Mater. 5(1) (2017) 67–80. 10.7569/JRM.2016.634130.

[119] L.C. Muller, S. Marx, H.C.M. Vosloo, E. Fosso-Kankeu, I. Chiyanzu, Polym. from Renew. Resour. 9(3–4) (2018) 111–32. 10.1177/2041247918803187.

[120] L.C. Muller, S. Marx, H.C.M. Vosloo, I. Chiyanzu, Polym. from Renew. Resour. 10(1–3) (2019) 3–18. 10.1177/2041247919830833.

[121] M.H. Tran, J.H. Yu, E.Y. Lee, Polymers (Basel). 13(9) (2021). 10.3390/polym13091491.

[122] J. Sternberg, S. Pilla, Green Chem. 22(20) (2020) 6922–35. 10.1039/d0gc01659d.

[123] A. Salanti, L. Zoia, M. Mauri, M. Orlandi, RSC Adv. 7(40) (2017) 25054–65. 10.1039/c7ra03416d.

[124] W. Zhao, Z. Liang, Z. Feng, B. Xue, C. Xiong, C. Duan, Y. Ni, ACS Appl. Mater. Interfaces 13(24) (2021) 28938–48. 10.1021/acsami.1c06822.

[125] V. Mimini, H. Amer, H. Hettegger, M. Bacher, I. Gebauer, R. Bischof, K. Fackler, A. Potthast, T. Rosenau, Holzforschung 74(2) (2020) 203–11. 10.1515/hf-2018-0298.

[126] R. Ménard, S. Caillol, F. Allais, ACS Sustain. Chem. Eng. 5(2) (2017) 1446–56. 10.1021/acssuschemeng.6b02022.

[127] M. Janvier, P.H. Ducrot, F. Allais, ACS Sustain. Chem. Eng. 5(10) (2017) 8648–56. 10.1021/acssuschemeng.7b01271.

[128] Q. Chen, K. Gao, C. Peng, H. Xie, Z.K. Zhao, M. Bao, Green Chem. 17(9) (2015) 4546–51. 10.1039/c5gc01340b.

[129] S. Sen, S. Patil, D.S. Argyropoulos, Green Chem. 17(11) (2015) 4862–87. 10.1039/c5gc01066g.

[130] M.A. Aristri, M.A.R. Lubis, S.M. Yadav, P. Antov, A.N. Papadopoulos, A. Pizzi, W. Fatriasari, M. Ismayati, A.H. Iswanto, Appl. Sci. 11(9) (2021) 1–29. 10.3390/app11094242.

[131] D.J. Dos Santos, L.B. Tavares, J.R. Gouveia, G.F. Batalha, Arch. Mater. Sci. Eng. 107(2) (2021) 56–63. 10.5604/01.3001.0015.0242.

[132] Y.C. Chen, S. Fu, H. Zhang, Colloids Surfaces A Physicochem. Eng. Asp. 585 (2020) 124164. 10.1016/J.COLSURFA.2019.124164.

[133] Y.Y. Wang, C.E. Wyman, C.M. Cai, A.J. Ragauskas, ACS Appl. Polym. Mater. 1(7) (2019) 1672–9. 10.1021/ACSAPM.9B00228.

[134] Y. Chen, H. Zhang, Z. Zhu, S. Fu, Int. J. Biol. Macromol. (2020). 10.1016/j.ijbiomac.2020.02.321.

[135] L.B. Tavares, C. V. Boas, G.R. Schleder, A.M. Nacas, D.S. Rosa, D.J. Santos, Express Polym. Lett. 10(11) (2016) 927–40. 10.3144/EXPRESSPOLYMLETT.2016.86.

[136] J.R. Gouveia, L.D. Antonino, G.E.S. Garcia, L.B. Tavares, A.N.B. Santos, D.J. do. Santos, Https://Doi.Org/10.1080/00218464.2020.1784148 97(15) (2020) 1423–39. 10.1080/00218464.2020.1784148.

[137] R. V. Gadhave, P. S. Kasbe, P.A. Mahanwar, P.T. Gadekar, Int. J. Adhes. Adhes. 95 (2019) 102427. 10.1016/J.IJADHADH.2019.102427.

[138] M.H. Hussin, N.H. Abd Latif, T.S. Hamidon, N.N. Idris, R. Hashim, J.N. Appaturi, N. Brosse, I. Ziegler-Devin, L. Chrusiel, W. Fatriasari, F.A. Syamani, A.H. Iswanto, L.S. Hua, S.S. Azry Osman Al Edrus, L.W. Chen, P. Antov, V. Savov, M.A. Rahandi Lubis, L. Kristak, R. Reh, J. Sedliačik, J. Mater. Res. Technol. (2022). 10.1016/j.jmrt.2022.10.156.

[139] A. Arias, E. Entrena-Barbero, G. Feijoo, M.T. Moreira, J. Environ. Chem. Eng. 10(1) (2022) 107053. 10.1016/j.jece.2021.107053.

[140] J. Saražin, A. Pizzi, S. Amirou, D. Schmiedl, M. Šernek, J. Renew. Mater. 9(5) (2021) 881–907. 10.32604/jrm.2021.015047.

[141] X. Xi, A. Pizzi, C. Gerardin, H. Lei, X. Chen, S. Amirou, Polymers (Basel). 11(11) (2019). 10.3390/polym11111802.

[142] X. Chen, A. Pizzi, H. Essawy, E. Fredon, C. Gerardin, N. Guigo, N. Sbirrazzuoli, Polymers (Basel). 13(3) (2021) 1–13. 10.3390/polym13030372.

[143] X. Chen, A. Pizzi, E. Fredon, C. Gerardin, X. Zhou, B. Zhang, G. Du, Int. J. Adhes. Adhes. 112(September 2021) (2022) 103001. 10.1016/j.ijadhadh.2021.103001.

[144] F.J. Santiago-Medina, M.C. Basso, A. Pizzi, L. Delmotte, J. Renew. Mater. 6(4) (2018) 413–25. 10.7569/JRM.2017.634172.

## *2. ATALA*

## *METODOLOGIA*

*“I never question anything…*

*Until after I’ve done it.”*

*Han Solo*

## 2.1. Lehengaiak eta kimikoak

Tesi honetarako erabili diren lehengaiak Euskal Herriko (Espainia) industria desberdinetako egur hondakinak izan dira. Alde batetik, Papelera Guipuzcoana Zikuñaga S.A.-k *Eucalyptus glubulus* laginak hornitu zituen, eta *Pinus radiata* zerrautsa, berriz, Ebaki XXI S.A. tik lortu ziren. III. Argitalpean likidotze-prozesuan erabilitako glizerol gordina Eibarreko Gipuzkoako Ingeniaritza Fakultateko jatetxean bildu zen. Bestalde, tesi honetan erabilitako produktu kimiko komertzialak M.1. taulan laburbiltzen dira.

M.1. Taula. Tesian erabilitako produktu kimiko komertzialak

| Produktu kimikoa | Laburdura | Purutasuna | Hornitzailea |
|---|---|---|---|
| Etanola | | | Scharlab |
| Metanola | | | |
| Etil azetatoa | | HPLC gradua | |
| Sodio sulfato anhidridoa | | ≥99% | |
| Dimetilformamida | DMF | HPLC ≥99,9% | |
| Litio bromuroa | | | Fisher Scientific |
| 1,4-dioxanoa | | ≥99,8% | |
| Piridina | | 99,50% | |
| Tetrahidrofurana | THF | Analitiko graduko erreaktibo | |
| Anhidrido ftalikoa | | 98% | |
| Azido sulfurikoa | | 96% | |
| Polietilen glikol -400 | PEG-400 | Teknikoa | |
| Glizerola | Gly | 99% | Panreac |
| Potasio hidroxidoa | KOH | 85% | |
| Sodio hidroxidoa | NaOH | | |
| 4,4'-difenilmetano diisozianatoa | MDI | | Merk |
| Dimetil karbonatoa | DMC | 99% | Alfa Aesar |
| Hexametilendiamina | HDMA | >98% | |
| Dibutyltin dilauratoa | DBTDL | 95% | Alfa Aesar |
| 3(Aminopropyl)trimetoxisil anoa | APTMS | | |

## 2.2. Lehengaien deslignifikazioa eta likore beltzen sonikazio-prozesua

Lan honetan erabili diren lignina laginak lortzeko, M.1. Irudian deskribatzen den prozesua jarraitu zen. Bertan, lehengaiak organosolv prozesu baten bidez deslignifikatu ziren M.2. taulan laburtutako erreakzio baldintzak erabiliz. Horretarako, 1,5 L-ko altzairu herdoilgaitzezko 5500 Steel Parr erreaktorea 4848 Parr kontrolagailuarekin erabili zen. Organosolv tratamendu bakoitzaren hiru ale egin ziren 50 gramo lehengai erabiliz.

M.2. Taula. Organosolv deslignifikazio prozesuen erreakzio-baldintzak

| | Disolbatzailea (w/w) | Solido-likido ratio | Tenperatura (°C) | Denbora (min) |
|---|---|---|---|---|
| *Eucalyptus globulus* | EtOH/$H_2O$ (50%) | 1:6 | 200 | 75 |
| *Pinus radiata* | | 1:8 | 210 | |

Likore beltzak (BL) pulpatik bereizi ziren huts bidezko iragazketaren bidez, 7-12 µm-ko atxikipen-ahalmeneko paper-iragazkiak erabiliz (Macherey-Nagel 640w). Iragazte-prozesuaren ondoren, BLak Sonoplus HD 3100 homogenizatzaile ultrasoniko batekin sonikatu egin ziren ondorengo baldintzak erabiliz: 35 °C, 60 min eta %35eko irteerako anplitudea. BLetako ligninak hauzpeatzeko, pH=2ko ur azidifikatutako bolumen bikoitza gehitu zen (BL bolumena kontuan izanik), eta ondoren, hauspeatutako lignina fase likidotik presio-iragazketaren bidez bereizi zen 2 L-ko altzairu herdoilgaitzezko ontzi bat eta 0,22µm-ko poroko diametroa zuen nylonezko filtro bat erabiliz. Azkenik, lignina ur destilatuarekin garbitu zen pH neutroa lortu arte.

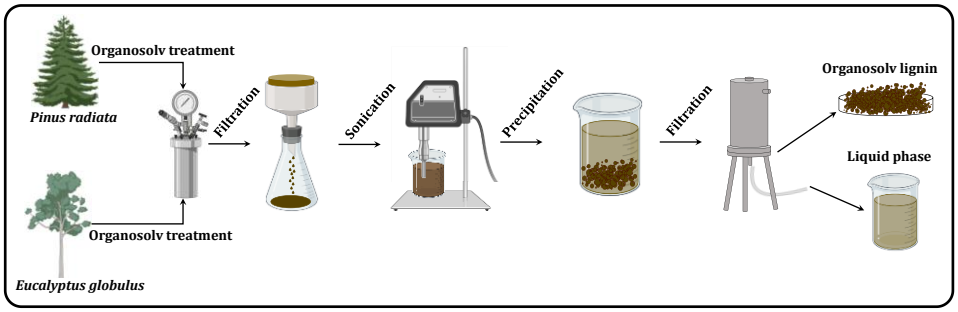


M.1. Irudia. Tesian jarraitutako deslignifikazio prozesuaren eskema

## 2.3. Biopoliolen sintesi-prozedura

***I. Argitalpenean*** sintetizatutako biopoliolak ondoren azaltzen moduan lortu ziren (M.2. Irudia).

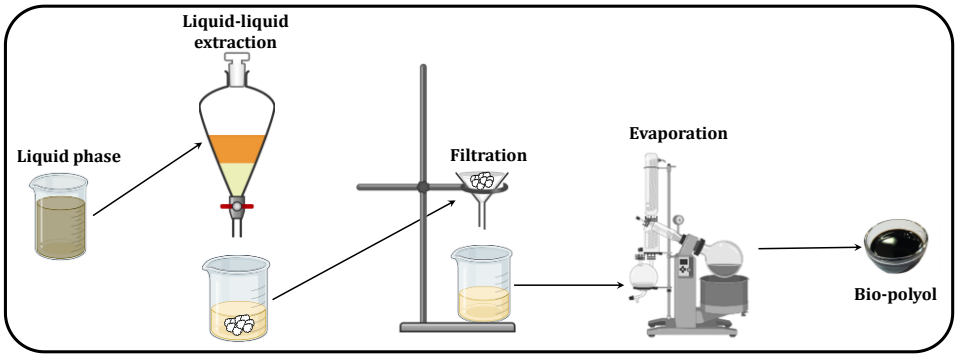


M.2. Irudia. **I. Argitalpeneko** biopoliolak lortzeko diagrama

Bestalde, lignina prezipitatzean geratzen den hondakin likidoa erabiliz, biopoliol desberdinak lortu ziren likido-likido erauzketa prozesu baten bidez.

Deslignifikazio prozesuaren eta ligninaren erauzketa prozesuaren ondoren geratzen den hondakin likidoari etil azetatoarekin likido-likido erauzketa bat egin zitzaion fase organikoa fase likidotik bereizteko. Horretarako, lau erauzketa egin ziren 1:0,25eko likido/etil azetato erlazioa erabiliz. Ondoren,

fase organikoa fase likidotik banandu eta iragazi zen, jarraian sodio sulfato anhidrikoarekin tratatu zen hezetasun arrastoak kentzeko. Azkenik, etil azetatoa lurrungailu birakari baten bidez lurrundu zen, biopoliolak lortuz.

***II.*** eta ***III. Argitalpenen*** biopoliolen sintesia mikrouhin bidezko likidotze erreakzio baten bidez egin zen, tenperatura-kontrolagailua eta barne-tenperaturako sentsorea duen CEM Microwave Discover System Model mikrouhin erreaktore bat erabiliz. Teknika hori erabiliz eta RSM metodologian oinarritutako Box Behnken diseinu esperimental baten bidez, ***II. Argitalpenean*** erreakzio baldintzak optimizatu ziren PU zurrunak eta elastikoak sintetizatzeko beharrezko ziren biopoliolak ekoizteko. Argitalpen honetan PEG-400 eta glizerol komertzialak erabili ziren disolbatzaile gisa eta azido sulfurikoa katalizatzaile gisa. Ondoren, ***III. Argitalpenean***, optimizatutako erreakzio-baldintzak erabiliz, glizerol komertziala glizerol gordin batengatik ordezkatu zen biopoliolak ekoizteko. Bi argitalpenetan M.3. Irudian azaltzen den, eta ondoren azaltzen den prozedura berbera erabili zen erreakzio egiteko.

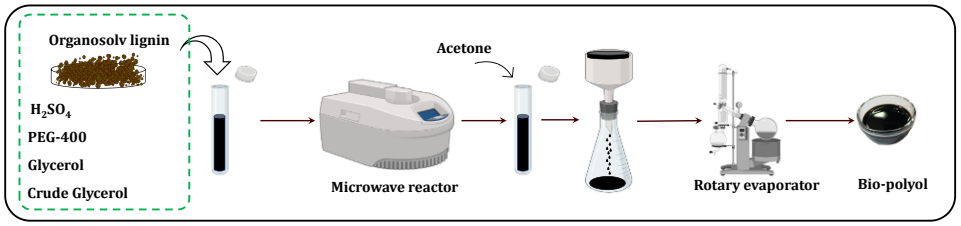


M.3. Irudia. **II**. eta **III. Argitalpenetan** ekoiztutako biopoliolen sintesia

Hasteko, aldez aurretik zehaztutako osagai bakoitzaren (lignina, PEG-400, glizerol teknikoa edo gordina eta azido sulfuriko) kantitate jakin pisatu zen erreaktorearen ontzian eta ondoren Vortexa erabiliz osagai guztiak nahastu ziren. Guztira 4 g pisatzen zuen lagina homogeneizatu ondoren, ontzia mikrouhin errektorean sartu eta 5 minutuko erreakzio martxan jarri zen etengabeko agitazioarekin. Erreakzio-denbora amaitu bezain laster, ontzia

50 °C arte hoztu zen erreaktorearen hozte-sistemaren bitartez. Ondoren, ontzia ur hotzarekin hoztu zen manipulatzeko tenperatura segurua lortzeko. Behin hoztuta, lortutako produktua azetonan disolbatu zen eta ondoren sortutako solidoak bereizteko iragazi egin zen. Bukatzeko, azetona lurrungailu birakari baten bidez lurrundu zen biopoliolak lortzeko.

### 2.3.1. Likidotze erreakzioaren eskalatze prozesua

***IV.*** eta ***V. Argitalpenetan*** erabilitako biopoliolak sintetizatzeko, likidotze erreakzioa eskalatu egin zen (x10), horretarako CEM Microwave Discover 2.0 erreaktore bat erabili zen, 100 ml-ko edukiera zuten ontziak erabiliz. Erreakzioak ***II.*** eta ***III. Argitalpenetan*** jarraitutako sintesi prozesu berarekin burutu ziren (ikusi M.3. Irudia).

## 2.4. Glizerol gordina lortzeko erabilitako sukaldeko olioaren transesterifikazio erreakzioa

Glizerol gordina lortzeko erabilitako sukaldeko olioaren transesterifikazio erreakzioa metanolarekin egin zen, 6:1eko proportzio molarrean (metanola : olioa). Erreakzioa KOH (olioaren %1 pisuan) bidez katalizatu zen eta azido oleikoa, 884 g/moleko pisu molekularrarekin, triglizerido nagusitzat hartu zen kalkuluak egiteko. Erreakzioa honela burutu zen: hasteko, olioa iragazi zen ezpurutasuna kentzeko; ondoren, berogailu-plaka baten bitartez olioa 60 °C-ra berotu zen matraze bolumetriko batean agitazio magnetikoa erabiliz (600 bira minutuko). 60 °C-ko tenperaturara iritsitakoan, aurrez prestatutako metanol/KOH nahasketa gehitu zen eta erreakzioa 120 minutuz mantendu zen errefluxu pean konbertsioa maximizatzeko. Erreakzioa bukatutzat jo eta nahastea 24 orduz utzi zen bereizte-inbutu batean, biodiesela eta glizerola bereizteko.

## 2.5. Ligninan oinarritutako poliuretano itsasgarrien sintesi prozedura

M.4. Irudian, ligninan oinarritutako eta isozianato komertziala erabiliz sintetizatutako poliuretano itsasgarrien (LPA) prozedura esperimentalaren diagrama irudikatzen da.

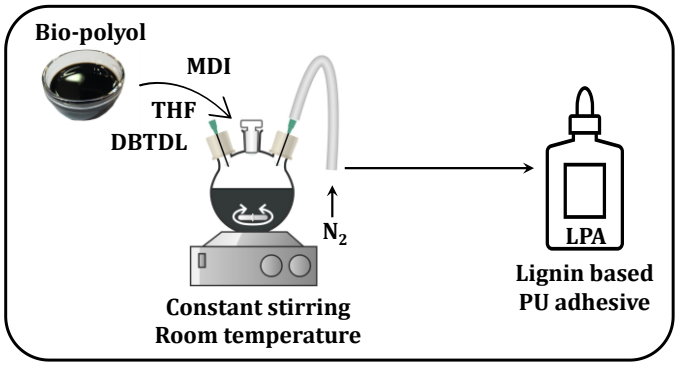


M.4. Irudia. LPA itsasgarrien sintesiaren prozedura esperimentala

Sintesia nitrogenozko atmosfera geldoan eta giro-tenperaturan egin zen "one-shot" metodoa erabiliz. Lehenbizi, biopoliola eta THF hiru ahoko matraze esferiko batean izuri ziren eta nahastea indartsu irabiatu zen. Ondoren, DBTDL katalizatzailea eta MDIa gehitu eta irabiatzen utzi zen nahasketa jariakorra izateari utzi zuen arte, eta horrela gel denbora lortu zen. LPAak sintetizatzeko erabilitako NCO:OH ratioak ***IV. Argitalpenean*** agertzen dira.

## 2.6. Isozianatorik gabeko poliuretanoak sintetizatzeko sintesiaren prozedura

Ligninan oinarritutako NIPU itsasgarrien (LNA) sintesia polikondentsazio erreakzio baten bidez gauzatu zen DMC eta HDMA erabiliz (M.5. Irudia).

Erreakzioa burutzeko Saražin et al. (2021)-en [140] lanean deskribatutako prozesua erabili zen aldaketa batzuekin.

Hidoxilo taldeen, DMCren eta HDMAren (OH:DMC:HDMA) arteko (1:2:2)ko ratio molarra erabili zen erreakzioa burutzeko. Hasieran, biopoliola DMCarekin eta aurrez zehaztutako ur kopuru batekin erreakzionatu zen 60 minutuz eta 65 °C-ko tenperaturan (ikusi ***V. Argitalpena***). Ondoren, HDMA gehitu zen eta nahasketa 90 °C-tara igo eta 120 minutu utzi zen. Erreakzioa, agitazio magnetikoarekin irabiatu zen eta errefluxu pean gauzatu zen. Azkenik, eta NIPU itsasgarrien itsaspen propietateak hobetzeko, 3-Aminopropiltirmetoxysilano deritzon akoplamendu agente gehitu zen.

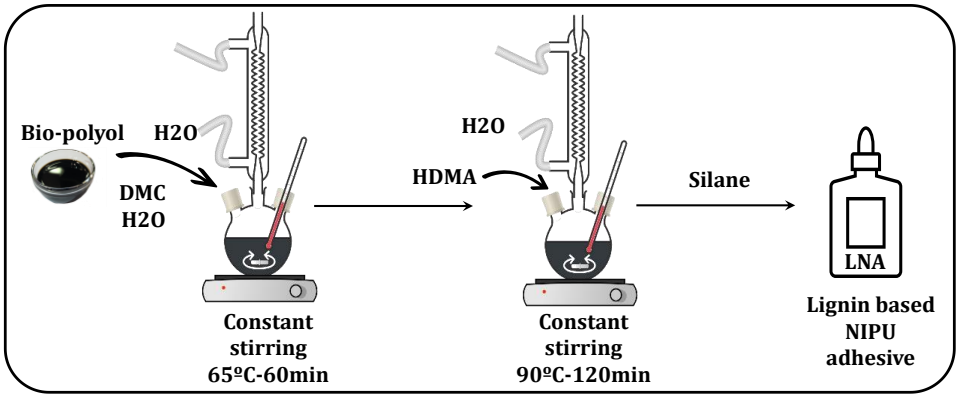


M.5. Irudia. LNA itsasgarriak polikondentsazio erreakzioaren bitartez sintetizatzeko prozedura

## 2.7. Karakterizazio metodoak

Lan honetako argitalpenetan erabilitako karakterizazio tekniken laburbilduma M.3 taulan agertzen da, eta ***II. Eranskinean*** zehatz-mehatz deskribatzen dira.

M.3. Taula. Lan honetako argitalpenetan erabilitako karakterizazio teknikak

| Karakterizazioa | Argitalpena | | | | | | |
|---|---|---|---|---|---|---|---|
| | I | II | | III | | V | VI |
| | Bp | L | Bp | CG | Bp | LPA itsasgarria | LNA itsasgarria |
| Konposizioa (GC-MS) | √ | x | x | √ | x | x | x |
| Estruktura kimikoa (ATR-FTIR) | √ | √ | x | √ | x | √ | √ |
| Pisu molekularra (GPC) | √ | √ | √ | x | √ | x | x |
| $I_{OH}$, $A_n$ | √ | x | √ | x | √ | x | x |
| Portaera reologikoa | √ | x | √ | x | √ | x | x |
| Degradazio termikoa (TGA) | √ | x | x | x | √ | √ | √ |
| Degradazio termikoaren zinetika eta bizi iraupenaren estimazioa (TGA) | x | x | x | x | x | √ | √ |
| Itsaspen-proba (ABES) | x | x | x | x | x | √ | √ |

L: Lignina; Bp: Biopoliola; CG: Glizerol gordina

# *3. ATALA*

# *EMAITZAK ETA EZTABAIDA*

# *3rd PART*

# *RESULTS AND DISCUSION*

# BIOPOLIOLEN LORPENA ETA SINTESIA

## OBTAINING AND SYNTHESIS OF BIO-POLYOLS

*Remember, concentrate on the moment.*

*Feel, don't think. Use your instincts."*

*Qui-Gon Jinn*

*“Always two there are, no more, no less.*

*A master and an apprentice”*

*Master Yoda*

# I. Argitalpena

# Lignina prezipitatu ondoren geratzen den hondakin likidotik lortutako biopoliol berriztagarriak

## LABURPENA

Lan honen helburua *Eucalytus globulus* eta *Pinus radiataren* likore beltzetan dagoen lignina prezipitatu ondoren geratzen den hondakin likidoak baloratzea izan zen bi biopoliol desberdin lortuz. *Eucalyptus globulus* eta Pinus radiataren likore beltz hauetatik lortutako biopoliolak (EOP eta POP) biskositatea, hidroxilo kopurua ($I_{OH}$) eta funtzionaltasuna ezagutzeko karakterizatu egin ziren American Society for Testing Materials (ASTM) arauak erabiliz. Bestalde, biopoliolen pisu molekularra GPC bidez neurtu zen, estruktura kimikoa eta konposizioa ATR-FTIR eta GC-MS bidez aztertu zen hurrenez hurren, eta bi biopoliolen degradazio termikoa TGA analisi baten bidez zehaztu zen. Egindako analisiak kontutan izanda bi biopoliolak PUak ekoizteko propietate egokiak zituztela ondorioztatu zen.

## 1. MATERIALAK ETA METODOAK

### 1.1. Materialak

Argitalpen honetan erabilitako lehengaiak, *Eucalyptus globulus*-en txirbilak eta *Pinus radiata*-ren zerrautsa, eta erreaktiboak **2. ATALAREN *2.1 puntuan*** deskribatzen den bezala lortu ziren.

### 1.2. Lehengaien deslignifikazioa eta likore beltzen sonikazio-tratamendua

Bi lehengaien organosolv desliginifikazio prozesuak eta eratutako LB-en sonikazio tratamenduak **2. ATALAREN *2.2 puntuan*** deskribatzen dira.

### 1.3. Likore beltzen karakterizazioa

*Eucalyptus globulus* (EOBL) eta *Pinus radiata* (POBL) LBk **I. Eranzkinean** deskribatuta dauden TAPPI arauekin karakterizatu egin ziren.

### 1.4. Biopoliolen lorpena

LB-tan dagoen lignina prezipitatu ondoren geratzen den hondakin likidoetatik biopoliolak lortzeko prozesua **2. ATALAREN *2.3 puntuan*** zehatz mehatz deskribatzen da.

### 1.5. Biopoliolen karakterizazioa

EOBLtik eta POBLtik lortutako EOP eta POP biopoliolak **2. ATALAREN *2.7 puntuko*** M.3. Taulan agertzen diren teknikak erabiliz karakterizatu ziren. Teknika hauek **II. Eranskinean** deskribatzen dira.

## 2. EMAITZAK ETA EZTABAIDA

### 2.1. Likore beltzak

Lbak karakterizatzean lortutako emaitzak P 1.1. Taulan agertzen dira. Espero zen bezala, ez zen alde nabarmenik hauteman bi lehengaien arteko pH-aren eta dentsitatearen balioetan. TDSari dagokionez, bi kasuetan OMri zegozkiola ondorioztatu ahal izan zen, nahiz eta POBL kasuan IM kopuru txiki bat ikusi zen. Neurtutako OMtik, %61,62 lignina zela zehaztu zen EOBLren kasuan, eta POBLren kasuan berriz, %53,92 baino ez zen lortu. Gainerako OMa hemizelulosetatik eratorritako degradazio-produktuei eta LBtan disolbatutako erauzketei egotzi dakieke.

P1.1. Taula. Likore beltzen karakterizazioa

| | Likore beltzak | |
|---|---|---|
| | ***Eucalyptus globulus*** | ***Pinus radiata*** |
| pH | 3,600 ± 0,035 | 3,787 ± 0,031 |
| Dentsitatea (g/mL) | 0,926 ± 0,003 | 0,911 ± 0,001 |
| TDS | 5,527 ± 0,373 | 2,313 ± 0,021 |
| IM | 0,027 ± 0,003 | - |
| OM | 5,509 ± 0,367 | 2,313 ± 0,021 |
| Lignina (%) | 2,970 ± 0,103 | 1,425 ± 0,076 |

## 2.2. Biopoliola

Lehen aipatu bezala, organosolv tratamenduak hirukoiztuta egin ziren lehengai bakoitzarekin, hasierako lehengaiarekiko biopoliol errendimenduak % 5,45 ± 0,53 (EOP) eta % 5,24 ± 0,28 izanik.

EOP eta POP biopoliolen estruktura kimikoa ATR-FTIR bidez aztertu zen. Lortutako kromatogramak P1.1a eta 1.1b. Irudietan irudikatzen dira. P1.1a Irudian ikus daitekeenez, bi polioletan unitate fenolikoen eto alkoholikoen OH luzapenari dagokion banda (3400 $zm^{-1}$) agertu zen. Bestalde, P1.1b. irudian irudikatutako hatz-markaren eskualdean (*fingerprint region*) (1800 $zm^{-1}$ – 800 $zm^{-1}$), karbohidratoei eta ligninari dagozkien banda bereizgarriak ikus daitezke. Ligninaren banda bereizgarriei dagokionez (1330 $zm^{-1}$ – 815 $zm^{-1}$), erabilitako lehengaiaren izaera desberdinei egotzi dakizkioken diferentzia txiki batzuk ikusi ziren; izan ere, zur bigunak G unitateez osatuta daude gehienbat, zur gogorra S eta G unitateen kantitate baliokide batez osatuta dauden bitartean. Zentzu horretan, 1270 $zm^{-1}$-ko eta 815 $zm^{-1}$-ko seinaleak G unitateei egozten zaizkie, 1330 $zm^{-1}$ eta 1114 $zm^{-1}$ seinaleak S unitateei, eta 1026 $zm^{-1}$-ko seinalea G eta S unitate biei egozten zaizkie [2–4]. Nabarmentzekoa da ere, 1270 $zm^{-1}$-eko uhin zenbakiko seinaleak, G eraztunari gehi C=O luzapenari dagokiona, askoz ere intentsitate handiagoa izan zuela POParen kasuan EOParen kasuan baino. Gainera, G unitateetako

CH taldeari dagokion seinalea (815 $zm^{-1}$) pinutik eratorritako POP biopolioletan bakarrik ikusi zen, EOP biopolioletan, berriz, S unitate gehiago ikusi ziren, lehengaien izaera desberdinagatik espero zitekeen bezala. S unitateetako C=O taldeari dagokion seinalea (1330 $zm^{-1}$), EOP biopoliolean ikusi zen bakarrik; bestalde, S unitateen CH aromatikoen deformazio bibrazioa (1114 $zm^{-1}$) bi biopolioetan ikusi zen, nahiz eta POParen kasuan intentsitate baxuagoa izan. Gainera, espero zen bezala, G unitateekin erlazionatutako eraztun aromatikoaren banda (1026 $zm^{-1}$) intentsitate handiagoa erakutsi zuen POPan EOPan baino. Azkenik, aril zetonen C=O taldeen luzatzea-bibrazioari (1674 $zm^{-1}$) eta CH taldearen deformazioari (1460 $cm^{-1}$) dagozkien banden intentsitatea [2] ondoren azaltzen den bezala aldatu egin zirela ikus daiteke: POP biopoliolean aril zetonen C=O taldeen luzatze-bibrazioa handitu egin zen, eta CH deformazioaren banda, berriz, murriztu zen, EOPren kasuan, berriz, kontrakoa gertatu zen. Lehen aipatu den bezala, karbohidratoekin lotutako seinaleak ere agertu ziren hatz-markaren eskualdean, horrela, 1603 $zm^{-1}$, 1424 $zm^{-1}$, 1114 $zm^{-1}$ eta 1026 $zm^{-1}$ uhin zenbakietan agertzen diren bandak karbohidratotik eratorritako konposatuen existentziaren adierazle dira [5].

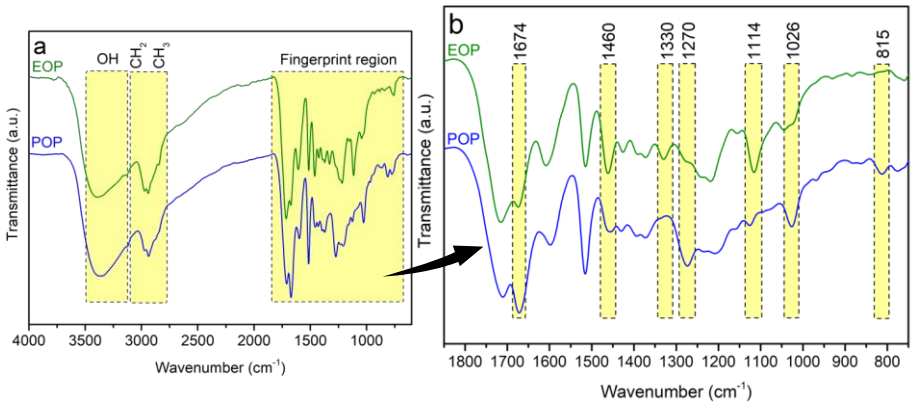


P1.1. Irudia. EOP eta POPen ATR-FTIR espektroak (a) eta (b) espektroen hatz-marken eremua

Biopoliolen konposizio kimikoa GC-MSren bidez zehaztu zen, eta lortutako kromatogramak P1.2. Irudian irudikatzen dira. Hobeto ulertzeko, kromatogramak, a, b eta c izeneko hiru gunetan mugatu ziren.

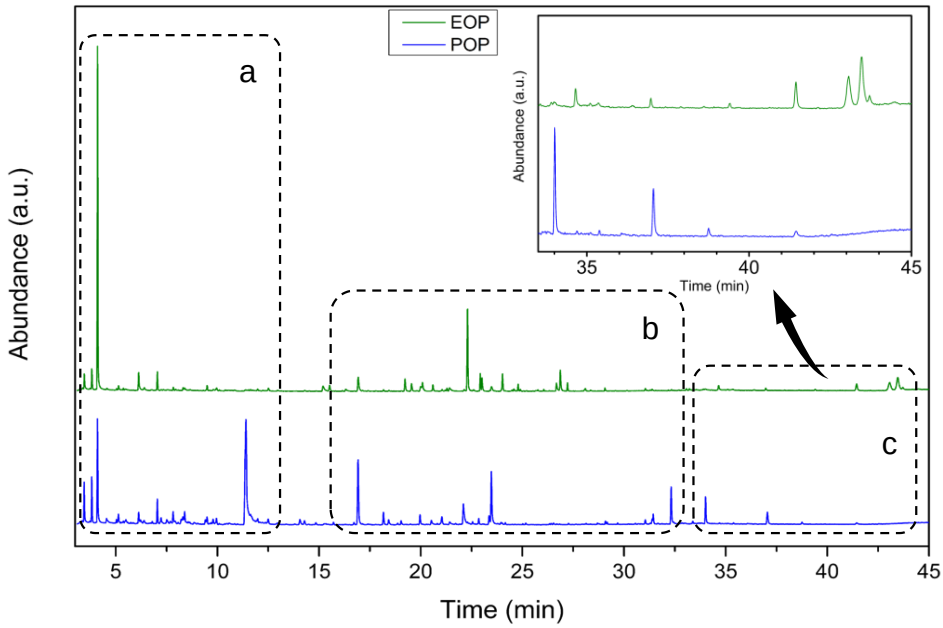


P1.2. Irudia. EOP eta POPen CG-MS kromatogramak

Lehenengo ***a*** eremua, karbohidratoen degradazio-konposatuekin erlazionatu daiteke, biopolioletan karbohidratoak zeudela egiaztatuz. Eremu honetan posible izan zen bi laginen arteko desberdintasun batzuk behatzea, lehengaien jatorri ezberdina zela eta. Horrela, zur gogorreko hemizelulosak batez ere pentosaz osatuta daudenez, nagusiki furfuralean deskonposatzen direnak, EOPren kasuan, konposatu ugariena furfurala izan zen, eta ez zen hidroximetilfurfuralaren (HMF) aztarnarik ikusi. Bestalde, zur-bigunetik datorren POP biopoliolaren kasuan, HMF izan zen konposatu ugariena, hau da, hexosen degradazio konposatu nagusia [6]. Horietaz gain, hemizelulosetatik eratorriko beste degradazio-konposatu batzuk ere ikusi

ziren, hala nola, azido glikoliko eta laktikoen esterifikaziotik eratutako etil glikolatoa eta etil laktatoa.

Aitzitik, ***b*** eta ***c*** bezala identifikatutako eskualdeetan, organosolv deslignifikazio prozesuan zehar ligninaren despolimerizatzearen ondorioz sortutako konposatuak irudikatzen dituzte, izan ere, prozesu hauetan ligninaren α eta β loturak hausten dira [7]. Hasteko, ***b*** eremuan ligninaren konposatu monomerikoak ikus daitezke. Lehen esan den bezala, EOP eta POP artean diferentziak aurkitu daitezke lehengaien jatorri ezberdina dela eta. Horrela, EOP biopoliola, S unitateetatik eratorritako konposatuetan aberatsagoa izan zen, siringaldehidoa ugariena izanik.

P1.2. Taula. CG-MS kormatogrametan ikusitako konposatuen zerrenda

| ED (min) | Konposatua | EOP | POP | Jatorria |
|---|---|---|---|---|
| 3,451 | Etil glikolatoa | ✓ | ✓ | C |
| 3,823 | Etil laktatoa | ✓ | ✓ | C |
| 4,107 | Furfurala | ✓ | ✓ | C |
| 6,129 | 5-Metilfurfurala | ✓ | ✓ | C |
| 7,042 | Etil 2-azetoxi-2-metillazetoazetatea | ✓ | ✓ | C |
| 11,045 | Hidroximetilfurfurala (HMF) | ✗ | ✓ | C |
| 16,992 | Banillina | ✓ | ✓ | G |
| 22,101 | Dihidrokoniferil alkohola | ✗ | ✓ | G |
| 22,305 | Siringaldehidoa | ✓ | ✗ | S |
| 22,934 | 4-propenil siringola | ✓ | ✗ | S |
| 23,014 | Homosiringaldehidoa | ✓ | ✗ | S |
| 23,475 | Koniferil aldehidoa | ✗ | ✓ | G |
| 24,025 | Siringilazetona | ✓ | ✗ | S |
| 26,863 | Sinapil aldehidoa | ✓ | ✗ | S |
| 34,011 | 4,4'-stilbenediol,3,3'-dimethoxy-(E) | ✗ | ✓ | G# |
| 37,053 | 3,4-Dibanilliltetrahidrofuranoa | ✗ | ✓ | G# |
| 38,755 | Secoisolariciresinol | ✗ | ✓ | G# |
| 41,443 | 4,4'-stilbenediol,3,3',5,5'-tetramethoxy- | ✓ | ✗ | S# |
| 41,451 | Dibenzilbutyrolactone | ✗ | ✓ | G# |
| 43,265 | Siringaresinola | ✓ | ✗ | S# |

ED (erretentzio denbora), C (Carbohydrate), G (Cuaiacol), S (Syringol), # Two phenolic rings

Hala eta guztiz ere, espero zen bezala, G unitateetatik eratorritako konposatuak ere ikusi ziren, proportzio txikiagoan bada ere. P1.2. Taulan laburbiltzen den bezala, azken konposatu hauek gehiengoak izan ziren POP biopoliolaren kasuan. Azkenik, $\boldsymbol{c}$ izenarekin mugatutako atalean, dimeroen eta trimeroen presentzia sumatu daiteke, nahiz eta ugaritasun gutxiarekin, konposatu horien lurrunkortasun baxua dela eta. Konposatu txiki horien ugaritasuna baxua izan bazen ere, haien presentziak ligninaren despolimerizaziotik eratorritako eta GC-MS-an ikusi ez daitezkeen konposatu handiagoak daudela adieraz dezakete.

EOP eta POP biopoliolak termograbimetrikoki aztertu ziren egitura kimikoaren eta degradazioaren arteko erlazioa aztertzeko. P1.3. Irudian, lagin bakoitzaren TGA termogramak eta dagozkien DTG kurbak irudikatzen dira. DTG kurbek bi biopoliolen arteko desberdintasunak agerian utzi zituen. Hasteko EOP biopoliolean hiru degradazio-eremu ezberdin bereizten dira. Lehenengo eta bigarren degradazio-eremu hauek % 37,64 masa-galera suposatu zuten, eta 120-260 °C tenperatura tartean kokatzen dira. Bi degradazio-urrats horiek ligninaren konposatu monomerikoen degradazioari [8] eta karbohidratoen degradazioarekin lotuta daude [9]. Horrela, 130°C-ko degradazio-tenperatura maximoa duen lehen urratsa lurrunkorragoak diren konposatuekin dago erlazionatuta eta %10,33ko masa galera suposatu zuen. Bigarren etapak 236 °C-ko degradazio-tenperatura maximoa du, eta masa-galeraren % 27,31a eragin zuten irakite-puntu altuagoko konposatu monomerikoen degradazioari dagokio. Azken degradazio-eremua (300-500 °C), 331 °C-ko degradazio-tenperatura maximoarekin, masa-galera handiena ekarri zuen, masa osoaren % 29,76a hain zuzen ere. Etapa hau ligninaren degradazioarekin erlazionatzen ohi da, eta beraz, biopolioleetan egon daitezkeen dimero, trimero eta oligomeroen degradazioari egotz dakioke [10].

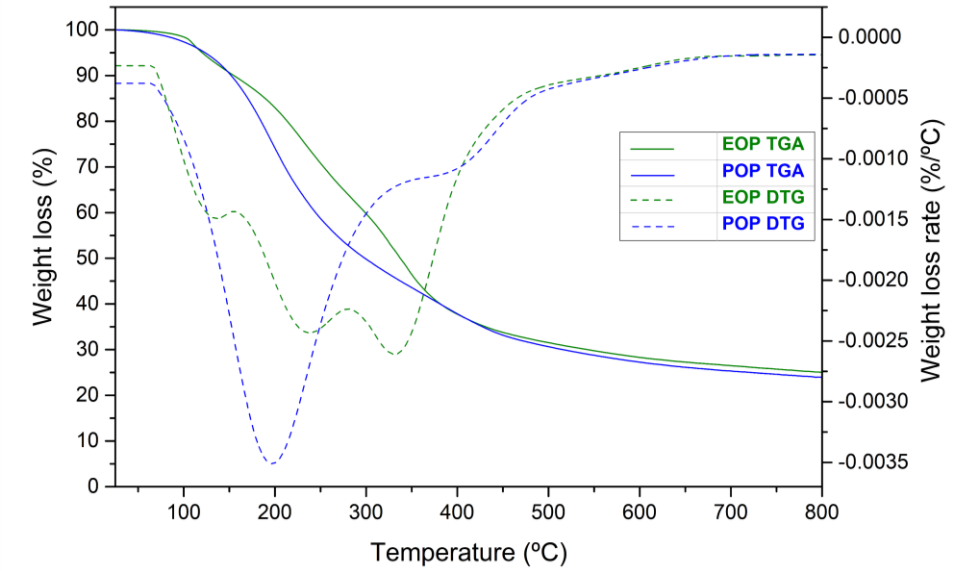


P1.3. Irudia. EOP eta POPen TGA eta DTG termogramak

POP biopoliolak, berriz, bi degradazio-urrats baino ez zituen izan. Lehenengoan masaren % 52,14ko galera suertatu izan zen eta 200 °C-ko degradazio-tenperatura izan zuen. Bestalde, lignina molekula handienen degradazio-eremu gisa identifika daitekeen zonak 380 °C inguruko degradazio-tenperatura izan zuen eta besaburu forma hartu zuen. Eremu hori degradazio osoaren %16,2 baino ez zen izan. Bi kasuetan, tenperatura 500 °C-tik gora igotzean, hasierako pisuaren %75 inguruko masa galdu zen, % 25,07ko (EOP) eta % 23,69ko (POP) hondakin solido bat geratuz.

Bio-poliol bakoitzaren pisu molekularraren banaketa $M_w$, $M_n$ eta PDI zehazteko aztertu zen. Espero zen bezala, biopoliolen jatorria zela eta, biek pisu molekular txikiko konposatuak izan zituzten, 848 g/mol eta 235 g/mol artekoak. Erabilitako kromatografoaren detekzio-muga 230 g/mol ingurukoa zenez, hemizelulosaren degradazio-konposatuak (furfural eta HMF, besteak beste) eta ligninaren monomero txikiak detekzio-tartetik kanpo geratu ziren. Hala ere, biopoliolak organosolv deslignifikazio-

prozesuan sortutako ligninaren despolimerizaziotik eratorritako dimeroak eta oligomeroak zituztela ondorioztatu daiteke. Gainera, bi biopolioletako batez besteko pisu molekularrak eta polidispertsitate-indizea oso antzekoak izan ziren, P1.3. Taulan laburbiltzen den bezala. PDIri dagokionez, biopoliolaren aplikagarritasunean eragin handia duen faktorea [11], bi biopolioletan balo txikiak lortu ziren, 1,493 (EOP) eta 1,579 (POP), hau da, banaketa nahiko homogeneoa zuten bi biopoliol lortu ziren. Gainera, lortutako balioak polieter (1,05) eta poliester (1,3) poliol komertzialen oso antzekoak izan ziren [11].

P1.3. Taula. EOP eta POPen $M_w$ (g/mol), $M_n$ (g/mol) eta PDI

| Biopoliol | $M_w$ (g/mol) | $M_n$ (g/mol) | PDI |
|---|---|---|---|
| EOP | 648 | 437 | 1,493 |
| POP | 563 | 357 | 1,579 |

P1.4. Irudian ikus daitekeen bezala, bi kromatogrametan atxikipen-denbora ia berdinak dituzten hiru seinale daude (24,8 min, 25,8 min eta 26,7 min). Hala ere, pisu molekularren banaketa kasu bakoitzean desberdina izan zela iradokitzen duten intentsitateetan desberdintasunak identifikatu ziren. Horrela, lehen seinalearen (24,8) intentsitatea handiagoa izan zen EOP biopoliolaren kasuan, POPean baino trimero eta oligomeroen ($M_w \approx 815$ g/mol) kontzentrazio handiagoa adieraziz TGAren bidez egindako analisian lortutako emaitzekin bat datorrena. Era berean, 25,8 eta 26,7 minutuko atxikipen denboretako seinaleak, hurrenez hurren, 274 g/mol eta 235 g/mol inguruko pisu molekularreko konposatuei zegozkien, biopolioletan dimeroak zeudela adieraziz. Azken seinale horrek intentsitate handiagoa izan zuen POP biopoliolaren kasuan EOP biopoliolaren kasuan baino, POP biopoliolean dimero gehiago zeudela adieraziz. Lortutako emaitzak kontutan hartuta, lortutako biopoliolen pisu molekularrak PUak sintetizatzeko beharrezkoa den pisu molekularren tartean (200-8000 g/mol) zeudela ondorioztatu daiteke [12].

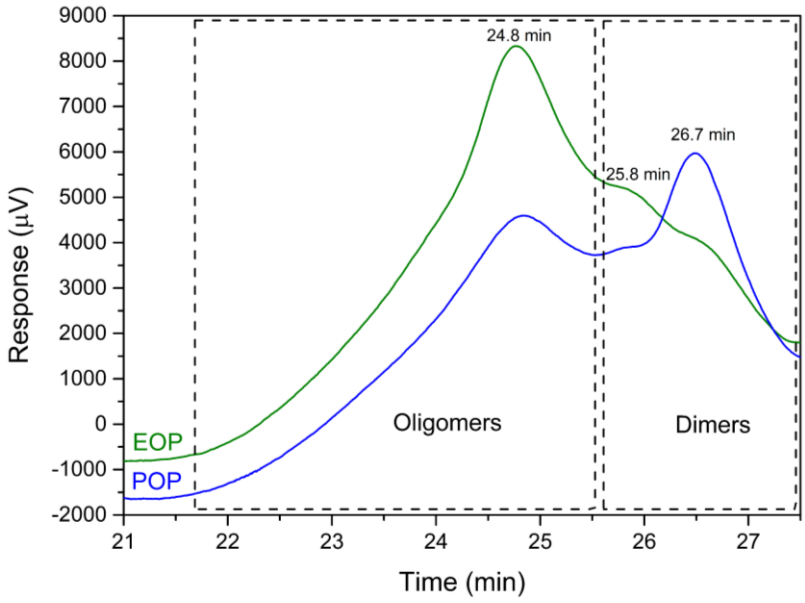


P1.4. EOP eta POPen pisu molekularraren banaketa

Aztertutako biopoliolen $A_n$, $I_{OH}$ eta *f*-ren balioak P1.4. Taulan laburbiltzen dira.

P1.4. Taula. EOP eta POPen $A_n$, $I_{OH}$ eta *f*

| **Biopoliol** | **$A_n$ (mg KOH/g)** | **$I_{OH}$ (mg KOH/g)** | ***f*** |
|---|---|---|---|
| EOP | 85,06 ± 2,51 | 618,07 ± 9,79 | 4,81 |
| POP | 64,34 ± 1,69 | 587,63 ± 0,63 | 3,74 |

Ikus daitekeenez, biopoliolek $A_n$ balio altuak aurkeztu zuten, 85,06 eta 64,31 mg KOH/g EOPrako eta POPerako, hurrenez hurren. $A_n$ balio altu hauek organosolv deslignifikazio-prozesuan sortutako azido organikoen (formikoa, lebulinikoa, glikolikoa eta laktikoa) ondorio izan ziren. Talde azidoek PUa sortzeko erreakzioaren efizientzia jaitsi dezaketenez [13]., hobe da $A_n$ balio baxuak izatea; hara ere, biomasa lignozelulosikotik datozen biopoliolen $A_n$ balioak 40 mg KOH/g baino handiagoak izan daitezke [12]. Arazo hori konpontzeko, biopoliolak neutralizatu egin daitezke NaOH edo MgOH bezalako baseak erabiliz [14].

EOP eta POP biopoliolen $I_{OH}$-ren balioak 618,07 mg KOH/g eta 587 mg KOH/g izan ziren, hurrenez hurren. Beste autore batzuek antzeko $I_{OH}$ balioak lortu zituzten lignina likidotzean [15-18]. Gosz et al., (2018)-ek Kraft pinu-lignina erabili zuen likuefakzio bidez biopoliolak ekoizteko, eta 610-670 mg KOH/g $I_{OH}$-ak balioak lortu zituen [15]. Era berean, Da Silva et al., (2019)-ek kraft lignina azido laktikoa katalizatzaile gisa erabiliz likuefaktatu zuen, 660 mg KOH/g-ko biopoliolak lortzeko [17]. Beste kasu batean, lignina komertzialaren likuefakzioaren ondoren 538 mg KOH/g-ko $I_{OH}$ balioak lortu ziren [18]. Lortutako $I_{OH}$ balioak altu samar izan ziren ligninatik eratorritako hidroxil talde erreaktibo ugariko konposatuak zeudelako [19] (dimeroak, trimeroak eta oligomeroak), deslignifikazio-prozesuan sortu zirenak eta disolbatuta geratu zirenak [19]. Bestalde, ligninetatik eratorriko konposatu horien presentziak, lortutako funtzionaltasun-balioak azaltzen ditu. $I_{OH}$-ren balioek zein funtzionaltasunekoek adierazten dute lortutako biopoliolak PUak fabrikatzeko aproposak direla, adibidez, 250-1000 mg KOH/g-ko $I_{OH}$ eta 3-8 bitarteko funtzionalitateak behar dituzten apar zurrunak, estaldura zurrunak eta elastoplastikoak sintetizatzeko [20].

Azkenik, biopoliolen portaera erreologikoa aztertu zen. Hasteko, biopoliolen propietate biskoelastikoak zehazteko oszilazio-saiakuntza bat egin zen. Horretarako, biopoliolaren likido- eta solido-maila neurtzeko hurrenez hurren erabiltzen diren galera-modulua (G'') eta biltegiratze-modulua (G') alderatu ziren [21]. P1.5. a eta b Irudietan ikus daitekeen bezala, G''-ren balioak G'-renak baino handiagoak izan ziren erabilitako maiztasun-tarte osoan, biopoliolak portaera likidoa dutela adieraziz. Gainera, bi biopoliolen pisu molekularrak kontutan hartuta (P1.3. Taula), espero zen bezala, EOP moduluen balioak POP moduluenak baino handiagoak izan ziren, hauek txikiagotu egiten baitira $M_w$-a murriztu ahala [22].

Horrez gain, biopoliolen jariakin portaera aztertzeko saiakuntza errotazional bat egin zen, biskositatearen ($\eta$), zizatzaile-tentsioaren ($\tau$) eta zizailatze-

abiaduraren ($\dot{\gamma}$) arteko erlazioa aztertuz. Parametroak Power-Lawren ekuaziora doitu ziren, **II. Eranskinaren *V. atalean*** adierazten den bezala. P1.5. Taulan lortutako balioen laburpena agertzen da eta P1.6.a irudian dagozkien fluxu-kurbak irudikatzen dira.

P1.5. Taulan laburbildutako datuen azterketatik ondoriozta daitekeenez, bi erreogramak doikuntza ona erakutsi zuten, $R^2$ balioek adierazten duten bezala. Gainera, lortutako n balioak unitatetik oso gertu zeudenez, biopoliolak Newtoniar fluido gisa jokatzen dutela esan daiteke. Newtoniar portaera hori P1.6.a Irudian antzeman daiteke, non biskositateak aplikatutako edozein deformazio-abiadurarako balio konstantea zuen. Beraz, sendotasun-indizea (κ), **II. Eranskinaren *V. atalean*** deskribatutakoa, biskositate konstantea (η) besterik ez dela esan daiteke [23].

P1.5. Taula. EOP eta POPren datuetan oinarritutako Power-Law funtzio linealak

| Biopoliol | κ(Pa·sⁿ) | n | $R^2$ |
|---|---|---|---|
| EOP | 0,016710 | 0,9650 | 0,9983 |
| POP | 0,005897 | 0,9226 | 0,9418 |

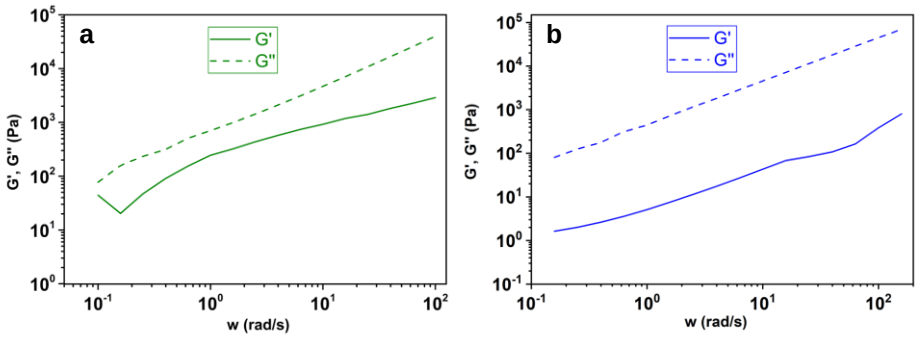


P1.5. Irudia. Biltegiratze-modulua (G') eta galera-modulua (G'') (Pa) ω(rad/s)-ren arabera. EOP (a) eta POP (b)

Dena den, biopoliolen portaera Newtoniarra berresteko, τ eta $\dot{\gamma}$ arteko erlazioa aztertu zen (P1.6. b Irudia).

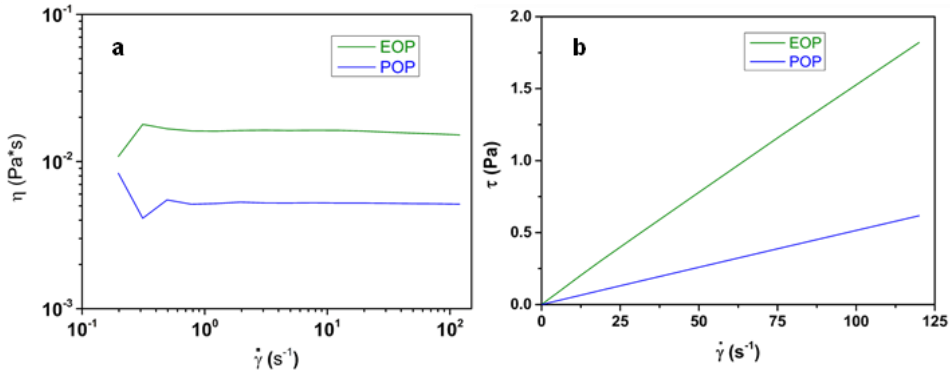


P1.6. Irudia. EOP eta POPen (a) Biskositatea (η) VS zizatzaile-abiadura ($\dot{\gamma}$) eta (b)zizatzaile-tentsioa (τ) VS zizatzaile-abiadura ($\dot{\gamma}$)

Bi biopoliolak erlazio lineala zutela baieztatu ahal izan zen, Newtoniar fluido batean espero den bezala, non malda biskositateari egokitu behar zaion. Hori baieztatuta geratu zen, P1.6. b Irudiko lerroen maldak bat etorri baitziren P1.5. Taulan adierazitako κ balioekin. Horrela, EOParen biskositatea 0,0168 Pa·s-koa izan zen; POPrena, berriz, 0,0059 Pa·s-koa izan zen. Balio horiek oso baxuak izan arren, bat datoz beste egile batzuek lortutakoekin [16, 17] eta 300 Pa·s-ren azpitik daudenez egokiak dira PUak sintetizatzeko [24]. EOPren biskositatearen balio altuagoa POPrekin alderatuta duen pisu molekular handiagoagatik azal daiteke, izan ere, biskositatea pisu molekularrarekin erlazionatuta baitago [25].

## 3. ONDORIOAK

Laburbilduz, likore beltzetan dagoen lignina prezipitatu ondoren geratzen den hondakin likidotik bi biopoliol ezberdin lortu ziren. Hasierako lehengaiarekiko lortutako errendimenduak % 5,43 eta %5,24 izan ziren EOP eta POPrentzat, hurrenez hurren. Biopoliol hauen batez besteko pisu molekularrak 648 g/mol izan ziren EOPrako eta 563 g/mol POPerako, eta polidispertsitate-indizeak 1,493 eta 1,579koak izan ziren, hurrenez hurren, polieter eta poliester poliol komertzialen oso antzekoak direnak. $I_{OH}$ eta

funtzionaltasun balioei dagokienez, 618 mg KOH/g eta 4,81 izan ziren EOPren kasuan, hurrenez hurren, eta 587 mg KOH/g eta 3,74 POPren kasuan. Lortutako $A_n$ balioak, biopoliolen jatorria zela eta, oso altuak suertatu ziren. Azkenik, EOP eta POP biopoliolen portaera erreologikoaren azterketak biopoliolak portaera Newtoniarra zutela frogatu zuen, 0,0168 Pa·s eta 0,0059 Pa·s-ko biskositate balioekin hurrenez hurren. Ezaugarri horiek guztiek biopoliolak PUak ekoizteko egokiak direla adierazten dute, eta beraz, organosolv likore beltzek arrakastaz balorizatu ziren.

## ERREFERENTZIAK

[1] Z. Chi, Z. Wang, Y. Liu, G. Yang, Chem. Eng. J. 331(August 2017) (2018) 317–25. 10.1016/j.cej.2017.08.121.

[2] L. Chen, X. Wang, H. Yang, Q. Lu, D. Li, Q. Yang, H. Chen, J. Anal. Appl. Pyrolysis 113 (2015) 499–507.

[3] J. Fernández-Rodríguez, X. Erdocia, C. Sánchez, M. González Alriols, J. Labidi, J. Energy Chem. 26(4) (2017) 622–31. 10.1016/j.jechem.2017.02.007.

[4] X. Jiang, (5) (2012) 827–33. 10.1002/ceat.201000400.

[5] A. Morales, F. Hernández-ramos, L. Sillero, R. Fernández-marín, 315(May) (2020). 10.1016/j.biortech.2020.123896.

[6] F. Hernández-Ramos, J. Fernández-Rodríguez, M.G. Alriols, J. Labidi, X. Erdocia, Fuel 280(February) (2020) 118524. 10.1016/j.fuel.2020.118524.

[7] Z. Zhang, M.D. Harrison, D.W. Rackemann, W.O.S. Doherty, I.M. O'Hara, Green Chem. 18(2) (2016) 360–81. 10.1039/c5gc02034d.

[8] M.M. Jensen, D.T. Djajadi, C. Torri, H.B. Rasmussen, R.B. Madsen, E. Venturini, I. Vassura, J. Becker, B.B. Iversen, A.S. Meyer, H. Jørgensen, D. Fabbri, M. Glasius, ACS Sustain. Chem. Eng. 6(5) (2018) 5940–9. 10.1021/acssuschemeng.7b04338.

[9] C. Girometta, D. Dondi, R.M. Baiguera, F. Bracco, D.S. Branciforti, S. Buratti, S. Lazzaroni, E. Savino, Cellulose 27(11) (2020) 6133–48. 10.1007/s10570-020-03208-4.

[10] A. Morales, B. Gullón, I. Dávila, G. Eibes, J. Labidi, P. Gullón, Ind. Crops Prod. 124(May) (2018) 582–92. 10.1016/j.indcrop.2018.08.032.

[11] J. D'Souza, R. Camargo, N. Yan, Polym. Rev. 57(4) (2017) 668–94. 10.1080/15583724.2017.1283328.

[12] S. Hu, X. Luo, Y. Li, ChemSusChem 7(1) (2014) 66–72. 10.1002/cssc.201300760.

[13] S. Hu, Y. Li, Ind. Crops Prod. 57 (2014) 188–94. 10.1016/j.indcrop.2014.03.032.

[14] W. Jiang, A. Kumar, S. Adamopoulos, Ind. Crops Prod. 124(March) (2018) 325–42. 10.1016/j.indcrop.2018.07.053.

[15] K. Gosz, P. Kosmela, A. Hejna, G. Gajowiec, Ł. Piszczyk, Wood Sci. Technol. 52(3) (2018) 599–617. 10.1007/s00226-018-0991-4.

[16] R. Briones, L. Serrano, J. Labidi, J. Chem. Technol. Biotechnol. 87(2) (2012) 244–9. 10.1002/jctb.2706.

[17] S.H.F. da Silva, I. Egüés, J. Labidi, Ind. Crops Prod. 137(March) (2019) 687–93. 10.1016/j.indcrop.2019.05.075.

[18] R. Mohammadpour, G. Mir Mohamad Sadeghi, J. Polym. Environ. 28(3) (2020) 892–905. 10.1007/s10924-019-01650-5.

[19] R. El Hage, N. Brosse, P. Sannigrahi, A. Ragauskas, Polym. Degrad. Stab. 95(6) (2010) 997–1003. 10.1016/j.polymdegradstab.2010.03.012.

[20] Y. LI, X. LUO, S. HU, Bio-based Polyols and Polyurethanes, Springer, 2015.

[21] Y.C. Tseng, Y.C. Hsieh, N.Y. Chin, W.Y. Huang, S.S. Hou, J.S. Jan, Polymer

(Guildf). 196(1) (2020) 122426. 10.1016/j.polymer.2020.122426.

[22] K. Behera, Y.H. Chang, F.C. Chiu, J.C. Yang, Polym. Test. 60 (2017) 132–9. 10.1016/j.polymertesting.2017.03.015.

[23] P. Parcheta, J. Datta, Polym. Test. 67(January) (2018) 110–21. 10.1016/j.polymertesting.2018.02.022.

[24] C.A. Cateto, M.F. Barreiro, A.E. Rodrigues, M.N. Belgacem, Ind. Eng. Chem. Res. 48(5) (2009) 2583–9. 10.1021/ie801251r.

[25] S.H.F. da Silva, P.S.B. dos Santos, D. Thomas da Silva, R. Briones, D.A. Gatto, J. Labidi, J. Wood Chem. Technol. 37(5) (2017) 343–58. 10.1080/02773813.2017.1303513.

*“Patience you must have my young Padawan”*

*Master Yoda*

## Publication II

# Organosolv lignin-based bio-polyols for polyurethane production: Process optimisation through response surface methodology

## ABSTRACT

The polyurethane industry relies on polyols of petrochemical origin. However, although the polyol industry is a growing business, the environmental consequences associated with the excessive petroleum consumption can be serious. Therefore, the use of renewable raw materials, such as lignin, to manufacture bio-polyols is being studied to replace partially or totally the use of petrochemical polyols. Lignin is the most abundant renewable phenolic polymer available on Earth and can be employed for different industrial applications, such as polyurethane manufacture, thus diminishing the dependence on oil. In this work, hardwood (*Eucalyptus globulus*) and softwood (*Pinus Radiata*) organosolv lignins were employed for producing bio-polyols, through microwave assisted liquefaction, with specific properties to be used in the synthesis of rigid and elastic polyurethanes. The reaction parameter values were optimised by response surface methodology to establish the most suitable conditions to produce bio-polyols from both type of lignins for rigid and elastic polyurethane formulation.

The effect of the independent variables catalyst concentration (%wt.), temperature (°C) and Polyethylene glycol/Glycerol weight ratio on the molecular weight and hydroxyl number index of bio-polyols was evaluated. The optimum reaction conditions of bio-polyols for rigid polyurethanes were virtually equal for the two lignins, 159-161°C, Polyethylene glycol/Glycerol

ratio of 3 and no catalyst. Conversely, the bio-polyols for elastic polyurethanes required different reaction parameters depending on the lignin used, 180 °C, 7.57 (Polyethylene glycol/Glycerol ratio) and 5% wt. of catalyst for hardwood lignin and 160 °C, 7.34 (Polyethylene glycol/Glycerol ratio) and 3.85% wt. of catalyst for softwood lignin. In addition, the bio-polyols obtained at optimised conditions were fully characterised and acid number, polydispersity index, functionality and the rheological behaviour of them was studied.

# 1. MATERIALS AND METHODS

## 1.1. Materials

The raw materials and chemicals used for this work were obtained as described in s***ection 2.1*** of the **2nd PART.**

## 1.2. Lignin obtaining procedure

Lignin used in this work were obtained after the organosolv delignification process and the subsequent ultrasound treatment of the black liquor described in ***section 2.2*** of the **2nd PART**.

## 1.3. Lignin characterisation

*Eucalyptus globulus* and *Pinus radiata* organosolv lignins obtained before (EOL and POL) and after ultrasound treatment (EOUL and POUL) were analysed using the techniques listed in Table 2.3 of the **2nd PART**, **(*section 2.6*)** and described in **Appendix II**.

## 1.4. Experimental design of microwave assisted lignin liquefaction

### 1.4.1. Microwave assisted lignin liquefaction procedure

Liquefaction reaction of lignins obtained after ultrasound treatment was carried out through the methodology described in ***section 2.3*** of the **2nd PART**.

### 1.4.2. Experimental design

A response surface methodology (RSM) was used to determine the effect of the independent variables: Catalyst concentration (%wt.) (Cat), Temperature (°C) (Temp) and Polyethylene glycol/Glycerol weight ratio (%wt.) (PEG/Gly) on the molecular weight ($M_w$) and hydroxyl number index ($I_{OH}$) of bio-polyols. A three block Box-Benkhen Design (BBD), which consisted in 15 experiment, with three central point was selected for the experimental design and optimisation.

A second-order polynomial equation (Equation P2.1) was used to fit the experimental data:

$$y = b_0 + \sum_{i=1}^{3} b_i x_i + \sum \sum_{i<j=2}^{3} b_{ij} x_i x_j + \sum_{i=1}^{3} b_{ii} x_i^2 + \varepsilon \qquad \text{Equation P2.1}$$

where $y_j$ represent the dependent variables ($M_w$ and $I_{OH}$), $b_0$, $b_i$, $b_{ii}$, $b_{ij}$ correspond to the regression coefficients estimated from the experimental results employing the least-squares method and $x_i$ and $x_j$ are the dimensionless normalised independent variables Cat, Temp and PEG/Gly, with a variation range from -1 to 1.

Through the evaluation of the lack of fit, the $R^2$ determination coefficient, the significance of the regression coefficients and the F-test value obtained from the analysis of variance, the suitability of the model was validated. The

experimental design, statistical analysis and regression model were generated employing the Statgraphics Centurion version XVI (Statpoint Technolgies Inc., Warrenton, VA, USA). Optimal conditions to produce polyols for rigid and elastic PU, predicted by the desirability function of the abovementioned software, were obtained by adjusting the dependent variables $M_w$ and $I_{OH}$. Microsoft Excel´s Data Analysis Add-In version 2016 (Microsoft, USA), was employed to fit the experimental data. Model validation was carried out by performing a triplicate of each experiment under optimal conditions and comparing them with the values predicted by the model.

Table P2.1. Experimental design involved in the study

| Variable | Definition | Units | Nomenclature | Value |
|---|---|---|---|---|
| Fixed | Time | min | | 5 |
| | SLR* | (w/w) | | 1/6 |
| Independent | Catalyst | (% wt.) | Cat | 0-5 |
| | Temperature | °C | Temp | 140-180 |
| | PEG/Gly ratio | (w/w) | PEG/Gly | 3-9 |
| Dependents | Molecular weight | g/mol | $M_w$ | |
| | Hydroxyl number | mg KOH/g | $I_{OH}$ | |

*Solid to liquid ratio (SLR)

The experimental variables considered in this study (Table P2.1), include the fixed variables, the independent variables, as well as the dependent ones, including the corresponding variation ranges of each variable.

### 1.4.3. Characterisation of the obtained bio-polyols

Bio-polyols synthesised to perform the experimental design were analysed to determine the molecular weight distribution ($M_w$, $M_n$ and $M_w/M_n$) as well

as the $I_{OH}$. For the determination of the molecular weight distribution, GPC was employed following the procedure described in **Appendix II**.

### 1.4.4. Characterisation of bio-polyols at the optimised reaction conditions

To validate the model, experiments were triplicated under the optimal conditions and the results ($M_w$ and $I_{OH}$ values) were compared with the theoretical ones. Once the model was validated, the bio-polyols obtained under the optimal conditions were further characterised employing the techniques listed in Table 2.3 of the **2nd PART**, **(*section 2.6*)**. These characterisation techniques are described in detail in **Appendix II.**

## 2. RESULTS AND DISCUSSION

### 2.1. Lignin characterisation

Since lignins with low molecular weight are desired to produce polyols [1], the obtained EOL and POL were ultrasonicated. These ultrasonicated lignins, called EOUL and POUL from the ultrasonication of EOL and POL respectively, showed lower molecular weight than the originals as summarised in Table P2.2.

Table P2.2. Mw (g/mol), Mn (g/mol) and PDI of organosolv lignins and ultrasonicated organosolv lignins

| Sample | $M_w$ (g/mol) | $M_n$ (g/mol) | PDI |
|---|---|---|---|
| EOL | 3632 | 952 | 3.81 |
| EOUL | 2837 | 888 | 3.20 |
| POL | 3529 | 1035 | 3.41 |
| POUL | 2924 | 911 | 3.21 |

In both cases, similar molecular weight reduction was achieved with respect to the original lignins. Concretely, a 21.8% reduction in the case of EOUL and 17.1% for POUL. The molecular weight reduction, although considerable, was far from that obtained by Wells et al. (2013) [2], who obtained a reduction of 85.9% under the studied conditions.

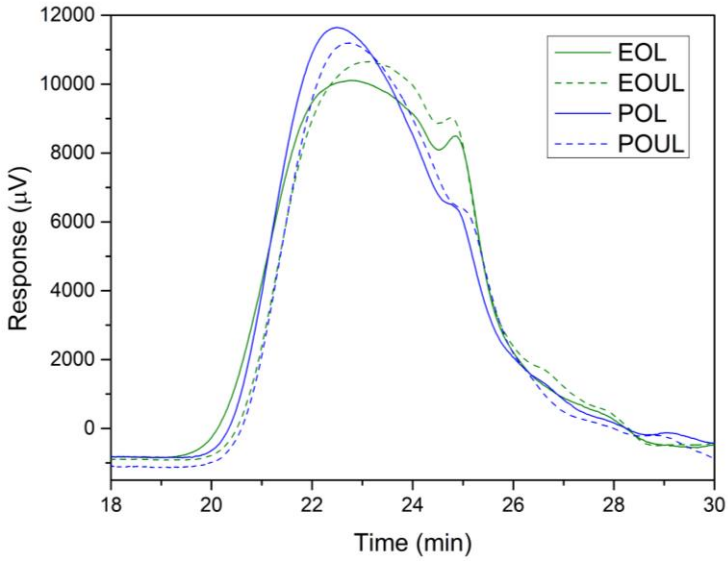


Figure P2.1. Molecular weight distribution of organosolv lignins

This difference could be due to a lower effect of cavitation because of the employed equipment. This decrease in the molecular weights can be observed in Figure P2.1 since the chromatograms corresponding to the ultrasonicated lignins (EOUL and POUL) exhibited lower retention times than the original ones.

ATR-FTIR spectroscopy was employed to characterise lignins to confirm that their chemical structure was not altered during the ultrasound fractionation process. As can be seen in Figure P2.2, no differences were observed between lignin samples from the same raw material before and after being subjected

to the ultrasonication process. Thus, it can be concluded that the ultrasound process did not produce any changes in the chemical structure of the lignins.

As can be observed, the fingerprint region of the ATR-FTIR spectra (Figure P2.2) showed the characteristic bands of lignin. In all samples a broad peak (3415 $cm^{-1}$) corresponding to OH stretching of phenolic units is observed. The vibration of aliphatic CH bonds was also visible at between 2970 $cm^{-1}$ and 2840 $cm^{-1}$. The band of carbonyl group, the vibration of the aromatic skeleton plus CO stretching and the stretching of CC plus C-O plus C=O at 1705 $cm^{-1}$, 1595 $cm^{-1}$ and 1213 $cm^{-1}$ respectively appeared in all samples. Nevertheless, since hardwood lignins are generally composed by an equal proportion of S and G units, whereas softwood lignin is predominantly constituted by G units several differences could be observed between lignin from hardwood and softwood. Thus, the spectra of lignin from *Eucalyptus globulus* showed more intense signal in the peaks at 1326 $cm^{-1}$, 1110 $cm^{-1}$ and 833 $cm^{-1}$. These bands correspond to the condensed S and G rings, the aromatic CH deformation of S units and to CH group out of plane in positions 2 and 6 in S units. On the other hand, in the case of lignin from *Pinus radiata*, the signals were more intense in the bands corresponding to the G units, i.e: vibration of the aromatic ring in G units (1510 $cm^{-1}$), G ring plus CO (1265 $cm^{-1}$), aromatic CH in plane deformation of G units (1029 $cm^{-1}$) and CH out of plane in position 2, 5 and 6 in G units (860 $cm^{-1}$ and 811 $cm^{-1}$) [3].

## 2.2. Optimisation of the conditions for obtaining suitable bio-polyols for PU applications

In the present study, microwave-assisted irradiation method was employed. A response surface methodology in combination with a Box-Behnken design was employed to accomplish the optimisation of the bio-polyols obtaining reaction conditions. Statgraphic software was used to establish the experiments set, which is summarised in Table P2.3, as well as the

experimental values that corresponded to the dependent variables ($Y_{IOH}$ and $Y_{Mw}$).

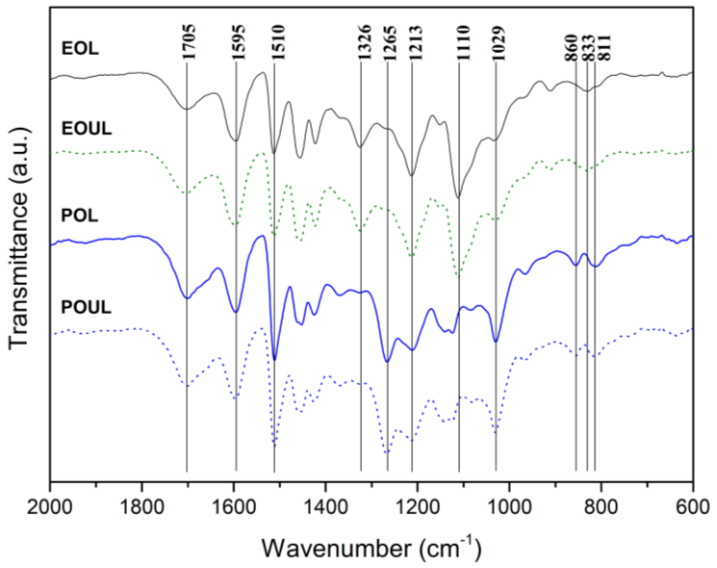


Figure P2.2. Fingerprint region of ATR-FTIR spectra of non-ultrasonicated and ultrasonicated organosolv lignins

Regarding Table P2.3, the $I_{OH}$ values ranged from 221.5 mgKOH/g (exp. 3) to 688.2 mgKOH/g (exp. 10) for *Eucalyptus globulus* bio-polyol, and from 211.3 mgKOH/g (exp. 1) to 592.6 mgKOH/g (exp. 4) for *Pinus radiata* bio-polyol. On the other hand, $M_w$ ranged between 1637 g/mol (exp. 13) and 5692 g/mol (exp. 6) and between 1372 g/mol (exp. 14) and 5469 g/mol (exp. 2) for the bio-polyols obtained from the liquefaction of lignin from *Eucalyptus globulus* and *Pinus radiata,* respectively.

In Table P2.4 the regression coefficients and their corresponding confidence levels according to Student's t-test (above 90%), as well as the $R^2$ determination coefficient, the adjusted $R^2$ and the statistical significance (Fisher's F-test) are summarised. $F_{\alpha=0.05}$, which is the value of the distribution that leaves an area behind the density function equal to 0.05 on its right (95% of confidence level), was calculated employing the free software R (version

4.1.1) were the degrees of freedom are expressed through Equation P2.2. On the other hand, the experimental *F* (*F*-exp) was determined using Equation P2.3.

$$\text{Degrees of freedom} = K; n-(K+1) \qquad \text{Equation P2.2}$$

$$F = \frac{R^2/K}{(1-R^2)/[n-(K+1)]} \qquad \text{Equation P2.3}$$

where *K* is the number of model parameters, *n* is the number of data points and $R^2$ is the determination coefficient.

Table P2.3. Independent normalised (Norm.) and not normalised (Not norm.) variables, Cat (%wt.) ($X_1$); Temperature (°C) ($X_2$) and PEG/Gly (w/w) ($X_3$), together with the dependent variables, average molecular weight ($Y_{Mw}$) (g/mol) and hydroxyl number ($Y_{IOH}$) (mgKOH/g), of the Box-Behnken experimental design

| Exp | Independent variables | | | | | | Dependent variables | | | |
|---|---|---|---|---|---|---|---|---|---|---|
| | Not norm. variables | | | Norm. Variables | | | *Eucalyptus globulus* | | *Pinus radiata* | |
| | Cat | T (°C) | PEG/Gly (w/w) | $X_1$ | $X_2$ | $X_3$ | $Y_{Mw}$ | $Y_{IOH}$ | $Y_{Mw}$ | $Y_{IOH}$ |
| 1 | 2.5 | 180 | 9 | 0 | 1 | 1 | 3532 | 236 | 3576 | 211 |
| 2 | 2.5 | 160 | 6 | 0 | 0 | 0 | 2904 | 312 | 5469 | 294 |
| 3 | 0 | 180 | 6 | -1 | 1 | 0 | 1752 | 222 | 1710 | 331 |
| 4 | 2.5 | 180 | 3 | 0 | 1 | -1 | 3753 | 563 | 4896 | 593 |
| 5 | 2.5 | 140 | 9 | 0 | -1 | 1 | 2169 | 243 | 4012 | 321 |
| 6 | 5 | 180 | 6 | 1 | 1 | 0 | 5926 | 290 | 4594 | 383 |
| 7 | 0 | 140 | 6 | -1 | -1 | 0 | 1662 | 261 | 1461 | 330 |
| 8 | 5 | 160 | 3 | 1 | 0 | -1 | 3854 | 688 | 5136 | 552 |
| 9 | 2.5 | 160 | 6 | 0 | 0 | 0 | 3005 | 263 | 4469 | 232 |
| 10 | 2.5 | 140 | 3 | 0 | -1 | -1 | 2269 | 485 | 2922 | 457 |
| 11 | 5 | 160 | 9 | 1 | 0 | 1 | 3623 | 224 | 4116 | 194 |
| 12 | 2.5 | 160 | 6 | 0 | 0 | 0 | 2700 | 290 | 4077 | 247 |
| 13 | 0 | 160 | 9 | -1 | 0 | 1 | 1637 | 326 | 1497 | 354 |
| 14 | 0 | 160 | 3 | -1 | 0 | -1 | 1771 | 645 | 1372 | 458 |
| 15 | 5 | 140 | 6 | 1 | -1 | 0 | 3472 | 248 | 3991 | 262 |

Table P2.4. Regression coefficient plus their statistical parameters

| Coefficients | *Eucalyptus globulus* | | *Pinus radiata* | |
|---|---|---|---|---|
| | $Y_{Mw}$ | $Y_{IOH}$ | $Y_{Mw}$ | $Y_{IOH}$ |
| $b_0$ | 2869.67[a] | 288.02[a] | 4671.67[a] | 257.78[a] |
| $b_1$ | 1256.63[a] | -0.43 | 1474.63[a] | -10.04 |
| $b_2$ | 673.88[a] | 13.85 | 298.75 | 18.42 |
| $b_3$ | -85.75 | -164.38[a] | -140.63 | -122.31[a] |
| $b_{12}$ | 591.00[b] | 20.40 | 88.50 | 29.96[c] |
| $b_{13}$ | -24.25 | -36.49 | -286.25 | -63.49[a] |
| $b_{23}$ | -30.25 | -11.99 | -602.50[c] | -61.37[a] |
| $b_{11}$ | 61.92 | 23.42 | -1276.96[a] | 31.27[c] |
| $b_{22}$ | 271.42 | -56.36[c] | -455.71 | 37.30[c] |
| $b_{33}$ | -210.33 | 159.27[a] | -364.46 | 100.30[a] |
| $R^2$ | 0.97 | 0.97 | 0.96 | 0.98 |
| $R^2$-adjusted | 0.92 | 0.90 | 0.87 | 0.95 |
| $F_{\alpha=0.05}$ | 4.773 | | | |
| *F*-exp | 19.516 | 15.463 | 11.795 | 28.588 |
| Area under *F*-exp | 0.002 | 0.004 | 0.007 | 0.001 |
| Significance level | 99.779 | 99.618 | 99.287 | 99.911 |

[a]Significant coefficients at the 99% of confidence level.
[b]Significant coefficients at the 95% of confidence level.
[c]Significant coefficients at the 90% of confidence level.

According to Table P2.4, the obtained $R^2$ determination coefficients were above 0.95 in all cases. Regarding the bio-polyol obtained from the liquefaction of *Eucalyptus globulus* lignin, $R^2$ of 0.97 was obtained for both $M_w$ and $I_{OH}$, while for the polyol obtained from the liquefaction of *Pinus radiata* lignin these values were 0.96 for $M_w$ and 0.98 for $I_{OH}$. This indicated that only a small number of total variations remained unexplained using the selected model, concretely 3% for the former and 4% and 2% for the latter. According with the obtained $R^2$ determination coefficients, it could be concluded that the model was appropriate to describe the interactions between the selected variables, since the $R^2$ determination coefficient indicate the validity of the design via the explanation of the total variations of the model [4].

Furthermore, the predictivity of the model obtained through Fisher's F-test confirmed that the selected model was statistically relevant since the *F*-experimental values were higher than the $F_\alpha$ values in all cases, which indicates that the models were statistically relevant above 95%. [5].

Regression coefficients presented in Table P2.4 showed a different behaviour depending on the used raw material. Thus, $X_1$, $X_2$ and the interaction $X_{12}$ were the most relevant independent variables for the molecular weight in the case of the bio-polyol obtained from *Eucalyptus globulus*, while in the case of the bio-polyol from *Pinus radiata* it was the independent variable catalyst concentration $X_1$, the interaction $X_{23}$ and the quadratic effect of $X_{11}$. On the other hand, the independent variables that demonstrated a significant relevance for the $I_{OH}$ were the effect of the PEG/Gly ($X_3$) and the quadratic effects $X_{22}$ and $X_{33}$ for the bio-polyol obtained from *Eucalyptus globulus*, whereas for the bio-polyol from *Pinus radiata* only the independent variables catalyst concentration ($X_1$) and temperature ($X_2$) did not show a significant effect, while the remaining variables were significantly relevant.

### 2.2.1. Average molecular weight ($M_w$)

Figure P2.3 shows the influence of the independent variables as well as their interactions on the molecular weight of bio-polyols obtained through the liquefaction of *Eucalyptus globulus* (2.3a, 2.3b and 2.3c) and *Pinus radiata* (2.3d, 2.3e and 2.3f).

Figures 2.3a and 2.3d represent the response surfaces in which the interaction effect between the independent variables $X_1$ and $X_3$ is shown. As is evident in both figures, the independent variable $X_3$ had almost no influence on the response ($M_w$). On the other hand, in both cases, an increment in the concentration of the catalyst increased the molecular weight of the obtained bio-polyols. It should be noted in Figure P2.3d that, for the bio-polyols that were obtained from the

liquefaction of lignin from *Pinus radiata*, the maximum value of $M_w$ was obtained for a catalyst concentration between 4% and 4.5%, after which the molecular weight decreased as the concentration increased. This behaviour could be explained by the influence of the quadratic term of the catalyst ($X_{11}$) on the molecular weight equation.

The influence of the independent variables $X_1$ and $X_2$ and their interaction on the molecular weight for a fixed value of the independent variable $X_3$ ($X_3$=0) is shown in Figure P2.3b and 2.3e. In both cases, an increase of the catalyst concentration ($X_1$) and the temperature ($X_2$) resulted in an increase of the molecular weight of the bio-polyols. As can be seen, the bio-polyol from the liquefaction of *Eucalyptus globulus* lignin reached the maximum molecular weight at one of the extremes of the design (Temperature of 80 ºC and Catalyst concentration of 5%). On the other hand, the bio-polyol from *Pinus radiata* lignin reached its maximum value of $M_w$ for a catalyst concentration around 4% and decreased from this point as the concentration increased due to the quadratic effect of the independent variable ($X_1$) on the molecular weight equation. As for temperature, the highest $M_w$ was obtained for a temperature of 175ºC and decreased as the temperature increased above this point, although the quadratic term $X_{22}$ was not significantly relevant (Table P2.4).

Figures P2.3c and 2.3f show the response surface of $M_w$ in function of temperature and PEG/Gly for a fixed value of concentration ($X_1$=0). According to the regression coefficients summarised in Table P2.4, the molecular weight of the bio-polyol from *Eucalyptus globulus* was not affected by the independent variable PEG/Gly whilst the influence of the temperature was significantly relevant. This is evident from Figure P2.3c, where it can be observed that a variation on the temperature had a significant impact on the molecular weight of the bio-polyol, whereas the PEG/Gly had little influence on the molecular weight regardless of the reaction temperature. On the other hand, in the case of bio-polyol from the liquefaction of lignin from *Pinus radiata* (Figure P2.3f), neither the independent

variable temperature nor PEG/Gly had a relevant significance in the molecular weight equation, although the interaction between both ($X_{23}$) proved to be significantly relevant. In Figure P2.3f, it can be noticed that the molecular weight of the bio-polyols is favoured by a high temperature and low PEG/Gly, obtaining the maximum when the temperature was at its highest (180 ºC) and the PEG/Gly was at its lowest, that is, at one of the extremes of the design.

One explanation for the high influence of the independent variables $X_1$ and $X_2$ on the $M_w$, could be that lignin during the microwave liquefaction process first degrades into small fragments that react with polyhydric alcohols (polyethylene glycol and glycerol) via ether bonds. Nevertheless, in the presence of catalyst and elevated temperatures, these lignin fragments can repolymerise, resulting in larger molecules and thus increasing the molecular weight [6,7].

### 2.2.2. Hydroxyl number ($I_{OH}$)

The influence of the independent variables and their interactions upon $I_{OH}$ of the liquefied bio-polyols are shown in Figures P2.4a, 2.4b and 2.4c (*Eucalyputs globulus*) and 2.4d, 2.4e and 2.4f (*Pinus radiata*). For a fixed value of the temperature ($X_2$=0), the influence of the independent variables $X_1$ and $X_3$ as well as the interactions between them are shown in Figures P2.4a and 2.4d. As mentioned above, the independent variable $X_1$ did not show significant influence on the $I_{OH}$ of the bio-polyols regardless the used raw material. On the other hand, the independent variable $X_3$ exhibited a significant influence in both cases, as indicated in Table P2.4. This behaviour is illustrated in the response surfaces curves. In both cases, an increase in the ratio resulted in a reduction of the hydroxyl number, whereas increasing the amount of glycerol in the mixture, i.e., reducing the PEG/Gly, drastically increased the hydroxyl number. It should be noted that, although the catalyst was not significantly influential, both the maximum and minimum hydroxyl value of the bio-polyols were obtained by using high concentrations of catalyst.

The response surfaces 2.4b and 2.4e were obtained by fixing the independent variable $X_3$ to 0. Figure 4b present a saddle point as a critical point, which means that the equilibrium is an inflection point between a relative maximum and a relative minimum. Therefore, this point does not serve as an optimal value. However, it is possible to identify the optimal region by visual observation of the surface [8]. Thus, to maximise the $I_{OH}$, a high temperature (180 ºC) and a catalyst concentration around 3.5% is preferable, while the minimum $I_{OH}$ value was obtained employing a reaction temperature around 170 ºC without catalyst. On the other hand, a clear minimum $I_{OH}$ value at 170 ºC and a catalyst concentration of 1.5% was observed in the case of the bio-polyol obtained from the liquefaction of *Pinus radiata* lignin (Figure P2.4e).

Finally, the response surfaces corresponding to the interaction of the independent variables temperature ($X_2$) and PEG/Gly ($X_3$), as well as their interactions, for a fixed value of $X_1$=0 are plotted in Figures P2.4c and 2.4f. Similarly, to Figures P2.4a and 2.4d, it is possible to appreciate the great influence of the independent variable $X_3$ on the $I_{OH}$. Thus, a lower PEG/Gly implied an increase in the $I_{OH}$, while a higher ratio resulted in a decrease of the hydroxyl number of the bio-polyols. Therefore, a minimum of hydroxyls was obtained for a PEG/Gly of almost 9 at a temperature of 170 ºC in the case of bio-polyol from the liquefaction of *Pinus radiata* lignin (Figure P2.4f). On the other hand, the response surface corresponding to the liquefaction of *Eucalyputs globulus* lignin (Figure P2.4c) exhibited a saddle point. In this case, the maximum $I_{OH}$ was obtained for a temperature of 165 ºC and a maximum PEG/Gly (3), whereas the minimum $I_{OH}$ corresponded to the maximum temperature (180 °C) and a PEG/Gly close to 8.

From the regression data summarised in Table P2.4 and the response surfaces, it can be noticed that the independent variable $X_3$ had the largest influence on the $I_{OH}$. This is due to the fact that polyethylene glycol has a lower number of free hydroxyls than glycerol, and therefore, as the amount of PEG increases with respect to glycerol, the hydroxyl number of the polyol decreases [9].

### 2.2.3. Optimisation and model validation

The aim of the optimisation was to determine the optimal reaction conditions for the synthesis of bio-polyols suitable for the manufacture of rigid and elastic polyurethanes. To do that, the desirability function of the Statgraphic Centurion XVI software was employed. In the optimisation of the bio-polyol conditions for the synthesis for rigid polyurethanes, the objective was to minimise the molecular weight while increasing the hydroxyl groups, whereas the opposite was sought for the optimisation of reaction conditions in the case of elastic polyurethane bio-polyols, i.e., an increase in the molecular weight of the bio-polyols while reducing the hydroxyl groups [10]. The optimised reaction settings for the above-mentioned bio-polyols are summarised in Table P2.5, where the not-normalised and the normalised values of the independent variables are included as well.

Table P2.5. Not-normalised and normalised values of the optimal points

| Origin | Independent variables | Rigid bio-polyol | | Elastic bio-polyol | |
|---|---|---|---|---|---|
| | | Not-norm. | Norm. | Not-norm. | Norm. |
| *Eucalyptus globulus* | $X_1$ | -1 | 0.00 | 1 | 5.00 |
| | $X_2$ | 0.0479 | 160.96 | 1 | 180.00 |
| | $X_3$ | -1 | 3.00 | 0.5246 | 7.57 |
| *Pinus radiata* | $X_1$ | -1 | 0.00 | 0.5430 | 3.86 |
| | $X_2$ | -0.0456 | 159.09 | 0.0066 | 160.13 |
| | $X_3$ | -1 | 3.00 | 0.4466 | 7.34 |

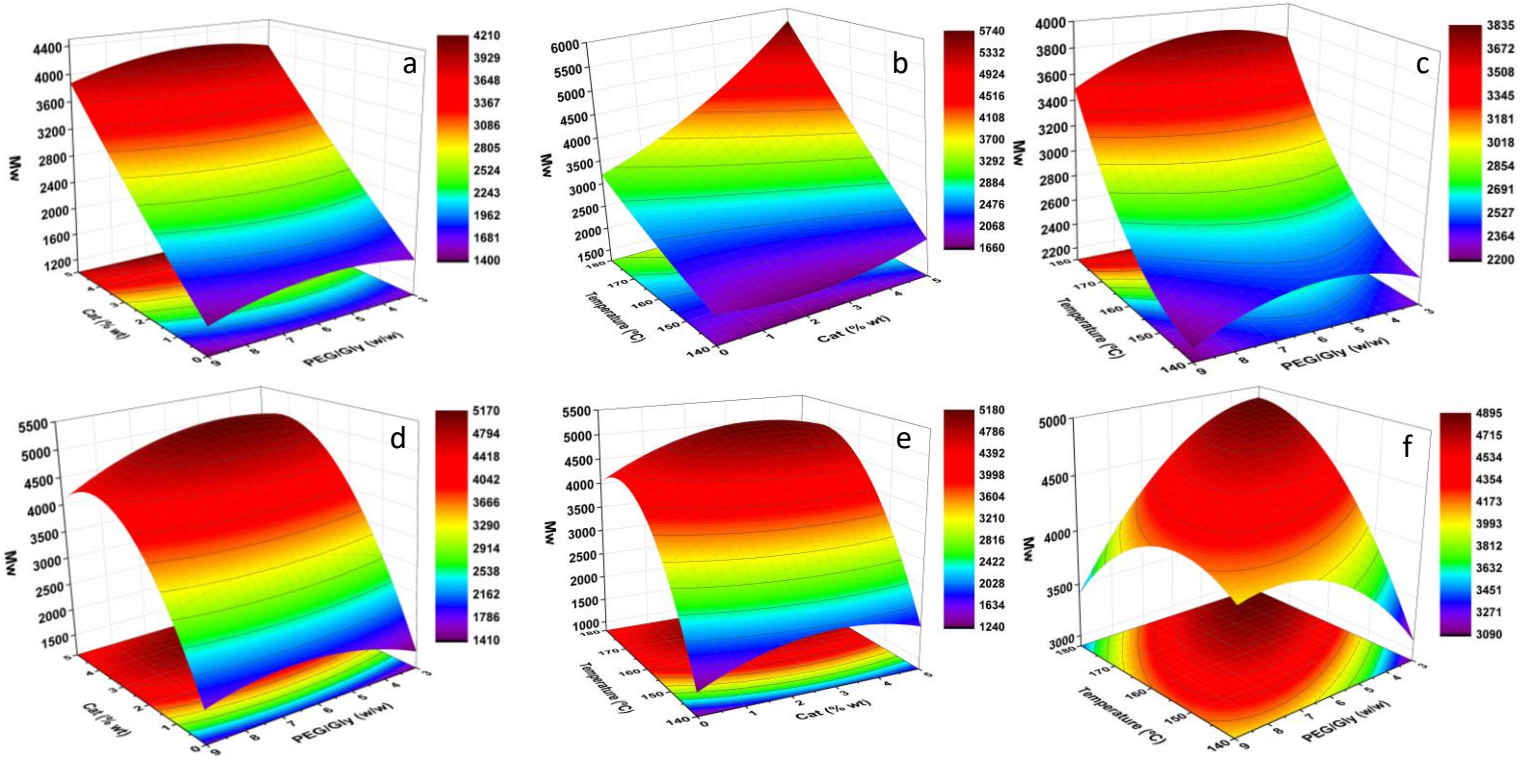


Figure P2.3. Response Surface for $M_W$: *Eucalyptus globulus* (a, b, c); *Pinus radiata* (d, e, f)

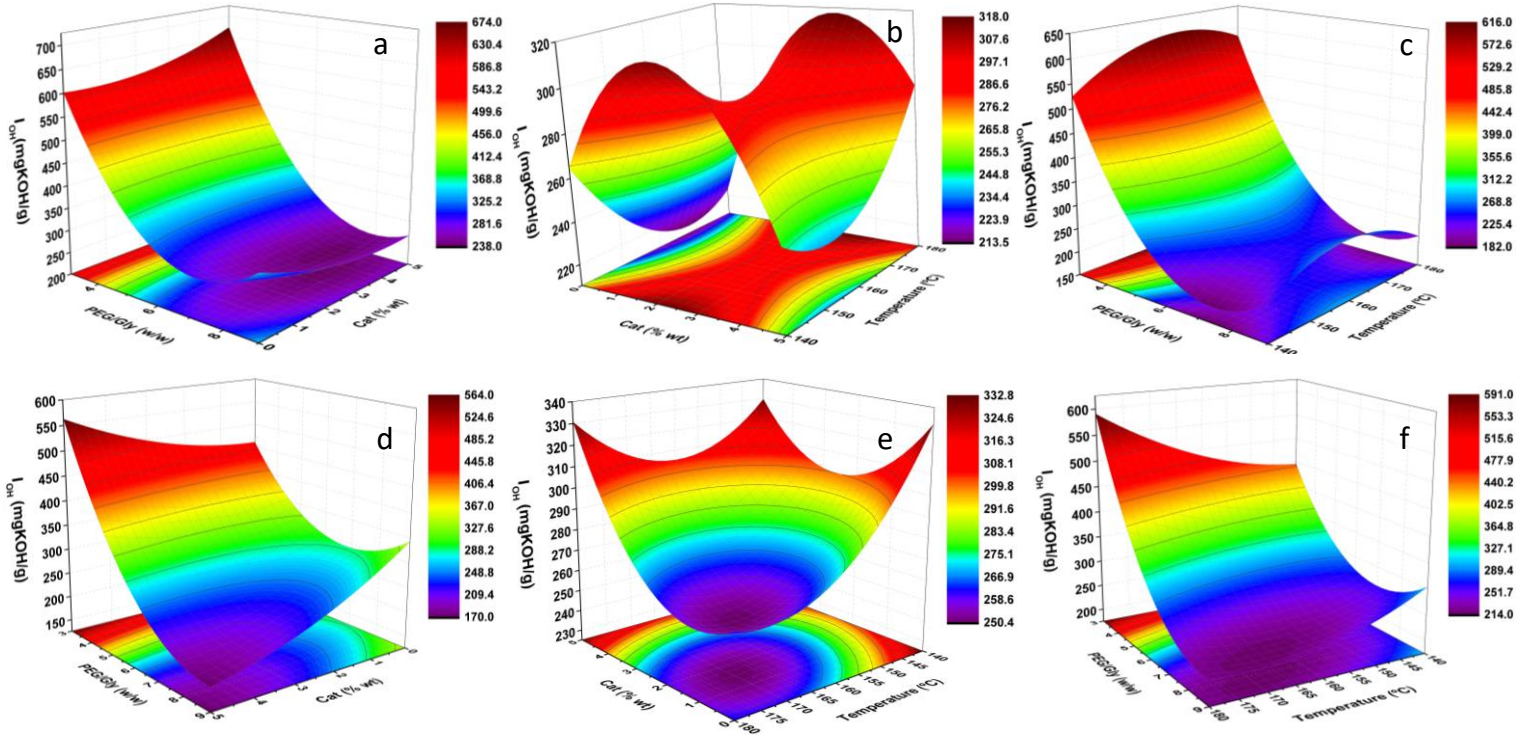


Figure P2.4. Response Surface for $I_{OH}$: *Eucalyptus globulus* (a, b, c); *Pinus radiata*

To verify the model, a triplicate of each experiment was performed under the optimal reaction conditions and the experimental results were compared with the theoretical results presented in Table P2.6. As a result of this comparison, it was established that the experimental results were in good concordance with the data predicted by the software, and therefore, the Box-Behnken design was validated.

Table P2.6. Theoretical values of $M_w$ and corrected $I_{OH}$ predicted by the software and experimental values at optimum conditions

| Parameter | Sample | Theoretical value | Experimental value |
|---|---|---|---|
| $M_w$ (g/mol) | EOPR[a] | 1532 | 1394 ± 12 |
| | EOPE[b] | 5593 | 4895 ± 325 |
| | POPR[c] | 1372 | 1383 ± 43 |
| | POPE[d] | 4891 | 5408 ± 765 |
| $I_{OH}$ (mg KOH/g) | EOPR | 599.2 | 595.2 ± 33.9 |
| | EOPE | 221.1 | 253.8± 60.6 |
| | POPR | 456.0 | 514.3± 42.7 |
| | POPE | 211.6 | 209.7 ± 3.7 |

[a]EOPR (*Eucalyptus globulus* Organosolv Polyols for Rigid PU)
[b]POPR (*Pinus radiata* Organosolv Polyol for Rigid PU)
[c]EOPE (*Eucalyptus globulus* Organosolv Polyol for Elastic PU)
[d]POPE (*Pinus radiata* Organosolv Polyol for Elastic PU)

### 2.2.4. Characterisation of the optimised bio-polyols

In reference to the molecular weight (Table P2.6), it should be noted that, as indicated in the previous section (2.2.1), an increase in the catalyst concentration resulted in an increase in the molecular weight of the bio-polyols. Hence, EOPE and POPE bio-polyols presented higher $M_w$ than EOPR and POPR bio-polyols in which no catalyst was used. In addition, the molecular weights of EOPE and POPE bio-polyols were higher than the ones of the employed lignins, EOUL and POUL respectively, in contrast to the reports of other authors. Thus, in the study by da Silva et al., (2017) [11] for the optimal liquefaction conditions of Kraft lignin, authors reported smaller molecular weights than the employed Kraft lignin for all points of the

experimental design. In another study, da Silva et al., (2019) [12] proved that the molecular weights of the bio-polyols obtained by liquefaction employing organic acids as catalyst were lower than the molecular weights of the Kraft lignin used. Similarly, Xue et al. (2015) [6] also obtained bio-polyols through liquefaction reactions with lower molecular weights than the ones of the employed original lignin using a catalyst concentration of 1.5%. The increase in molecular weight can be explained as the repolymerisation reactions of lignin are favoured by the presence of acid catalyst [13]. On the other hand, a concentration of sulphuric acid over 3% could enhance the repolymerisation reactions of lignin [7]. According to the literature, the molecular weight of polyols for rigid and elastic PU should be between 300-1000 (g/mol) and 2000-10000 (g/mol), respectively [10]. Considering the obtained results, though the molecular weights of EOPR and POPR bio-polyols were slightly above the stipulated range, it could be considered that the obtained bio-polyols are suitable for PU fabrication.

Regarding the $I_{OH}$ of the studied bio-polyols, EOPR and POPR showed higher values than EOPE and POPE. This increment could be explained by two main reasons: firstly, an increase in catalyst concentration could decrease the hydroxyl number of the bio-polyol [9] and secondly, an increase in glycerol content, with a higher number of free hydroxyl than PEG, could enhance the hydroxyl number of the final bio-polyol [14]. According to the literature, bio-polyols for rigid PUs, EOPR and POPR, are in the range of $I_{OH}$ required for the manufacture of rigid PUs (200-1000 mg KOH/g). However, the bio-polyols EOPE and POPE were slightly above the range of 28-160 mg KOH/g, which is the one required for the manufacture of elastic PU [15].

In the literature, most of the existing works are focused on two parameters: hydroxyl number and yield. Nevertheless, parameters such as the number average molecular weight ($M_n$), polydispesrity index (PDI), acid number ($A_n$) and functionality (*f*) should be considered in the synthesis of polyols [16].

Thus, although these parameters were not considered in the experimental design, they are summarised in Table P2.7 together with the obtained yield. Bio-polyols *f* and the liquefaction yield (η) were calculated using the Equations P2.4 and 2.5:

$$f = \frac{M_n \cdot I_{OH}}{1000 \cdot 56.1} \qquad \text{Equation P2.4}$$

$$\eta = \frac{M}{M_0} \cdot 100 \qquad \text{Equation P2.5}$$

Where, $M$ is the final bio-polyol mass and $M_0$ is the mass of the initial mixture of the liquefaction procedure.

Table P2.7. Mn (g/mol), PDI (Mw/Mn), An (mg KOH/g), f and yield (%) of bio-polyols at optimum conditions

| Sample | $M_{n\,(g/mol)}$ | PDI ($M_w/M_n$) | $A_n$ (mg KOH/g) | *f* | Yield (%) |
|---|---|---|---|---|---|
| EOPR | 380 ± 7 | 3.69 ± 0.08 | 2.74 ± 0.00 | 4.03 ± 0.15 | 98.63 ± 0.71 |
| EOPE | 524 ± 28 | 9.37 ± 1.12 | 33.01 ± 0.00 | 2.36 ± 0.44 | 71.98 ± 1.41 |
| POPR | 387 ± 4 | 3.58 ± 0.08 | 5.36 ± 0.23 | 3.55 ± 0.26 | 98.93 ± 0.10 |
| POPE | 778 ± 7 | 6.95 ± 0.91 | 30.56 ± 0.15 | 2.91 ± 0.08 | 87.56 ± 3.30 |

The polydispersity index indicated that the EOPE and POPE bio-polyols had wider molecular weight distribution than EOPR and POPR bio-polyols. The reason for this could be due to a higher number of repolymerisation reactions in the synthesis of EOPE and POPE bio-polyols, as discussed previously. Wider molecular weight distributions of EOPE and POPE indicates that the chain length variability of these bio-polyols is higher than in EOPR and POPR. This variability has a direct impact on the properties of the polyurethane, hence a bio-polyol with lower PDI is preferable for the manufacture of polyurethane foams, as a wide variability of the bio-polyol chain lengths could result in softening of the foam or in a mechanical collapse due to stresses that occur in the weaker regions of the foam [17].

In the synthesis of polyurethanes, the $A_n$ value of bio-polyols is an important parameter to be considered, since acid groups could decrease the efficiency of the reaction [18]. According to the literature, the bio-polyols studied in this work showed an $A_n$ index within the range reported by other authors, usually ranging from 0 to 40 mg KOH/g [7]. As it can be seen in Table P2.7, those bio-polyols in which no catalyst was used (EOPR and POPR) showed a lower $A_n$ index than in the bio-polyols with higher acid concentration (EOPE and POPE). This is because the number of acid substances generated during the liquefaction tended to increase, as the catalyst concentration increased [12]. Furthermore, as expected, the bio-polyols with the lowest acid number (EOPR and POPR) showed the highest hydroxyl number, since there is a direct correlation between the increase of acid number and the decrease hydroxyl number values [19].

Regarding functionality, to the best of our knowledge, no work has been reported indicating the functionality of polyols obtained by liquefaction of lignin with PEG and glycerol. A summary of the functionalities obtained in this study is presented in Table P2.7. Obtained values for EOPR and POPR bio-polyols (4.03 ± 0.15 and 3.55 ± 0.26), as well as for EOPE and POPE bio-polyols (2.36 ± 0.44 and 2.91 ± 0.08) are suitable for the synthesis of rigid and elastic PUs, whose functionalities should be between 3-8 and 2-3 [10].

Finally, as summarised in Table P2.7, significant differences were found in the obtained yields between the bio-polyols for rigid PUs and those for elastic PUs. Thus, the EOPR and POPR bio-polyols showed quite similar yields between them, 98.63 ± 0.71% and 98.93 ± 0.10% respectively. These results are very similar to those published by other authors who used the same microwave liquefaction reaction time that was employed in this work. For instance, da Silva et al., (2017) [11] documented a yield of 95.27% for the liquefaction of Kraft lignin using 3% catalyst, while Sequeiros et al., (2013) [20][20]obtained yields over 94% for all points of their experimental design

employing organosolv lignin from olive tree pruning. Xue et al., (2015) [6] liquefied alkaline lignin from corncob waste applying a catalyst concentration of 1.5% to obtain a yield of 94.47%. On the other hand, Gosz et al., (2018) [21] obtained a yield of 93% by liquefying pine Kraft lignin with 1,4-butanediol and crude glycerol without catalyst. In contrast, EOPE and POPE bio-polyols exhibited significantly lower yields, 71.98 ± 1.41% and 87.56 ± 3.30%. Two reasons could explain the large difference between the yields of bio-polyols for rigid PU (EOPR and POPR) and bio-polyols for elastic PU (EOPE and POPE). On the one hand, as mentioned above, an increase in the concentration of the acid catalyst enhances the lignin repolymerisation reactions, which increases the solid residue, leading to a reduction in the final yield. On the other hand, an excess of glycerol in the mixture promotes the reaction yield. This is because during the reaction the glycerol can be condensed into polyglycerol forming water as a by-product. Such water fragments the lignin into smaller and more reactive molecules through hydrolysis, enhancing the reaction yield [21].

To analyse the relationship between chemical structure and degradation, the bio-polyols were subjected to a thermogravimetric analysis. The TGA thermograms and their corresponding DTG derivative thermogravimetric curves are presented in Figure P2.5. Through the study of the DTG curves, three degradation stages were observed which are summarised in Table P2.8.

Table P2.8. Main degradation stages on TGA-DTG analysis

| Sample | 1st degradation stage | | 2nd degradation stage | | 3rd degradation stage | |
|---|---|---|---|---|---|---|
| | T interval(°C) | $T_{max}$ (°C) | T interval(°C) | $T_{max}$ (°C) | T interval (°C) | $T_{max}$ (°C) |
| EOPR | 40-120 | 70 | 130-246 | 208 | 246-417 | 356 |
| POPR | 40-120 | 68 | 132-260 | 218 | 260-430 | 371 |
| EOPE | 40-120 | 78 | 135-293 | 225 | 293-452 | 380 |
| POPE | 40-120 | 80 | 139-298 | 230 | 298-452 | 399 |

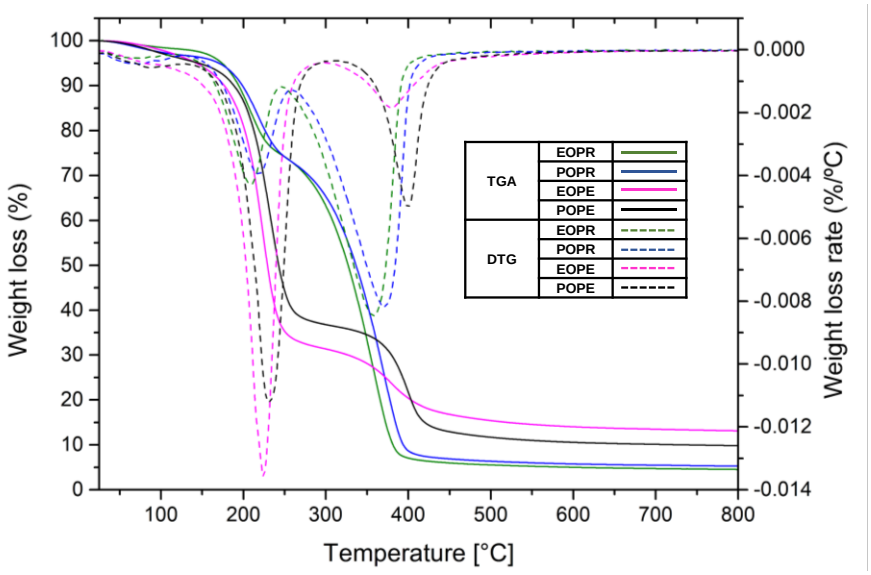


Figure P2.5. TGA thermograms and DTG curves of bio-polyols

The first degradation stage corresponds to the weight loss of the humidity of the samples. The second degradation stage correspond to the degradation of glycerol (153-267 °C) and the third degradation stage corresponded to the degradation of PEG (267-392°C) and lignin [22]. Since lignin degradation takes place between 300-500 °C, this third degradation region of bio-polyols reaches higher temperatures than if only PEG were present. It can be observed that, as the $M_w$ of bio-polyols increases, the degradation temperature is delayed; moreover, the lower the reaction yield, the lower the weight loss. An explanation for this, is that the lower the yield, the higher the lignin repolymerisation reactions, which results in a greater solid residue and, therefore, a lower final amount of lignin in the bio-polyol. These results confirmed that the combination of the liquefying solvents and lignin was successful.

Finally, to determine the rheological behaviour of the bio-polyols, a rotational test was performed. Through this test, the relationship between viscosity (η), shear stress (τ) and shear rate ($\dot{\gamma}$), which were fitted to the

Ostwald-de Waele (power-law) equation (Equation P2.6), was studied to determine the bio-polyols' fluid behaviour as well as their viscosity.

$$\tau = k \cdot \dot{\gamma}^{n} \qquad \text{Equation P2.6}$$

where n and k are adjustment parameters dependent on both the measurement conditions and the nature of the fluid. Depending on the value of the flow index parameter (n) the fluid could be Newtonian when n=1, pseudoplastic if n<1 and dilatant for n>1. The parameter k, also called consistency index, which is associated to the apparent viscosity of the fluid at a shear rate of 1 $s^{-1}$, exhibits higher values as the viscosity increases. In Table P2.9 and Figures P2.6a and 2.6b, a summary of the data, obtained by the software and the flow curves, are presented.

Table P2.9. Power-Law Linear functions based on the rheological data from bio-polyol samples

| Sample | Function | $k$ (Pa*s$^n$) | $n$ | $R^2$ |
|---|---|---|---|---|
| EOPR | $\tau = 0.2623 \cdot \dot{\gamma}^{0.9709}$ | 0.2623 | 0.9709 | 0.9995 |
| POPR | $\tau = 0.4394 \cdot \dot{\gamma}^{1.0043}$ | 0.4394 | 1.0043 | 0.9998 |
| EOPE | $\tau = 0.8137 \cdot \dot{\gamma}^{0.9541}$ | 0.8137 | 0.9541 | 0.9995 |
| POPE | $\tau = 1.1885 \cdot \dot{\gamma}^{0.9525}$ | 1.1885 | 0.9525 | 0.9998 |

The high values of $R^2$ reported in Table P2.9 indicated that all the rheograms are well fitted. Therefore, it could be concluded that the selected model was adequate to evaluate the rheological behaviour of the bio-polyols. Considering that the flow index parameter ($n$) of all bio-polyols is very close to unity, it could be concluded that all bio-polyols behave as Newtonian fluids. However, analysing the Figure 6a, the rheograms corresponding to EOPE and POPE showed a pseudoplastic behaviour, i.e., the viscosity ($\eta$) decreased as the shear rate ($\dot{\gamma}$) increased, while EOPR and POPR bio-polyols exhibit a clearly Newtonian behaviour, where the viscosity remained constant regardless the applied shear rate. Figure P2.6b, where the relationship between the shear stress (τ) and shear rate ($\dot{\gamma}$) is represented,

confirms that EOPR and POPR bio-polyols behaved as Newtonian fluids since their graphical representation is a line passing through the origin, while the representation of EOPE and POPE bio-polyols subtly exhibited the characteristic curve of pseudoplastics fluids, where τ decreases as $\dot{\gamma}$ increases.

It is well known that the power-law becomes Newton's Law when a fluid behaves in a Newtonian way and therefor the viscosity of the fluid corresponds to any point along the *plateau* in the Figure P2.6a, i.e., the consistency index *k* is equal to the viscosity. Therefore, the viscosities for EOPR and POPR are 0.2626 Pa·s and 0.4394 Pa·s respectively. On the other hand, the viscosities of EOPE and POPE are in the range of 0.7286-0.6676 Pa·s and 1-0.9310 Pa·s respectively at the studied shear rate. As it was expected, since viscosity and molecular weight are closely related [11], the bio-polyols with the highest viscosities were those with the highest molecular weight. According to literature, these viscosities values are suitable for PU production since they are below 300 Pa·s [23] and are similar to the viscosities obtained by other authors by liquefying lignin [6,12,22].

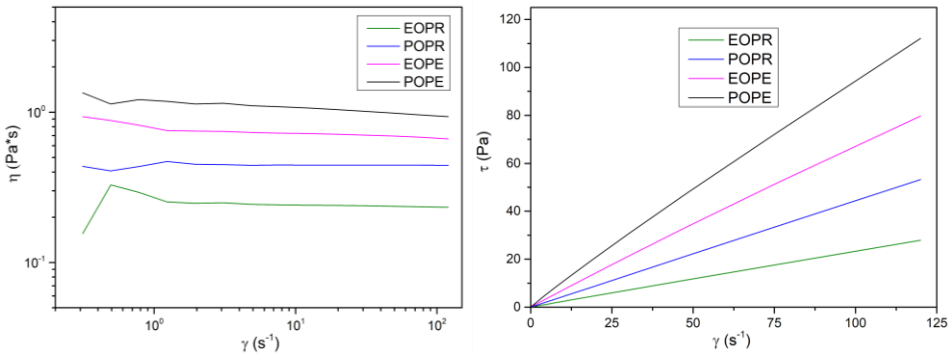


Figure P2.6. Viscosity (η) VS shear rate ($\dot{\gamma}$) and (b) shear stress (τ) VS shear rate ($\dot{\gamma}$) of bio-polyols at optimum point

## 3. CONCLUSIONS

Through Box Behnken experimental design and employing response surface methodology, the optimal lignin liquefaction reaction conditions using microwave irradiation technology for obtaining bio-polyols to formulate rigid and elastic polyurethanes were obtained. Two different organosolv lignins were employed: *Eucalyptus globulus* lignin and *Pinus radiata* lignin. Four optimum points were obtained, of which two for bio-polyols for rigid polyurethanes (EOPR and POPR), and two for bio-polyols for elastic polyurethanes (EOPE and POPE). The $R^2$ determination coefficients obtained for the studied parameters ($M_w$ and $I_{OH}$) were 0.97 and 0.97 for *Eucalyptus globulus* lignin, while for *Pinus radiata* lignin the coefficients were 0.96 and 0.98. The elevated $R^2$ coefficients together with Fisher's F-test confirmed that the selected models were appropriate and that the models were well adjusted. The optimum reaction conditions for EOPR and POPR bio-polyols were virtually equals, around 160°C and PEG/Gly ratio of 3, noteworthy is the absence of catalyst in both cases. On the other hand, the optimum reaction conditions were 180°C and polyethylene glycol/glycerol ratio of 7.57 for EOPE and 160.13°C and polyethylene glycol/glycerol ratio of 7.34 for POPE. The high concentration of catalyst, 5% and 3.85% respectively, is remarkable in both cases. The molecular weight of EOPR and POPR bio-polyols at the optimum points was slightly higher than that required for the manufacture of rigid polyurethanes. Similarly, the hydroxyl number of EOPE and POPE bio-polyols was slightly higher than the required for the manufacture of elastic PUs. However, considering the rest of the studied parameters: $A_n$, PDI, *f* and the rheological behaviour, it could be concluded that the bio-polyols were suitable for the synthesis of polyurethanes. Nevertheless, before their use, the bio-polyols should be neutralised due to the high acid number value and for polyurethane foams preparation the high polydispersity should be taken into account.

## REFERENCES

[1] Y.Y. Li, X. Luo, S. Hu, Bio-based Polyols and Polyurethanes, 2015, pp. 1–79.

[2] T. Wells, M. Kosa, A.J. Ragauskas, Ultrason. - Sonochemistry 20(6) (2013) 1463–9. 10.1016/j.ultsonch.2013.05.001.

[3] L. Chen, X. Wang, H. Yang, Q. Lu, D. Li, Q. Yang, H. Chen, J. Anal. Appl. Pyrolysis 113 (2015) 499–507. 10.1016/j.jaap.2015.03.018.

[4] A. Morales, B. Gullón, I. Dávila, G. Eibes, J. Labidi, P. Gullón, Ind. Crops Prod. 124(July) (2018) 582–92. 10.1016/j.indcrop.2018.08.032.

[5] R. Fernández-Marín, F. Hernández-Ramos, A.M. Salaberria, M.Á. Andrés, J. Labidi, S.C.M. Fernandes, Int. J. Biol. Macromol. 186(January) (2021) 218–26. 10.1016/j.ijbiomac.2021.07.048.

[6] B.L. Xue, J.L. Wen, R.C. Sun, Materials (Basel). 8(2) (2015) 586–99. 10.3390/ma8020586.

[7] S. Hu, X. Luo, Y. Li, ChemSusChem 7(1) (2014) 66–72. 10.1002/cssc.201300760.

[8] M.A. Bezerra, R.E. Santelli, E.P. Oliveira, L.S. Villar, L.A. Escaleira, Talanta 76(5) (2008) 965–77. 10.1016/j.talanta.2008.05.019.

[9] Y. Jin, X. Ruan, X. Cheng, Q. Lü, Bioresour. Technol. 102(3) (2011) 3581–3. 10.1016/j.biortech.2010.10.050.

[10] M. Ionescu, in: De Gruyter (Ed.), Polyols for Polyrethanes, Boston, Berlin, 2019, pp. 1–10.

[11] S.H.F. da Silva, P.S.B. dos Santos, D. Thomas da Silva, R. Briones, D.A.

Gatto, J. Labidi, J. Wood Chem. Technol. 37(5) (2017) 343–58. 10.1080/02773813.2017.1303513.

[12] S.H.F. da Silva, I. Egüés, J. Labidi, Ind. Crops Prod. 137(March) (2019) 687–93. 10.1016/j.indcrop.2019.05.075.

[13] Y. Lee, E.Y. Lee, J. Wood Chem. Technol. 36(5) (2016) 353–64. 10.1080/02773813.2016.1156132.

[14] F. Chen, Z. Lu, J. Appl. Polym. Sci. 111 (2009) 508–16. 10.1002/app.29107.

[15] Y.Y. Li, X. Luo, S. Hu, Bio-based Polyols and Polyurethanes, 2015, pp. 1–79.

[16] F. Hernández-Ramos, M.G. Alriols, T. Calvo-Correas, J. Labidi, X. Erdocia, ACS Sustain. Chem. Eng. (2021). 10.1021/acssuschemeng.0c09357.

[17] J. D'Souza, R. Camargo, N. Yan, Polym. Rev. 57(4) (2017) 668–94. 10.1080/15583724.2017.1283328.

[18] S. Hu, Y. Li, Ind. Crops Prod. 57 (2014) 188–94. 10.1016/j.indcrop.2014.03.032.

[19] S.H. Lee, M. Yoshioka, N. Shiraishi, J. Appl. Polym. Sci. 78(2) (2000) 319–25. 10.1002/1097-4628(20001010)78:2<319::AID-APP120>3.0.CO;2-Z.

[20] A. Sequeiros, L. Serrano, R. Briones, J. Labidi, J. Appl. Polym. Sci. 130(5) (2013) 3292–8. 10.1002/app.39577.

[21] K. Gosz, P. Kosmela, A. Hejna, G. Gajowiec, Ł. Piszczyk, Wood Sci. Technol. 52(3) (2018) 599–617. 10.1007/s00226-018-0991-4.

[22] R. Briones, L. Serrano, J. Labidi, J. Chem. Technol. Biotechnol. 87(2) (2012) 244–9. 10.1002/jctb.2706.

[23] C.A. Cateto, M.F. Barreiro, A.E. Rodrigues, M.N. Belgacem, Ind. Eng. Chem. Res. 48(5) (2009) 2583–9. 10.1021/ie801251r.

*“All mentors have a way of seeing more of our faults*

*than we would like. It’s the only way we grow”*

*Senator Padmé Amidala*

## III. Argitalpena

# Findu gabeko glizerolaren balorizazioa poliuretanoak ekoizteko likidotutako ligninazko biopoliolen ekoizpenerako erabiliz

## LABURPENA

Lan honetan, erabilitako sukaldetzeko landare-oliotik transesterifikazio erreakzioaren bidez azpiproduktu bezala lortutako findu gabeko glizerola (*crude glycerol* CG) erabiliz, poliuretanoak sintetizatzeko propietate egokiko biopolioloak ekoiztu ziren. Biopoliolak sintetizatzeko ***II. Argitalpenean*** optimizatutako erreakzio baldintzak eta metodologia bera erabili ziren. Organosolv ligninen likidotze erreakzioetan ***II. Argiltalpeneko*** lehengai eta erreaktibo berak erabili ziren, hau da, Eucalyptus globulus eta Pinus radiatik lortutako organosolv ligninak, PEG, glizerola eta $H_2SO_4$ katalizatzaila, baina lan honetan, glizerol komertzialaren ordez, CGa erabili zen. Biopoliolen hainbat parametro zehaztu ziren, $I_{OH}$, $A_n$, $M_w$, *f* eta errendimendua hain zuzen ere. PU zurrunak ($EOPR_{CG}$ eta $POPR_{CG}$ deiturikoak) nahiz elastikoak ($EOPE_{CG}$ eta $POPE_{CG}$) sintetizatzeko beharrezko ezaugarriak zituzten biopoliolak formulatu ziren. $EOPR_{CG}$ eta $POPR_{CG}$ biopoliolek 534 ± 4 (mg KOH/g)-ko eta 383 ± 8 (mg KOH/g)-ko $I_{OH}$ balioak lortu zuten hurrenez hurren, eta $EOPE_{CG}$-renak eta $POPE_{CG}$-renak berriz txikiagoak izan ziren, 228 ± 36 (mg KOH/g) and 173 ± 16 (mg KOH/g). Biopoliolen $A_n$-ren balioak 1,91 eta 25,09 (mg KOH/g) artekoa izan zen, eta *f*-ak 4,16 eta 3,14koak $EOPR_{CG}$ eta $POPR_{CG}$-rako hurrenez hurren, $EOPE_{CG}$ eta $POPE_{CG}$-rako, berriz, 3,51 eta 2,08koak izan ziren.

# 1. MATERIALAK ETA METODOAK

## 1.1. Materialak

Argitalpen honetan erabilitako lehengaiak, *Eucalyptus globulus*-en txirbilak, *Pinus radiata*-ren zerrautsa, janaria prestatzeko landare-olio erabilia eta erreaktibo kimikoak **2. ATALAREN *2.1 puntuan*** deskribatzen den moduan lortu ziren.

## 1.2. Ligninak lortzeko prozedura

Erabilitako organosolv ligninak **2. ATALAREN *2.2 puntuan*** deskribatutako organosolv deslignifikazio eta ultrasoinu prozesuen bitartez lortu ziren. Lignina hauek, EOUL eta POUL bezala deituak, **II. Argitalpenean** karakterizatu ziren.

## 1.3. Glizerol gordina lortzeko sukalde landare-olioaren transesterifikazio erreakzioa

CG-a **2. ATALAREN *2.4 puntuan*** deskribatzen den transesterifikazioaren bidez lortu zen.

## 1.4. Biopoliolen sintesia mikrouhin bidezko likidotze erreakzioa erabiliz

EOUL eta POUL ligninen likidotze erreakzioa **2. ATALAREN *2.3 puntuan*** deskribatutako metodologia erabiliz egin zen.

Katalizatzailearen kontzentrazioa, erreakzio-tenperatura eta erreakzioan erabilitako PEG/CG erlazioa **II. Argitalpenean** egindako optimizazio prozesuan lortu ziren, eta jarraian laburbiltzen dira (P3.1 Taula).

P3.1. Taula. ***II. Argitalpenean*** optimizatutako likidotze-erreakzio baldintzak

| Biopoliol | Biopoliol zurruna | | Biopoliol elastikoa | |
|---|---|---|---|---|
| | $EOPR_{CG}$ | $POPR_{CG}$ | $EOPE_{CG}$ | $POPE_{CG}$ |
| Kat (% wt.) | 0 | 0 | 5 | 3,86 |
| Tenperatura (°C) | 161 | 159 | 180 | 160 |
| PEG/CG (% wt.) | 3/1 | 3/1 | 7,57/1 | 7,34/1 |

Non biopoliol zurruna eta Biopoliol elastikoa, PU zurrunak eta elastikoa sintetizatzeko biopoliolak diren

### 1.5. Glizerol gordinaren karakterizazioa

Findu gabeko glizerola **2. ATALAREN** ***6. Puntuko*** 2.3 Taulan adierazitako teknikak erabiliz karakterizatu zen. Teknika horiek **II. Eranskinean** deskribatzen dira. Bestalde, dentsitatea, pH-a eta biskositatea neurtu ziren. Dentsitatea CGaren bolumen ezagun bat pisatuz kalkulatu zen. pH giro tenperaturan zehaztu zen Crison basic 20 pH-metro bat erabiliz, neurketak egiteko CGaren 1,00 ± 01 g pisatu eta ur desionizatuaren 50 mL-tan disolbatu ziren. Errautsen edukia ISO 2098-1972 arauaren arabera zehaztu zen, non CG 1g hiru orduz erretzen da 750 °C-tan labe batean.

### 1.6. Biopoliolen karakterizazioa

**2. ATALAREN** ***2.7 puntuko*** M.3 Taulan azaltzen den bezala, lan honetan ekoiztutako biopoliolak $M_w$, $M_n$, PDI, $I_{OH}$, $A_n$ eta $f$ parametroak zehazteko karakterizatu ziren. Gainera, TGA bitartez biopoliolen degradazio termikoa aztertu zen, eta haien portaera erreologikoa determinatu zen. Karakterizazio hauek guztiak **II. Eranskinean** zehatz mehatz azalduta daude.

## 2. EMAITZAK ETA EZTABAIDA

### 2.1. Glizerol gordinaren karakterizazioa

Atal honetan CGaren propietate fisikoak eta konposizioa biltzen dira.

Lortutako CGaren pH-a 10,55 ± 0,02 izan zen. pH balio hau erabilitako KOH katalizatzailearen hondarrak egon daitezkeela adierazte du baita transesterifikazio erreakzioan sortutako potasio gatzak daudela ere. pH balio hori bat dator beste egile batzuek NaOH edo KOH katalizatzaile gisa erabiliz transesterifikazio bidez lortutako CG pH balioekin [1–3]. Espero zen bezala, CGaren dentsitatea (1,03 ± 0,07 g/zm$^3$) glizerol puruarena (1,259 g/zm$^3$) baino txikiagoa izan zen, horren arrazoia, CGan dauden gantz-azido (*fatty acids* FA), gantz-azidoen ester metilikoak (*fatty acids methyl ester* FAME), ura eta metanol-traza bezalako ezpurutasun arinagoei egotzi daiteke [2]. CGaren ur-edukia nabarmen aldatzen da fabrikazio-industriaren arabera. Adibidez, xaboiaren industrian lortutako CGa % 3,6 ur inguru izan ohi du, eta estearina ekoiztean lortutako CGak, berriz, % 55,3 inguru izan dezake. Bestalde, transesterifikazio bidez lortutako CGak % 8,15 eta % 43,2 arteko ura izaten du, baina purifikazio-gastuak merkatzeko, gomendagarria da % 12tik ez igotzea [5]. Beraz, lan honetan lortutako ur edukia (11,64 ± 1,61) transesterifikazio erreakzio bidez lortutako CG baten espezifikazioen barruan dago. Ur horrek triglizeridoak hidroliza ditzake gantz-azido askeak sortzeko, eta horiek erreakzioaren errendimendua murrizten duten xaboiak sortzen dituzte [4].

CGaren oinarrizko analisiak materia organikoaren % 46,00 ± 1,29a karbonoari (C) zegokiola adierazi zuen. Balio handi hori glizerola baino C eduki handiagoa duten xaboiak, FAMEak eta glizeridoak bezalako ezpurutasun kopuru handiari egotzi dakioke. Hu et al., (2012)-ek [2] antzeko balioak lortu zituen hainbat soja eta olio begetaletatik lortutako CGerako. Bestalde, lortutako $N_2$ (0,15 ± 0,01%), $H_2$ (8,17 ± 0,33%) eta $O_2$ (35,6 ± 1,58%) balioak bat etorri ziren landare-olio desberdinetatik lortutako CGa aztertzean lortutako balioekin [2,6,7]. Hala ere, $S_2$-ren kontzentrazioa (%1,33 ± 0,04) aipatutako azterlanetan lortutako balio maximoak (% 0,078) baino handiagoa izan zen.

CGaren konposizio kimikoa GC-MS bidez aztertu zen. P3.1. Irudian ikusi daitekeen bezala, glizerolaz gain (% 41,84 ± 0,17), CGa beste konposatu batzuetan aberatsa zela ikusi zen, hala nola gantz-azidoetan (% 11,46% ± 6,01) eta FAMEetan (% 26,31 ± 7,68), besteak beste.

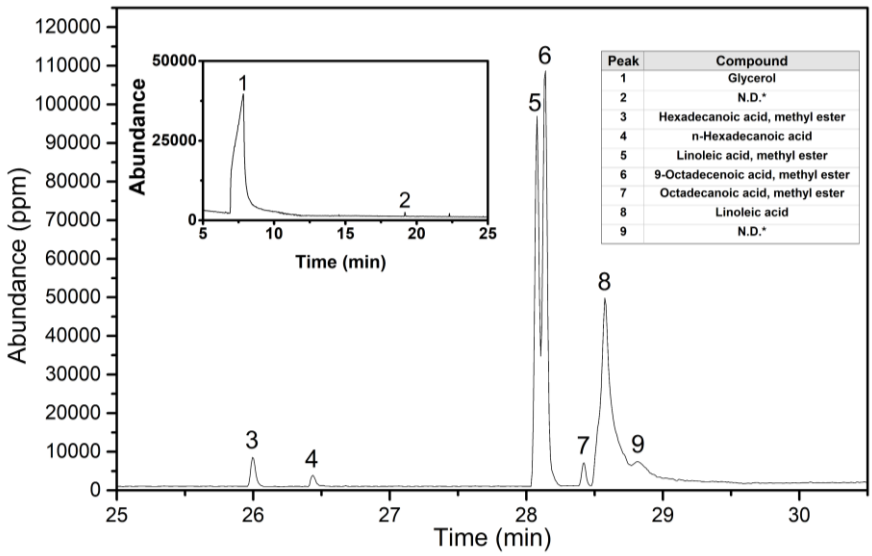


P3. 1. Irudia. CGaren CG-MS kromatograma

CGaren egitura kimikoa ATR-FTIR analisiaren bidez zehaztu zen, eta glizerol komertzial batekin alderatu zen (P3.2. Irudia). CGak glizerolaren talde funtzional nagusiak zituela baieztatu ahal izan zen: OHren luzatzea (3300 $zm^{-1}$) eta flexioa (920 $zm^{-1}$), CHren luzatze asimetrikoa (2920 $zm^{-1}$) eta simetrikoa (2851 $zm^{-1}$), CO alkohol primarioaren (1456 $zm^{-1}$) eta sekundarioaren (1110 $zm^{-1}$) luzatzea eta $H_2O$ren flexioa (1650 $zm^{-1}$) [1,8]. Horiez gain, CGaren ezpurutasunei egozgarri diren beste seinale bereizgarri batzuk ere ikusi ziren. Lehenengoa, konposatu asegabeen C=C taldeen luzatzearekin erlazionatutako seinale txiki bat da (3015 $zm^{-1}$) [1]; bigarrena, berriz, esterren edo gantz-azidoen azido karboxilikoen C=O taldeen (1745 $zm^{-1}$) presentzia adierazten du [9].

3015 $zm^{-1}$-ko uhin-zenbakian eta konposatu asegabeekin erlazionatutako C=C (3015 $zm^{-1}$). Azkenik, $COO^-$ karboxilato ioien (1560 $zm^{-1}$) presentziarekin lotutako seinale bat ikusi zen, CG laginean xaboiak zeudenaren adierazgarri [1,9].

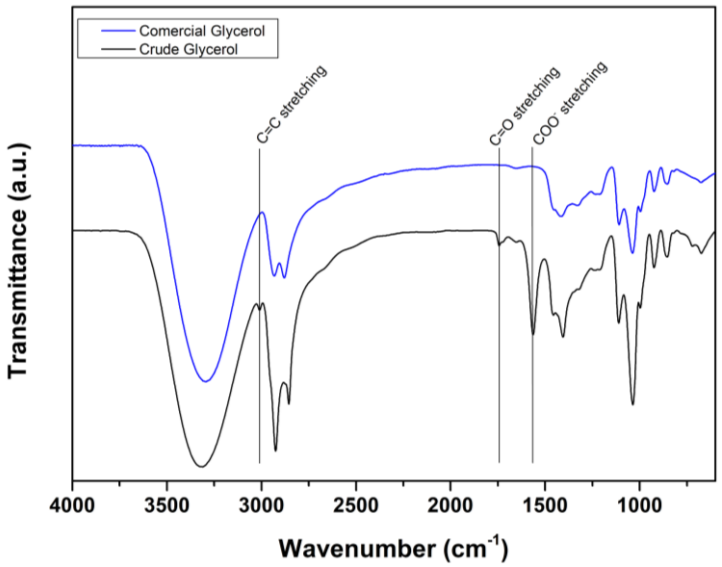


P3.2. Irudia. CGaren eta glizerol komertzialaren ATR-FTIR espektroak

## 2.2. Biopoliolen karakterizazioa

P3.2. Taulan, biopoliolen karakterizatzean lortutako datuak laburbiltzen dira. Ezinbestekoa da $M_w$ egokia duten biopoliolak lortzea, nahi diren segmentu biguneko propietateak dituzten PUak ekoizteko. Izan ere, PUen azken aplikazioaren arabera, $M_w$-a 300-1000 (g/mol) edo 2000-10000 (g/mol) artekoa izan behar da PU zurrunetarako eta elastikoetarako, hurrenez hurren [10].

P3.2. Taula. Biopololen $M_W$, $I_{OH}$, $A_n$, *f*, biopoliolaren pisu ekibalentea (EW) eta errendimendua

| | $EOPR_{CG}$ | $EOPE_{CG}$ | $POPR_{CG}$ | $POPE_{CG}$ |
|---|---|---|---|---|
| $M_n$(g/mol) | 442 ± 34 | 941 ± 30 | 453 ± 24 | 780 ± 20 |
| $M_w$ (g/mol) | 1742 ± 275 | 8818 ± 127 | 1431 ± 362 | 5530 ± 131 |
| PI | 4,25± 0,55 | 9,38 ± 0,16 | 3,14 ± 0,63 | 7,10 ± 0,31 |
| $I_{OH}$ (mgKOH/g) | 554 ± 4 | 228 ± 36 | 383 ± 8 | 173 ± 16 |
| $A_n$ (mgKOH/g) | 1,91 ± 0,06 | 20,94 ± 2,75 | 4,21 ± 0,90 | 25,09 ± 2,59 |
| *f* | 4,16 ± 0,10 | 3,51 ± 0,68 | 3,14 ± 0,16 | 2,08 ± 0,27 |
| EW | 101,20 ± 0,66 | 248,98 ± 38,77 | 146,68 ± 3,23 | 325,36 ± 30,16 |
| Errendimendua (%) | 93,55 ± 3,00 | 70,75 ± 0,47 | 90,60 ± 0,56 | 79,35 ± 0,83 |

Espero zen bezala, zenbat eta azido kontzentrazio handiagoa, orduan eta $M_w$ altuagoa. Beraz, katalizatzailerik gabe sintetizatutako biopoliolak ($EOPR_{CG}$ eta $POPR_{CG}$) katalizatzailea erabiliz sintetizatutako $EOPE_{CG}$ eta $POPE_{CG}$ baino $M_w$ txikiagoa izan zuten, P3.3. Irudian ikus daitekeen bezala. $M_w$-ren balioen handitzea ligninaren birpolimerizazio-erreakzioen handitzearen ondorio da, hauek azido sulfuriko bezalako katalizatzaile azido baten aurrean areagotzen bait dira [11]. Gainera, $EOPE_{CG}$ biopoliolaren $M_w$-a $POPE_{CG}$-rena baino handiago izan zen; izan ere, katzalizatzailearen kontzentrazioa % 3tik gora handitzen den heinean, birpolimerizazio-erreakzioak ere handitu egiten baitira [12]. Gainera, CGan dauden glizerolaren, FFAren eta FAMEen arteko polimerizazio-erreakzioek ere biopoliolen $M_w$-a handitu dezakete [13]. Hala ere, katalizatzaile azidoaren gehikuntzak eragindako ligninaren birpolimerizazio-erreakzioek garrantzi handiagoa izan zuten; horrela, CG kantitate handiagoa baina katalizatzailerik gabeko biopoliolak ($EOPE_{CG}$ eta $POPE_{CG}$) $M_w$ baxuenak lortu zituzten. PDIa ere erabakagarria da PUen azken aplikaziorako; izan ere, polimeroen kateen luzeraren aldakortasunarekin lotuta dago, eta, kate horien luzeraren arabera, PUak nahi ez den portaera izan lezake [14]. Ligninaren birpolimerizazio-erreakzioek PDIan ere eragina

zutela ikusi zen. Horrela, $EOPE_{CG}$ biopoliolak $M_w$ eta PDI balio altuenak lortu zituen, $POPE_{CG}$-tik jarraitua. PU ezberdinak sintetizatzeko biopoliolak izan behar dituzten propietateak kontutan hartuta, $EOPE_{CG}$ eta $POPE_{CG}$ biopoliolek PU elastikoak ekoizteko eskatzen diren parametroen barruan zeudela ondorioztatu zen. Bestalde, $EOPR_{CG}$ eta $POPR_{CG}$ biopoliolen pisu molekularrak Pu zurrunak sintetizatzeko behar direnak baino pixka bat handiagoak izan arren, horiek fabrikatzeko egokitzat hartu daitezke.

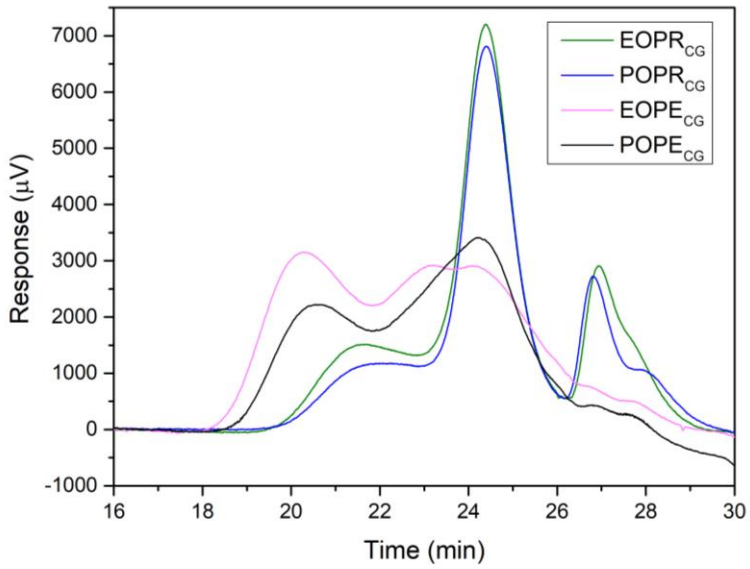


P3.3. Irudia. Likidotutako biopoliolen pisu molekularren banaketa

Jakina da PU zurrunen sintesirako beharrezkoa den $I_{OH}$-a 200-1000 mg KOH/g artean dagoela, PU elastikoetarako, berriz, balio hau 28-160 mg KOH/g artean dago [15]. Era berean, $A_n$-ren balio altuek erreakziorako kaltegarriak direla jakina da ere, erreakzioaren eraginkortasuna murriztu baitezakete, eta, beraz, $A_n$ baxuko biopoliolak erabiltzea komeni dira [16]. Bi parametro hauek, $I_{OH}$ eta $A_n$, estuki lotuta daude, $A_n$-ren gorakadak poliolaren $I_{OH}$ kopurua gutxitzen baitu [17]. Korrelazio hori lan honetan sintetizatutako biopolioleetan ikusi ahal izan zen. Horrela, $I_{OH}$ balio altuenak zuten biopoliolek ($EOPE_{CG}$ eta $POPE_{CG}$) $A_n$ balio baxuenak izan zituzten. Bestalde,

$EOPE_{CG}$ eta $POPE_{CG}$ sistemetan ikusitako $A_n$-ren balioen hazkundea azido sulfurikoa katalizatzaile gisa erabiltzearen ondorio izan zen. $EOPE_{CG}$ eta $POPE_{CG}$ biopolioleekin alderatuta, $EOPR_{CG}$ eta $POPR_{CG}$ biopolioleetako $I_{OH}$ balio altuagoak nagusiki bi arrazoirengatik azaldu daitezke. Lehenengoa, erreakzioan $I_{OH}$-a murrizten duen katalizatzailerik ez dagoelako [18]. Bestalde, $EOPR_{CG}$ eta $POPR_{CG}$ biopoliolen sintesian erabilitako glizerol kantitate handiagoak $I_{OH}$-ren indizearen handitzea ekarri zuen [19].

PUen azken aplikazioaren arabera funtzionalitate desberdineko biopoliolak behar dira. Adibidez, PU zurrunen sintesirako, gurutzaketa handiko sareak sortzen dituzten 3-8 bitarteko funtzionalitate altuko biopoliolak hobesten dira; aldiz, apar malguak, elastomeroak edo itsasgarriak bezalako PU elastikoak sintetizatzeko, gurutzaketa dentsitate txikiko materialak sortzen dituzten 2-3 bitarteko funtzionalitateak nahiago dira, kate polimerikoen mugikortasuna ahalbidetzen baitute [10]. Beraz, $EOPR_{CG}$ eta $POPR_{CG}$ biopoliolek lortutako funtzionalitateak, 4,16 eta 3,14 hurrenez hurren, PU zurrunak sintetizatzeko beharrezkoak diren funtzionalitate tartean zeuden. $EOPE_{CG}$ eta $POPE_{CG}$ biopoliolen kasuan, lehenengoak 2,08ko funtzionalite balioa izan zuen, PU elastikoak sintetizatzeko egokia, aldiz, $POPE_{CG}$-ren funtzionalitatea 3 baino altuagoa izan zen, gutxigatik izan bazen ere. Hori dela medio, eta lortutako $I_{OH}$ eta $M_w$ balioak kontutan hartuta, PU elastikoak sintetizatzeko egokia izan zitekeela ondorioztatu zen. Hidroxilo talde batetik eratorritako katea edo poliolaren pisu baliokidea (EW) ere kontuan hartu beharreko parametroa da (P3.1. Ekuazioa). Kate labur batek PUaren uretano taldeen arteko lotura-dentsitate handiagoa dakar, eta, beraz, kohesio handiagoa, batez ere bigarren mailako hidrogeno-loturen bidez, funtzionaltasun handi batekin batera egitura zurruna ematen duena. Bestalde, kate luze batek uretano-loturen kontzentrazioa gutxitzen du, haien arteko kohesioa txikituz, eta funtzionaltasun baxuko eta mugikortasun handiko kate batekin batera, PU elastiko sortuz [20]

$$EW = \frac{56.1 \cdot 100}{\text{Corrected } I_{OH}}$$ P3.1 Ekuazioa

Espero zen bezala, eta P3.2 Taulan laburtutako datuen arabera, $EOPR_{CG}$ eta $POPR_{CG}$ biopoliolek PU zurrunak sintetizatzeko egokiak diren EW balioak baxuak lortu zituzten, berriz, $EOPE_{CG}$ eta $POPE_{CG}$ biopoliolak egitura malguagoko poliuretanoak sintetizatzeko beharrezkoak diren EW balio altuagoak erakutsi zuten.

PUak ekoizteko ezaugarri egokiak dituzten biopoliolak lortzeko aztertu diren propietateak garrantzitsuak badira ere, errendimendua funtsezko beste faktore bat da prozesua industrialki bideragarria izan dadin. Ligninaren likidotze-prozesuan, katalizatzaileak eragin esanguratsua du erreakzioaren errendimenduan, katalizatzaile azido bat dagoenean ligninaren birpolimerizazio-erreakzioak areagotzen baitira, hondakin solido gehiago sortuz eta, beraz, erreakzioaren errendimendua murriztuz [12]. Uraren presentziak ere eragina izan dezake errendimenduan, izan ere, hidrolisiaren bitartez ligninaren zatiketa sustatu baitezake, erreakzioaren errendimendua handituz [21]. Ur hori likidotze-erreakzioan sor daiteke, glizerola poliglizerolean kondentsatzen denean; beraz, zenbat eta glizerol gehiago, orduan eta ur gehiago egongo da eta, beraz, errendimendua altuagoa izango da [22]. P3.2. Taulan laburbildutako emaitzen arabera, CG gehiago eta katalizatzailerik gabeko $EOPR_{CG}$ eta $POPR_{CG}$ biopoliolak, $EOPE_{CG}$ eta $POPE_{CG}$ biopoliolak baino errendimendu handiagoa izan zuten. CGaren glizerol kantitate txikiagoa eta FA eta FAME bezalako ezpurutasunak direla medio, likidotze erreakzioaren errendimendua murriztuta ikusi daiteke [16], dena den, poliolen arteko CGren kantitate alde txikiak ezin du azaldu $EOPE_{CG}$ eta $POPE_{CG}$ biopoliolen errendimendu txikiak, eta, beraz, katalizatzailearen eraginaren ondorio dela esan daiteke. Hori baieztatu ahal izan zen,

katalizatzaile kontzentrazio handiagoa zuen $EOPE_{CG}$ biopoliolaren errendimendua $POPE_{CG}$-rena baino txikiagoa izan zela ikusita.

Biopoliolen egitura kimikoaren eta degradazioaren arteko erlazioa zehazteko, analisi termograbimetrikoa egin zitzaien. P3.4. Irudian, lagin bakoitzaren TGA termogramak eta dagozkien DTG kurbak irudikatzen dira. DTG kurbetatik, $EOPE_{CG}$ eta $POPE_{CG}$ biopoliolek lau degradazio-eremu zituztela ondorioztatu zen; $EOPR_{CG}$ eta $POPR_{CG}$, berriz, 3 baino ez. Bestalde, $EOPE_{CG}$, $POPE_{CG}$ eta $POPR_{CG}$ biopolioletan, $EOPR_{CG}$ biopoliolean ikusi ez zen azken degradazio-eremu bat identifikatu zen. Detektatutako degradazio-eremuen tenperatura tarteak eta horien gehieneko degradazio-tenperaturak P3.3. Taulan azaltzen dira.

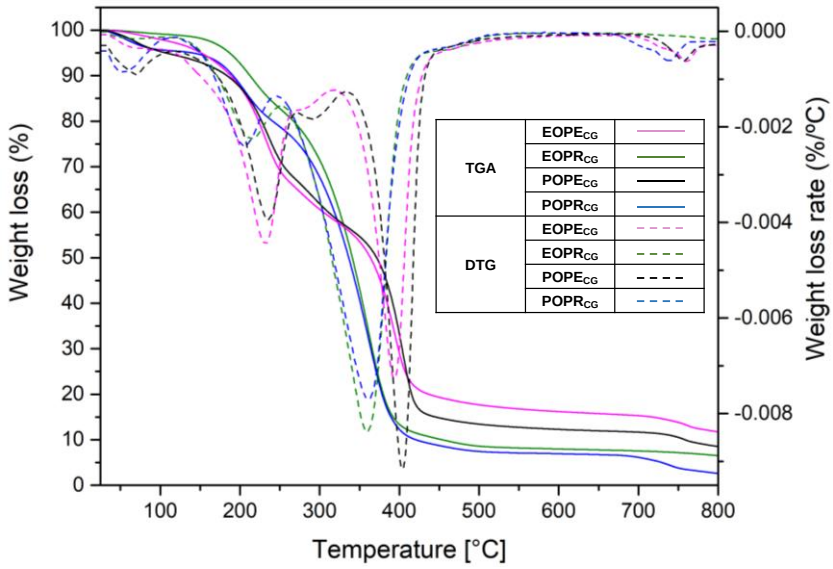


P3.4. Likidotutako biopoliolen TGA eta DTG termogramak

Lagin guztietan hezetasunarekin eta disolbatzailearekin erlazionatzen den lehen degradazio-eremu bat detektatu ahal izan zen, 30-110 °C artekoa. Hala ere, $POPR_{CG}$ eta $POPE_{CG}$ laginetan gertatuko pisu-galera nabarmenagoa izan zen ziurrenik prozesuan erabilitako azetonaren presentziagatik. Bigarren

degradazio-eremua (115-270 °C) eta hirugarrena (275-335 °C) glizerolaren eta PEGaren degradaziorekin erlazionatuta daude [23]. Ligninaren β-O-4 eta C-C loturen degradazioa 250-400 °C artekoa bada ere, lignina molekularen pisu molekularraren eta birpolimerizazio-mailaren arabera, degradazio hori tenperatura desberdinetan gerta daitekeela azpimarra behar da [24]. Horrek azalduko luke $EOPE_{CG}$ eta $POPE_{CG}$ laginetan lau degradazio-eremu eta $EOPR_{CG}$ eta $POPR_{CG}$ laginetan hiru baino ez egotea. Beraz, lignina pisu molekular handieneko $EOPE_{CG}$ eta $POPE_{CG}$ laginetan, ligninaren degradazioa 315-450 °C artean gertatu zen bitartean, $EOPR_{CG}$ eta $POPR_{CG}$ biopolioleetan tenperatura baxuagoetan gertatu zen, PEGaren degradazioarekin gainjarriz. Azkenik, 690 eta 775 °C artean, masa-galera txiki bat ikusi zen, ziurrenik laginetan ezpurutasun ez-organikoak zeudelako. Hala ere, ezin izan zen argi eta garbi zehaztu degradazio horren jatorria.

P3.3. Taula. TGA-DTG kurben degradazio-faseen tarte-tenperatura ($T_{int}$) eta degradazio-tenperatura maximoa ($T_m$)

| | | $EOPE_{CG}$ | $EOPR_{CG}$ | $POPE_{CG}$ | $POPR_{CG}$ |
|---|---|---|---|---|---|
| 1. Etapa | Tinter (°C) | 30-100 | 30-110 | 30-110 | 30-110 |
| | Tmax (°C) | 72 | 70 | 70 | 56 |
| 2. Etapa | Tinter (°C) | 115-267 | 125-255 | 120-267 | 120-250 |
| | Tmax (°C) | 233 | 214 | 235 | 205 |
| 3. Etapa | Tinter (C) | 267-315 | 214-430 | 267-335 | 250-430 |
| | Tmax (°C) | 283 | 360 | 291 | 361 |
| 4. Etapa | Tinter (°C) | 315-440 | - | 335-450 | - |
| | Tmax (°C) | 391 | - | 403 | - |
| 5. Etapa | Tinter (°C) | 705-775 | - | 705-775 | 690-770 |
| | Tmax (°C) | 758 | | 758 | 740 |

Azkenik, biopolioleen propietate biskoelastikoak eta jariakin portaera zehazteko laginei azterketa erreologiko bat egin zitzaien, **II. Eranskinean** deskribatutako metodologia erabiliz. Portaera biskoelastikoa aztertzeko, oszilazio-saiakuntza bat egin zen, biltegiratze-modulua (G') galera-moduluarekin (G'') alderatuz (P3.5. Irudia).

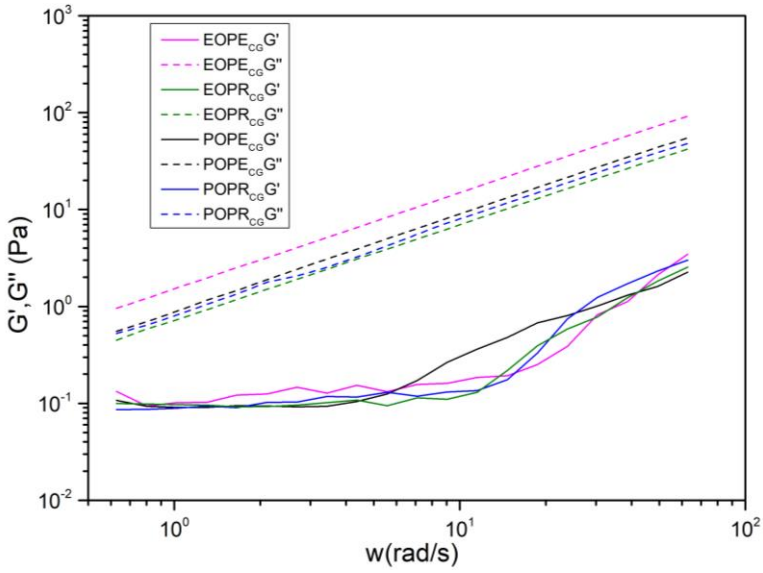


P3.5. Irudia. Biopoliolen biltegiratze-modulua (G') eta galera-modulua (G'') (Pa) ω(rad/s)-ren arabera

P3.5. Irudiko erreogramen analisitik biopoliolek jarrera likidoa zutela ondorioztatu zen, kasu guztietan G''-ren balioak G'-renak baino handiagoak izan baitziren maiztasun-tarte osorako. Gainera, espero zen bezala, biopoliolen pisu molekularrak handitzean moduluak ere handitu egin ziren, eta, beraz, $EOPE_{CG}$ eta $POPE_{CG}$ moduluek $EOPR_{CG}$ eta $POPR_{CG}$ moduluak baino handiagoak izan ziren [25]. Biopoliolen jariakin portaera eta biskositatea saiakuntza errotazional baten bidez aztertu zen. Saiakuntza horretan, η-ren, τ-ren eta $\dot{\gamma}$-ren arteko erlazioa aztertu zen. Parametro hauek, **II. Eranskinaren *V. atalean*** adierazten den Power-Law ekuaziora doitu ziren eta lortutako datuak P3.4. Taulan azaltzen dira. Bestalde, lortutako fluxu-kurbak P3.6a eta 3.6b irudietan irudikatzen dira.

P3.4. Taula. Aztertutako biopolioleen datuetan oinarritutako Power-Law funtzio linealak

| Lagina | Funtzioa | $k$ (Pa·s$^n$) | $n$ | $R^2$ |
|---|---|---|---|---|
| $EOPE_{CG}$ | $\tau = 1{,}4299 \cdot \dot{\gamma}^{1{,}0176}$ | 1,4299 | 1,0176 | 0,9985 |
| $EOPR_{CG}$ | $\tau = 0{,}7290 \cdot \dot{\gamma}^{0{,}9911}$ | 0,7290 | 0,9911 | 0,9995 |
| $POPE_{CG}$ | $\tau = 0{,}9352 \cdot \dot{\gamma}^{0{,}9978}$ | 0,9352 | 0,9978 | 0,9988 |
| $POPR_{CG}$ | $\tau = 0{,}7927 \cdot \dot{\gamma}^{1{,}0011}$ | 0,7927 | 1,0011 | 0,9939 |

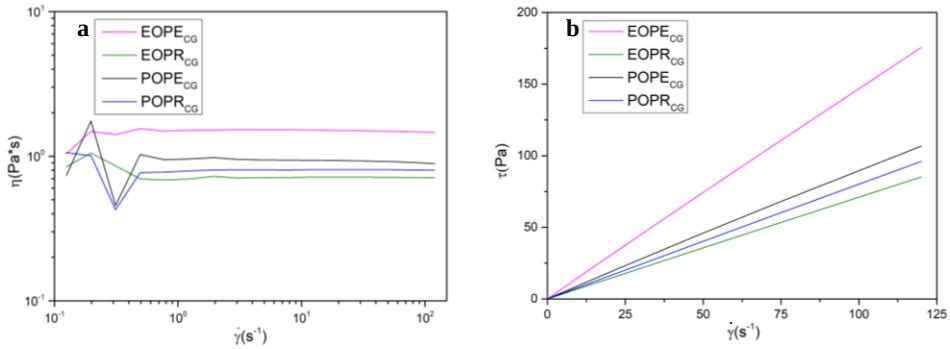


P3.6. Irudia. Biopoliolen (a) Biskositatea (η) VS zizatzaile-abiadura ($\dot{\gamma}$); (b)zizatzaile-tentsioa (τ) VS zizatzaile-abiadura ($\dot{\gamma}$)

Kasu guztietan 0,99tik gorako $R^2$ balioak lortu ziren, erreogramak ondo doituta zeudela eta, beraz, portaera erreologikoa ebaluatzeko aukeratutako eredua egokia zela adieraziz. Gainera, fluxu-indizearen balioak unitatearen berdinak edo oso antzekoak izan zirenez, biopoliolak Newtoniar portaera izan zutela ondorioztatu zen. Biopoliolen portaera hori P3.6a irudian ikusi ahal izan zen, zeinean biskositatea konstante mantendu zen aplikatutako edozein $\dot{\gamma}$ baliorako, eta P3.6b. Irudian irudikatzen den τ-ren eta $\dot{\gamma}$-ren arteko portaera aztertuz baieztatu egin zen. Kasu guztietan, parametro horien irudikapen grafikoak jatorritik igarotzen zen lerro zuzen bat eman zuela ikusi zen, eta haren maldak biopoliol bakoitzaren κ balioaren berdinak zirela. Gainera, espero zen bezala, biopolioleen $M_w$-a zenbat eta handiagoa izan, orduan eta biskositate handiagoa izan zuten [26]. Horrela, biopoliol bakoitzaren biskositatea bat etorri zen bere κ balioarekin [27], hau da, 1,4299 Pa·s ($EOPE_{CG}$)-rentzat, 0,7920 Pa·s (EOPRCG)-rentzat, eta 0,9352 eta

0,7927 Pa·s $POPE_{CG}$ eta $POPR_{CG}$-rentzat. Beraz, balio horiek 300 Pa·s baino txikiagoak zirenez, biopoliolak PUak ekoizteko egokiak zirela ondorioztatu zen.

## 2.3. Glizerol gordinak biopoliolen parametroetan duen eragina

Beste egile batzuek biomasa lignozelulosikoa likuefaktatzean lortutako emaitzak, besteak beste glizerola eta CG disolbatzaile gisa erabilita, P3.5. Taulan laburbiltzen dira. Dena den, argitalpen honetan erabilitako erreakzio-baldintzak ***2. Argitalpenean*** lortutako baldintza optimoak direnez, lehenik eta behin bi argitalpenetan lortutako emaitzak alderatzen dira.

Erreakzio-errendimenduak nahiko antzekoak izan ziren bi argitalpenetan, baina ezpurutasuna eta glizerol-eduki txikiagoren ondorioz, CG disolbatzaile gisa erabiltzean erreakzioaren errendimendua murriztu egin zen [16].

Gainera, glizerol-molekulen kantitate txikiagoaren eta talde hidroxiloak kontsumi ditzaketen ezpurutasunen ondorioz, CGrekin sintetizatutako biopoliolen $I_{OH}$-a glizerol komertzialarekin sintetizatutako biopolioleena baino txikiagoa izan zen [28].

$A_n$-ren portaera ***2. Argitalpenean*** ikusitakoaren berdina izan zen, hau da, katalizatzailearen kontzentrazioa zenbat eta handiagoa izan, orduan eta handiagoa $A_n$-en balioak. Hala ere, CG disolbatzaile gisa erabiltzean, $A_n$-en balioak apur bat txikiagoak izan ziren, CG-ko ezpurutasun organikoek konposatu azidoen kontsumoa eragin baitezakete [28].

$M_w$-ei dagokienez, 2. Argitalpenean lortutakoekin alderatuta, CG disolbatzaile gisa erabiltzean handitu egin zirela esan behar da, bereziki $EOPE_{CG}$ biopoliolean. Gorakada hori glizerolaren eta ezpurutasunen (FFA eta FAME) arteko polimerizazio-erreakzioek eragin dezakete [29]. Gainera, hazkunde horren ondorioz CGarekin sintetizatutako biopolioleen PDIak ere

handitu egin ziren Hu et al., (2014b)-ek [16] jakinarazi zuen bezala. Era berean, EOPECG-ren funtzionalitatea beharrezko den balioaren baino zerbait gainetik egon arren, ondorioztatu ahal izan zen bi argitalpenetan lortutako funtzionalitateak ere antzekoak izan zirela kasu guztietan, eta egokiak nahi diren PUak sintetizatzeko. CGrekin sintetizatutako biopolioleen biskositateei dagokienez, ***2. Argitalpenkekoekin*** alderatuta, aurreikus zitekeen bezala, handitu egin ziren laginen $M_w$-a handitu ahala edo $POPE_{CG}$-ren kasuan bezala, ia berdin mantendu ziren.

Jarraian, alderaketa bibliografikoa egiten da. $EOPR_{CG}$ eta $POPR_{CG}$ biopolioleen errendimenduak, CGa erabili arren, biomasa lignozelulosikoa edo lignina likidotzeko prozesuetan lortutako balio tipikoen artean aurkitzen dira (P3.5 Taula). Bestalde, Tran et al., (2021)-ek [35] azetonan disolbagarria den lignina CG eta 1,4-butanodiola disolbatzaile gisa eta azido sulfurikoa katalizatzaile gisa erabiliz likidotzean lortutako errendimenduak $EOPE_{CG}$ eta $POPE_{CG}$-ren oso antzekoak izan ziren.

Nabarmentzekoa da P3.5. Taulan laburbiltzen diren azterlan gehienetan poliolak aparrak fabrikatzeko erabili zirela. Azterlan horietan, $I_{OH}$-ren balioak 100 mg KOH/g eta 811,8 mg KOH/g artekoak izan ziren, beraz, $EOPR_{CG}$ eta $POPR_{CG}$ biopolioleen $I_{OH}$ balioak bat etorri ziren bibliografian aurkitutako balioekin.

P3.5. Taulan adierazitako azterlan gutxik adierazten zuten poliolen PDIa, eta egiten zutenak PU aparren sintesirako polioleez ari ziren. Lan horietan adierazitako PDIak $EOPR_{CG}$ eta $POPR_{CG}$ biopolioleen PDIen antzekoak izan ziren. Lee and Lin, (2008)-ek PUzko itsasgarriak ekoizteko poliolak sintetizatu zituzten, 310 mg KOH eta 287 mg KOH $I_{OH}$-rekin, Taiwaneko akazia eta Txinako izeia PEG, glizerola eta azido sulfurikoarekin egindako likuefazioaren bidez. Balio horiek lan honetan sintetizatutako $EOPE_{CG}$ eta $POPE_{CG}$ biopolioleen balioen oso antzekoak izan ziren. Antzera, Jiang et al.,

(2021)-ek [37] PUzko itsasgarriak sintetizatu zituen biomasa lignozelulozikotik (Norvegiako izeia) eratorritako poliolak erabiliz, nahiz eta kasu horretan lortutako $I_{OH}$-ak handiagoak izan (825 eta 623 mg KOH/g). Zoritxarrez, ez zen aurkitu PUzko poliol mota horren PDIa eta funtzionaltasuna adierazten duen lanik. Azkenik, $A_n$-ren balioak, ligninaren likidotze prozesuetan lortzen diren ohiko balioen artean daude (0-40 mg KOH/g).

3.5. Taula. Glizerol komertziala edo glizerol gordina erabiliz niomasa lignozelulosikoaren eta ligninaren likidotze buruzko bibliografia

| Lehengaia | Disolbatzailea | Errendimendua (%) | $I_{OH}$ | $A_n$ | Mw | PDI | *f* | Katalizatzailea $H_2SO_4$ | Erabilpena | Ref, |
|---|---|---|---|---|---|---|---|---|---|---|
| *Eucalyptus globulus* organosolv lignin | PEG + G | 98,63 ± 0,71 | 595,15 ± 33,92 | 2,74 ± 0,00 | 1394 ± 12 | 3,69 ± 0,08 | 4,03 ± 0,15 | - | PU zurruna | Pending publication |
| | | 71,98 ± 1,41 | 253,84 ± 60,59 | 33,01 ± 0,00 | 4895 ± 325 | 9,37 ± 1,12 | 2,36 ± 0,44 | 5% | PU elastikoa | |
| *Pinus radiata* organosolv lignin | | 98,93 ± 0,14 | 514,28 ± 42,70 | 5,63 ± 0,23 | 1383 ± 43 | 3,58 ± 0,08 | 3,55 ± 0,26 | - | PU zurruna | |
| | | 87,56 ± 3,30 | 209,67 ± 3,70 | 30,56 ± 0,15 | 5408 ± 765 | 6,95 ± 0,91 | 2,91 ± 0,08 | 3,86% | PU elastikoa | |
| *Eucalyptus globulus* Kraft lignin | PEG + G | 95,27 | 537,95 | - | 1775 | 3.51 | - | 3% | - | [26] |
| Olive tree pruning organosolv lignin | PEG + G | 99,07 | 811.8 | - | - | - | - | 1% | - | [30] |
| *Eucalyptus globulus* kraft lignin | PEG + G | >86 | 100-660,08 | 0,8-10,70 | 1459-1990 | - | - | 3, 6, 9 (azido organikoak) | - | [31] |
| Enzymatic hydrolysis lignin of cornstalk | PEG + G | >90 | 191-409 | - | - | - | - | 15% | - | [18] |
| Alkaline corncob lignin | PEG + G | 97,47 | 484.03 | - | 525 | 1,13 | - | 1,5% | PU aparra | [32] |
| Sugarcane bagasse Organosolv lignin | CG | - | 435 | - | - | - | - | - | PU aparra | [33] |
| Softwood Kraft lignin | | - | 515 | - | - | - | - | | | |
| Hardwood Lignosulphonate | | - | 529 | - | - | - | - | | | |

| Lehengaia | Disolbatzailea | Errendimendua (%) | $I_{OH}$ | $A_n$ | Mw | PDI | *f* | Katalizatzailea $H_2SO_4$ | Erabilpena | Ref, |
|---|---|---|---|---|---|---|---|---|---|---|
| Kraft lignin (softwood) | CG | >0,61 (g/g CG) | 412 | | 5088 | 2,2 | - | - | PU aparra | [34] |
| Organosolv lignin (sugarcane bagasse) | | | 224 | | 7867 | 4,9 | - | | | |
| Lignosulphonate (hardwood) | | | 592 | | 7384 | 3,3 | - | | | |
| Acetone soluble lignin | CG + 1,4-BDO | 72,64 | ≈1100 | ≈4 | - | - | - | 1% | PU aparra | [35] |
| Kraft pine lignin | CG + 1,4-BDO | 93 | 670 | - | - | - | - | - | PU aparra | [21] |
| Repeseed cake | PEG + G | 84 | 586 | - | - | - | - | 80:20:3 (PEG: G : $H_2SO_4$) | - | [23] |
| Data seeds | | 96 | 395 | - | - | - | - | | | |
| Olive stone | | 92 | 496 | - | - | - | - | | | |
| Corncob | | 91 | 504 | - | - | - | - | | | |
| Apple pomace | | 97 | 428 | - | - | - | - | | | |
| Wheat straw | | - | 350 | 28 | 1270 | 1,22 | | - | PU aparra | [19] |
| Taiwan acacia | PEG + G | 95,2 | 310 | 25,6 | - | - | - | 3:1:0,09 (disolbatzaile: biomasa: $H_2SO_4$) | Itsasgarriak | [36] |
| China fir | | 98,4 | 287 | 38,0 | - | - | - | | | |
| Norway spruce | EG | 99,7 | 825-623 | 48,2-47,8 | - | - | - | 4,5 g | Itsasgarriak | [37] |

# 3. ONDORIOAK

Lan honetan, lignina likidotzearen erreakzioaren bidez, PU elastikoak eta zurrunak ekoizteko beharrezko ezaugarriak zituzten biopoliolak arrakastaz sintetizatu ziren. Likidotze erreakzioa mikrouhin erreaktore bat eta PEG eta CGa disolbatzaile gisa erabiliz gauzatu zen, ***2. Azterlanean*** optimizatutako erreakzio-baldintzak erabiliz. CGaren eragina nabarmena izan zen lortutako emaitzak ***2. Azterlanean*** lortutakoekin alderatzean. Likidotze errendimenduak behera egin zuten kasu guztietan, nahastean glizerol gutxiago baitzegoen. Horrela, $EOPR_{CG}$ eta $POPR_{CG}$ biopoliolen errendimenduak %90etik gorakoak izan ziren, eta $EOPE_{CG}$ eta $POPE_{CG}$-renak berriz, nabarmen txikiagoak izan ziren, %70 eta % 80 artekoak, erreakzioan erabilitako azido sulfurikoaren eraginaren ondorioz. CG-aren glizerol-eduki baxuagoak, biopoliolen $I_{OH}$-an eragina izan zuen. Azterlan honetan 554 eta 383 mg KOH/g bitarteko $I_{OH}$ balioak lortu ziren $EOPR_{CG}$ eta $POPR_{CG}$ biopoliolentzat, hurrenez hurren, eta 228 eta 173 mg KOH/g bitarteko balioak $EOPE_{CG}$ eta $POPE_{CG}$ biopoliolentzat. Bestalde, lortutako $A_n$ balioak ligninaren likidotze prozesuetan lortzen diren ohiko balioen artean egon ziren. Funtzionaltasunei dagokienez, $EOPE_{CG}$-ren kasuan lortutako balioa nahi baino pixka bat altuago izan bazen ere, lortutako balioak PUak ekoizteko egokiak zirela esan daiteke. Oro har, eta beste parametro guztiak aztertuta, parametro batzuen emaitzek okerrera egin badute ere, CGa ligninaren likuefakzio erreakzioetan erabil daitekeela ondorioztatu zen biopoliolak ekoizteko.

## ERREFERENTZIAK

[1] S. Kongjao, S. Damronglerd, M. Hunsom, Korean J. Chem. Eng. 27(3) (2010) 944–9. 10.1007/s11814-010-0148-0.

[2] S. Hu, X. Luo, C. Wan, Y. Li, J. Agric. Food Chem. 60(23) (2012) 5915–21. 10.1021/jf3008629.

[3] C.V. Rodrigues, K.O. Santana, M.G. Nespeca, J. Eduardo de Oliveira, S.I. Maintinguer, Int. J. Hydrogen Energy 41(33) (2016) 14641–51. 10.1016/j.ijhydene.2016.06.209.

[4] L.R. Kumar, S.K. Yellapu, R.D. Tyagi, X. Zhang, Bioresour. Technol. 293(August) (2019) 122155. 10.1016/j.biortech.2019.122155.

[5] C.A.G. Quispe, C.J.R. Coronado, J.A. Carvalho, Renew. Sustain. Energy Rev. 27 (2013) 475–93. 10.1016/j.rser.2013.06.017.

[6] J.C. Thompson, B.B. He, Appl. Eng. Agric. 22(2) (2006) 261–5. 10.13031/2013.20272.

[7] M.D. Bohon, B.A. Metzger, W.P. Linak, C.J. King, W.L. Roberts, Proc. Combust. Inst. 33(2) (2011) 2717–24. 10.1016/j.proci.2010.06.154.

[8] A. Hejna, P. Kosmela, M. Klein, K. Formela, M. Kopczyńska, J. Haponiuk, Ł. Piszczyk, J. Polym. Environ. 26(8) (2018) 3334–44. 10.1007/s10924-018-1217-4.

[9] M. Nanda, Z. Yuan, W. Qin, Austin J. Chem. Eng. 1(1) (2014) 1–7.

[10] M. Ionescu, in: De Gruyter (Ed.), Polyols for Polyrethanes, Boston, Berlin, 2019, pp. 1–10.

[11] Y. Lee, E.Y. Lee, J. Wood Chem. Technol. 36(5) (2016) 353–64.

10.1080/02773813.2016.1156132.

[12] S. Hu, X. Luo, Y. Li, ChemSusChem 7(1) (2014) 66–72. 10.1002/cssc.201300760.

[13] X. Luo, S. Hu, X. Zhang, Y. Li, Bioresour. Technol. 139 (2013) 323–9. 10.1016/j.biortech.2013.04.011.

[14] J. D'Souza, R. Camargo, N. Yan, Polym. Rev. 57(4) (2017) 668–94. 10.1080/15583724.2017.1283328.

[15] Y.Y. Li, X. Luo, S. Hu, Bio-based Polyols and Polyurethanes, 2015, pp. 1–79.

[16] S. Hu, Y. Li, Ind. Crops Prod. 57 (2014) 188–94. 10.1016/j.indcrop.2014.03.032.

[17] S.H. Lee, M. Yoshioka, N. Shiraishi, J. Appl. Polym. Sci. 78(2) (2000) 319–25. 10.1002/1097-4628(20001010)78:2<319::AID-APP120>3.0.CO;2-Z.

[18] Y. Jin, X. Ruan, X. Cheng, Q. Lü, Bioresour. Technol. 102(3) (2011) 3581–3. 10.1016/j.biortech.2010.10.050.

[19] F. Chen, Z. Lu, J. Appl. Polym. Sci. 111 (2009) 508–16. 10.1002/app.29107.

[20] M. Ionescu, in: De Gruyter (Ed.), Polyols for Polyurethanes, Boston, Berlin, 2019, pp. 307–20.

[21] K. Gosz, P. Kosmela, A. Hejna, G. Gajowiec, Ł. Piszczyk, Wood Sci. Technol. 52(3) (2018) 599–617. 10.1007/s00226-018-0991-4.

[22] M. Ionescu, Z.S. Petrović, Eur. J. Lipid Sci. Technol. 120(6) (2018) 1–9.

10.1002/ejlt.201800004.

[23] R. Briones, L. Serrano, J. Labidi, J. Chem. Technol. Biotechnol. 87(2) (2012) 244–9. 10.1002/jctb.2706.

[24] A. Morales, B. Gullón, I. Dávila, G. Eibes, J. Labidi, P. Gullón, Ind. Crops Prod. 124(May) (2018) 582–92. 10.1016/j.indcrop.2018.08.032.

[25] K. Behera, Y.H. Chang, F.C. Chiu, J.C. Yang, Polym. Test. 60 (2017) 132–9. 10.1016/j.polymertesting.2017.03.015.

[26] S.H.F. da Silva, P.S.B. dos Santos, D. Thomas da Silva, R. Briones, D.A. Gatto, J. Labidi, J. Wood Chem. Technol. 37(5) (2017) 343–58. 10.1080/02773813.2017.1303513.

[27] P. Parcheta, J. Datta, Polym. Test. 67(January) (2018) 110–21. 10.1016/j.polymertesting.2018.02.022.

[28] S. Hu, C. Wan, Y. Li, Bioresour. Technol. 103(1) (2012) 227–33. 10.1016/j.biortech.2011.09.125.

[29] X. Luo, S. Hu, X. Zhang, Y. Li, Bioresour. Technol. 139 (2013) 323–9. 10.1016/j.biortech.2013.04.011.

[30] A. Sequeiros, L. Serrano, R. Briones, J. Labidi, J. Appl. Polym. Sci. 130(5) (2013) 3292–8. 10.1002/app.39577.

[31] S.H.F. da Silva, I. Egüés, J. Labidi, Ind. Crops Prod. 137(March) (2019) 687–93. 10.1016/j.indcrop.2019.05.075.

[32] B.L. Xue, J.L. Wen, R.C. Sun, Materials (Basel). 8(2) (2015) 586–99. 10.3390/ma8020586.

[33] L.C. Muller, S. Marx, H.C.M. Vosloo, J. Renew. Mater. 5(1) (2017) 67–

80. 10.7569/JRM.2016.634130.

[34] L.C. Muller, S. Marx, H.C.M. Vosloo, I. Chiyanzu, Polym. from Renew. Resour. 10(1–3) (2019) 3–18. 10.1177/2041247919830833.

[35] M.H. Tran, J.H. Yu, E.Y. Lee, Polymers (Basel). 13(9) (2021). 10.3390/polym13091491.

[36] W.-J. Lee, M.-S. Lin, J. Appl. Polym. Sci. 109(1) (2008) 23–31. 10.1002/app.28007.

[37] W. Jiang, R. Hosseinpourpia, V. Biziks, S.A. Ahmed, H. Militz, S. Adamopoulos, Polymers (Basel). 13(19) (2021) 1–18. 10.3390/polym13193267.

# SYNTHESIS OF POLYURETHANE AND NON-ISOCYANATE POLYURETHANE WOOD ADHESIVES

*“In my experience, when you think you understand The Force,*

*you realize just how little you know”*

*Ashoka Tano*

## Publication IV

# Synthesis, characterisation, and thermal degradation kinetic of lignin-based polyurethane wood adhesives

## ABSTRACT

In this work, different PU wood adhesives were synthesised using different ligno-based bio-polyols obtained in ***Publication II***. The synthesis of PUs was carried out by one-shot method using THF as solvent and MDI as diisocyanate employing different NCO:OH ratios (2.0:1, 2.5:1, and 3.0:1). The chemical structure of the formulated wood adhesive PUs was determined through ATR-FTIR and the shear strength was analysed using Automated Bonding Evaluation System (ABES). Through this technique it was concluded that an NCO:OH ratio of 2.5:1 was the formulation that showed the best shear strength for a pressing time of 120 s. Employing this ratio and the same synthesis procedure, two new PUs were synthesised using the bio-polyols obtained in ***Publication III***.

Finally, a study of thermal degradation kinetics employing the OFW and KAS isoconversional methods of the PUs synthesised with an NCO:OH ratio of 2.5:1 was carried out. On the one hand, the $E_a$ of each system were estimated for the different α ratios, obtaining values of 226 (KJ/mol) ($LPA_{EOPE}$), 180.8 (KJ/mol) ($LPA_{EOPECG}$), 146.9 (KJ/mol) ($LPA_{POPE}$) and 143.4 (KJ/mol) ($LPA_{POPECG)}$. In addition, the pre-exponential factor was determined with which an estimation of the lifetime of the polymers was performed.

# 1. MATERIALS AND METHODS

## 1.1. Materials

The raw materials, *Eucalyptus globulus* chips and *Pinus radiata*, as well as the used vegetable oil and chemicals employed in this work were obtained as described in ***section 2.1*** of the **2nd PART.**

## 1.2. Lignin obtaining procedure

Lignins used in this work were obtained after the organosolv delignification process and the subsequent ultrasound treatment of the black liquor described in ***section 2.2*** of the **2nd PART**. These lignins called EOUL (*Eucalyptus globulus* organosolv lignin) and POUL (*Pinus radiata* organosolv lignin) were characterised in ***Publication II***.

## 1.3. Crude glycerol obtaining procedure

CG was obtained by the transesterification reaction outlined in **section 2.4** of the **2nd PART**.

## 1.4. Synthesis of bio-polyols through microwave assisted liquefaction

The liquefaction of organosolv lignins (EOUL and POUL) were performed following the methodology detailed in the ***section 2.3.1*** of the **2nd PART**.

The catalyst concentration, as well as the reaction temperature and the PEG/CG ratio involved in the reaction, were obtained from the optimisation carried out in ***Publication II*** and are summarised below (Table P4.1).

Table P4.1. Liquefaction reaction conditions optimised in ***Publication II***

| Bio-polyol | EOPE & $EOPE_{CG}$ | POPE & $POPE_{CG}$ |
|---|---|---|
| Cat (% wt.) | 5 | 3.86 |
| Temperature (°C) | 180 | 160 |
| PEG/CG (% wt.) | 7.57/1 | 7.34/1 |

## 1.5. Synthesis of lignin-based polyurethane adhesives

The synthesis of the different lignin-based polyurethane adhesives (LPA) using the above-mentioned bio-polyols, i.e., EOPE, $EOPE_{CG}$, POPE and $POPEC_{CG}$ was carried out following the procedure described in the ***section 2.5*** of the **2nd PART**. Three different NCO:OH ratios were employed in the synthesis of PUs using EOPE and POPE bio-polyols, viz. 2.0:1, 2.5:1 and 3.0:1. For the synthesis of PUs with $EOPE_{CG}$ and $POPEC_{CG}$, the ratio giving the best shear strength value was employed. Table P4.2 shows the recipe used for each of the synthesised LPA.

Table P4.2. Recipe used for the synthesis of LPAs

| | | $LPA_{EOPE}$ | $LPA_{POPE}$ | $LPA_{EOPECG}$ | $LPA_{POPECG}$ |
|---|---|---|---|---|---|
| Bio-polyol (g) | | 2.5 | 2.5 | 2.5 | 2.5 |
| THF (g) | | 1.5 | 1.5 | 1.5 | 1.5 |
| DBTDL (wt%)* | | 0.2 | 0.2 | 0.2 | 0.2 |
| NCO:OH | 2.0:1 | 3.68 | 2.03 | - | - |
| | 2.5:1 | 4.6 | 2.53 | 3.96 | 3.40 |
| | 3.0:1 | 5.52 | 3.04 | - | - |

## 1.6. Characterisation of the obtained bio-polyols

Important parameters, such as such as molecular weight distribution ($M_w$, $M_n$ and PDI), hydroxyl number ($I_{OH}$), acid number ($A_n$) and functionality (*f*) of the bio-polyols obtained in the reaction scale-up were determined.

Furthermore, the thermal degradation of bio-polyols was studied through a thermogravimetric analysis (TGA) and their rheological behaviour was assessed. This characterisation was conducted according to the methodologies explained in **Appendix II**.

### 1.7. Characterisation of lignin-based polyurethane adhesives

The LPAs were characterised through ATR-FTIR to determine both their chemical structure and their degree of microphase separation and miscibility. In addition, thermogravimetric analysis was employed to study the thermal degradation, the thermal degradation kinetic by OFW and KAS methods and the lifetime estimation of the PUs by OFW method. In addition, the shear strength of the LPAs was assessed by adhesion test employing an automated bonding evaluation system (ABES). For these characterisations, the procedures described in **Appendix II** were used. The curing process of the PUs was carried out at room temperature for 7 days.

## 2. RESULTS AND DISCUSSION

### 2.1. Bio-polyols characterisation

The bio-polyols were characterised to establish their suitability for the synthesis of polyurethane adhesives. Therefore, the molecular weight distribution ($M_w$, $M_n$, PDI), hydroxyl number ($I_{OH}$), acid number ($A_n$), functionality (*f*), and the chain derived from a hydroxyl group (EW) of the different samples were analysed, and a summary of the results is presented in Table P4.3.

Table P4.3. Characterisation of bio-polyols employed to synthesise PUs

| Sample | $M_n$ | $M_w$ | PDI | $I_{OH}$ | $A_n$ | *f* | EW |
|---|---|---|---|---|---|---|---|
| EOPE | 739±43 | 3934 ± 98 | 5.33±0.18 | 330 ± 3 | 35 ± 0.36 | 4.16 | 153.7 |
| POPE | 707±32 | 4079 ± 50 | 6.29±0.92 | 182 ± 51 | 25 ± 0.00 | 2.29 | 271 |
| $EOPE_{CG}$ | 852±8 | 6644 ± 89 | 7.79±0.18 | 284 ± 1 | 17 ± 0.24 | 4.29 | 186.4 |
| $POPE_{CG}$ | 933±85 | 11035 ± 1059 | 12.63±0.00 | 182 ± 30 | 20 ± 0.64 | 2.83 | 277.7 |

$M_n$ and $M_W$ (g/mol), $I_{OH}$ and $A_n$ (mgKOH/g)

As expected, the obtained results were like those obtained in our previous works (data not published), although, expectedly, due to the scale-up of the

reaction, they differed slightly. Thus, the $M_w$ was within the range required for this type of PU (2000-10000 g/mol) except for $POPE_{CG}$ which has a $M_w$ of 11035 g/mol [1]. As with this type of bio-polyols synthesised through liquefaction reactions, the $A_n$ in all cases was high, but within the usual values [2]. However, the $I_{OH}$ values resulted to be higher than 28-160 mg KOH/g, which are the values suggested for the synthesis of these PUs [3]. This is especially pronounced for EOPE and $EOPE_{CG}$, while POPE and $POPE_{CG}$ were practically in the required range. In addition, *f* of POPE and $POPE_{CG}$ bio-polyols was between 2 and 3 in both cases, whereas that of the EOPE and $EOPE_{CG}$ bio-polyols was 4.16 and 4.29 respectively. The EW of POPE and $POPE_{CG}$ resulted to be higher than the EOPE and $EOPE_{CG}$, i.e., the chains derived from the hydroxyl groups of POPE and $POPE_{CG}$ were higher than those obtained for bio-polyols synthesised with organosolv lignin from *Eucalyptus globulus* [4]. This, together with the low functionality, the $I_{OH}$, and $M_w$, suggests that POPE and $POPE_{CG}$ bio-polyols could be more suitable for the synthesis of PU adhesives.

Differences with respect to our previous studies can be explained by the scale-up of the reaction and the type of vessel employed in each case. In fact, the vessel used in the scale-up was of round bottom flask type whereas in the previous studies it was of the test tube type, which makes more difficult the homogenisation of the sample. Therefore, although the $I_{OH}$ and *f* of EOPE and $EOPE_{CG}$ bio-polyols were slightly higher than the required values, the bio-polyols were suitable for synthesising PU adhesives.

### 2.2. Lignin-based polyurethane adhesive characterisation

A total of six PU adhesives were synthesised, three with each of the bio-polyols (EOPE and $EOPE_{CG}$), following the procedure summarised in Table P4.2. Aliquots of the PUs were taken every 30 minutes, with the aim of following the reaction, until the gel time was reached, and then they were

analysed by ATR-FTIR. The ATR-FTIR spectra are shown in Figure P4.1 and the most characteristic bands are listed in Table P4.4.

Table P4.4. ATR-FTIR band assignments of PU spectra synthesised with EOPE and POPE bio-polyols

| Wavenumber ($cm^{-1}$) | Band assignment |
|---|---|
| 3400 | O-H stretching |
| 3290 | N-H stretching vibration of urethane groups |
| 2970-2940-2870 | CH stretching of CH3 and CH2 |
| 2270 | Antisymetric stretching vibration of NCO |
| 1730-1706 | C=O stretching |
| 1599 | C-C stretching of the aromatic ring of MDI |
| 1507 | N-H vending vibration |
| 1407 | C-H stretching of the aromatic ring of MDI |
| 1308 | C-N stretching of urethane group |
| 1225 | C-N stretching of urethane group |
| 1096 | C-O-C stretching |

As observed, in all cases, as the reaction progresses in time, the band assigned to the O-H stretching (3400 $cm^{-1}$) decreases as a consequence of the reaction between the NCO groups of MDI and OH groups of bio-polyols to create urethane (NHCO) groups. The creation of urethane groups was confirmed by the appearance of the peaks at 3290 $cm^{-1}$, related with the stretching vibration of N-H groups, 1730 $cm^{-1}$ and 1706 $cm^{-1}$ bands corresponding to the C=O stretching vibration and the N-H vending vibration at 1507 $cm^{-1}$ [5]. These bands increased as the isocyanate groups were consumed to create urethane bonds. It is also observable the C-N stretching bands of urethane group at 1308 $cm^{-1}$ and 1225 $cm^{-1}$ [6]. The C-C and C-H absorptions bands which correspond to the stretching of the aromatic ring of the MDI are observed at 1599 $cm^{-1}$ and 1407 $cm^{-1}$ [7].

Two aspects are noteworthy; the first one is that surprisingly in the cured $LPA_{EOPE}$ samples, isocyanate remains unconsumed in all cases, while in the

$LPA_{POPE}$ samples, the band corresponding to the NCO anti-symmetric vibration (2270 $cm^{-1}$) is not observed in the cured samples. The reason for this is probably that lignin from *Eucalyptus globulus* is more sterically hindered than lignin form *Pinus radiata*, since the former has more syringyl groups [8]. This unreacted isocyanate in $LPA_{EOPE}$ samples, besides being toxic, could react with the OH of the beech veneer strip or the water adsorbed by wood to form covalent bonds increasing the shear strength, leading to undesired behaviour of the PU [9]. The second is that, as the reaction progresses, the contribution of the bands corresponding to the C=O groups which are related to the free urethanes (1730 $cm^{-1}$) and the one assigned to the urethane groups linked through hydrogen bonds (1709 $cm^{-1}$) [10] gradually changes.

Using ATR-FTIR spectra, the degree of separation and miscibility of the micro-phase of a PU can be determined [11]. In fact, analysing this area of the spectra corresponding to carbonyl stretching, the different C=O species present in PUs known as free C=O groups not associated by hydrogen bonds (free C=O and free C=O ester), H-bonded C=O in disordered hard segment (HS), H-bonded C=O in ordered HS and H-bonded C=O in disordered soft segment (SS), can be determined [12]. The analysis of the micro-phase separation is of interest because the mechanical properties of PUs, among others, depend to a large extent on it [13].

Through the deconvolution of the absorbance bands of C=O groups, the degree of micro-phase separation could be determined, the curve fitting of the different cured PUs samples was carried out through a Gaussian curve shape obtaining $R^2$ values above 0.999 in all cases and the spectra are shown in Figure P4.2. Table P4.5 summarised the theoretical hard segment ($HS_t$) percentage of each PU calculated as indicated in **Appendix II**, as well as the percentages of the different C=O species, which were calculated by deconvolution of such bands in the ATR-FTIR spectra.

As expected, the higher the NCO:OH ratio, the higher the $HS_t$ content, moreover the percentage of $HS_t$ was similar for PUs with the same isocyanate to hydroxyl ratio. The trend of free urethane carbonyl groups in HS in the $LPA_{EOPE}$ formulations was to decrease, although for the 2.5 the value was slightly lower than in 3.0. Consequently, the H-bonded urethane carbonyl groups in both disordered and ordered HS followed the opposite trend, i.e., they increased with increasing MDI content, except in formulation 2.5 which was the lowest, despite it showed H-bonded urethane carbonyl groups in Soft-Hard segment. On the other hand, $LPA_{POPE}$ formulations showed the same behaviour as $LPA_{EOPE}$, i.e., the H-bonded urethane carbonyl groups in disordered and ordered HS decreased in formulation 2.5 which is the opposite to what would be expected, since as the HS increases, the H-bonded urethane C=O groups tends to increase [10].

According to the procedure described by Niemczyk et al., (2017) [14], the mass fraction of the hard and soft segments of a PU, as well as their degree of micro-mixing, can be determined. Thus, it is possible to determine different parameters such as the proportion of H-bonded C=O groups ($X_{HB}$), the maximum mass fraction of the rigid segment mixed in the soft phase ($W_H$), if assuming that all the H-bondend C=O groups are only found in the rigid domains, the weight fraction of the mixed phase ($MP_W$), the soft segment weight fraction ($SS_W$) and the hard segment weight fraction ($HS_W$). The equations for the calculation of these parameters are listed in **Appendix II**. In Table P4.6 the corresponding values of these parameters are indicated for each formulation.

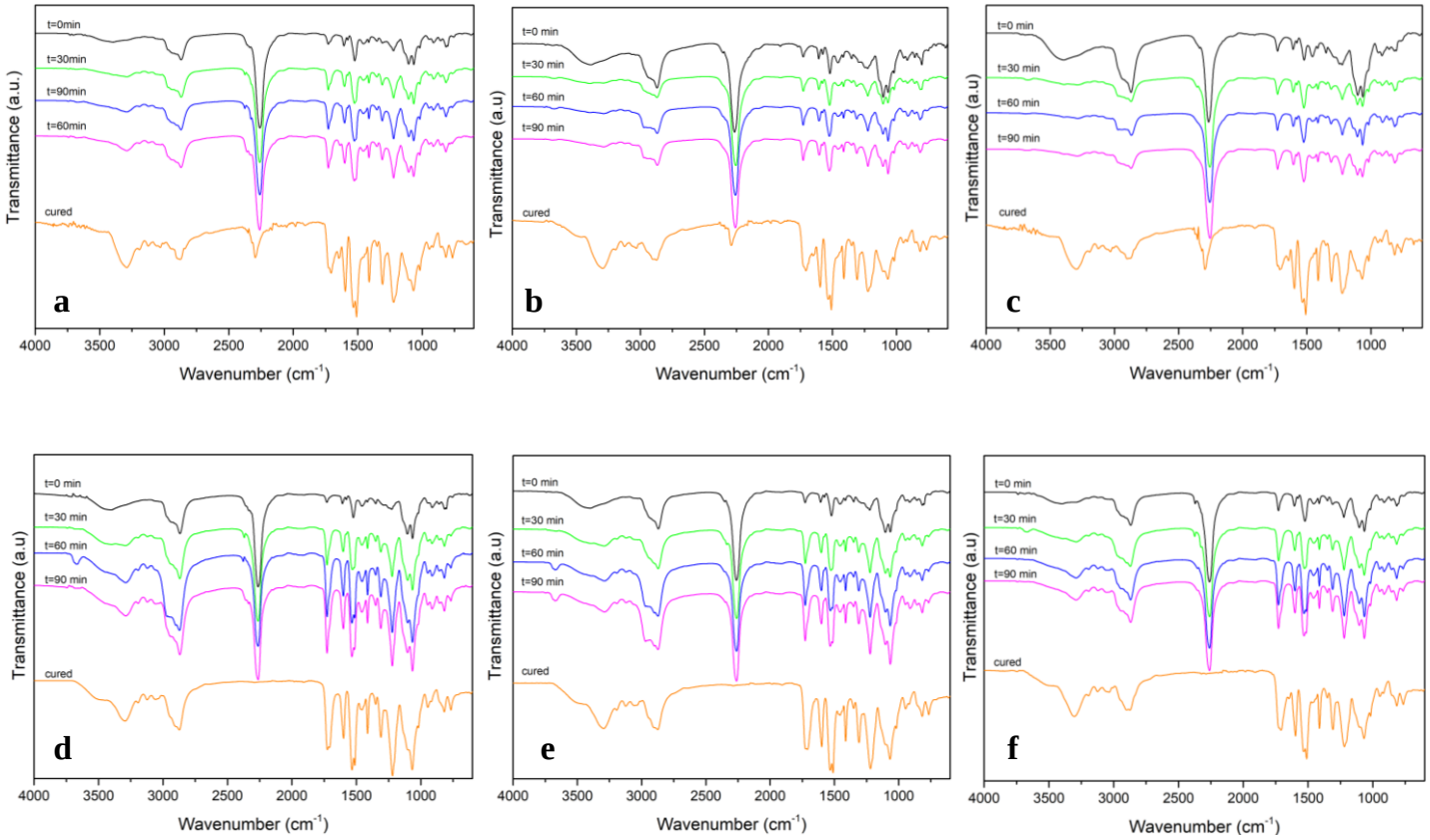


Figure P4.1. ATR-FTIR spectra of the LPA formulations at different reaction times and cured. a, b, and c are the 2.0, 2.5 and 3.0 $LPA_{EOPE}$ formulations and d, e and f are the $LPA_{POPE}$ equivalents

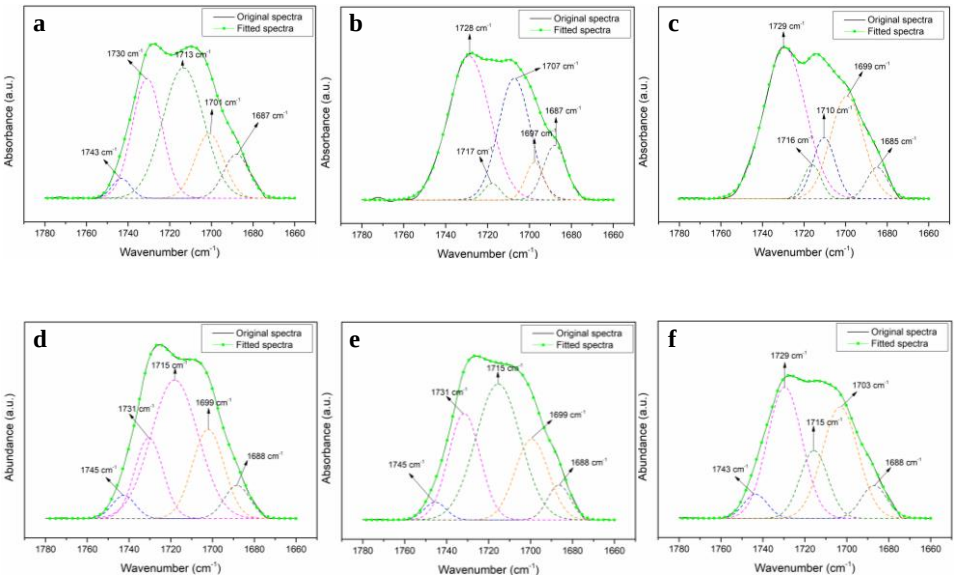


Figure P4.2. ATR-FTIR spectra in the absorbance region of the carbonyl groups of the different LPAs. a, b and c are the 2.0, 2.5 and 3.0 $LPA_{EOPE}$ formulations and d, e and f are the $LPA_{POPE}$ equivalents

Table P4.5. Percentages of C=O urethane species in cured LPAs

| | NCO/OH | NCO (mol) | $HS_t$ (%) | A | B | C | D | E | F |
|---|---|---|---|---|---|---|---|---|---|
| | 2.0:1 | 2.00 | 33.60 | 3.01 | 29.02 | 43.76 | --- | 15.02 | 9.19 |
| $LPA_{EOPE}$ | 2.5:1 | 2.50 | 38.74 | 2.24 | 29.56 | 39.15 | 8.10 | 10.46 | 10.49 |
| | 3.0:1 | 3.00 | 43.15 | 2.59 | 46.59 | 20.16 | --- | 25.70 | 4.64 |
| | 2.0:1 | 2.00 | 34.33 | 4.10 | 17.43 | 50.29 | --- | 21.67 | 6.51 |
| $LPA_{POPE}$ | 2.5:1 | 2.50 | 39.52 | 2.92 | 25.23 | 45.67 | --- | 20.19 | 5.98 |
| | 3.0:1 | 3.00 | 43.95 | 2.76 | 38.83 | 26.36 | --- | 27.05 | 5.00 |

A: 1745-1743 $cm^{-1}$ Free C=O in Soft Segment (%)
B: 1732-1729 $cm^{-1}$: Carbonyl-carbonyl interactions in Soft Segment (%)
C: 1714-1713 $cm^{-1}$: Free urethane C=O in Hard Segment (%)
D: 1706 $cm^{-1}$: H-bonded C=O in Soft-Hard Segment (%)
E: 1701-1697 $cm^{-1}$: H bonded urethane C=O in disordered Hard Segment (%)
F: 1686-1688 $cm^{-1}$: H bonded urethane C=O in ordered Hard Segment (%)

Table P4.6. Relevant parameters estimated for the determination of microphase of different formulations

| Sample | NCO:OH | *z* | $X_{HB}$ | $W_H$ | $MP_W$ | $SP_W$ | $HS_W$ |
|---|---|---|---|---|---|---|---|
| $LPA_{EOPE}$ | 2.0:1 | 0.336 | 0.316 | 0.257 | 0.086 | 0.750 | 0.250 |
| | 2.5:1 | 0.387 | 0.308 | 0.304 | 0.118 | 0.730 | 0.270 |
| | 3.0:1 | 0.431 | 0.556 | 0.252 | 0.109 | 0.677 | 0.323 |
| $LPA_{POPE}$ | 2.0:1 | 0.343 | 0.318 | 0.263 | 0.090 | 0.747 | 0.253 |
| | 2.5:1 | 0.395 | 0.323 | 0.307 | 0.121 | 0.726 | 0.274 |
| | 3.0:1 | 0.440 | 0.503 | 0.280 | 0.123 | 0.684 | 0.316 |

z is the $HS_t$ fraction

According to the analysis of the data presented in Table P4.6, the mass fraction of the H-bonded urethane groups ($X_{HB}$) tended to increase with increasing the HS content except for $LPA_{EOPE}$ 2.5 formulation which had the lowest value. Furthermore, in all cases the $X_{HB}$ content was low. This could be explained by the cross-linked and sterically hindered nature of the lignobased bio-polyol. This unique chemical conformation may inhibit hydrogen bonding between the carbonyl group of the urethane groups of a rigid segment chain and the NH urethane groups of adjacent rigid segment chains [15].

When analysing the mass fraction of the rigid segment mixed in the soft phase ($W_H$), the same behaviour to $X_{HB}$ was observed, i.e, it tends to increase with increasing the isocyanate content, therefore, the mass fraction of the mixed also increased. This was in agreement with the expected result, since increasing the MDI content in the mixture the degree of phase separation tends to be lower, in other words, the amount of hard segment mixed into the soft phase increases [14]. However, in the 3.0 formulations of both PUs, a decreasing behaviour was observed, thus in the case of $LPA_{EOPE}$ the lowest amount of rigid segment mixed in the soft phase was observed, while in the case of $LPA_{POPE}$ this formulation showed an intermediate value between

formulations 2.0 and 2.5. In general, $LPA_{EOPE}$ $W_H$ and $MP_W$ values were slightly lower than those of $LPA_{POPE}$, i.e., the former exhibited higher phase separation or lower miscibility between the HS and the SS. An explanation for this may lie in the nature of the lignin used to synthesise the PUs. Thus, lignin from *Eucalyptus globulus* with a higher number of syringyl groups in its structure, presented a greater steric hindrance that increases phase separation and decreases the miscibility. This greater phase separation in $LPA_{EOPE}$, even if relatively small, could result in better mechanical properties of the PU [16].

The SS content predictably decreases with increasing HS content, which has a great influence on the final mechanical properties of the PU, since it is responsible for providing flexibility and mobility to the chains [17], so it is necessary to find a balance between the chain mobility offered by the SS and the stiffness conferred by HS. On the other hand, it should be noted that the theoretical value of HS content was higher than the calculated one, indicating that the presence of lignin as well as its origin affected to the HS formation.

The ABES testing was carried out to measure the bonding strength of the different PU adhesives formulation. Such tests are able to determine the tensile strength required to disrupt the adhesive bond and indicate the shear strength of an adhesive [6]. Figure P4.3a and 3b shows the shear strength test results of PUs synthesised with EOPE and POPE bio-polyols and employing different NCO:OH ratios.

At first glance, it is evident that there is a big difference between PUs synthesised with EOPE (Figure P4.3a) and those synthesised with POPE (Figure P4.3b). When using NCO:OH ratios of 2.0 and 2.5 othe PUs synthesised with the POPE bio-polyol reached lower shear strength values. On the contrary, when using a ratio of 3.0:1 the shear strength of the PU increased rapidly reaching a value of 4.08 (MPa) at pressing time of 120 s.

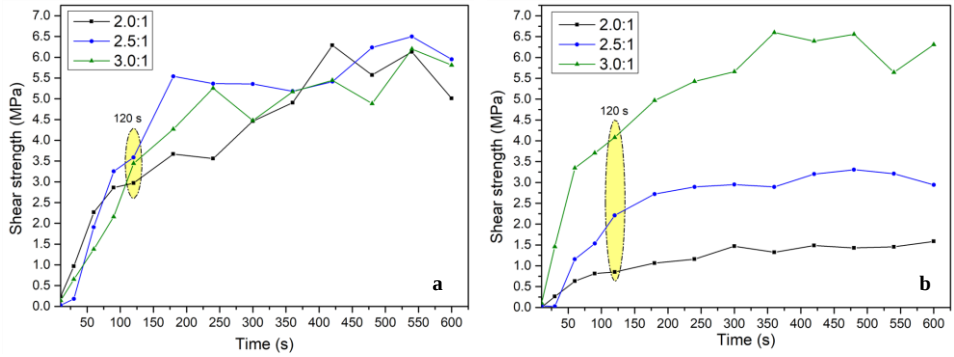


Figure P4.3. Shear strength of lignin-based polyurethane adhesives; (a) $LPA_{EOPE}$, (b) $LPA_{POPE}$

The shear strength continued increasing up to 5.66 MPa at 180 s and after this pressing time, the undesirable failure of the substrate occurred. From Figure P3.4a it can be noted that very similar high shear strength values were obtained regardless of the formulations used. This behaviour was probably caused by the unreacted isocyanate in these formulations, which interacted with the hydroxyl groups of the veneer strips to form additional covalent bonds that distorted the results. In addition, as with the PU formulated with POPE and a NCO:OH ratio of 3.0:1, at elevated pressing times, substrate failure occurred. Considering the values presented in Table P4.6, there was no significant difference in terms of $HS_W$ and $SS_W$ between the $LPA_{EOPE}$ and $LPA_{POPE}$ formulations, therefore, the previously mentioned unreacted isocyanate is the only explanation for the high results obtained with 2.0 and 2.5 $LPA_{POPE}$ formulations.

Three typical stages were observed, caused by the behaviour of the adhesive in the curing process [18]. In the first stage, a delay in the development of bond strength is observed, which can be associated with energy loss due to water evaporation. The second zone is related to the chain elongation process and cross-linking between the chains. The third stage depends on the behaviour of the adhesive against temperature and humidity, so during this

stage the shear strength can increase or decrease depending on the nature of the adhesive [19]. This last stage is only visible in the 2.5 and 3.0 formulations of PUs synthesised with POPE.

Nevertheless, considering a pressing time of 120 s, which is a common pressing time in industry, it was observed that the highest shear strength value (3.58 MPa) was obtained with the 2.5:1 NCO:OH ratio in the PUs formulated with EOPE, while a value of 4.08 MPa was achieved in the PUs formulated with POPE using the 3.0:1 NCO:OH ratio. For this reason, this ratio was selected to formulate the PUs based on the bio-polyols synthesised using CG ($EOPE_{CG}$ and $POPE_{CG}$).

### 2.3. Characterisation of LPA employing bio-polyols formulated with CG

Employing the respective quantities of reagents summarised in Table P4.2, two PU adhesives were synthesised using the bio-polyols formulated with CG and NCO:OH ratio of 2.5:1, namely, $LPA_{EOPECG}$ and $LPA_{POPECG}$. Finally, a comparison with the PU adhesives synthesised with the same NCO:OH ratio of the previous section was performed.

The ATR-FTIR spectra of both cured PU adhesives as well as the analysis of the region belonging to the carbonyl groups are represented in Figure P4.4 and Figure P4.5a and 5b, respectively. The spectra exhibit the same characteristic bands as those described above. It should be highlighted that also, in this case, isocyanate remains unreacted when the PU was formulated using the bio-polyol from *Eucalyptus globulus* lignin. Therefore, it can be confirmed that due to its higher steric hindrance, part of the isocyanate cannot react with the hydroxyl groups of the bio-polyol.

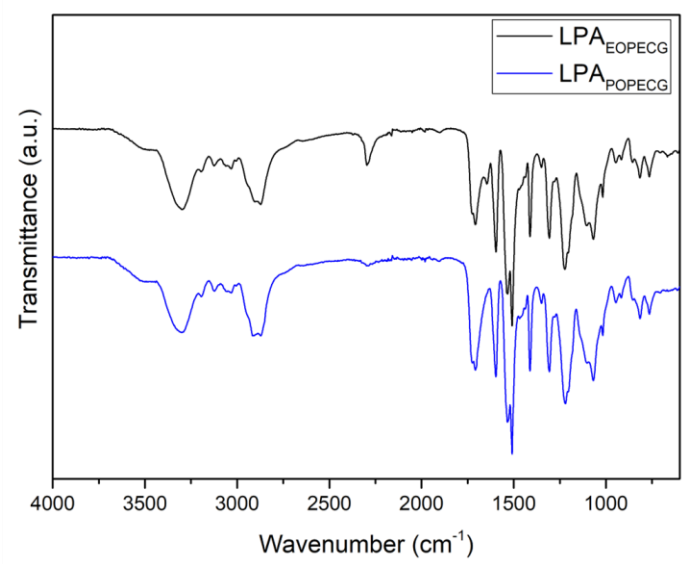


Figure P4.4. ATR-FTIR spectra of cured LPAs of $LPA_{EOPECG}$ and $LPA_{POPECG}$ samples

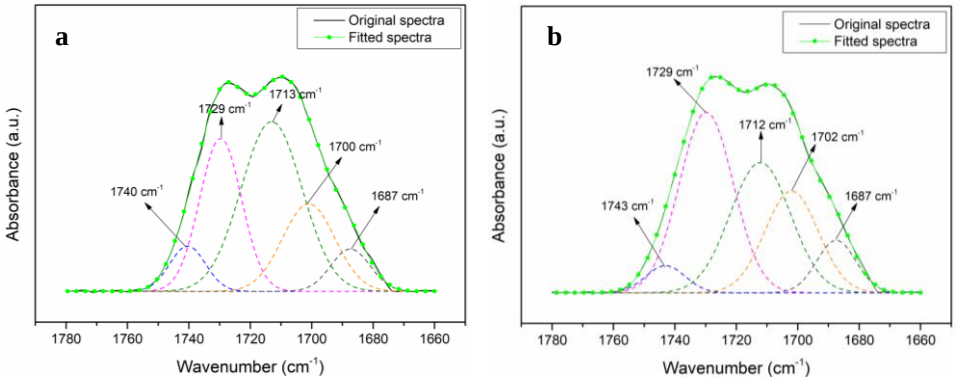


Figure P4.5. ATR-FTIR spectra of the absorbance region of the carbonyl groups of $LPA_{EOPECG}$ (a) and $LPA_{POPECG}$ (b) obtained through a Gaussian curve shape. The obtained $R^2$ values were above 0.999

From the deconvolution of the area corresponding to the carbonyl groups represented in Figures P4.5a and P4.5b, the $X_{HB}$, $W_H$, $MP_W$, $SS_W$ and $HS_W$ parameters were calculated and summarised in Table P4.7.

Compared to their respective homologues, for both PUs synthesised using the bio-polyol formulated with CG, the theoretical content of HS was lower. However, $X_{HB}$ was higher in the case of $LPA_{EOPECG}$. Likewise, both $W_H$ and $MP_W$ were lower. This indicates that for this PUs there was a lower amount of HS mixed in the soft phase and therefore the segregation of the micro-phases was higher. Such behaviour could be explained by the higher molecular weight of the $EOPE_{CG}$ and $POPE_{CG}$ bio-polyols with respect to EOPE and POPE, which would allow the phase separation [20].

Table P4.7. Relevant parameters estimated for the determination of microphase separation in GC-formulated LPAs

| Sample | NCO:OH | *z* | $X_{HB}$ | $W_H$ | $MP_W$ | $SP_W$ | $HS_W$ |
|---|---|---|---|---|---|---|---|
| $LPA_{EOPECG}$ | 2.5:1 | 0.362 | 0.335 | 0.274 | 0.099 | 0.737 | 0.263 |
| $LPA_{POPECG}$ | 2.5:1 | 0.346 | 0.303 | 0.269 | 0.093 | 0.747 | 0.253 |

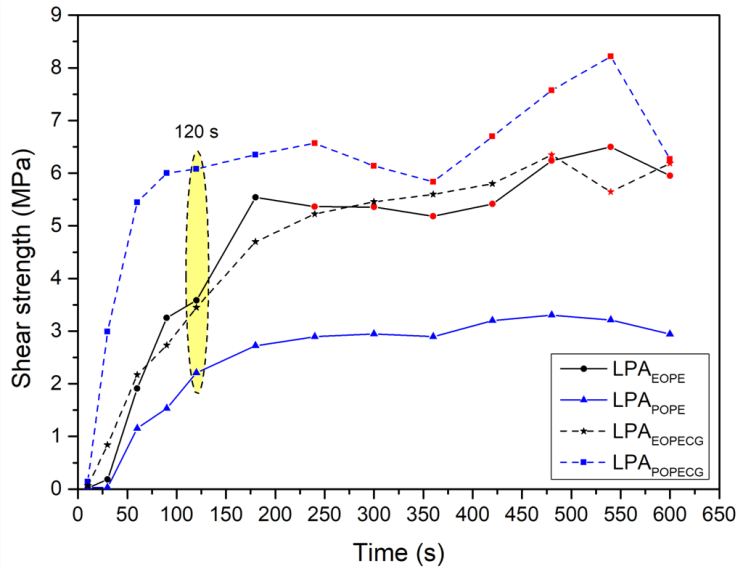


Figure P4.6. Shear strength of lignin-based polyurethane adhesives. The red point indicated the substrate failure

The shear strength of the $LPA_{EOPECG}$ and $LPA_{POPECG}$ adhesives were measured and compared with their counterparts $LPA_{EOPE}$ and $LPA_{POPE}$ in Figure P4.6. As

expected, the results obtained agreed with what was projected after studying the degree of microphase separation of PUs, since the mechanical properties of polyurethanes can be improved by increasing the microphase separation [13]. Thus, $LPA_{POPECG}$ showed the best shear strength results (6.06 MPa) due to its lower weight fraction of the mixed phase. Nevertheless, as happened with $LPA_{EOPE}$, at pressing times higher than 180 s, substrate failure occurred. On the other hand, $LPA_{EOPECG}$ with a shear strength value of 2.6 MPa behaved very similar to its homologue $LPA_{EOPE}$ despite having a lower degree of phase separation, which may be a consequence of the unreacted isocyanate in both samples. The obtained shear strength values were in the range of those reported by other authors, such as Nacas et al., (2017) [9] who obtained a shear strength of 6.8 MPa using Kraft lignin and MDI with a NCO:OH ratio of 1.2:1. Magina et al., (2021) [6] used lignosulphonates together with MDI and different quantities of PEG200 to synthesise different wood adhesives. They concluded that the best formulation was the one with an NCO:OH ratio of 2.1:1 obtaining a shear strength value close to 3 MPa. Gouveia et al., (2020) [21] studied the effect of lignin hydroxypropylation by synthesising various PU wood adhesives using KL and hydroxypropylated KL with MDI and a NCO:OH ratio of 1.1:1. They concluded that the best shear strength value was obtained with unmodified lignin (4.5 MPa), while hydroxpropylation improved elasticity and tensile strength at the expense of shear strength. Vieira et al., (2022) [22] obtained a wood PU adhesive based on oxyalkylated Kraft lignin using a 1.3:1 ratio with a shear strength of 3.1 MPa.

The thermostability of the LPAs was studied through a thermogravimetric analysis. According to the DTG curves represented in Figure P4.7, the major weight loss of the samples took place between 225 °C and 450 °C. Regardless of the polyol used in the PU formulation, the degradation zones were the same although the maximum degradation temperatures varied slightly.

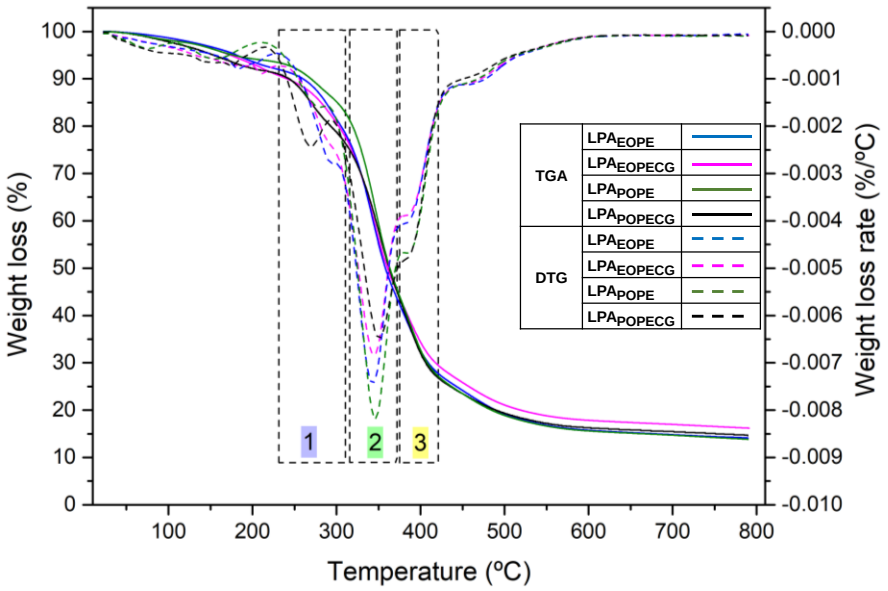


Figure P4.7. TGA and DTG curves of the different LPAs

The first degradation zone (225-310 °C) corresponds to the H-bonded urethane groups of the HS [23] and the cleavage of unstable ether linkages of lignin (β-O-4, α-O-4 and 4-O-5) [24]. The region with the highest mass loss, region 2, which is located between 310-375 °C, is associated with the degradation of the soft segment of the polyurethane [8]. The last mass loss area, region 3 (375-420 °C), is considered the degradation area of the diisocyanate and the aromatic rings of lignin [25]. A similar final residue was obtained for all PUs due to the presence of lignin in the samples. It can also be observed that the maximum degradation temperature at the first mass loss step was higher in $LPA_{EOPE}$ and $LPA_{EOPECG}$ than in $LPA_{POPE}$ and $LPA_{POPECG}$, which means a higher stability of the formers. Generally, since the first degradation zone corresponds to the degradation of the H-bonded urethane groups, PUs with less amount of these, tend to be less stable, as less energy will be required to break them. However, this is not the case for $LPA_{EOPE}$, which despite having more H-bond urethane groups than $LPA_{POPE}$ is more stable. Nevertheless, since the $X_{HB}$ values were very similar in all cases, the

higher stability of the $LPA_{EOPE}$ and $LPA_{EOPECG}$ samples could be explained since, as mentioned above, in PUs with lignin, in this first degradation zone there is also degradation of ether linkages, which are more abundant in hardwoods such as *Eucalyptus globulus* than in softwood as *Pinus radiata* [26].

Using different heating rates (1, 2, 5 and 10 °C/min) and the isoconversional methods of OFW and KAS described in **Appendix II**, the activation energy ($E_a$) of each system was calculated. In addition, the average lifetime of the PUs was estimated through the OFW method, for which the pre-exponential factor A was determined. The calculation of both $E_a$ and $A$ was performed from the slope and the intercept of the plots of $\ln(\beta)$ and $\ln\left(\frac{\beta}{T_p^2}\right)$ versus 1000/Tp. In these graphs, the conversion rates from 5% to 90% for each system were ploted. FigureP4.8a, 8b, 8c and 8d showed the different TGA curves obtained with each heating rate for the different systems. In all cases, as expected, as the heating rate increases, the degradation curve shifted towards higher temperatures. The final residue of each PU was between 16.5-17 % ($LPA_{EOPE}$), 14-16 % ($LPA_{EOPECG}$), 13.9-15.8 % ($LPA_{POPE}$) and 11.8-13.8 % ($LPA_{POPECG}$).

From Figure P4.9, it could be concluded that the model was well selected since linear and parallel straight lines and very high correlation coefficients were obtained. Nevertheless, in the $LPA_{POPECG}$ samples (Figure P4.9d and 4.9h), the line corresponding to the conversion of 0.9 was not properly fitted, so it was not considered for the calculation of the $E_a$ and $A$.

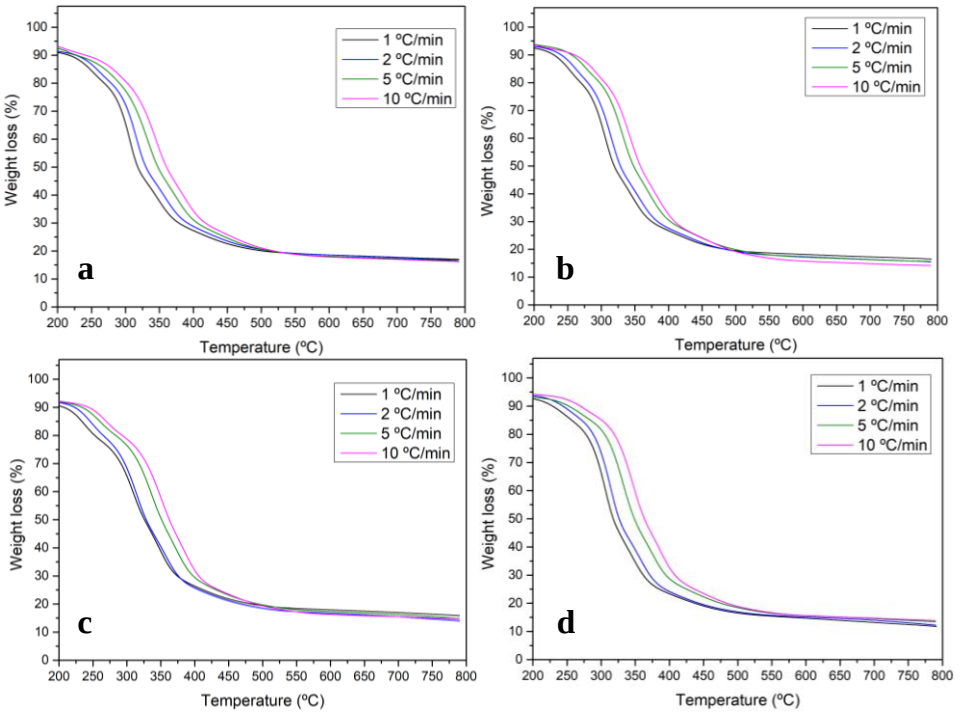


Figure P4.8. TGA curves at the different heating rates for $LPA_{EOPE}$ (a), $LPA_{EOPECG}$ (b), $LPA_{POPE}$ (c) and $LPA_{POPECG}$ (d)

According to the results obtained and outlined in Tables P4.8 and P4.9 and taking into account that the $E_a$ is the impediment to the degradation process [27], the synthesised PUs will degrade in the following order from the slowest one to the fastest one for α=0.05: $LPA_{EOPE}$ > $LPA_{EOPECG}$ > $LPA_{POPE}$ > $LPA_{POPECG}$. Due to the nature of the bio-polyols, different behaviour was observed in the decomposition reaction mechanism between PUs formulated with different bio-polyols as shown in Figure P4.10. The $E_a$ follows the same trend for $LPA_{EOPE}$ and $LPA_{EOPECG}$, both samples presented a high value at the beginning, which decreased to a minimum and then increased again. While in $LPA_{POPE}$ and $LPA_{POPECG}$, the minimum $E_a$ value was obtained at the beginning and then increased. However, in the case of $LPA_{POPECG}$ the last two values tend to decrease because of the poor fitting.

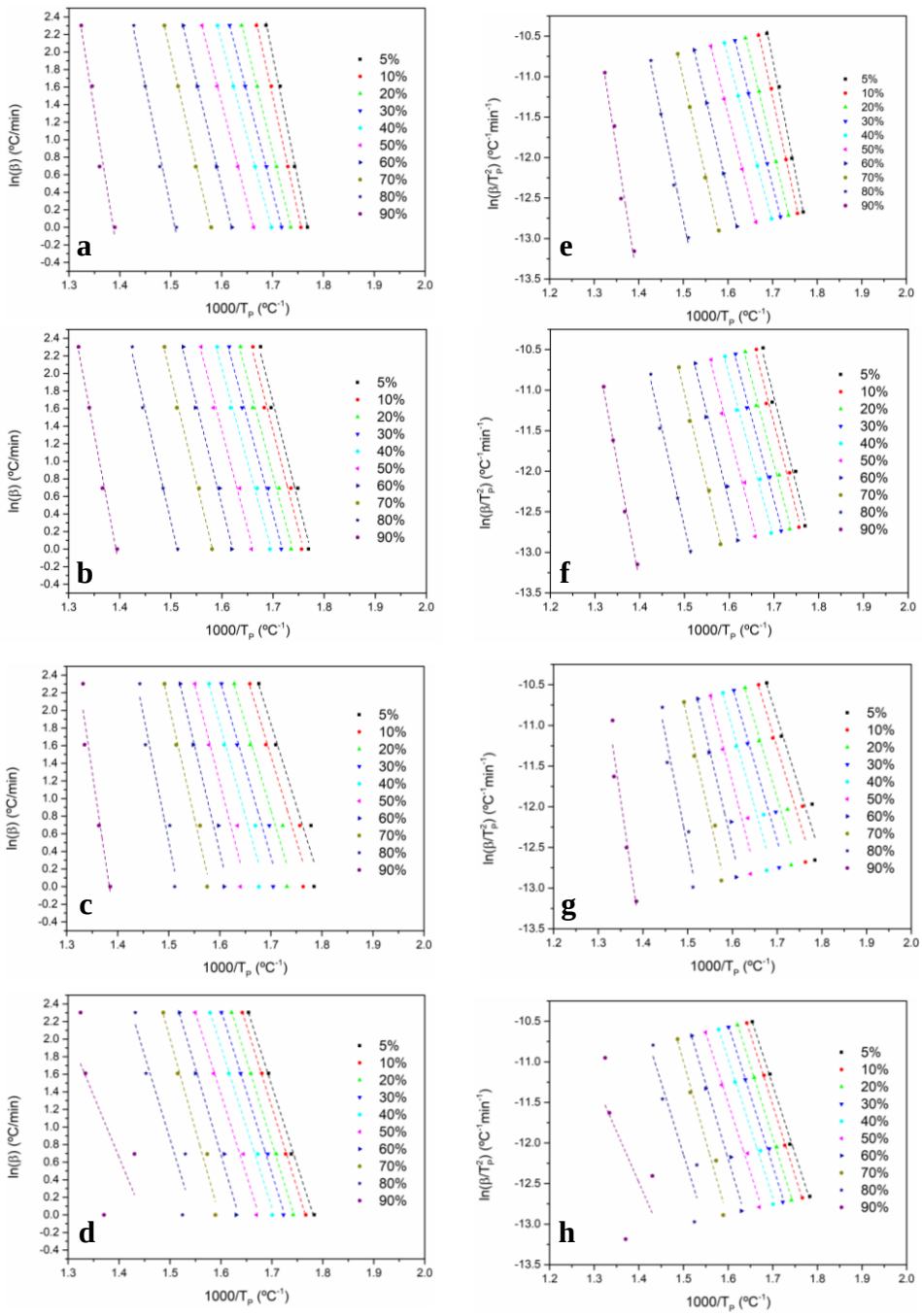


Figure P4.9. (a-d) OFW plots of ln(β) vs. 1000/$T_P$ and (e-h) KAS plots of ln(β/$T^2_P$) vs. 1000/$T_P$ for different conversion values. Where $LPA_{EOPE}$ (a-e), $LPA_{EOPECG}$ (b-f), $LPA_{POPE}$ (c-g) and $LPA_{POPECG}$ (d-h)

Table P4.8. Activation energies ($E_a$) (KJ/mol) and correlation coefficients of the linear regression of the PU samples for the decomposition obtained through the OFW method

| | $LPA_{EOPE}$ | | $LPA_{EOPECG}$ | | $LPA_{POPE}$ | | $LPA_{POPECG}$ | |
|---|---|---|---|---|---|---|---|---|
| α | $R^2$ | $E_a$ | $R^2$ | $E_a$ | $R^2$ | $E_a$ | $R^2$ | $E_a$ |
| 0.05 | 0.9976 | 226.0 | 0.9830 | 180.8 | 0.9432 | 146.9 | 0.9970 | 143.4 |
| 0.1 | 0.9989 | 209.8 | 0.9849 | 179.0 | 0.9464 | 152.0 | 0.9995 | 154.9 |
| 0.2 | 0.9995 | 188.8 | 0.9899 | 174.4 | 0.9526 | 156.3 | 0.9992 | 157.1 |
| 0.3 | 0.9998 | 177.6 | 0.9923 | 171.1 | 0.9508 | 158.7 | 0.9972 | 154.8 |
| 0.4 | 0.9999 | 171.0 | 0.9920 | 168.7 | 0.9481 | 164.2 | 0.9947 | 152.2 |
| 0.5 | 0.9999 | 179.2 | 0.9893 | 175.4 | 0.9467 | 179.1 | 0.9919 | 153.4 |
| 0.6 | 0.9997 | 190.3 | 0.9926 | 184.0 | 0.9689 | 193.0 | 0.9900 | 164.0 |
| 0.7 | 0.9991 | 198.9 | 0.9964 | 190.3 | 0.9785 | 202.2 | 0.9762 | 172.9 |
| 0.8 | 0.9913 | 219.1 | 0.9939 | 199.6 | 0.9468 | 228.5 | 0.8829 | 158.8 |
| 0.9 | 0.9677 | 284.1 | 0.9929 | 243.4 | 0.9412 | 307.5 | 0.4439* | 116.9 |

*Not considered for calculating the average

Table P4.9. Activation energies ($E_a$) (KJ/mol) and correlation coefficients of the linear regression of the PU samples for the decomposition obtained through the KAS method

| | $LPA_{EOPE}$ | | $LPA_{EOPECG}$ | | $LPA_{POPE}$ | | $LPA_{POPECG}$ | |
|---|---|---|---|---|---|---|---|---|
| α | $R^2$ | $E_a$ | $R^2$ | $E_a$ | $R^2$ | $E_a$ | $R^2$ | $E_a$ |
| 0.05 | 0.9974 | 228.2 | 0.9811 | 180.5 | 0.9359 | 145.0 | 0.9967 | 141.2 |
| 0.1 | 0.9988 | 211.0 | 0.9832 | 178.6 | 0.9397 | 150.2 | 0.9994 | 145.1 |
| 0.2 | 0.9995 | 188.8 | 0.9887 | 173.6 | 0.9467 | 154.5 | 0.9990 | 147.2 |
| 0.3 | 0.9998 | 176.9 | 0.9914 | 170.0 | 0.9446 | 156.9 | 0.9968 | 144.8 |
| 0.4 | 0.9999 | 169.8 | 0.9910 | 167.4 | 0.9418 | 162.6 | 0.9938 | 142.1 |
| 0.5 | 0.9999 | 178.2 | 0.9880 | 174.2 | 0.9406 | 178.0 | 0.9906 | 143.0 |
| 0.6 | 0.9997 | 189.6 | 0.9917 | 183.0 | 0.9655 | 192.4 | 0.9885 | 153.4 |
| 0.7 | 0.9990 | 198.4 | 0.9960 | 189.3 | 0.9762 | 201.9 | 0.9730 | 162.1 |
| 0.8 | 0.9904 | 219.2 | 0.9932 | 198.6 | 0.9418 | 229.2 | 0.8671 | 147.6 |
| 0.9 | 0.9650 | 286.8 | 0.9922 | 243.8 | 0.9368 | 311.3 | 0.3914* | 104.8 |

*Not considered for calculating the average

Consequently, the values of the preexponential factor (A) estimated with the OFW method and presented in Table P4.10, followed the same tendency. This factor is indicative of the collision frequency between molecules, i.e., it is an

indication of the availability of chemical groups which are susceptible to degradation [27]. Thus, the higher the value of A, the more difficult it is for the polymer to degrade. Therefore, $LPA_{EOPE}$ and $LPA_{EOPECG}$ polyurethanes remained more stable at 5% of conversion, while $LPA_{POPE}$ and $LPA_{POPECG}$ will degrade more easily at this conversion rate.

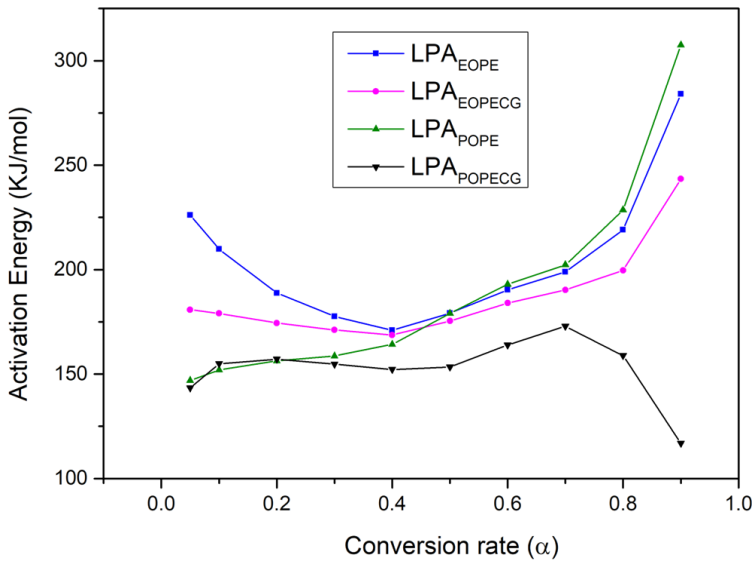


Figure P4.10. $E_a$ calculated through OFW method vs. α

Table P4.10. Preexponential factor (A) of the PU samples for the decomposition obtained through the OFW method

| | A ($min^{-1}$) | | | |
|---|---|---|---|---|
| α | $LPA_{EOPE}$ | $LPA_{EOPECG}$ | $LPA_{POPE}$ | $LPA_{POPECG}$ |
| 0.05 | 3.7E+18 | 9.7E+11 | 9.8E+08 | 6.6E+10 |
| 0.1 | 1.5E+17 | 2.1E+14 | 8.4E+11 | 2.3E+11 |
| 0.2 | 2.1E+15 | 1.0E+14 | 2.3E+12 | 5.0E+11 |
| 0.3 | 2.0E+14 | 5.2E+13 | 3.6E+12 | 3.5E+11 |
| 0.4 | 4.6E+13 | 2.8E+13 | 9.3E+12 | 2.1E+11 |
| 0.5 | 8.6E+13 | 6.9E+13 | 1.2E+14 | 2.0E+11 |
| 0.6 | 7.1E+14 | 2.1E+14 | 1.1E+15 | 9.7E+11 |
| 0.7 | 1.9E+15 | 3.5E+14 | 3.8E+15 | 3.1E+12 |
| 0.8 | 1.8E+16 | 5.4E+14 | 1.4E+17 | 1.1E+11 |
| 0.9 | 3.0E+17 | 6.9E+16 | 3.1E+21 | 2.3E+07 |

Finally, the lifetime of the synthesised PUs was evaluated, and the results are plotted in Figure P4.11. The determination of the lifetime of a material is of great interest in order to develop a specific product with the required specifications to perform the task for which it is conceived [28]. The estimation of the lifetime of the polymers can be determined employing the activation energies and the preexponential factors obtained through the Ozawa-Flynn-Wall method. Usually, the lifetime estimation is carried out for a 5% of weight loss or 5% conversion [29]. The obtained data must be treated prudently since they correspond to the degradation of PUs in an inert atmosphere, and therefore these values will vary in contact with an oxidising atmosphere, as the materials will degrade differently.

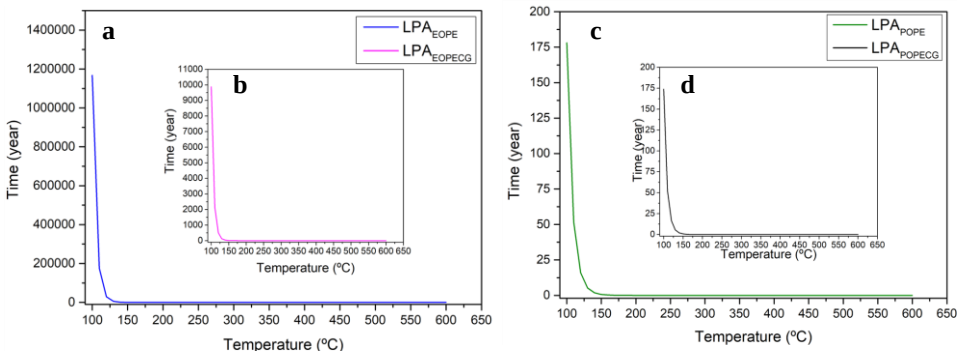


Figure P4.11. Estimated lifetime of LPA$_{EOPE}$ (a), LPA$_{EOPECG}$ (b), LPA$_{POPE}$ (c) and LPA$_{POPECG}$ (d)

As expected, the obtained results were consistent with the $E_a$ values of the PUs. Consequently, the PU with the highest lifetime expectation was LPA$_{EOPE}$, followed by LPA$_{EOPECG}$, then LPA$_{POPE}$ and finally LPA$_{POPECG}$. It should be noted that the difference between LPA$_{EOPE}$ and LPA$_{EOPECG}$ was very high because of the widely differing $E_a$ values, while there was almost no difference between LPA$_{POPE}$ and LPA$_{POPECG}$. Furthermore, it can be observed, that as the temperature increased, the degradation of the polymers was greatly accelerated in all cases.

# 3. CONCLUSIONS

This study demonstrated the applicability of a bio-polyols synthesised through the liquefaction process of lignin with polyhydric alcohols (PEG and Glycerol) by microwave irradiation in the formulation of PU adhesives. Moreover, the results indicate that it is possible to substitute commercial glycerol by a non-purified crude glycerol obtained from used vegetable oil. Based on the results, it was determined that the origin of the lignin had a great effect on the PUs. On the one hand, it was observed that when the bio-polyol derived from *Eucalyptus globulus* lignin was used, isocyanate remained unreacted in all cases, whereas with its counterpart derived from *Pinus radiata* lignin this was not the case due to the higher steric hindrance of the former. Furthermore, it was observed that due to the steric hindrance, the phase separation was higher in the PUs synthesised with EOPE bio-polyol regardless of the glycerol used. However, the origin of the glycerol also showed a significant influence on the microstructure since bio-polyols synthesised using CG showed higher molecular weights that favoured the phase separation. When studying the thermal degradation of the PUs it was found that the nature of the lignin also plays an important role, since despite having less H-bonded urethane groups in their structure, the PUs synthesised with EOPE proved to be more stable due to the higher amount of aryl ether bonds in their structure. Consequently, the estimated lifetime of the PUs at 5% degradation followed the same order $LPA_{EOPE}$ > $LPA_{EOPECG}$ > $LPA_{POPE}$ > $LPA_{POPECG}$.

## REFERENCES

[1] M. Ionescu, in: De Gruyter (Ed.), Polyols for Polyrethanes, Boston, Berlin, 2019, pp. 1–10.

[2] S. Hu, X. Luo, Y. Li, ChemSusChem 7(1) (2014) 66–72. 10.1002/cssc.201300760.

[3] Y.Y. Li, X. Luo, S. Hu, Bio-based Polyols and Polyurethanes, 2015, pp. 1–79.

[4] M. Ionescu, in: De Gruyter (Ed.), Polyols for Polyurethanes, Boston, Berlin, 2019, pp. 307–20.

[5] F. Ren, R. Zhou, F. Sun, H. Ma, Z. Zhou, W. Xu, RSC Adv. 7(47) (2017) 29779–85. 10.1039/c7ra04454b.

[6] S. Magina, N. Gama, L. Carvalho, A. Barros-Timmons, D.V. Evtuguin, Materials (Basel). 14(22) (2021) 1–18. 10.3390/ma14227072.

[7] M. Fuensanta, J.M. Martín-Martínez, Front. Mech. Eng. 6(June) (2020) 1–10. 10.3389/fmech.2020.00034.

[8] P. Cinelli, I. Anguillesi, A. Lazzeri, Eur. Polym. J. 49(6) (2013) 1174–84. 10.1016/j.eurpolymj.2013.04.005.

[9] A.M. Nacas, N.M. Ito, R.R.D. Sousa, M.A. Spinacé, D.J. Dos Santos, J. Adhes. 93(1–2) (2017) 18–29. 10.1080/00218464.2016.1177793.

[10] M. Fuensanta, J.M. Martín-Martínez, J. Adhes. Sci. Technol. 34(24) (2020) 2652–71. 10.1080/01694243.2020.1780774.

[11] Y. Liu, L. Liu, Y. Liang, J. Appl. Polym. Sci. 137(45) (2020) 1–9. 10.1002/app.49414.

[12] M. Fuensanta, J.M. Martín-Martínez, Polymers (Basel). 13(18) (2021). 10.3390/polym13183097.

[13] M. Gholami, V. Haddadi-Asl, I.S. Jouibari, J. Plast. Film Sheeting 38(4) (2022) 502–41. 10.1177/87560879221088939.

[14] A. Niemczyk, A. Piegat, Á. Sonseca Olalla, M. El Fray, Eur. Polym. J. 93(May) (2017) 182–91. 10.1016/j.eurpolymj.2017.05.046.

[15] X. Luo, A. Mohanty, M. Misra, Ind. Crops Prod. 47 (2013) 13–9. 10.1016/j.indcrop.2013.01.040.

[16] K. Kojio, S. Nozaki, A. Takahara, S. Yamasaki, J. Polym. Res. 27(6) (2020) 64–7. 10.1007/s10965-020-02090-9.

[17] S. Arévalo-Alquichire, M. Morales-Gonzalez, K. Navas-Gómez, L.E. Diaz, J.A. Gómez-Tejedor, M.A. Serrano, M.F. Valero, Polymers (Basel). 12(3) (2020). 10.3390/polym12030666.

[18] J.M.M. Ferra, M. Ohlmeyer, A.M. Mendes, M.R.N. Costa, L.H. Carvalho, F.D. Magalhes, Int. J. Adhes. Adhes. 31(3) (2011) 127–34. 10.1016/j.ijadhadh.2010.11.013.

[19] B.M. De Morais Lemos Esteves, L.P.V. Cruz-Lopes, A.P. Fernandes, J.M. Martins, I. De Jesus Domingos, J.V. Ferreira, S.H.F. Da Silva, J. Labidi, Wood Res. 64(1) (2019) 105–16.

[20] D.-K. Lee, H.-B. Tsai, R.-S. Tsai, P.H. Chen, Polym. Eng. Sci. 47(5) (2007) 695–701. 10.1002/pen.20742.

[21] J.R. Gouveia, L.D. Antonino, G.E.S. Garcia, L.B. Tavares, A.N.B. Santos, D.J. do. Santos, Https://Doi.Org/10.1080/00218464.2020.1784148 97(15) (2020) 1423–39. 10.1080/00218464.2020.1784148.

[22] F.R. Vieira, N. Gama, S. Magina, A. Barros-Timmons, D. V. Evtuguin, P.C.O.R. Pinto, Polymers (Basel). 14(23) (2022). 10.3390/polym14235305.

[23] J. D'Souza, R. Camargo, N. Yan, J. Appl. Polym. Sci. 131(16) (2014) 1–10. 10.1002/app.40599.

[24] C. Zhang, H. Wu, M.R.K. Kessler, Polymer (Guildf). 69(1) (2015) 52–7. 10.1016/j.polymer.2015.05.046.

[25] L.B. Tavares, C. V. Boas, G.R. Schleder, A.M. Nacas, D.S. Rosa, D.J. Santos, Express Polym. Lett. 10(11) (2016) 927–40. 10.3144/EXPRESSPOLYMLETT.2016.86.

[26] X. Erdocia, F. Hernández-ramos, A. Morales, N. Izaguirre, P.L. De Hoyos-martínez, J. Labidi, Lignin-Based Materials for Biomedical Applications, Elsevier Inc., 2021, pp. 61–104.

[27] N.L. Batista, M.L. Costa, K. Iha, E.C. Botelho, J. Thermoplast. Compos. Mater. 28(2) (2015) 265–74. 10.1177/0892705713484740.

[28] J.H. Flynn, J. Therm. Anal. Calorim. 44(2) (1995) 499–512. 10.1007/BF02636139.

[29] L. Núñez, F. Fraga, M.R. Núñez, M. Villanueva, J. Appl. Polym. Sci. 78(6) (2000) 1239–44. 10.1002/1097-4628(20001107)78:6<1239::aid-app90>3.0.co;2-

*“If no mistake you have made, losing you are.*

*A different game you should play.”*

*Master Yoda*

## Publication V

# Lignin-based non isocyanate polyurethane adhesives. Synthesis and determination of adhesion properties and thermal degradation kinetic


## ABSTRACT

In this work, different non-isocyanate adhesives were synthesised through polycondensation reaction of a ligno-based bio-polyol with dimethyl carbonate (DMC) and hexamethylenediamine (HDMA). The bio-polyols were obtained in previous works (***Publication II and III***). The formulated NIPU adhesives called, $LNA_{EOPE}$, $LNA_{EOPECG}$, $LNA_{POPE}$ and $LNA_{POPECG}$ were characterised and subjected to shear strength test employing an ABES system with undesirable results. To improve the adhesion properties of NIPU adhesives, different amounts (5%, 15% and 25%) of (3-Aminopropyl) trimethoxysilane (APTMS) were added. The best result was obtained by adding 15% APTMS in all cases except for $LNA_{EOPE}$, in which the best results were obtained by adding 25% APTMS. A thermal degradation study of silanised NIPUs called $CLNA_{EOPE-25}$, $CLNA_{EOPECG-15}$, $CLNA_{POPE-15}$ and $CLNA_{POPECG-15}$ was carried out using OFW and KAS isoconversional methods. With them, the $E_a$, the pre-exponential factor A and an estimation of the lifetime of the polymers were determined.


## 1. MATERIALS AND METHODS

### 1.1. Materials

The raw materials, *Eucalyptus globulus* chips and *Pinus radiata*, as well as the used vegetable oil and chemicals employed in this work were obtained as described in s***ection 2.1*** of the **2nd PART.**

### 1.2. Lignin obtaining procedure

Lignins used in this work were obtained after the organosolv delignification process and the subsequent ultrasound treatment of the black liquor described in ***section 2.2*** of **2nd PART**. These lignins called EOUL (*Eucalyptus globulus* organosolv lignin) and POUL (*Pinus radiata* organosolv lignin) were characterised in ***Publication II***.

### 1.3. Crude glycerol obtaining procedure

CG was obtained by the transesterification reaction outlined in **section 2.4** of the **2nd PART**.

### 1.4. Lignin based bio-polyols

For this work, the same lignin-based bio-polyols that were employed and characterised in ***Publication IV*** were used. These bio-polyols were synthesised through liquefaction of the different organosolv lignins (EOUL and POUL) following the procedure that is described in ***section 2.3.1*** of the **2nd PART**.

Table P5.1 summarises the main parameters of these bio-polyols to facilitate the reading of this publication. The discussion about the characterisation of the bio-polyols is detailed in ***Publication IV***.

Table P5.1. Most relevant parameters of the bio-polyols synthesised in the ***Publication IV***

| Sample | $M_n$ | $M_w$ | PI | $I_{OH}$ | $A_n$ | *f* |
|---|---|---|---|---|---|---|
| EOPE | 739 ± 43 | 3934 ± 98 | 5.33 ± 0.18 | 330 ± 3 | 35 ± 0.36 | 4.16 |
| POPE | 707 ± 32 | 4079 ± 50 | 6.29 ± 0.92 | 182 ± 51 | 25 ± 0.00 | 2.29 |
| $EOPE_{CG}$ | 852 ± 8 | 6644 ± 89 | 7.79 ± 0.18 | 284 ± 1 | 17 ± 0.24 | 4.29 |
| $POPE_{CG}$ | 933 ± 85 | 11035 ± 1059 | 12.63 ±0.00 | 182 ± 30 | 20 ± 0.64 | 2.83 |

## 1.5. Synthesis of lignin based non-isocyanate polyurethane adhesives

Using the bio-polyols synthesised by the liquefaction process described in the previous section, called EOPE, $EOPE_{CG}$, POPE and $POPE_{CG}$, different lignin based non-isocyanate polyurethane adhesives (LNA) labelled as $N_{EOPE}$, $N_{EOPECG}$, $N_{POPE}$ and $N_{POPECG}$ were synthesised. The synthesis was performed following the procedure described in the ***section 2.6*** of the ***2nd PART***.

## 1.6. Characterisation of the obtained non-isocyanate polyurethane adhesives

The pH of the different NIPUs was determined using a digital pH meter "CRISON basic 20" at room temperature. The solids content of the NIPUs were calculated by weighing a certain amount of sample which was dried in an oven at 100°C for 24 hours and employing the formula presented in Equation P5.1. A triplicate of each sample was performed. The NIPUs without the silane coupling agent were cured in an oven for 24 hours at 120 °C and 150 °C.

$$Solid\ content\ (\%) = \frac{W_2}{W_1} \times 100 \qquad \text{Equation P5.1}$$

Where $W_2$ is the final weight (g) of the sample after 24 hours at 100 °C and $W_1$ is the initial weight (g) of the sample.

Then, the non-cured and cured NIPUs were characterised to determine the molecular weight distribution through GPC the chemical structure as well as the microphase separation and miscibility through ATR-FTIR. The NIPUs with the 3-Aminopropyltrimethoxysilane coupling agent were cured at 120°C in an oven for 24 hours and characterised by ATR-FTIR and thermogravimetric analysis. The shear strength of the NIPUs with and without coupling agent was carried out at 120 °C through ABES. Such

characterisations were performed according to the procedures described in **Appendix II.**

## 2. RESULTS AND DISCUSSION

### 2.1. Characterisation of the synthesised lignin based non-isocyanate polyurethane adhesives

In aqueous formulations it is important to obtain as high solids content as possible. This is because of the higher latent heat of evaporation of water than that of organic solvents, which hinders the drying process and therefore prevents such formulation from meeting the requirements of modern industry [1]. On the other hand, pH can affect the curing process and the adhesion performance of the resulted adhesives [2]. Table P5.2 summarised the solids contents as well as the pH obtained for each NIPU formulation according to the Equation P5.1.

Table P5.2. Solid content and pH of the different LNA formulation

| Sample | Solid content (wt.%) | pH |
|---|---|---|
| $LNA_{EOPE}$ | 52.58 ± 0.43 | 11.54 ± 0.04 |
| $LNA_{EOPECG}$ | 49.58 ± 0.24 | 11.47 ± 0.02 |
| $LNA_{POPE}$ | 44.53 ± 0.30 | 11.57 ± 0.01 |
| $LNA_{POPECG}$ | 45.20 ± 0.25 | 11.49 ± 0.03 |

The solid content as well as the pH of the synthesised NIPUs were within the range reported by other authors when synthesising NIPUs adhesives with lignin or tannins with DMC and HDMA. Thus, Saražin et al., (2021) [3] obtained an organosolv lignin based NIPU adhesive with a solid content of 46% and a pH of 11. Likewise, Chen et al., (2022) [2] synthesised different NIPUs employing tannins and reacting them with DMC and HDMA and different concentrations of glycerol diglycidyl ether (GDE). When the concentration of the GDE was zero, the solids content of the obtained NIPU

adhesive was 54.38% and the pH was 11.1, the latter decreased as the concentration of GDE increased. Despite this, the authors did not find significant differences in the adhesion properties of the NIPUs.

Employing the bio-polyols summarised in section 1.4 called EOPE, $EOPE_{CG}$, POPE and $POPE_{CG}$, four different LNAs were synthesised following the instructions described in section 1.5 and the different steps of the reaction were analysed through ATR-FTIR (Figure P5.1). In the first step of the reaction, the addition of DMC, the appearance of three characteristic DMC bands can be observed, viz. 1751 $cm^{-1}$, 1457-1452 $cm^{-1}$ and 1284-1272 $cm^{-1}$, corresponding to stretching of C=O in the ester group, CH deformation in $CH_3$ and C-O stretching in the ester group of DMC [4]. The appearance of these characteristic bands indicates that the DMC reacted properly with the bio-polyols. In addition, the broad bands between 3423 $cm^{-1}$ and 3401 $cm^{-1}$ could be associated with the water in the medium in which the reaction was carried out.

In the second stage of the reaction, the hexamethylenediamine was added to form urethane groups through reaction with DMC. The formation of urethane groups could be confirmed by the appearance of three bands at wavenumbers 3360-3336 $cm^{-1}$, 1720-1686 $cm^{-1}$ and 1531-1525 $cm^{-1}$. The first one (3360-3336 $cm^{-1}$), which appears as a small peak, since it was overlapped by the reaction water band, correspond to the N-H stretching vibration of urethane groups [4], carbonyl (C=O) groups belonging to free urethane groups (1730 $cm^{-1}$) and H-bonded urethane groups (1686 $cm^{-1}$) [5] and the N-H vending vibration at 1531-1525 $cm^{-1}$ [6]. In addition to urethane bonds, the reaction between HDMA and DMC could create urea bonds which are confirmed by the appearance of a peak between 1646-1636 $cm^{-1}$ wavenumbers [7]. These groups that were created by the reaction between DMC and HDMA during the NIPU synthesis had a major importance on the morphology and final properties of the material. This is due, among other

reasons, to their ability to form double H-bonds generating stronger interactions [8] and thus increasing the mechanical strength [9].

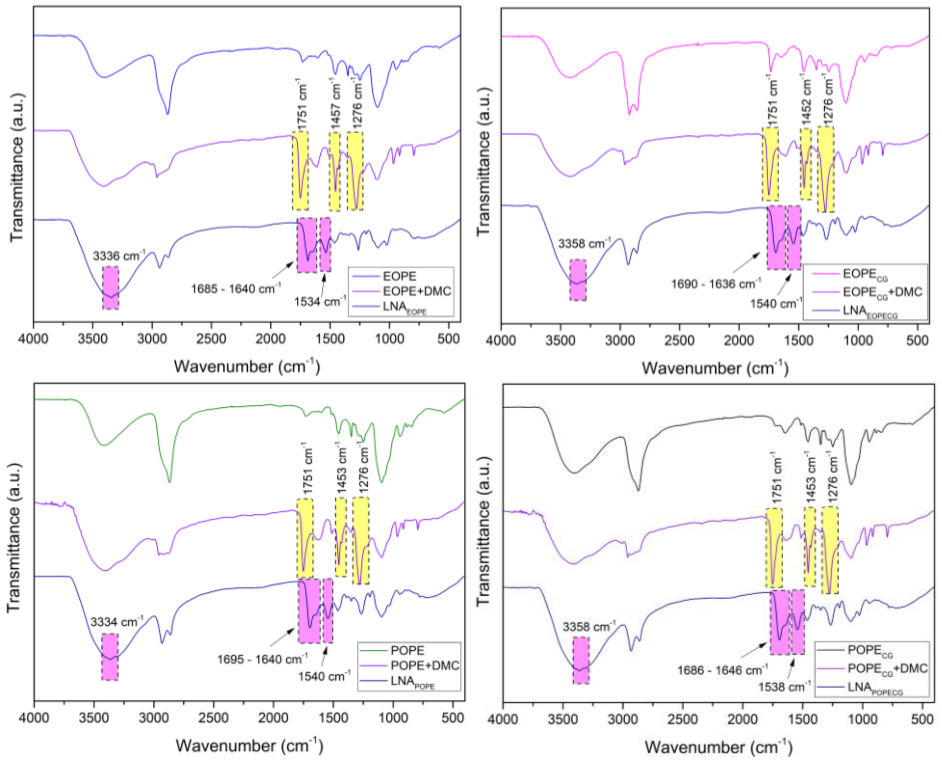


Figure P5.1. ATR-FTIR spectra of the different steps of the LNA reaction. a, b, c and d correspond to the LNAs formulated with EOPE, EOPECG, POPE and POPECG respectively.

Afterwards, the NIPUs were cured employing three different temperatures, i.e., 100 °C, 120 °C and 150 °C. To do so, the NIPUs were poured into an aluminium mould and placed in the oven at the above-mentioned temperatures for 24 hours. Then, the cured samples were analysed through GPC to determine the variation of the molecular weight distribution (Figure P5.2), and through ATR-FTIR to analyse the chemical structure of the samples (Figure P5.3).

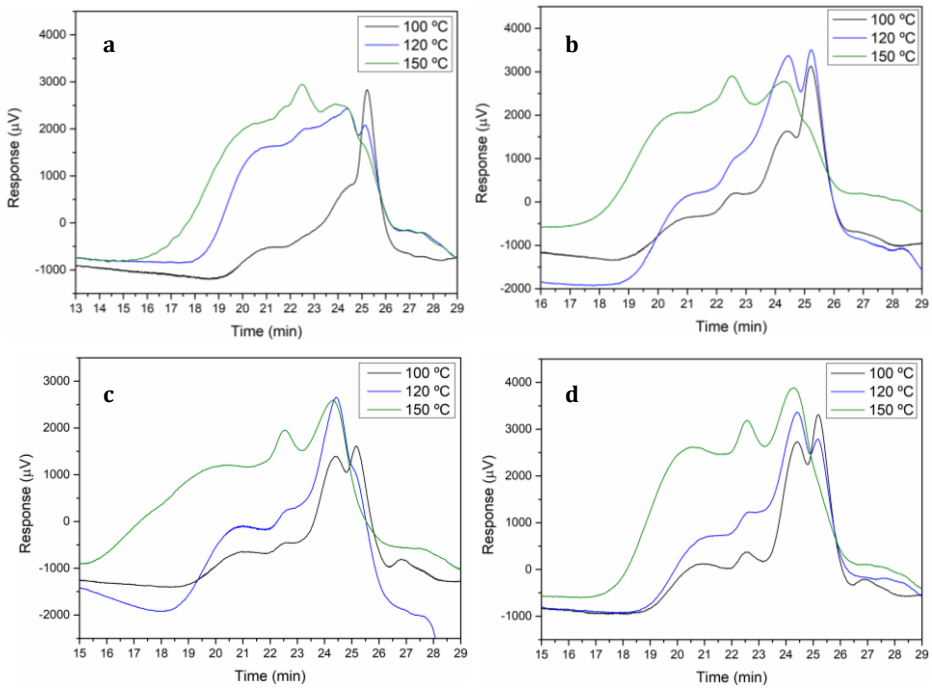


Figure P5.2. Molecular weight distribution of the synthesised LNAs

As shown in Figure P5.2, in all cases the chromatograms follow the same pattern. The samples cured at 100 °C showed four peaks, although the intensities vary depending on the samples. Those sample cured at 120 °C also presented four peaks, however the last one at 25.2 min lost intensity with respect to the previous peak at 24.3 min, and even almost disappeared in the case of $LNA_{POPE}$. For the samples cured at 150 °C, this peak disappeared or almost disappeared in all cases. This could be explained by the fact that the smaller unreacted molecules took part in the increasing polymerisation with increasing temperature. It is also remarkable that, except for $LNA_{EOPE}$, the first peak that corresponds to the higher molecular weight, starts roughly at the same retention time, which means that there is not much difference between the higher molecular weight fragments of the samples cured at 100 °C or 120 °C. However, as the curing temperature increased to 150 °C the retention time of this peak decreased remarkably in all cases, indicating that the molecular weights of the samples increased due to the higher degree of

polymerisation. This increase in molecular weights is well reflected in Table P5.3 where the average molecular weights corresponding to the different retention times are listed.

Table P5.3. Average molecular weight (MW) (g/mol) of LNAs by retention time (min)

| Sample | 100 °C | | 120 °C | | 150 °C | |
|---|---|---|---|---|---|---|
| | $R_T$ | $M_w$ | $R_T$ | $M_w$ | $R_T$ | $M_w$ |
| $LNA_{EOPE}$ | 21.28 | 18025 | 21.27 | 29894 | 20.61 | 57316 |
| | 22.53 | 3270 | 22.75 | 4374 | 21.78 | 8473 |
| | 24.17 | 873 | 24.38 | 998 | 22.45 | 3165 |
| | 25.22 | 365 | 25.14 | 342 | 23.87 | 908 |
| | - | - | - | - | 25.01 | 368 |
| $LNA_{EOPECG}$ | 21.67 | 20519 | 21.02 | 21901 | 20.69 | 39312 |
| | 22.71 | 4088 | 22.59 | 3458 | 21.93 | 8222 |
| | 24.46 | 889 | 24.45 | 872 | 22.52 | 3172 |
| | 25.22 | 365 | 25.23 | 352 | 24.34 | 876 |
| | 26.47 | 237 | 26.82 | 236 | 25.09 | 362 |
| $LNA_{POPE}$ | 20.93 | 20291 | 20.98 | 23838 | 17.89 | 147950 |
| | 22.60 | 3667 | 22.60 | 3281 | 20.29 | 46757 |
| | 24.40 | 908 | 24.43 | 816 | 22.53 | 4992 |
| | 25.17 | 365 | 25.11 | 339 | 24.31 | 823 |
| | 26.82 | 239 | - | - | - | - |
| $LNA_{POPECG}$ | 20.92 | 20957 | 21.22 | 21333 | 20.58 | 37083 |
| | 22.60 | 3324 | 22.64 | 3774 | 22.58 | 3730 |
| | 24.41 | 808 | 24.39 | 909 | 24.27 | 775 |
| | 25.18 | 364 | 25.18 | 354 | - | - |
| | 26.83 | 237 | - | - | - | - |

The chemical structure of LNAs cured at different temperatures is represented in Figure P5.3. It was evident that, as the LNAs were cured, the water in the samples was evaporated revealing a sharp peak (3358-3302 $cm^{-1}$) associated to the N-H vibration band which was masked in the non-cured samples (Figure P5.1). It is noteworthy that, in general, all the bands related with urethane groups became wider as the curing temperature was increased. In addition, in all LNA samples, as the curing temperature

increased, a band around wavenumber 3480 $cm^{-1}$ belonging to free $NH_2$ appeared, which was indicative of micro-phase separation [10]. In addition, in the region corresponding to Amide I, the bands belonging to carbonyl urethane and urea groups (1740-1644 $cm^{-1}$) [11] (amplified in each figure) revealed that as the curing temperature increased, a shoulder towards lower wavenumbers appeared. Therefore, the microphase distribution varied as the curing temperature increased. However, this variation in the microphase structure was not very significant between the samples cured at 120 °C and 150 °C. On the other hand, H-bonded C-O around 1097 $cm^{-1}$ [12], increased as well. Therefore, from both GPC and ATR-FTIR characterisation, it was evident that as the curing temperature went higher, cross-linking of the LNAs increased and therefore the H-bonded urethane groups increased generating different degrees of phase separation. However, in general, no major differences were observed between the samples cured at 120 °C and 150 °C, so it was decided to use the former for the adhesion test.

Prior to measure the shear strength, the micro-phase separation of the LNAs at 120 °C was studied, since the micro-phase separation of PUs, generated by the immiscibility between the HS and SS of the polymer, is determinant in the final properties of the PUs [13]. While the SS are responsible for providing the elastomeric behaviour, the HS provide stability as they behave as crosslinkers [14]. The degree of separation as well as the miscibility of the micro-phases of a PU can be determined by different techniques such as Nuclear magnetic resonance spectroscopy [15], Differential scanning calorimetry [16], Dynamic thermomechanical analyser [17] Atomic force microscopy [18] and through ATR-FTIR [19] among others.

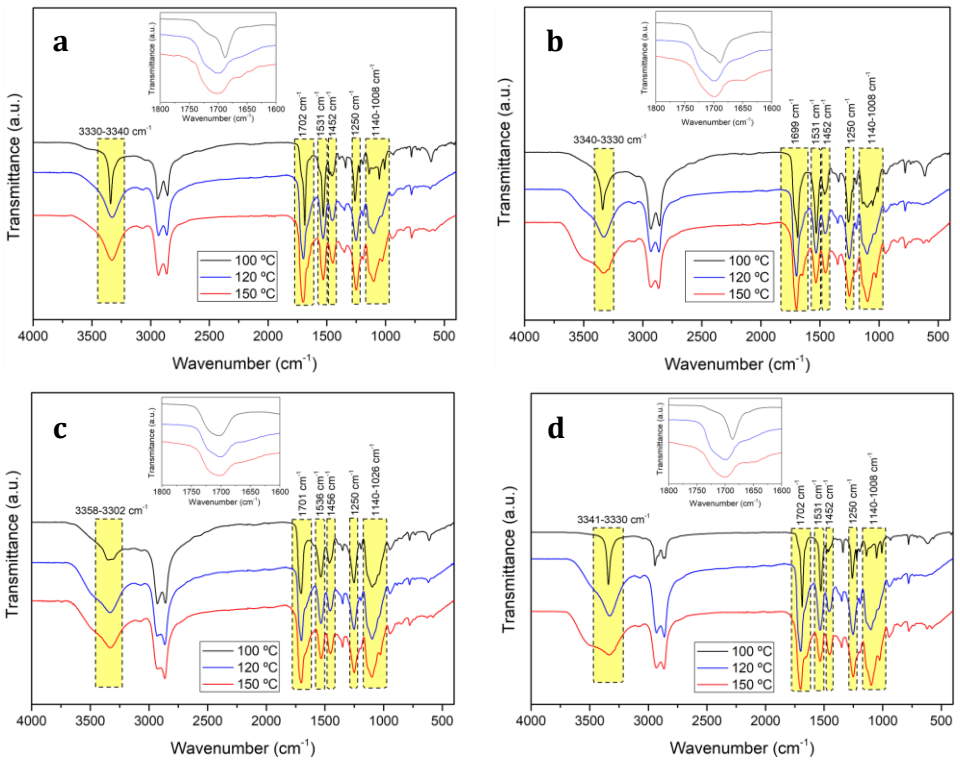


*Figure P5.3. ATR-FTIR spectra of LNAs cured at different temperatures: a) $LNA_{EOPE}$; b) $LNA_{EOPECG}$; c) $LNA_{POPE}$; d) $LNA_{POPE}$*

To analyse the microphase separation employing ATR-FTIR technology it is necessary to study the contribution of the different bands corresponding to the carbonyl groups of the PU, i.e., free C=O groups, H-bonded C=O in disordered and ordered HS and H-bonded C=O groups in disordered SS [5]. To carry out such analysis it is necessary to perform a deconvolution of the absorbance bands of the C=O groups. In addition, the H-bonded C=O groups ($X_{HB}$), the maximum mass fraction of the rigid segment mixed in the soft phase ($W_H$), the weight fraction of the mixed phase ($MP_W$), the soft segment weight fraction ($SS_W$) and the hard segment weight fraction ($HS_W$) could be calculated using the equations summarised in Appendix II.

In Table P5.4 the theoretical $HS_t$ % of the different LNAs, determined as indicated in **Appendix II**, are shown, as well as the percentages of the

different carbonyl and urea species which were calculated from the deconvolution of the bands at wavenumbers between 1750-1640 $cm^{-1}$ of the ATR-FTIR spectrum depicted in Figure P5.4.

*Table P5.4. Percentage of C=O urethane and urea species in cured LNAs*

| | T (°C) | HSt (%) | A | B | C | D |
|---|---|---|---|---|---|---|
| $LNA_{EOPE}$ | 120 | 30.379 | 12.599 | 67.143 | 15.845 | 4.413 |
| $LNA_{EOPECG}$ | 120 | 28.045 | 13.006 | 70.479 | 11.765 | 4.749 |
| $LNA_{POPE}$ | 120 | 31.112 | 15.305 | 63.154 | 18.383 | 3.158 |
| $LNA_{POPECG}$ | 120 | 26.581 | 15.717 | 64.995 | 17.171 | 2.117 |

A:1720-1714 $cm^{-1}$ Free urethane C=O in Hard Segment
B:1702-1699 $cm^{-1}$ H-bonded C=O urethane in disordered Hard Segment
C:1663-1660 $cm^{-1}$ H-bonded urea in disordered Hard Segment
D:1644-1638 $cm^{-1}$ H-bonded urea in ordered Hard Segment

The spectra shown in Figure P5.4 were fitted through Gaussian method and a good fit was obtained with $R^2$ values which were above 0.999 in all cases. The groups involved in all cases were the same. In the $LNA_{EOPE}$ and $LNA_{POPE}$ samples the amount of free urethane C=O in HS was lower and consequently the amount of H-bonded C=O urethane in HS was higher.

The presence of urea groups in all cases was noteworthy. These groups tend to increase phase separation compared to urethane groups mainly due to their higher polarity which affects the solubility, and the formation of double H-bonds among other considerations [8]. Using the results of the contribution of each group (Table P5.4), the $X_{HB}$, $W_H$, $MP_W$, $SS_W$ and $HS_W$ parameters were calculated (Table P5.5)

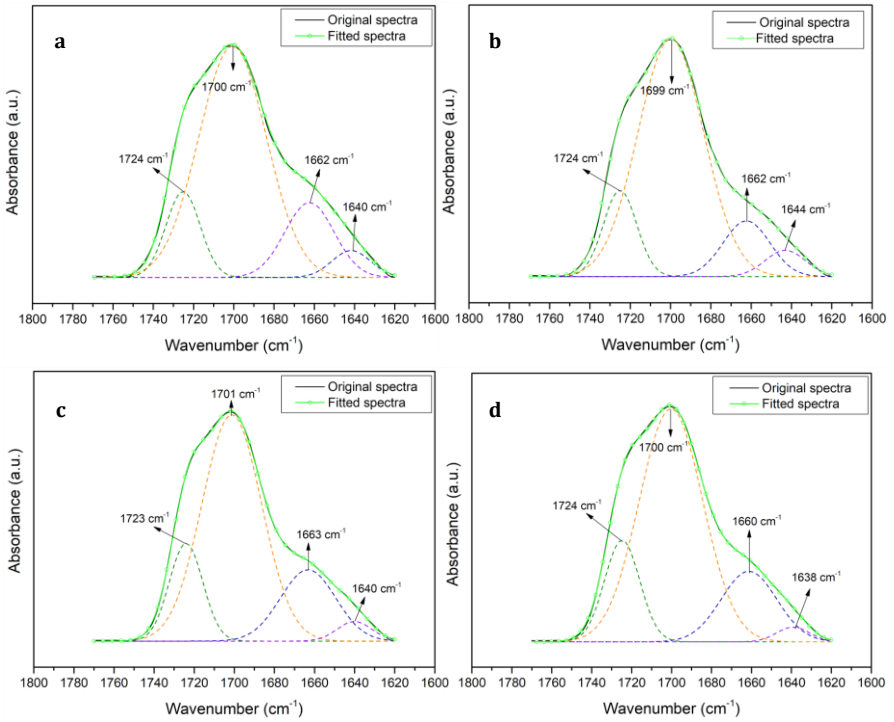


Figure P5.4. ATR-FTIR spectra of the absorbance region of the carbonyl group of the different LNAs cured at 120 °C. a) $LNA_{EOPE}$; b) $LNA_{EOPECG}$; c) $LNA_{POPE}$; d) $LNA_{POPECG}$

Table P5.5. Relevant parameter for the determination of microphase separation in LNAs

| | T (°C) | z | $X_{HB}$ | $W_H$ | $MP_W$ | $SP_W$ | $HS_W$ |
|---|---|---|---|---|---|---|---|
| $LNA_{EOPE}$ | 120 | 0.304 | 0.853 | 0.060 | 0.018 | 0.715 | 0.285 |
| $LNA_{POPE}$ | 120 | 0.311 | 0.822 | 0.074 | 0.023 | 0.712 | 0.288 |
| $LNA_{EOPECG}$ | 120 | 0.280 | 0.848 | 0.056 | 0.016 | 0.735 | 0.265 |
| $LNA_{POPECG}$ | 120 | 0.266 | 0.817 | 0.062 | 0.017 | 0.751 | 0.249 |

z is the $HS_t$ fraction

The mass fraction of H-bonded urethane or/and urea group ($X_{HB}$) in $LNA_{EOPE}$ and $LNA_{EOPECG}$ was very similar and the same for $LNA_{POPE}$ and $LNA_{POPECG}$. However, the distribution of these H-bond urethane and/or urea groups was different. In general, the values of $W_H$ and consequently $MP_w$ were low in all cases, however, the samples $LNA_{EOPECG}$ and $LNA_{POPECG}$ showed a slightly lower phase miscibility than $LNA_{EOPE}$ and $LNA_{POPE}$.

The tensile strength which is necessary to break the adhesive bonds of the LNA adhesive formulations were carried out employing an Automatic Bond Evaluation System (ABES) by measuring the shear strength. In Figure P5.5, the results of the shear strength test of the different LNAs are represented. As mentioned above, a temperature of 120 °C was selected and different pressing times were used.

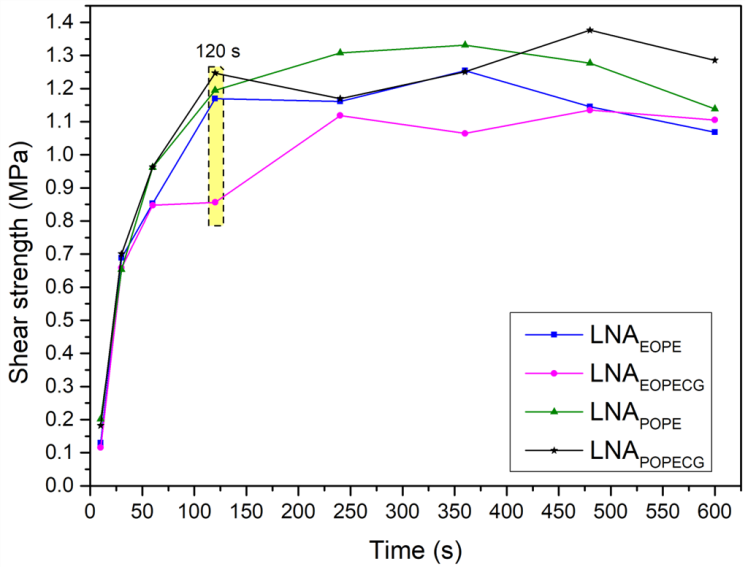


Figure P5.5. Shear strength of LNA adhesives

Analysis of the shear strength results revealed the usual behaviour of adhesive curing process in this type of test [20]. A first stage where a delay in the development of the bond strength is observed, which is related with the loss of energy caused by the evaporation of the water in the sample. The second zone, almost linear, corresponds to the process of elongation and crosslinking of the chains during the curing process [21]. The last stage is a zone where the shear strength can increase or decrease depending on the behaviour of the adhesive with respect to temperature and/or humidity [22]. Similar maximum values were obtained in all cases, although they were achieved at different retention times. Thus, the maximum shear strength for

$LNA_{EOPECG}$ and $LNA_{POPECG}$ were obtained at a pressing time of 480 s, being the highest value for $LNA_{POPECG}$ 1.38 MPa and 1.13 MPa for $LNA_{POPECG}$. On the other hand, the maximum shear strength values for $LNA_{EOPE}$ and $LNA_{POPE}$ were 1.25 MPa and 1.33 MPa respectively and were reached at a pressing time of 360 s.

To improve both the adhesion and crosslinking properties of the NIPUs, a silane coupling agent (3-aminopropyltrimethoxysilane) (APTMS) was added. The silane coupling agent acts by hydrolysing rapidly in basic aqueous media forming silanol and methanol as residue. These hydrolysed molecules tend to condense with adjacent silanol molecules forming oligomers. Then the OH groups of the oligomers form H-bonds with the OH groups of the surface and finally during the curing process covalent bonds are formed, leaving the amino group free to form covalent bonds or physical interactions with other groups [23]. This amino group can interact via H-bonds with the NH groups of urethane and urea groups as well as with the amino-terminal groups of the NIPUs increasing the amount of H-bonded groups [4]. The coupling agent was added at different molar ratios (5, 15 and 25%) with respect the $I_{OH}$ of the bio-polyols, assuming that all of them reacted to form urethane and urea bonds. Once the coupling agent was added, the samples were magnetically stirred for 24 hours, and then the shear strength was determined, and the results are represented in Figure P5.6. Additionally, to characterise them, the different LNAs with the silane coupling agent (CLNA) were cured at 120 °C employing an aluminium mould.

As expected, the higher the APTMS concentration, the higher the shear strength. Nevertheless, in the $CLNA_{POPECG}$ formulations, better results were obtained with an APTMS concentration of 15%. Thus, in $CLNA_{EOPE}$ formulation, the maximum shear strength value was obtained with the addition of 25% APTMS (3.90 MPa) and a pressing time of 300 s. At the same

pressing time but with 15% APTMS the value was slightly lower (3.68 MPa) while with 5% the maximum value (2.25 MPa) was obtained at the maximum pressing time. In the $CLNA_{EOPECG}$ formulation a maximum value of 3.41 MPa was reached at 25% APTMS (240 s) while adding 15 and 5% the maximum shear strength values, 2.70 MPa and 1.93 MPa, were achieved at 360 s.

The addition of 25% of APTMS in the $CLNA_{POPE}$ formulation reached a maximum shear strength value of 3.21 MPa at 600 s, 2.68 MPa at 480 s with the addition of 15% and 1.49 MPa at 360s with 5%. Finally, as mentioned above, for the $CLNA_{POPECG}$ formulation the highest values were obtained when 15% APTMS was added-In this case the maximum shear strength (3.50 MPa) was obtained at a pressing time of 240 s as in the formulation with 5% (2.46 MPa), while by adding 25% APTMS the maximum value (3.20 MPa) was attained at 480 s. Considering the pressing time used as a reference (120 s), it was observed that except for the $CLNA_{EOPE}$ formulation, an increase from 15% to 25% of APTMS would not be justified since very similar shear strength values were obtained.

These results were significantly lower than those obtained by Saražin et al., (2021) [3] using organosolv lignin to synthesise a NIPU adhesive. However, in this study an epoxy-based silane coupling agent was used, which can create C-N bonds with the amino-terminal groups facilitating the curing process; moreover, higher curing temperatures were used. Thus, they obtained a lignin based NIPU adhesive with a shear strength above 7 MPa adding 22% of coupling agent and using a curing temperature of 200 °C and 10 min of pressing time. Chen et al., (2022) [2] synthesised a NIPU wood adhesive by reacting mimosa tannins with DMC, HDMA and glycerol diglycidyl ether obtaining a maximum shear strength value around 1.4-1.5 MPa. Therefore, the following formulations were selected as optimal:

$CLNA_{EOPE}$ with 25% of APTMS ($CLNA_{EOPE-25}$), $CLNA_{EOPE-15}$, $CLNA_{POPE-15}$ and $CLNA_{POPECG-15}$, in the latter three 15% APTMS was used.

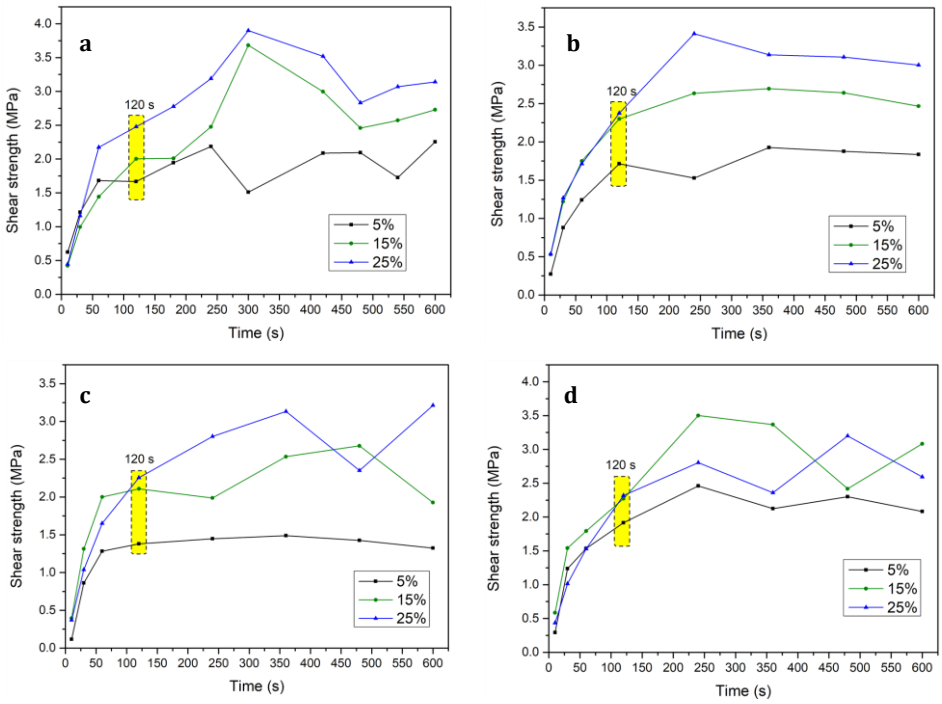


Figure P5.6. Shear strength of different CLNA. a) $CLNA_{EOPE}$; b) $CLNA_{EOPECG}$; c) $CLNA_{POPE}$; d) $CLNA_{POPECG}$

## 2.2. Characterisation of the synthesised lignin based non-isocyanate polyurethane adhesives with silane coupling agent

The optimised CLNA formulations were characterised through ATR-FTIR to determine their chemical structure as well as to analyse the microphase structure. In addition, through TGA, the thermal stability of the samples was studied and using the isoconversional methods of OFW and KAS, described in **Appendix II**, the *Ea*, *A* and a lifetime estimation of each system was determined. Unfortunately, in this case the molecular weight of the samples could not be determined as they were insoluble in the mobile phase used.

The chemical structure of CLNAs is compared with LNAs and the obtained ATR-FTIR spectra are shown in Figure P5.7. Few differences could be observed between the chemical structure of CLNA and LNA samples. However, there were some signals that indicated the incorporation of the APTMS. One of them was the appearance, in all cases, of a signal at wavenumber 694 $cm^{-1}$ corresponding to the C-Si-C vibration [24]. On the other hand, it was observed that the signal related to the H-bonded urea increased as a possible consequence of the reaction between the terminal carbonate groups and the amino groups of the APTMS. The band at 1100 $cm^{-1}$ assigned to the Si-O-C bond [25] was more pronounced. In addition, around 805 $cm^{-1}$ wavenumber a small band shoulder which was not visible in $CLNA_{POPE-15}$appeared. This band is related to the Si-O-Si deformation vibration [26] of the oligomers formed through the condensation of the APTMS molecules.

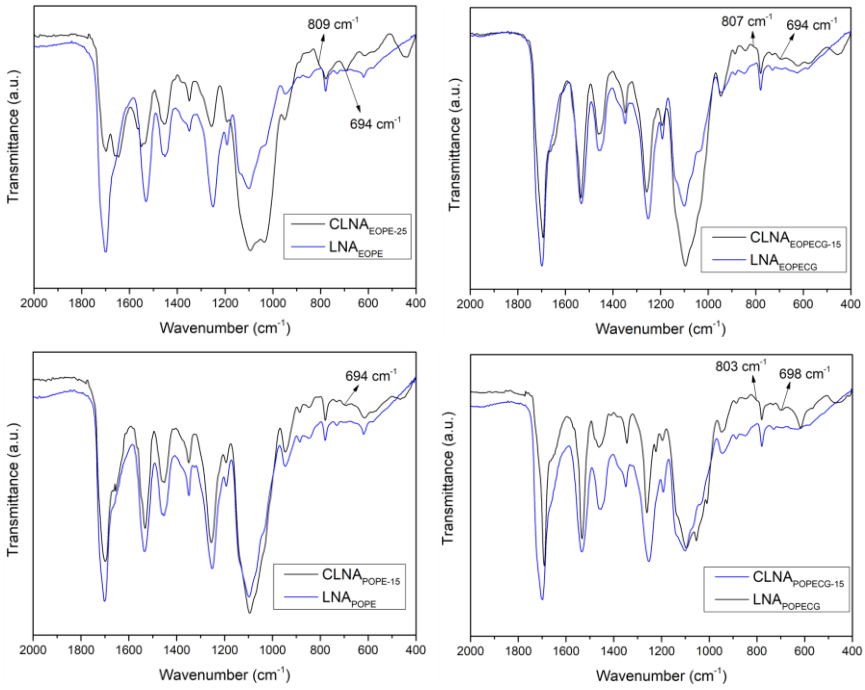


Figure P5.7. ATR-FTIR spectra of CLNA and LNA samples.

The analysis of the carbonyl region (1750-1640 $cm^{-1}$) is depicted in Figure P5.8. The spectra were fitted through Gaussian method and a good fit was obtained with $R^2$ values which were above 0.999 in all cases. In Table P5.6 the percentages of the carbonyl and urea species presented.

Table P5.6. Percentage of carbonyl and urea species in cured CLNAs

| | T (°C) | HSt(%) | A | B | C | D |
|---|---|---|---|---|---|---|
| $CLNA_{EOPE-25}$ | 120 | 30.379 | 11.156 | 41.488 | 35.830 | 11.525 |
| $CLNA_{EOPECG-15}$ | 120 | 28.045 | 17.608 | 52.516 | 15.493 | 14.382 |
| $CLNA_{POPE-15}$ | 120 | 31.112 | 11.925 | 58.385 | 27.272 | 1.996 |
| $CLNA_{POPECG-15}$ | 120 | 26.581 | 24.409 | 27.599 | 35.250 | 12.742 |

A:1723-1711 $cm^{-1}$ Free urethane C=O in Hard Segment
B:1701-1691 $cm^{-1}$ H-bonded C=O urethane in disordered Hard Segment
C:1675-1654 $cm^{-1}$ H-bonded urea in disordered Hard Segment
D:1644-1630 $cm^{-1}$ H-bonded urea in ordered Hard Segment

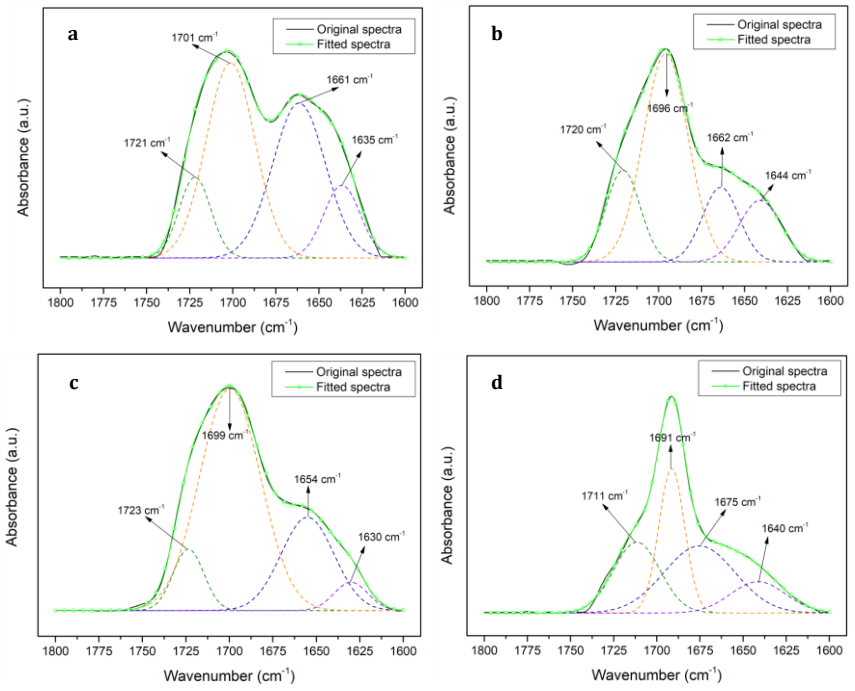


Figure P5.8. ATR-FTIR spectra of the absorbance region of the carbonyl group of the different CLNAs cured at 120 °C. a) $CLNA_{EOPE-25}$; b) $CLNA_{EOPECG-15}$; c) $CLNA_{POPE-15}$; d) $CLNA_{POPECG-15}$

When comparing the carbonyl and urea species of the samples with the APTMS coupling agent (Table P5.6 and Figure P5.7) and those obtained without the APTMS (Table P5.4 and Figure P5.4), is evident that the percentage of H-bonded urea group in both ordered and disordered HS increased considerably despite the decrease of the H-bonded urethane CO. This could be because the H-bond between the urea groups were promoted by the addition of the coupling agent. On the one hand, the higher increase of H-bond urea group in the $CLNA_{EOPE-25}$ sample compared to the other samples was expected due to the higher amount of APTMS used. On the other hand, among the samples in which 15% of APTMS was used, the sample $CLNA_{POPECG-15}$ surprisingly showed a much higher increase than the other two, achieving a slightly higher amount of H-bond urea group than those obtained by $CLNA_{EOPE-25}$. It was also worth noting that the samples synthesised with CG showed an increase in free urethane groups.

Table P5.7. Relevant parameters for the determination of microphase separation in CLNs

| | T (°C) | z | $X_{HB}$ | $W_H$ | $MP_W$ | $SP_W$ | $HS_W$ |
|---|---|---|---|---|---|---|---|
| $CLNA_{EOPE-25}$ | 120 | 0.304 | 0.869 | 0.054 | 0.016 | 0.713 | 0.287 |
| $CLNA_{EOPECG-15}$ | 120 | 0.280 | 0.796 | 0.074 | 0.021 | 0.740 | 0.260 |
| $CLNA_{POPE-15}$ | 120 | 0.311 | 0.860 | 0.060 | 0.019 | 0.707 | 0.293 |
| $CLNA_{POPECG-15}$ | 120 | 0.266 | 0.721 | 0.092 | 0.024 | 0.759 | 0.241 |

z is the $HS_t$ fraction

Because of the decrease in H-bonded urethane CO groups in $CLNA_{EOPECG-15}$ and $CLNA_{POPECG-15}$, an increase in the miscibility between the microphases was observed. On the contrary, since both H-bonded urethane and urea groups increased in $CLNA_{EOPE-25}$ and $CLNA_{POPE-15}$ samples, the mass fraction of HS mixed in SS decreased slightly with respect to the samples without APTMS as can be seen in Table P5.7. This microphase configuration affected the adhesion behaviour of the samples. A greater phase separation between HS and SS usually improves the material behaviour, as was the case with

sample $CLNA_{EOPE-25}$, which obtained the highest shear strength value. However, the second-best result was not obtained with $CLNA_{POPE-15}$, as expected, but was obtained with the sample with the least phase separation. Thus, $CLNA_{POPECG-15}$ with lower amount of APTMS obtained a maximum value only 0.4 MPa lower than the one obtained by $CLNA_{EOPE-25}$. Furthermore, this value was obtained using a shorter pressing time. Therefore, it can be concluded that a higher amount of urea groups helped favourably in the adhesion properties of the synthesised NIPUs.

The thermal stability of the formulated CLNAs was studied through TGA. Figure P5.9 shows the TGA and DTG curves obtained for each sample, which indicates that there were three main degradation zones besides the moisture evaporation zone (30-120 °C).

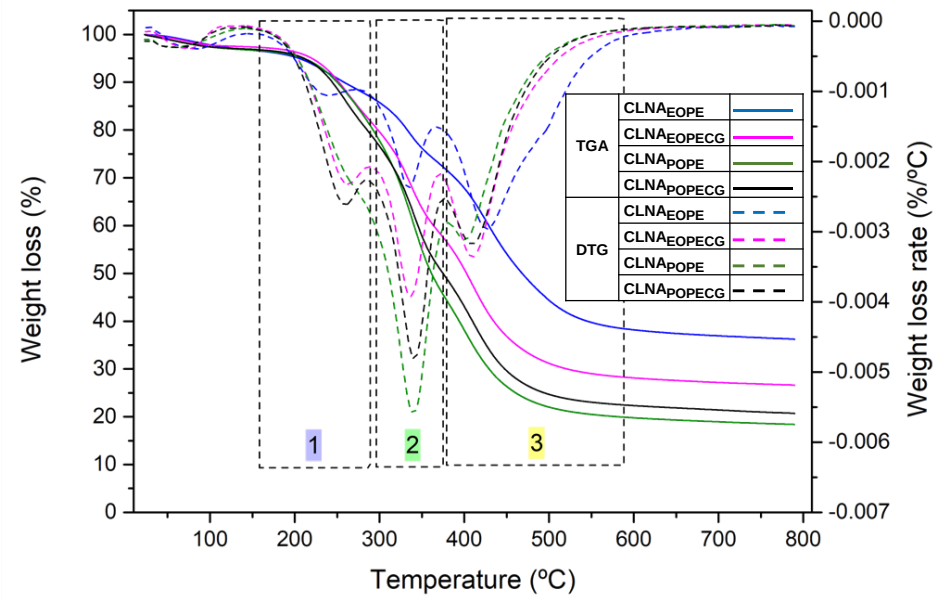


Figure P5. 9. TGA and DTG curves of the synthesised CLNAs

The first degradation zone (150-280 °C) is associated with the following events: the cleavage of H-bonded urethane and urea groups [27], the

cleavage of unstable β-O-4, α-O-4 and 4-O-5 ether bonds of lignin [28] and the presence of unreacted HDMA [2], which boiling point is 204 °C. The mass loss zone between 280-380 °C is related with the degradation of the soft segment [29] (bio-polyol) and it was the area with the highest mass loss, except in the case of $CLNA_{EOPE\text{-}25}$. The last degradation area (380-580 °C) is attributed to the cleavage of covalent C-C [30], the aromatic rings of lignin [31] as well as the degradation of APTMS [32]. The degradation of the latter takes place in two stages, the first between 380-450 °C, corresponding to the intercalated silane and the second between 450-550 °C, belonging to grafted silane [33]. Depending on the sample and thus on the amount of APTMS used, the final residue was different. Therefore, an increase of APTMS was reflected in an increase in the final residue.

Employing OFW and KAS isoconversional methods, which are described in **Appendix II**, and using different heating rates (1, 2, 5 and 10 °C/min) the $E_a$ and the pre-exponential factor (A) of the synthesised CLNAs was calculated. Both, $E_a$ and A, were calculated from the slope and intercept of the plots of $\ln(\beta)$ and $\ln\left(\frac{\beta}{T_p^2}\right)$ versus 1000/Tp where the conversion rates (α) from 5% to 90% for each system were plotted.

The most commonly used isoconversional method, since it is not necessary to know the reaction order, is the OFW method [34]. Nevertheless, a second method (KAS) was employed to validate the model. In both cases, a linear fit must be obtained for the model to be applicable [35]. In Figure P5.10 a-d and P5.10 e-f, the fitted plots of the CLNAs using OFW and KAS methods are outlined, and the obtained $R^2$ determination coefficients and $E_a$ of each CLNA are summarised in Table P5.8 (OFW) and Table P5.9 (KAS). Through OFW methods the pre-exponential factor was obtained for every conversion rate to make an estimation of the half-life of the polymer. This estimation was carried out using the OFW method.

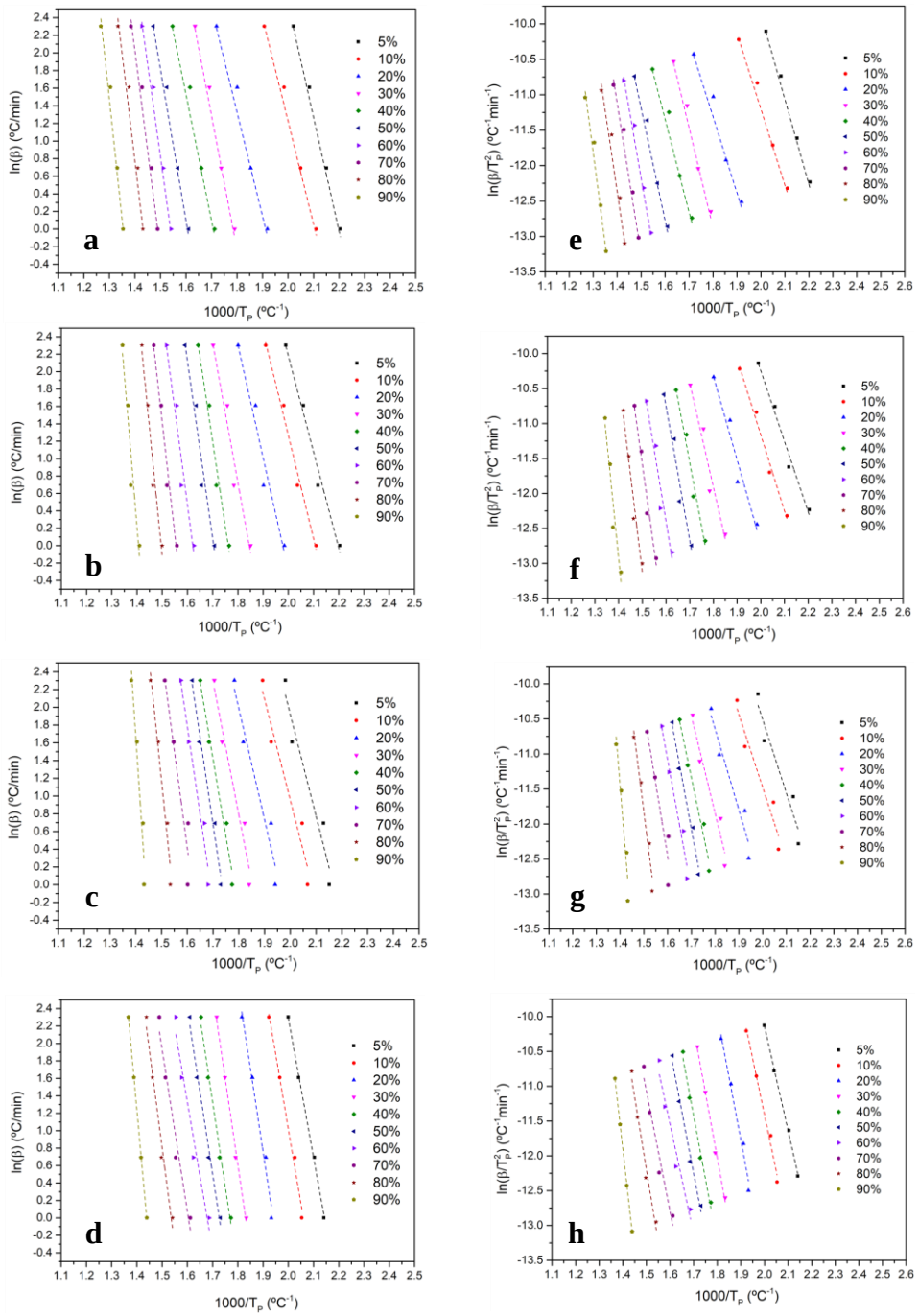


Figure P5.10. (a-d) OFW plots of ln(β) vs. 1000/$T_P$ and (e-h) KAS plots of ln($\beta/T^2_P$) vs. 1000/$T_P$ for different conversion values of $CLNA_{EOPE-25}$ (a-e), $CLNA_{EOPECG-15}$ (b-f), $CLNA_{POPE-15}$ (c-g) and $CLNA_{POPECG-15}$(d-h)

As mentioned above, OFW and KAS methods must fit a linear regression, furthermore, as shown in Figure P5.10 the lines must follow a parallel trend to each other. Therefore, since both conditions are fulfilled, it can be concluded that the selected models were correct.

In addition, the $R^2$ determination coefficients reported in Tables P5.8 and P5.9 reveal a good fit of the regressions. Moreover, as it can be observed, the $E_a$ values obtained by the two methods were very similar, which confirms the good selection of the methods.

The dependence of the $E_a$ with respect to the conversion degree is different in each case as can be seen in Tables P5.8 and P5.9 and Figure P5.11. Thus, for a α of 5%, the sample $CLNA_{POPECG\text{-}15}$ showed the highest value, followed by $CLNA_{EOPE\text{-}25}$, $CLNA_{POPE\text{-}15}$ and $CLNA_{EOPECG\text{-}15}$.

Table P5.8. Activation energies ($E_a$) (KJ/mol) and correlation coefficients of the linear regression of the PU samples for the decomposition obtained through OFW method

| | $CLNA_{EOPE\text{-}25}$ | | $CLNA_{EOPECG\text{-}15}$ | | $CLNA_{POPE\text{-}15}$ | | $CLNA_{POPECG\text{-}15}$ | |
|---|---|---|---|---|---|---|---|---|
| α | $R^2$ | $E_a$ | $R^2$ | $E_a$ | $R^2$ | $E_a$ | $R^2$ | $E_a$ |
| 0.05 | 0.998 | 100.1 | 0.9842 | 87.3 | 0.9413 | 90.7 | 0.9982 | 126.2 |
| 0.1 | 0.992 | 91.2 | 0.9877 | 93.9 | 0.9492 | 90.1 | 0.9909 | 142.6 |
| 0.2 | 0.983 | 93.9 | 0.9542 | 102.7 | 0.9487 | 99.4 | 0.9850 | 158.4 |
| 0.3 | 0.9918 | 120.3 | 0.9552 | 126.8 | 0.9589 | 118.6 | 0.9953 | 164.3 |
| 0.4 | 0.9823 | 113.5 | 0.9750 | 153.2 | 0.9792 | 137.0 | 0.9901 | 161.0 |
| 0.5 | 0.9908 | 134.2 | 0.9586 | 161.0 | 0.9840 | 154.3 | 0.9889 | 157.1 |
| 0.6 | 0.9903 | 161.0 | 0.9496 | 173.4 | 0.9692 | 157.1 | 0.9590 | 141.2 |
| 0.7 | 0.9832 | 173.3 | 0.9770 | 203.9 | 0.9134 | 173.4 | 0.9643 | 154.4 |
| 0.8 | 0.9731 | 183.7 | 0.9674 | 232.0 | 0.9697 | 223.8 | 0.9801 | 184.9 |
| 0.9 | 0.9806 | 211.0 | 0.9393 | 276.3 | 0.9451 | 341.8 | 0.9999 | 264.0 |

Table P5.9. Activation energies ($E_a$) (KJ/mol) and correlation coefficients of the linear regression of the PU samples for the decomposition obtained through KAS method

| | $CLNA_{EOPE-25}$ | | $CLNA_{EOPECG-15}$ | | $CLNA_{POPE-15}$ | | $CLNA_{POPECG-15}$ | |
|---|---|---|---|---|---|---|---|---|
| α | $R^2$ | $E_a$ | $R^2$ | $E_a$ | $R^2$ | $E_a$ | $R^2$ | $E_a$ |
| 0.05 | 0.9976 | 97.4 | 0.9813 | 83.9 | 0.9308 | 87.4 | 0.9979 | 124.7 |
| 0.1 | 0.9902 | 86.6 | 0.9854 | 90.5 | 0.9395 | 86.4 | 0.9897 | 134.2 |
| 0.2 | 0.9791 | 89.7 | 0.9464 | 99.2 | 0.9393 | 95.6 | 0.9831 | 149.5 |
| 0.3 | 0.9904 | 116.8 | 0.9486 | 124.0 | 0.9523 | 115.4 | 0.9947 | 154.9 |
| 0.4 | 0.9786 | 109.2 | 0.9718 | 151.4 | 0.9761 | 134.5 | 0.9889 | 151.3 |
| 0.5 | 039891 | 130.3 | 0.9535 | 159.3 | 0.9819 | 152.4 | 0.9876 | 147.2 |
| 0.6 | 0.9888 | 158.1 | 0.9437 | 171.8 | 0.9651 | 155.1 | 0.9530 | 130.9 |
| 0.7 | 0.9807 | 170.7 | 0.9747 | 203.5 | 0.9034 | 171.7 | 0.9594 | 143.6 |
| 0.8 | 0.9694 | 181.2 | 0.9643 | 232.7 | 0.9666 | 224.3 | 0.9776 | 173.7 |
| 0.9 | 0.9781 | 209.3 | 0.9344 | 278.6 | 0.9415 | 347.8 | 0.9998 | 252.1 |

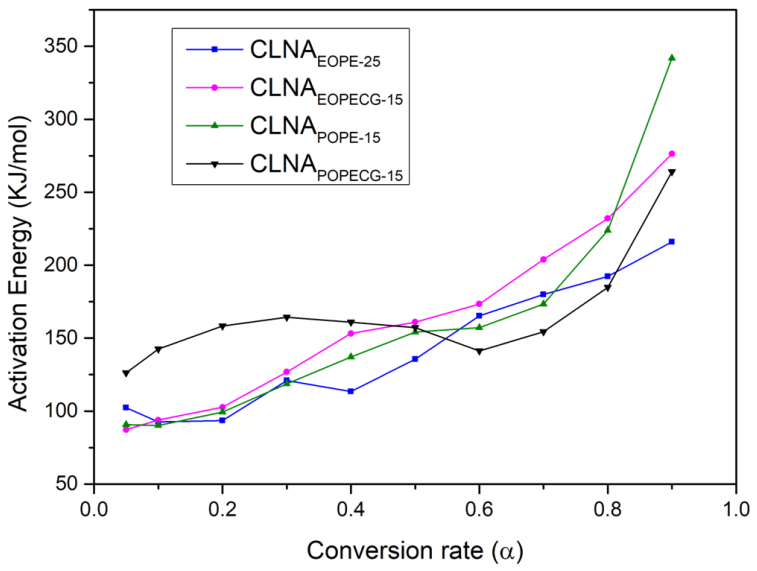


Figure P5.11. $E_a$ vs. α of different CLNAs calculated with OFW method.

As the conversion degree increased, different behaviour was observed in the samples, in this way, the $E_a$ of $CLNA_{EOPE-25}$ decreased at 10% of conversion

and increased again until reach a maximum value of 211.0KJ/mol at 90% of conversion. The tendency for the $CLNA_{EOPECG-15}$ as well as for $CLNA_{POPE-15}$ was to increase with the degree of conversion. Finally, $E_a$ increased in $CLNA_{POPECG-15}$ until it reached a value of 161.0 KJ/mol at 40% of conversion, thereafter it decreased progressively up to 60% of conversion and increased again until it reached a final value of 264.0 KJ/mol. These different behaviours, as well as the differences in $E_a$ with increasing the conversion rate, indicates that the decomposition process throughout the reaction did not follow the same reaction mechanism, as $E_a$ is a function of α. This could be explained by the different nature of the bio-polyols, the different amount of H-bonded urethane and urea groups presented in the samples as well as the interaction of APTMS with them.

Furthermore, as can be seen at 5% degradation the highest $E_a$ values corresponds to the samples with the highest content of H-bonded urea groups ($CLNA_{POPECG-15}$ and $CLNA_{EOPE-25}$), since the stability of the urea groups is greater than that of the urethane groups [36]. Therefore, the greater the urea groups, the greater the stability of the NIPU. On the other hand, comparing $CLNA_{EOPECG-15}$ and $CLNA_{POPE-15}$ samples with similar urea and urethane groups, it was observed that the obtained $E_a$ values were very similar, though slightly lower for $CLNA_{EOPECG-15}$ due to the lower amount of H-bonded groups.

In Table P5.10 the A values calculated with OFW method are summarised. As this factor refers to the availability of chemical groups that would be susceptible to degrade [35], a higher value indicates a higher resistance to degradation.

Table P5.10. A ($min^{-1}$) of the CLNA samples obtained through OFW method

| | A ($min^{-1}$) | | | |
|---|---|---|---|---|
| α | $CLNA_{EOPE-15}$ | $CLNA_{EOPECG-15}$ | $CLNA_{POPE-15}$ | $CLNA_{POPECG-15}$ |
| 0.05 | 1.2E+09 | 3.5E+07 | 6.2E+07 | 5.1E+11 |
| 0.1 | 7.7E+07 | 1.4E+08 | 4.2E+07 | 2.8E+12 |
| 0.2 | 3.3E+07 | 5.4E+08 | 1.9E+08 | 2.7E+13 |
| 0.3 | 3.5E+09 | 3.8E+10 | 6.2E+09 | 1.9E+13 |
| 0.4 | 3.8E+08 | 3.9E+12 | 1.7E+11 | 4.1E+12 |
| 0.5 | 6.8E+09 | 8.9E+12 | 3.9E+12 | 1.1E+12 |
| 0.6 | 4.5E+11 | 2.6E+13 | 3.9E+12 | 2.7E+10 |
| 0.7 | 2.0E+12 | 2.7E+15 | 3.2E+13 | 1.2E+11 |
| 0.8 | 5.0E+12 | 1.4E+17 | 1.1E+17 | 1.0E+13 |
| 0.9 | 1.0E+14 | 3.2E+19 | 1.2E+25 | 1.0E+18 |

As it was expected, the A values followed the same trend as the $E_a$ values. As mentioned above, the pre-exponential factor is used to estimate the lifetime of the polymer through OFW method and is usually carried out at 5% of conversion [37]. Therefore, the polymers with the highest expected lifetime those with the highest A value at a α=5%, i.e., $CLNA_{POPECG-15}$ > $CLNA_{EOPE-25}$ > $CLNA_{POPE-15}$ > $CLNA_{EOPECG-15}$.

The lifetime versus temperature of the formulated CLNAs is represented in Figure P5.12.

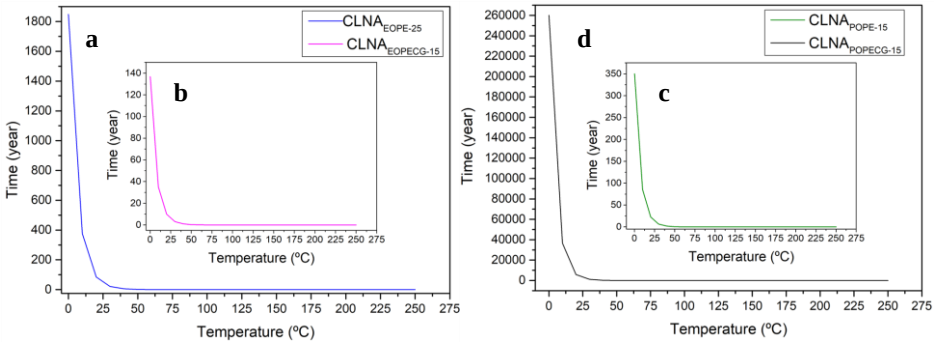


Figure P5.12. Lifetime estimation of a) $CLNA_{EOPE-25}$; b) $CLNA_{EOPECG-15}$; c) $CLNA_{POPE-15}$; d) $CLNA_{POPECG-15}$

Accordingly, with the higher values of A, the lifetime of the polymers was as follows from highest to lowest $CLNA_{POPECG-15}$ > $CLNA_{EOPE-25}$ > $CLNA_{POPE-15}$ > $CLNA_{EOPECG-15}$. In all cases the degradation of the CLNAs increases rapidly with increasing temperature. Thus, above 40°C the lifetime decreases sharply from years to days in all cases except $CLNA_{POPECG-15}$. However, it should be noted that these results were obtained from degrading the CLNAs in an inert atmosphere ($N_2$) and that oxidising atmosphere the polymers will degrade differently.

## 3. CONCLUSIONS

Four different NIPU adhesives were synthesised, characterised, and subjected to adhesion test employing an ABES with poor results between 1.13-1.38 MPa. To improve the adhesion properties, a coupling agent (APTMS) was employed in different amounts and the optimal formulations ($CLNA_{EOPE-25}$, $CLNA_{EOPECG-15}$, $CLNA_{POPE-15}$ and $CLNA_{POPECG-15}$) were selected based on the shear strengths obtained at a pressing time of 120 s. A kinetic degradation study was carried out employing the isoconversional OFW and KAS methods and the $E_a$, A and half-life of the selected CLNAs were determined. From the obtained $E_a$ values, it was concluded that the degradation mechanisms were different in each sample, leading to the following order of stability of the CLNAs: $CLNA_{POPECG-15}$ > $CLNA_{EOPE-25}$ > $CLNA_{POPE-15}$ > $CLNA_{EOPECG-15}$.

## REFERENCES

[1] F. Zhang, X. Wei, Z. Xiao, J. Appl. Polym. Sci. 127(3) (2013) 1730–6. 10.1002/app.37763.

[2] X. Chen, A. Pizzi, E. Fredon, C. Gerardin, X. Zhou, B. Zhang, G. Du, Int. J. Adhes. Adhes. 112(September 2021) (2022) 103001. 10.1016/j.ijadhadh.2021.103001.

[3] J. Saražin, A. Pizzi, S. Amirou, D. Schmiedl, M. Šernek, J. Renew. Mater. 9(5) (2021) 881–907. 10.32604/jrm.2021.015047.

[4] F.J. Santiago-Medina, M.C. Basso, A. Pizzi, L. Delmotte, J. Renew. Mater. 6(4) (2018) 413–25. 10.7569/JRM.2017.634172.

[5] M. Fuensanta, J.M. Martín-Martínez, Polymers (Basel). 13(18) (2021). 10.3390/polym13183097.

[6] F. Ren, R. Zhou, F. Sun, H. Ma, Z. Zhou, W. Xu, RSC Adv. 7(47) (2017) 29779–85. 10.1039/c7ra04454b.

[7] N. Kébir, M. Benoit, C. Legrand, F. Burel, Eur. Polym. J. 96(August) (2017) 87–96. 10.1016/j.eurpolymj.2017.08.046.

[8] I. Yilgör, E. Yilgör, G.L. Wilkes, Polymer (Guildf). 58 (2015) A1–36. 10.1016/j.polymer.2014.12.014.

[9] S. Sakurai, Y. Okamoto, H. Sakaue, T. Nakamura, L. Banda, S. Nomura, J. Polym. Sci. Part B Polym. Phys. 38(13) (2000) 1716–28. 10.1002/1099-0488(20000701)38:13<1716::AID-POLB50>3.0.CO;2-X.

[10] H. Huang, H. Pang, J. Huang, P. Yu, J. Li, M. Lu, B. Liao, Constr. Build. Mater. 284 (2021) 122388. 10.1016/j.conbuildmat.2021.122388.

[11] Z. Shen, L. Zheng, C. Li, G. Liu, Y. Xiao, S. Wu, J. Liu, B. Zhang, Polymer (Guildf). 175(May) (2019) 186–94. 10.1016/j.polymer.2019.05.010.

[12] F. Dong, S. Maganty, S.J. Meschter, J. Cho, Prog. Org. Coatings 114(September 2017) (2018) 58–67. 10.1016/j.porgcoat.2017.09.018.

[13] V. Costa, A. Nohales, P. Félix, C. Guillem, D. Gutiérrez, C.M. Gõmez, J. Appl. Polym. Sci. 132(12) (2015) 1–10. 10.1002/app.41704.

[14] S. Arévalo-Alquichire, M. Morales-Gonzalez, K. Navas-Gómez, L.E. Diaz, J.A. Gómez-Tejedor, M.A. Serrano, M.F. Valero, Polymers (Basel). 12(3) (2020). 10.3390/polym12030666.

[15] S. D'Hollander, C.J. Gommes, R. Mens, P. Adriaensens, B. Goderis, F. Du Prez, J. Mater. Chem. 20(17) (2010) 3475–86. 10.1039/b923734h.

[16] J. Balko, B. Fernández-D'Arlas, E. Pöselt, R. Dabbous, A.J. Müller, T. Thurn-Albrecht, Macromolecules 50(19) (2017) 7672–80. 10.1021/acs.macromol.7b00871.

[17] J. Zhou, H. Li, X. Lu, Polym. Adv. Technol. 29(8) (2018) 2308–16. 10.1002/pat.4342.

[18] S. Abdollahi Baghban, M. Khorasani, G.M.M. Sadeghi, J. Appl. Polym. Sci. 135(46) (2018) 1–13. 10.1002/app.46744.

[19] A. Niemczyk, A. Piegat, Á. Sonseca Olalla, M. El Fray, Eur. Polym. J.

93(May) (2017) 182–91. 10.1016/j.eurpolymj.2017.05.046.

[20] B. Esteves, J. Martins, J. Martins, L. Cruz-Lopes, J. Vicente, I. Domingos, Maderas Cienc. y Tecnol. 17(2) (2015) 277–84. 10.4067/S0718-221X2015005000026.

[21] J.M.M. Ferra, M. Ohlmeyer, A.M. Mendes, M.R.N. Costa, L.H. Carvalho, F.D. Magalhes, Int. J. Adhes. Adhes. 31(3) (2011) 127–34. 10.1016/j.ijadhadh.2010.11.013.

[22] B.M. De Morais Lemos Esteves, L.P.V. Cruz-Lopes, A.P. Fernandes, J.M. Martins, I. De Jesus Domingos, J.V. Ferreira, S.H.F. Da Silva, J. Labidi, Wood Res. 64(1) (2019) 105–16.

[23] B. Arkles, Gelest, Inc. (2014) 1–76.

[24] S. Cichosz, A. Masek, Materials (Basel). 13(13) (2020) 1–19. 10.3390/ma13132901.

[25] A.A. Issa, A.S. Luyt, Polymers (Basel). 11(3) (2019). 10.3390/polym11030537.

[26] M. Baloch, M. Alberro, J. Labidi, Polymers (Basel). 13(4) (2021) 1–15. 10.3390/polym13040643.

[27] J. D'Souza, R. Camargo, N. Yan, J. Appl. Polym. Sci. 131(16) (2014) 1–10. 10.1002/app.40599.

[28] C. Zhang, H. Wu, M.R.K. Kessler, Polymer (Guildf). 69(1) (2015) 52–7. 10.1016/j.polymer.2015.05.046.

[29] P. Cinelli, I. Anguillesi, A. Lazzeri, Eur. Polym. J. 49(6) (2013) 1174–84.

10.1016/j.eurpolymj.2013.04.005.

[30] O.S.H. Santos, M. Coelho da Silva, V.R. Silva, W.N. Mussel, M.I. Yoshida, J. Hazard. Mater. 324 (2017) 406–13. 10.1016/j.jhazmat.2016.11.004.

[31] L.B. Tavares, C. V. Boas, G.R. Schleder, A.M. Nacas, D.S. Rosa, D.J. Santos, Express Polym. Lett. 10(11) (2016) 927–40. 10.3144/EXPRESSPOLYMLETT.2016.86.

[32] S. Thanomchat, K. Srikulkit, Adv. Mater. Sci. Eng. 2015 (2015). 10.1155/2015/741242.

[33] W. Shen, H.P. He, J. Zhu, P. Yuan, R.L. Frost, J. Colloid Interface Sci. 313(1) (2007) 268–73. 10.1016/j.jcis.2007.04.029.

[34] A. Singh, R. Kumar, P.K. Soni, V. Singh, J. Macromol. Sci. Part B Phys. 59(12) (2020) 775–95. 10.1080/00222348.2020.1802850.

[35] N.L. Batista, M.L. Costa, K. Iha, E.C. Botelho, J. Thermoplast. Compos. Mater. 28(2) (2015) 265–74. 10.1177/0892705713484740.

[36] Y. Yang, X. Cao, H. Luo, X. Cai, J. Polym. Res. 25(11) (2018). 10.1007/s10965-018-1634-z.

[37] L. Núñez, F. Fraga, M.R. Núñez, M. Villanueva, J. Appl. Polym. Sci. 78(6) (2000) 1239–44. 10.1002/1097-4628(20001107)78:6<1239::aid-app90>3.0.co;2-x.

*4. ATALA*

# ONDORIOAK ETA ETORKIZUNEKO LANAK

## ONDORIOAK

Ondorio orokor gisa, *Eucalyptus globulus*etik eta *Pinus radiata*tik eratorritako ligninak mikrouhin bidezko likidotze erreakzioa erabiliz biopoliolak sintetizatzeko erabil daitezkeela ikusi da. Gainera, likidotze prozesua eskalagarria izan daitekeela ere frogatu da, sintetizatuko biopoliolen ezaugarriak aldaketa nabarmenik jasan gabe. Zurean aplikatzeko Isozianato eta isozianatorik gabeko formulatutako poliuretanozko itsasgarriek zizailatzearekiko erresistentzia handia eta egonkortasun handia erakutsi zuten. Beraz, sintetizatutako itsasgarriak zur-industrian erabiltzeko kontutan hartu beharreko alternatiba bat izan daitekeela ondorioztatu zen.

Argitalpen bakoitzerako hurrengo ondorio espezifikoak atera ziren:

- **I. Argitalpena**: Ligninaren prezipitazio-prozesuan sortutako hondakin likidoak $M_w$ baxuko eta $I_{OH}$ balio altuako biopoliolak lortzeko aukera egiaztatu zen. Lortutako ezaugarriak PUak ekoizteko egokiak zirela ondorioztatu zen, hala ere, lortutako errendimendu baxuak zirela eta, lan honetan ez ziren PUak sintetizatu.
- **II. Argitalpena**: Box Behnken diseinu esperimental baten bidez eta RSM metodologia erabiliz, hainbat biopoliol mota sintetizatzeko erreakzio-baldintzak optimizatu ziren. Diseinu esperimentala mikrouhin erradiazioaren teknologia erabiliz burutu zen, eta doikuntza ona zuela frogatu zen, 0,97tik gorako determinazio-koefizienteak ($R^2$) lortuz. Gainera, Fisherren F probaren bidez modeluaren doikuntza egokia berretsi zen. Horrela, ***I. Argitalpenean*** lortutako ligninak erabiliz, PU zurrunak eta elastikoak formulatzeko beharrezko ezaugarriak zituzten biopoliolak lortu ziren.
- **III. Argitalpena**: ***II. Argitalpenean*** optimizatutako erreakzio-baldintzak erabiliz, eta metodologia berari jarraituz, gradu teknikoko

glizerolaren ordez sukaldatzeko landare-oliotik datorren findu gabeko glizerol gordin bat ligninaren likidotze prozesuan erabil daitekeela ondorioztatu zen. Hala ere, zenbait desberdintasun ikusi ziren ***II. Argitalpenean*** lortutako emaitzekin alderatuta, errendimendu txikiagoak eta $I_{OH}$ txikiagoak besteak beste. Dena den, lortutako biopoliolak PUen sintesirako behar diren ezaugarriak zituztela ondorioztatu zen.

- **IV. Argitalpena**: Lan honetan mikrouhin bidezko likidotze erreakzioaren eskalatze bat egin zen, ***II. eta III. Argitalpenetan*** lortutakoen oso antzeko ezaugarriak zituzten biopoliolak lortuz, eskalatzea posible dela frogatuz. Gainera, ligninatik eratorritako biopoliolak erabiliz, zuraren industrian erabil daitezkeen PU itsasgarriak sintetizatu daitezkeela frogatu zen. Emaitzarik onenak, 2,5:1eko NCO:OH erlazioa erabiltzean lortu ziren. Bestalde, ligninaren jatorriak PUen mikroegituran eragina dutela egiaztatu zen, Eucalyptus globulus-etik eratorritako lignina erabiltzean fase-bereizketa handiagoa gertatzen dela ondorioztatuz.
- **V. Argitalpena**: Argitalpen honetan, ***IV. Argitalpenean*** lortutako biopoliolak erabiliz, zuraren industrian erabilgarria den isozianato gabeko poliuretano itsasgarriak ekoiztu ziren. Horretarako, polikondentsazio erreakzio bat erabili zen DMC eta HDMA. ABES saiakuntzan lortutako emaitzak onak izan ez zirenez, silanozko akoplamendu-agente bat erabiltzea erabaki zen polimeroaren erretikulazioa eta zizailuarekiko erresistentzia-balioak hobetzeko asmoz.

## ETORKIZUNEKO LANAK

Jarraian, hemen aurkeztutako lana osa dezaketen ikerketa-ildo batzuk proposatzen dira.

- Poliuretanoen sintesia, ***I. Argitalpenean*** lortutako biopoliolak erabiliz.

- Poliuretanozko aparren sintesia, ***II. Argitalpenean*** optimizatutako biopoliolak erabiliz.

- Tesi honetan jarraitutako ikerlerro guztien bizi-zikloaren azterketa (LCA).

- ***V. Argitalpenean*** NIPUak ekoizteko erabilitako diaminaren ordez, ingurumena gehiago errespetatzen duen konposatu batengatik ordezkatzea.

*This party is Over*

*Mace Windu*

# IRUDI ETA TAULEN LABURPENA

## LIST OF FIGURES & TABLES

# IRUDIAK - FIGURES

## Sarrera

## Metodologia



## Emaitzak eta eztabaida - Results and discussion

### I. Argitalpena

## Publication II



## III. Argitalpena

## Publication IV

## Publication V

# TAULAK - TABLES

## Sarrera



## Metodologia



# Emaitzak eta eztabaida - Results and discussion

## I. Argitalpena

## Publication II

## III. Argitalpena



## Publication IV

## Publication V

## II. Eranskina

# ERANSKINAK

## APPENDIX

# I. ERANSKINA Likore beltzak karakterizatzeko prozedura

## I. pH-ren determinazioa

*Eucalyptus globulus* eta *Pinus radiata* deslignifikazio prozesuaren ondoren lortutako LBen pHa "CRISON basic 20" pH metro digital baten bitartez zehaztu zen.

## II. Dentsitatearen determinazioa

LBen dentsitatea grabimetrikoki neurtu zen hauen bolumen ezagun bat pisatuz. Horretarako, aurrez pisatutako eta hezetasunik gabeko arragoak erabili ziren.

## III. Disolbatutako solido totalak (TDS)

Organosolv LBen TDSaren zehaztapena National Renewable Energy Laboratory (NREL)-en LPA-012 arauan deskribatutako prozeduraren arabera egin zen. Prozedura honetan, 5,0 ± 0,01 g LB pisatzen dira, aurretik pisatutako eta hezetasunik gabeko arrago batean. Ondoren, arragoak 24 orduz labe batean sartzen dira 105 ± 3 °C-ko tenperaturan, denbora hau igarotzean labetik atera eta lehorgailu batean hozten uzten dira segurtasunez pisatu ahal izateko. Azkenik, TDS kalkulua A.I.1 Ekuazioa erabiliz egiten da.

$$TDS\ (\%) = \frac{(m_f - m_i)}{m} \times 100 \qquad \text{A.I.1 Ekuazioa}$$

non $m_f$ arragoaren gehi laginaren pisua den (g)-tan labean 24 ordu eman ondoren, $m_i$ arrago lehorraren pisua den (g)-tan eta m hasierako likore beltzaren laginaren pisua den.

## IV. Materia inorganikoa eta organikoa (IM, OM)

LBen IMa TAPPI T-211 om-93 arauaren egokitzapen baten bidez zehaztu zen.

TDSa kalkulatzeko erabilitako arragoa lagin lehorrarekin labean sartu zen 3 orduz eta 525 °C-ko tenperaturan. Ondoren, arragoa lehorgailu batean hoztu eta pisatu egin zen. IMa A.I.2 Ekuazioa erabiliz kalkulatu zen.

$$IM\ (\%) = \frac{(m_f - m_i)}{m} \times 100 \qquad \text{A.I.2 Ekuazioa}$$

non $m_f$ erretako lagina duen arragoaren pisua den (g), $m_i$ arrago lehorraren pisua den (g) eta m hasierako LBren laginaren pisua den (g).

OMa TDS eta IMren arteko diferentzia bezala kalkulatu zen A.I.3 Ekuazioa erabiliz.

$$OM\ (\%) = TDS(\%) - IM(\%) \qquad \text{A.I.3 Ekuazioa}$$

## V. Lignina edukia

LBtan disolbatutako lignina frakzioa grabimetrikoki determinatu zen.

Hasteko, lignina LBtatik ***2. zatiko 2.2 ATALEAN*** deskribatzen den bezala prezipitatu eta iragazi zen. Ondoren, lignina 50 ± 2 °C-ko tenperatura erabiliz lehortu zen labe batean. Lehortu eta gero, lehorgailu batean hoztu eta pisatu egin zen. Lignina kontzentrazioa A.I.4 Ekuazioa erabiliz kalkulatu zen.

$$Lignina\ edukia\ (\%) = \frac{(m_f - m_i)}{(V \times \rho)} \times 100 \qquad \text{A.I.4 Ekuazioa}$$

non $m_f$ lignina duen filtro lehorraren pisua (g) den, $m_i$ filtro lehorraren pisua (g) den, eta LBren bolumena (mL) eta dentsitatea (g/mL) V eta ρ diren, hurrenez hurren.

# II. ERANSKINA Biopoliolak eta poliuretanoak karakterizatzeko prozedura

## I. Konposizio kimikoa

Argitalpenean lortutako biopoliolaren konposizio kimikoa Gasen Kromatografia-Masen Espektrometria (GC-MS) teknika erabiliz analizatu zen. Biopoliol lagina HPLC graduko etil azetatoan disolbatu egin zen matraze aforatu batean. Ondoren, disoluzioaren µL bat Agilent CG(7890A) eta MS (5975C) Triple-Axis Detektagailua duen GC-MSn injektatu zen. Gas kromatografoak HP-5MS((%5 fenil)-metilpolisiloxano, 30 m x 0,25 mm)-ko zutabe kapilar batez ekipatuta zegoen eta Helioa gas garraiatzaile gisa erabili zen. Tenperatura programa 50 °C-tan hasi zen; ondoren, tenperatura 8 °C/min-ko abiadurarekin 120 °C-ra igo zen eta horrela 5 minutu mantendu zen. Gero, tenperatura 280 °C-ra igo zen 8 °C/min-ko abiaduraz eta 10 minutuz tenperatura horretan mantendu zen, azkenik 10 °C/min-ko berotze abiadura erabiliz tenperatura 300 °C-ra igo zen (2 min). Kalibrazioa Sigma-Aldrich-ek hornitutako ondoren aipatzen diren konposatuak erabiliz egin zen: fenola, orto, meta eta para kresola, guaiakola, katekola, 3-metilkatekola, 4-metilkatekola, 4-etilkatekola, 3-metoxikatekola, siringola, 4-hidroxibenzaldehidoa, azetobanillona, beratrola, azido 4-hidroxibenzoikoa, 4-hidroxi-3-metoxifenilazetona, banillina, azido banillinikoa, siringaldehidoa, 3,5-dimetoxi-4-hidroxiazetofenone eta azido siringikoa.

## II. Estruktura kimikoa

***I. Argitalpenean*** lortutako biopoliolen, ***II. Argitalpenea***n erauzitako lignina laginak eta ***IV. eta V. Argitalpenetan*** sintetizatutako PU eta NIPU laginen egitura kimikoa Islapen Total Indargetua – Fourierren Transformatuaren bidezko espektroskopia infragorria (ATR-FTIR) bidez aztertu zen. Analisiak

egiteko, Universal Attenuated Total Reflectance (ATR) osagarriaz eta diamantezko leiardun Islapen kristal batez hornitutako PerkinElmer Spectrum Two FTIR espektrometro bat erabili zen. Lagin bakoitzerako guztira 20 ekorketa egin ziren, 4 $cm^{-1}$-ko bereizmenarekin, 4000 eta 600 $cm^{-1}$ artean.

PU eta NIPUen mikrofaseen arteko banaketa eta nahaskortasun maila ATR-FTIR espektro bidez zehaztu zen eta hidrogeno zubien (H-zubi) bitartez elkartutako uretano eta urea taldeen pisu frakzioa A.II.1. Ekuazioarekin kalkulatu zen.

$$X_{HB} = \frac{A_{Hb}}{K' A_{Fc} + A_{Hb}} \qquad \text{A.II.1. Ekuazioa}$$

non, $X_{HB}$ uretano eta urea taldeen H-zubien bidez elkartutako frakzio masikoa den, $A_{HB}$ H-zubien bidez lotutako C=O uretano taldeen (1708-1704 $cm^{-1}$, 1697-1694 $cm^{-1}$ eta 1688-1686 $cm^{-1}$) eta urea taldeen (1675-1654 $cm^{-1}$ eta 1644-1630 $cm^{-1}$) absorbantzia den, $A_{FC}$ C=O uretano talde askeen absorbantzia da ((1730-1728 $cm^{-1}$) eta K' balio konstantea H-zubien bidez lotutako C=O taldeen eta C=O talde askeen arteko iraungipen-koefizientea den.

Fase bigunean nahastutako HS-ren gehieneko masa frakzioa ($W_H$) kalkultzeko, A.II.2. Ekuazioa erabili zen.

$$W_H = \frac{(1 - X_{HB}) \times z}{[(1 - X_{HB}) \times z + (1 - z)]} \qquad \text{A.II.2. Ekuazioa}$$

non z HS-ren frakzio teorikoa den. MDIn oinarritutako PUetarako A.II.3.1. ekuazioarekin eta NIPUetarako A.II.3.2. ekuazioarekin kalkulatu zen.

$$HS_t\ \% = \frac{n M_{MDI}}{(n+1) M_{MDI} + \bar{M}_{nPolyol}} \times 100 \qquad \text{A.II.3.1. Ekuazioa}$$

$$HS_t\ \% = \frac{nM_{DMC}+nM_{HDMA}}{(n+1)M_{DMC+}\ (n+1)M_{HDMA}+\bar{M}_{nPolyol}} \times 100 \qquad \text{A.II.3.2. Ekuazioa}$$

non $M_{MDI}$, $M_{DMC}$ eta $M_{HDMA}$ MDI diisozianatoaren, DMCren eta HDMAren pisu molekularrak diren, $M_{nPoliol}$ biopoliolaren batez besteko pisu molekularra kopurua den (g/mol) eta n mol kopurua den.

Fase nahastearen (*mixed phase* $MP_W$), segmentu bigunaren (*soft segment* $SS_W$) eta segmentu zurrunaren (*hard segment* $HS_W$)-ren pisu frakzioa A.II.4., A.II.5. eta A.II.6. Ekuazioen bitartez kalkulatu ziren.

$$MP_W = z \times W_H \qquad \text{A.II.4. Ekuazioa}$$

$$SS_w = MP_W + (1 - z) \qquad \text{A.II.5. Ekuazioa}$$

$$HS_w = 1 - SS_W \qquad \text{A.II.6. Ekuazioa}$$

## III. Pisu molekularraren banaketa

Lignina eta biopoliolen laginen pisu molekularraren banaketa, Gel-Iragazketako Kromatografiaren (*Gel Permeation Chromatography* GPC) bidez aztertu zen batezbesteko pisu molekularra pisuan ($M_W$) eta kopuruan ($M_n$), baita polidispertsitate indizea (PDI) ($M_W/M_n$) gisa adierazita, zehazteko. Horretarako, Varian Polymer Laboratories-en bi kolumna PolarGel -M (300 mm x 7.5 mm) seriean dituen eta errefrakzio-indizearen detektagailua duen Jasco LC Netll/ADC kromatografo bat erabili zen. Litio bromurodun (% 0.1) N,N-dimetilformamidazko disoluzio bat erabili zen fase mugikor gisa eta analisiak ondorengo baldintzekin gauzatu ziren: 700 $mm^3$/min-ko fluxua, 40 °C-ko tenperatura eta 20µL-ko injekzio bolumena. Kalibrazio-kurba, Sigma Aldrichek hornitutako poliestirenozko patroi diferenteak (2600-70000 g/mol) erabiliz egin zen.

## IV. Oinarrizko analisia

Oinarrizko analisia Leco TruSpec micro elemental analizatzailea erabiliz gauzatu zen 1050°C-ko tenperatua erabiliz. Analisietan erabilitako gas eramailea (helio 3X purua) eta probarako gasa (oxigeno 4X estra purua) Nippon Gasek hornitu zituen. Kalibrazioa Leco sulfamethazina (C=51.78%; H=5.07%; S=11.5%) erabiliz egin zen. Analisiak burutzeko 2 mg-ko laginak erabili ziren.

## V. Hidroxilo-zenbakiaren ($I_{OH}$) eta azido-zenbakiaren ($A_n$) determinazioa

***I., II.*** eta ***III. Argitalpenentan*** lortutako biopoliolen $I_{OH}$-a eta $A_n$-a, biak (mg KOH/lagin g) gisa definituak, ASTM D4274 [1] eta ASTM D974 [2] estandar metodoak erabiliz zehaztu ziren.

Biopoliol desberdinen $I_{OH}$-ak neurtzeko, ASTM D4274 estandar metodoa erabiliz, 0,5-1 g lagin, 700 mL piridinan 115 g anhidrido ftalico disolbatuz sortutako ftalazio erreaktiboaren 25mL-tan disolbatu ziren. Soluzioa ordubetez berotu zen 115 °C-tan, errefluxu eta etengabeko irabiaketa erabiliz. Erreakzioa amaitutakoan, 50 mL piridina isuri ziren kondentsadoretik. Azkenik, bukaerako soluzioa 0,5 M den NaOH disoluzioa erabiliz baloratu zen. $I_{OH}$-a kalkulatzeko, A.II.7. Ekuazioa erabili zen.

$$I_{OH} = \frac{(B-A)\times M \times 56.1}{w} + A_n \qquad \text{A.II.7 Ekuazioa}$$

non B eta A, zuria eta biopoliol lagina baloratzeko beharrezko NaOH bolumena (mL) diren, hurrenez hurren. M NaOH-ren molaritatea den, W laginaren pisua den (g) eta $A_n$ laginaren azido zenbakia den.

Biopoliolen $A_n$-a kalkulatzeko, biopoliol bakoitzaren 0,4 g disolbatu egin ziren 1,4-dioxano:ura (4:1 b/b) den 50 mL disoluzio batean eta ondoren 0,1

M-eko KOH/etanol disoluzio batekin baloratu zen. $A_n$ balioak zehazteko A.II.8. Ekuazioa erabili zen.

$$A_n = \frac{(C-B)\times M \times 56.1}{w} \qquad \text{A.II.8 Ekuazioa}$$

non C KOH disoluzioa titulatzeko beharrezkoa izan zen bolumena (mL) den, B soluzio zuria baloratzeko beharrezkoa izan zen bolumena (mL) den, M KOH disoluzioaren molaritatea den eta *w* (g) analizatutako biopoliolaren lagina den.

Lignina oinarritutako biopoliolen kolore iluna zela eta, ezin izan zen fenolftaleina indikatzailea erabiliz titulatu. Hori dela eta, titulazio potentziometriko bat egin zen Tiamo 2.5 softwarra duen Automatic 888 (Titrando Metrohm) titratzaile automatiko bat erabiliz.

## VI. Portaera erreologikoa

***I., II.*** eta ***III. Argitalpenetako*** biopoliolen portaera erreologikoa aztertzeko proba oszilatorioak zein errotazionalak burutu ziren. Lehenengoarekin, biltegiratze modulua (G') eta galera modulua (G'') zehaztu ziren, eta bigarrenarekin, berriz, biskositatea (η) eta zizailadura-esfortzua (τ) zizail-tasaren ($\dot{\gamma}$) arabera determinatzeko erabili zen. Neurketak Hakke viscotester IQ (Thermo Fisher Scientific) eta Rhemometric Scientific Advanced Rheometric Expansion System (ARES) ekipamenduan erabiliz gauzatu ziren A.1. Taulan ikusi daitekeen bezala.

Neurketak giro tenperaturan egin ziren eta aztertutako biopoliolaren arabera erabilitako geometria desberdina izan zen. Horrela, ***I. Argitalpenean***, moduluak zein likatasuna neurtzeko, 25 mm eta 35 mm-ko plater paraleloen geometria erabili zen, hurrenez hurren. Test oszilatorioa egiteko, 0,1 eta 100 rad·s$^{-1}$ bitarteko maiztasun-ekorketa bat erabili zen %

10eko tentsio finkoan. Errotazional saiakuntzarako 0,02 eta 120 $s^{-1}$ bitarteko zizailatze-abiadura ekorketa erabili zen.

A. 2. Taula. **I., II. eta III Argitalpenetan** sintetizatutako biopoliolen karakterizazio erreologikoa aztertzeko erabilitako proba eta ekipamendu desberdinak

| | Erreometroa | | | |
|---|---|---|---|---|
| | ARES | | HAAKE | |
| Argitalpena | Oszilatorioa | Errotazionala | Oszilatorioa | Errotazionala |
| I | √ | ✗ | ✗ | √ |
| II eta III | ✗ | ✗ | √ | √ |

***II.*** eta ***III. Argitalpenetan***, moduluen eta biskositatearen determinazioak egiteko, 12.54 mm-ko pistoi-erradiodun zilindro ardazkideen geometria erabili zen (CC 25 DIN/Ti egokigailua) 1 mm-ko eraztun hutsunearekin. Neurketak egiteko I. Argitalpenean erabilitako baldintzak erabili ziren.

Errotazional saiakuntzen parametroak Power-Law ekuaziora (A.II.9. Ekuazioa) egokitu ziren.

$$\tau = \kappa \cdot \dot{\gamma}^{n} \qquad \text{A.II.9. Ekuazioa}$$

non *n* fluxu-indizea eta κ sendotasun-indizea doikuntza-parametroak diren, fluidoaren izaeraren eta neurketa-baldintzen araberakoak. κ, fluidoaren itxurazko biskositatearekin erlazionatzen da $1s^{-1}$-ko zizaila abiadurarekin, eta biskositatea gora egin ahala, handitu egiten dira κ-ren balioak [3]. Fluxu-indizea berriz, fluidoaren portaera adierazten du; hala, n=1 bada, fluido Newtonianoa da, pseudoplastikoa n<1 bada eta dilatantea n>1 denean.

### VII. Analisi termograbimetrikoa (TGA)

***I., II.*** eta ***III. Argitalpenetako*** biopoliolak eta ***IV.*** eta ***V. Argitalpenetako*** PU eta NIPUak analisi termograbimetrikoen bidez aztertu ziren TGA/SDTA RSI analyser 851 (Mettler Toledo) erabiliz. 3 eta 5 mg bitarteko laginak pisatu

ziren aluminiozko kapsuletan eta $N_2$-ko atmosferapean (10 mL·min$^{-1}$), 25 °C-tik 800 °C-ra berotu ziren, 10 °C·min$^{-1}$-ko berotze abiadura erabiliz.

## VIII. Degradazio termikoaren zinetika eta bizi iraupenaren estimazioa

***IV.*** eta ***V. Argitalpenentan*** sintetizatutako PU eta NIPUen degradazio termikoaren zinetika eta bizi iraupenaren estimazioa egin ahal izateko, aurreko puntuan deskribatutako TGA ekipamendua eta prozedura bera erabili ziren. Hala ere, kasu honetan lau berotze abiadura diferente erabili ziren, zehazki, 1, 2, 5 eta 10 °C·min$^{-1}$. Aktibazio-energia (*activation energy* $E_a$) kalkulatzeko bi metodo ezberdin hautatu ziren: Ozawa-Flynn-Wall (OFW) [4] (A.II.10. Ekuazioa) eta Kissinger-Akahira-Sunose [5] (A.II.11. Ekuazioa).

non $\beta$ berotze abiadura den, $T_p$ tenperatura exotermiko maximoa den berotze abiadura jakin batean. $E_a$ aktibazio energia den, $A$ faktore preesponentziala den, $R$ gasen konstante unibertsala eta $f(\alpha)$ mekanismoak zehaztutako funtzioa diren.

$$\ln(\beta) = ln\left(\frac{AE_a}{Rf(\alpha)}\right) - 5.331 - 1.052\frac{E_a}{RT_p} \qquad \text{A.II.10. Ekuazioa}$$

$$\ln\left(\frac{\beta}{T_p^2}\right) = ln\left(\frac{AR}{E_a}\right) - \frac{E_a}{RT_p} \qquad \text{A.II.11. Ekuazioa}$$

Bi kasuetan, $Ea$-ren eta $A$-ren balioak, $\ln(\beta)$ eta $\ln\left(\frac{\beta}{T_p^2}\right)$ versus $1/T_p$ grafikoen malda eta interzeptutik lor daitezke.

PU eta NIPUen bizi iraupena OFW metodoa erabiliz estimatu zen A.II.12. ekuazioa-z baliatuz.

$$\ln t = \frac{E}{RT} + \ln\left[-\frac{\ln(1-\alpha)}{A}\right] \qquad \text{A.II.12. Ekuazioa}$$

## IX. PUen eta NIPUen adhesio saiakuntzak ABES erabiliz

PU eta NIPU itsasgarrien adhesio saiakuntzak (***IV.*** eta ***V. Argitalpenak***) burutzeko, Viseuko Institutu Politeknikoko Zurezko Ingeniaritzako Departamentuko Automated Bonding Evaluation System (ABES, Crovallis, OR, USA) erabiliz burutu ziren. Probak egiteko, 117 mm x 20 mm eta 0,5 mm-ko lodierako pagoz (*Fagus sylvatica*) egindako xaflak erabili ziren. Horretarako, itsasgarrien 10 mg aplikatu ziren, eta pago-xaflaren ertzaren 5 mm-tan banatu ziren, 100 $mm^2$-ko itsaspen-eremua izateko. Ondoren, itsasgarria zuen xafla eta itsasgarririk gabeko beste xafla bat ABESean jarri ziren eta saiakuntzak 120 °C-tan burutu ziren prentsa denbora desberdinak erabiliz.

## ERREFERENTZIAK

[1] S.T. Methods, Test 08(Reapproved 2010) (2000) 3–6. 10.1520/D4671-05.2.

[2] ASTM, i (2013) 1–7. 10.1520/D0974-12.2.

[3] D. Chimene, C.W. Peak, J.L. Gentry, J.K. Carrow, L.M. Cross, E. Mondragon, G.B. Cardoso, R. Kaunas, A.K. Gaharwar, ACS Appl. Mater. Interfaces 10(12) (2018) 9957–68. 10.1021/acsami.7b19808.

[4] T. Ozawa, Bull. Chem. Soc. Jpn. 38(11) (1695) 1881–6. 10.1246/bcsj.38.1881.

[5] S. Vyazovkin, Molecules 25(12) (2020). 10.3390/molecules25122813.

# APPENDIX III. Publications & Conferences

## Contributions included in this thesis

The following publications are directly related to the thesis presented here.

**Publication 0:**

Book chapter.

Biorefinery: A Sustainable Approach for the Production of Biomaterials, Biochemicals and Biofuels. **(Under edition)**

Tittle: Current Approaches for Polyurethane Production from Lignin.

Authors: **Fabio Hernández-Ramos**, Pedro L. de Hoyos-Martínez, Sebastian Barriga, Xabier Erdocia and Jalel Labidi

**Publication I:**

Paper in Scientific Journal.

Renewable Biopolyol from Residual Aqueous Phase Resulting after Lignin Precipitation **(Published)**

Journal: ACS Sustainable Chemistry & Engineering. https://dx.doi.org/10.1021/acssuschemeng.0c09357

Authors: Fabio Hernández-Ramos, María González Alriols, Tamara Calvo-Correas, Jalel Labidi and Xabier Erdocia.

**Publication II:**

Paper in Scientific Journal.

Organosolv lignin-based bio-polyols for polyurethane production: Process optimisation through response surface methodology. **(Under revision)**

Journal: Industrial Crops & Products.

Authors: **Fabio Hernández-Ramos**, Vincent Novi, María González Alriols, Jalel Labidi and Xabier Erdocia

**Publication III:**

Paper in Scientific Journal.

Valorisation of crude glycerol in the production of liquefied lignin bio-polyols for polyurethane formulations. **(In process)**

Authors: **Fabio Hernández-Ramos**, María González Alriols, M. Mirari Antxustegi, Jalel Labidi and Xabier Erdocia

**Publication IV:**

Paper in Scientific Journal.

Synthesis, characterisation, and thermal degradation kinetic of lignin-based polyurethane wood adhesives. **(In process)**

Authors: **Fabio Hernández-Ramos**, Jalel Labidi, Xabier Erdocia and Bruno Esteves

**Publication V:**

Paper in Scientific Journal.

Lignin-based non isocyanate polyurethane adhesives. Synthesis and determination of adhesion properties and thermal degradation kinetic. **(In process)**

Authors: Fabio Hernández-Ramos, Jalel Labidi, Xabier Erdocia and Bruno Esteves

# Contributions not included in this thesis

During this thesis different book chapters as well as scientific publications not directly related to the work presented here have been collaborated on.

**Book Chapters:**

Erdocia, X., **Hernández-Ramos, F.**, Morales, A., Labidi, J., 2021. Lignin depolymerization for monomers production by sustainable processes, Micro and Nanolignin in Aqueous Dispersions and Polymers: Interactions, Properties, and Applications. https://doi.org/10.1016/B978-0-12-823702-1.00005-0

Erdocia, X., **Hernández-ramos, F.**, Morales, A., Izaguirre, N., Hoyos-martínez, P.L. De, Labidi, J., 2021. Lignin extraction and isolation methods, in: Lignin-Based Materials for Biomedical Applications. Elsevier Inc., pp. 61–104. https://doi.org/10.1016/c2019-0-01345-3

Fernández-Rodríguez, J., Erdocia, X., **Hernández-Ramos, F.**, Alriols, M.G., Labidi, J., 2019. Lignin Separation and Fractionation by Ultrafiltration, in: Separation of Functional Molecules in Food by Membrane Technology. pp. 229–265. https://doi.org/10.1016/b978-0-12-815056-6.00007-3

Fernández-Rodríguez, J., Alriols, M.G., **Ramos, F.H.**, Labidi, J., 2018. Energetic assessment of lignin extraction processes by simulation, Computer Aided Chemical Engineering. Elsevier Masson SAS. https://doi.org/10.1016/B978-0-444-64235-6.50268-0

**Scientific Journals:**

Gómez-Cruz, I., Romero, I., Contreras, M. del M., Labidi, J., **Hernández-Ramos, F.**, Roseiro, L.B., Duarte, L.C., Castro, E., Carvalheiro, F., 2022. Combined Extraction and Ethanol Organosolv Fractionation of Exhausted Olive Pomace for Bioactive Compounds. Adv. Sustain. Syst. 6. https://doi.org/10.1002/adsu.202100361

Egüés, I., **Hernandez-Ramos, F.**, Rivilla, I., Labidi, J., 2021. Optimization of ultrasound assisted extraction of bioactive compounds from apple pomace. Molecules 26. https://doi.org/10.3390/molecules26133783

Fernández-Marín, R., **Hernández-Ramos, F.**, Salaberria, A.M., Andrés, M.Á., Labidi, J., Fernandes, S.C.M., 2021. Eco-friendly isolation and characterization of nanochitin from different origins by microwave irradiation: Optimization using response surface methodology. Int. J. Biol. Macromol. 186, 218–226. https://doi.org/10.1016/j.ijbiomac.2021.07.048

Rajhi, I., **Hernandez-Ramos, F.**, Abderrabba, M., Dhia, M.T. Ben, Ayadi, S., Labidi, J., 2021. Antioxidant, antifungal and phytochemical investigations of capparis spinosa L. Agric. 11. https://doi.org/10.3390/agriculture11101025

Sillero, L., Morales, A., Fernández-Marín, R., **Hernández-Ramos, F.**, Davila, I., Erdocia, X., Labidi, J., 2021. Study of different extraction methods of bioactive molecules from different tree species. Chem. Eng. Trans. 86, 31–36. https://doi.org/10.3303/CET2186006

Sillero, L., Morales, A., Fernández-Marín, R., **Hernández-Ramos, F.**, Dávila, I., Erdocia, X., Labidi, J., 2021. Life Cycle Assessment of various biorefinery approaches for the valorisation of almond shells. Sustain. Prod. Consum. 28, 749–759. https://doi.org/10.1016/j.spc.2021.07.004

Fernández-Rodríguez, J., Erdocia, X., **Hernández-Ramos, F.**, Gordobil, O.,

González Alriols, M., Labidi, J., 2020. Direct lignin depolymerization process from sulfur-free black liquors. Fuel Process. Technol. 197, 106201. https://doi.org/10.1016/j.fuproc.2019.106201

**Hernández-Ramos, F.**, Fernández-Rodríguez, J., Alriols, M.G., Labidi, J., Erdocia, X., 2020. Study of a renewable capping agent addition in lignin base catalyzed depolymerization process. Fuel 280, 118524. https://doi.org/10.1016/j.fuel.2020.118524

Morales, A., **Hernández-Ramos, F.**, Sillero, L., Fernández-Marín, R., Dávila, I., Gullón, P., Erdocia, X., Labidi, J., 2020. Multiproduct biorefinery based on almond shells: Impact of the delignification stage on the manufacture of valuable products. Bioresour. Technol. 315. https://doi.org/10.1016/j.biortech.2020.123896

Sepperer, T., **Hernandez-Ramos, F.**, Labidi, J., Oostingh, G.J., Bogner, B., Petutschnigg, A., Tondi, G., 2019. Purification of industrial tannin extract through simple solid-liquid extractions. Ind. Crops Prod. 139, 111502. https://doi.org/10.1016/j.indcrop.2019.111502

**Hernandez, F.**, Erdocia, X., Labidi, J., 2018. Phenolic monomers production by the direct depolymerization of lignin contained in Kraft black liquor in the presence of metal catalyst. Chem. Eng. Trans. 70, 1597–1602. https://doi.org/10.3303/CET1870267

# Contributions to conferences

**BIOPOL 2022** (14th to 16th November, Alicante - Spain): **Fabio Hernández-Ramos**, María González Alriols, Jalel Labidi, Xabier Erdocia; *Lignin Based Polyurethane* adhesives (Oral comunication)

**SUSTENG 2022** (31st Aug – 4th Sep 2022, Rethymno, Crete, Greece): **F. Hernández-Ramos**, M. Gonzalez Alriols, J. Labidi, X. Erdocia; *Valorisation of crude glycerol in the production of liquefied lignin biopolyols* (Oral comunication)

**MZT 2021** (November 29-30, Bilbao – Spain): **F. Hernández-Ramos**, L. Sillero, A. Morales, R. Fernández-Marín, I. Dávila, X. Erdocia: *Euskal baso eta nekazaritza industrietatik eratorritako biomasaren prozesaketa goi-mailako bio-findegi batean* (Oral comunication)

**BIORESTEC 2021** (May 17-19, Garda – Italy): **Fabio Hernández-Ramos**, María González Alriols, Jalel Labidi, Xabier Erdocia; *Polyol from residual aqueous phase resulting after the precipitation of lignin* (Poster)

**PRES 2018** (25-29 Aug, Prague, Czech Republic): **F. Hernández**, X. Erdocia, J. Labidi; *Phenolic monomers production by the direct depolymerization of lignin contained in Kraft black liquor in the presence of metal catalyst* (Poster)

*I must not fear. Fear is the mind-killer. Fear is the little-death that brings total obliteration. I will face my fear. I will permit it to pass over me and through me. And when it has gone past I will turn the inner eye to see its path. Where the fear has gone there will be nothing. Only I will remain.*

*Litany of Bene Gesserit against fear*

*Frank Herbert, Dune*

Ingurumenarekin gero eta kontzientziatuago dagoen gizarte honetan, eta gero eta murriztaileagoak diren legeak direla eta, biomasaren balorizazioa etorkizun handiko alternativa bihurtu da historikoki industria petrokimikotik eratorritako bioerregaiak eta produktu kimikoak ekoizteko. Eskuragarri dauden biomasa moten artean, biomasa lignozelulosikoa da erakargarriena, ugaria, merkea eta ingurumena errespetazen duelako.

Biomasa lignozelulosikoaren osagaien artean, lignina, bere izaera fenolikoagatik eta funtzionaltasun altuagatik, bioerregaiak, produktu kimikoak eta oinarri biologikoko materialak garatzeko hautagai ezin hobea da. Gainera, lignina pepergintzan azpiproduktu gisa sortzen da, eta, beraz, oso eskuragarri eta merkea den lehengaia da. Ligninarekin ekoiztu daitezkeen materialen artean plastikoak, mintzak, hidrogelak, piliolak eta poliuretanoak aurki daitezke.

eman ta zabal zazu

Universidad del País Vasco

Euskal Herriko Unibertsitatea

**Tesi hau Espainiako Gobernuaren eta Eusko Jaurlaritzaren laguntza ekonomikoari esker burutu da**

BioRP

Biorefinery Processes Research Group